IMT Institute for Advanced Studies, Lucca

Lucca, Italy

Deterministic Shift Extension of Affine Models for Variance Derivatives

PhD Program in Computer Decision and System Science,
curriculum: Management Science

XXVIII Cycle

By

Gabriele Pompa

2015

Program Coordinator: Prof. Rocco De Nicola, IMT Institute for Advanced Studies Lucca

Supervisor: Prof. Fabio Pammolli, IMT Institute for Advanced Studies Lucca

Supervisor: Prof. Roberto Renò, University of Verona

The dissertation of Gabriele Pompa is currently under review.

IMT Institute for Advanced Studies, Lucca

2015

Contents

Abstract

The growing demand for volatility trading and hedging has lead today to a liquid market for derivative securities written on it, which made these instruments a widely accepted asset class for trading, diversifying and hedging. This growing market has consistently driven the interest of both practitioner and academic researchers, which can find in VIX and derivatives written on it a valuable source of informations on S&P500 dynamics, over and above vanilla options. Their popularity stems from the negative correlation between VIX and SPX index, which make these instruments ideal to take a pure position on the volatility of the S&P500 without necessarily taking a position on its direction. In this respect futures on VIX enable the trader to express a vision of the markets future volatility and call options on VIX offer protection from market downturns in a clear-cut way. From the theoretical point of view, this has lead to the need of a framework for consistently pricing volatility derivatives and derivatives on the underlying, that is the need to design models able to fit the observed cross-section of option prices of both markets and properly price and hedge exotic products. The consistent pricing of vanilla options on S&P500 and futures and options on VIX is a requirement of primary importance for a model to provide an accurate description of the volatility dynamics. Since equity and volatility markets are deeply related, but at the same time show striking differences, the academic debate around the relevant features should a model incorporate in order to be coherent with both markets is still ongoing. In this thesis we leverage on the growing literature concerning the developing of models for consistently pricing volatility derivatives and derivatives on the underlying and propose the Heston++ model, which is an affine model belonging to the class of models analyzed by Duffie et al. (2000) with a multi-factor volatility dynamics and a rich jumps structure both for price and volatility. The multi-factor Heston (1993) structure enables the model to better

capture VIX futures term structures along with maturity-dependent smiles of options. Moreover, both correlated and idiosyncratic jumps in price and volatility factors help in reproducing the positive sloping skew of options on VIX, thanks to an increased level of the skewness of VIX distribution subsumed by the model. The key feature of our approach is to impose an additive displacement, in the spirit of Brigo and Mercurio (2001), on the instantaneous volatility dynamics which, acting as lower bound for its dynamics, noticeably helps in capturing the term structure of volatility. Both increasing the fit to the at-the-money term structure of vanilla options, as already pointed out in Pacati et al. (2014), and remarkably capturing the different shapes experienced by the term structure of futures on VIX. Moreover, we propose a general affine framework which extends the affine volatility frameworks of Leippold et al. (2007), Egloff et al. (2010) and Branger et al. (2014) in which the risk-neutral dynamics of the S&P500 index features several diffusive and jump risk sources and two general forms of displacement characterize the dynamics of the instantaneous variance process, which is affine in the state vector of volatility factors. The instantaneous volatility is modified according to a general affine transformation in which both an additive and a multiplicative displacement are imposed, the first supporting its dynamics, the second modulating its amplitude. We calibrate the Heston++ model jointly and consistently on the three markets over a sample period of two years, with overall absolute (relative) estimation error below 2.2% (4%). We analyze the different contributions of jumps in volatility. We add two sources of exponential upward jumps in one of the two volatility factors. We first add them separately as an idiosyncratic source of discontinuity (as in the SVVJ model of Sepp (2008b)) and then correlated and synchronized with jumps in price (as in the SVCJ model of Duffie et al. (2000)). Finally, we let the two discontinuity sources act together in the full-specified model. For any model considered, we analyze the impact of acting a displacement transformation on the volatility dynamics. In addition, we perform the analysis restricting factor parameters freedom to satisfy the Feller condition. Our empirical results show a decisive improvement in the pricing performance over non-displaced

models, and also provide strong empirical support for the presence of both price-volatility co-jumps and idiosyncratic jumps in the volatility dynamics.

Introduction

The recent financial crisis has raised the demand for derivatives directly linked to the volatility of the market. This growing demand has lead today to a liquid market for VIX derivatives, futures and options written on the CBOE VIX volatility index Carr and Lee (2009).

Their popularity stems from the negative correlation between VIX and SPX index, which make these instruments ideal to take a position on the volatility of the S&P500 without necessarily taking a position on its direction. In this respect futures on VIX enable the trader to express a vision of the market's future volatility and call options on VIX offer protection from market downturns in a clear-cut way.

This growing market has consequently driven the interest of both practitioner and academic researchers, finding in volatility and derivatives written on it a valuable source of informations on the returns dynamics over and above vanilla options (Andersen et al., 2002; Bardgett et al., 2013; Chung et al., 2011; Kaeck and Alexander, 2012; Mencía and Sentana, 2013; Song and Xiu, 2014).

Indeed equity and volatility markets are deeply related, but at the same time show striking differences. The academic debate around the relevant features should a model incorporate in order to be consistent with both markets is still ongoing (Bardgett et al., 2013; Branger et al., 2014; Mencía and Sentana, 2013).

In this thesis we leverage on the growing literature concerning the building of models for consistent pricing volatility derivatives and derivatives on the underlying and propose the Heston++ model, which is a an affine model with a multi-factor volatility dynamics and a rich jumps structure both in price and volatility.

The multi-factor Heston (1993) structure enables the model to better capture futures term structures along with maturity-dependent smiles. Moreover, both correlated and idiosyncratic jumps in price and volatility factors help in reproducing the positive sloping skew of options on VIX, thanks to an increased level

of the skewness of VIX distribution subsumed by the model.

Nevertheless, the key feature of our approach is to impose an additive displacement, in the spirit of Brigo and Mercurio (2001), on the instantaneous volatility dynamics which, acting as lower bound for its dynamics, noticeably helps in capturing the term structure of volatility expressed both through the ATM term structure of vanilla options, as already pointed out in Pacati et al. (2014), and through the term structures of futures on VIX.

Moreover, we propose a general affine framework which allows for a general affine transformation of the instantaneous volatility, both imposing an additive displacement which support its dynamics, and a multiplicative displacement which modules its amplitude.

Overall, we conduct an extensive analysis with the Heston++ model and its several nested specifications and we find an outstanding ability in fitting the two SPX and VIX options surfaces together, along with very different shapes of the term structure of VIX futures, with an overall absolute (relative) pricing error of 2.2% (4%), showing a decisive improvement in the pricing performance over non-displaced models.

Moreover the remarkable ability of the Heston++ model in capturing features of the VIX options skew, without compromising the ability in fit the smile of the vanilla surface, provide a strong empirical support for the presence of two sources of upward jumps in volatility, one synchronized and correlated with the price dynamics, the second one independent and idiosyncratic.

The thesis is structured as follows:

- **Chapter 1** introduces the mathematical infrastructure of affine models in the footsteps of Duffie et al. (2000).
- **Chapter 2** presents the market of VIX and volatility derivatives and the growing contributions of the literature.
- **Chapter 3** introduces the Heston++ model and gives closed-form pricing formulas for SPX and VIX derivatives. Moreover, the general displaced affine framework is introduced.
- **Chapter 4** describes the empirical analysis conducted with the Heston++ model and its nested specifications and presents the results.

Chapter 1

Affine Models: preliminaries

(With a bit of philosophy). The problem of valuing financial securities, describing the dynamics of the term structure of interest rates, pricing options and estimating credit-risk instruments would in general depend on (and require) the knowledge with *certainty* of just an *infinite* amount of state variables X describing the system under exam. A *reductionist* approach is a must. If one accepts the idea of giving at most a probabilistic description (and in addition of only a few) of the state variables really driving the quantities to be evaluated, then interestingly a particular property of the dynamics of X is able to dramatically reduce the complexity of the problem. This is the *affinity* property.
(Keeping discussion informal). An affine process is a stochastic process X in which the drift vector, which governs the deterministic component of the dynamics of X, the instantaneous covariance matrix, which describes how diffusive randomness enters in each component X_i of X and spreads through the others X_j, and the jump arrival intensities, responsible for discontinuities in the dynamics of X, are all very simple functions of the value of X at that time, that is affine functions.
(Taking it seriously). Prominent examples among affine processes in term-structure literature are the Gaussian model of Vasicek (1977) and square-root CIR model of Cox et al. (1985). Duffie and Kan (1996) introduce a general multivariate class of affine jump diffusion models of interest-rates term-structures. Concerning the option pricing literature most of subsequent models built on the particular affine stochastic-volatility model for currency and equity prices proposed by Heston (1993). These were, among many, the models proposed by Bates (1996), Bakshi

et al. (1997), Duffie et al. (2000), Eraker (2004) and Christoffersen et al. (2009), that brought successively jumps in returns and in volatility factor(s), either idiosyncratic or simultaneous and correlated, while maintaining the simple property that the (logarithm of the) characteristic function, which - entirely and univocally - describes the statistical and dynamical properties of the state vector X, is an affine function of X itself. A property that is crucial and guarantees an otherwise usually hopeless mathematical tractability of asset-pricing and risk-measures problems.
In this respect, a truly breakthrough has been made by Duffie et al. (2000), who study in full generalities the properties of affine jump diffusion models, from their characterization, to the problem of pricing, deriving in particular closed-form expressions for a wide variety of valuation problems, trough a *transform analysis*.
This opens the way to richer - but still tractable - models both for equity and other derivatives, such as those written on the volatility of an underlying process, that will be introduced in the next Chapter.
This Chapter is structured as follows: in Section 1.1 we will introduce affine processes, substantially following Duffie et al. (2000), then in Section 1.2 we will derive their pricing formula for call options on equity, which is based on Fourier transform analysis, and connect it to the widespread formula of Geman et al. (1994), which is based on a change of numeraire technique.

1.1 Definition

We will refer to the notation in Duffie et al. (2000). The n-dimensional jump-diffusion process (Duffie et al., 2000, sec. 2.2) $X_t = (x_1, x_2, ..., x_n)^T$, solving the SDE

$$dX_t = \mu(t, X_t)dt + \sigma(t, X_t)dW_t + dZ_t \tag{1.1}$$

where W_t is an n-dim standard Wiener and Z_t is a n-dim pure jump process, is said an *affine* jump-diffusion (AJD) process if the following dependencies holds:

$$\begin{aligned}
drift\ vector: &\quad \mu(t,X) = K_0 + K_1 X \ \text{ for } \ (K_0, K_1) \in \mathbb{R}^n \times \mathcal{M}_{n\times n} \\
covariance\ matrix: &\quad (\sigma(t,X)\sigma^T(t,X))_{ij} = (H_0)_{ij} + (H_1)_{ij} \cdot X \\
&\qquad\qquad = (H_0)_{ij} + \textstyle\sum_{k=1}^n (H_1^{(k)})_{ij} X_k \\
&\quad \text{for } \ (H_0, H_1) \in \mathcal{M}_{n\times n} \times \mathcal{T}_{n\times n\times n} \ \text{ with } \ H^{(k)} \in \mathcal{M}_{n\times n} \\
jump\ intensities: &\quad \lambda(t,X) = \lambda_0 + \lambda_1 \cdot X \ \text{ for } \ (\lambda_0, \lambda_1) \in \mathbb{R} \times \mathbb{R}^n \\
short\ rate: &\quad R(t,X) = R_0 + R_1 \cdot X \ \text{ for } \ (R_0, R_1) \in \mathbb{R} \times \mathbb{R}^n
\end{aligned} \tag{1.2}$$

A more formal definition of affine process X_t can be found in Duffie et al. (2003), where a (regular) affine process is characterized in three equivalent ways: stating the form of its infinitesimal generator $\mathcal{A}$ (Theorem 2.7), giving the expression for its characteristic triplet (Theorem 2.12) and requiring the infinite decomposability property of its associated distribution (Theorem 2.15). In particular, the previous requirements corresponds to their characterization of *admissible* parameters, as given in their Definition 2.6. In this thesis we will deal in particular with 3-dimensional state vectors X_t consisting of log-price x_t and two volatility factors $\sigma^2_{i,t}$, as:

$$X_t = \begin{pmatrix} x_t \\ \sigma^2_{1,t} \\ \sigma^2_{2,t} \end{pmatrix} \tag{1.3}$$

or eventually permutations of these components. According to the specification analysis developed in Dai and Singleton (2000), under some non-degeneracy conditions and a possible reordering of indices (associated to a permutation of the components of the state vector), it is sufficient for affinity of the diffusion (1.1) that the volatility matrix $\sigma(t,X)$ is of the following *canonical* form:

$$\sigma(t,X)_{n\times n} = \Sigma_{n\times n}\sqrt{V}_{n\times n} = \Sigma_{n\times n} \begin{pmatrix} \sqrt{V_1(X)} & 0 & \cdots & 0 \\ 0 & \sqrt{V_2(X)} & \cdots & 0 \\ \vdots & \vdots & \ddots & \vdots \\ 0 & 0 & \cdots & \sqrt{V_n(X)} \end{pmatrix} \tag{1.4}$$

where $\Sigma, V \in \mathcal{M}_{n\times n}$ with $V_{ii} = V_i(X) = a_i + b_i \cdot X$, with $a_i \in \mathbb{R}$ and $b_i \in \mathbb{R}^n$. This sufficient conditions have been extended by Collin-Dufresne et al. (2008) and Cheridito et al. (2010) to allow for the possibility of a number m of independent

Wiener processes possibly greater than the number of state variables $n \leq m$:

$$\sigma(t,X)_{n\times m} = \Sigma_{n\times m}\sqrt{V}_{m\times m} = \Sigma_{n\times m}\begin{pmatrix} \sqrt{V_1(X)} & 0 & \cdots & 0 \\ 0 & \sqrt{V_2(X)} & \cdots & 0 \\ \vdots & \vdots & \ddots & \vdots \\ 0 & 0 & \cdots & \sqrt{V_m(X)} \end{pmatrix} \tag{1.5}$$

where $\Sigma \in \mathcal{M}_{n\times m}$ ($n \leq m$) and $V \in \mathcal{M}_{m\times m}$, with diagonal elements defined as before. The *extended canonical* form (1.5) is not the most general condition, but in the present contest it will be sufficient. Indeed, we will consider only affine models in which the state vector's components follow only CIR (Cox et al., 1985) diffusions (+ jumps) and no Gaussian components will be present (Cheridito et al., 2010; Collin-Dufresne et al., 2008).
At any time $t \in [0,T]$ the distribution of X_t, as well as the effects of any discounting, is described by the *characteristic* $\chi(K,H,\lambda,\text{jumps},R)$ w.r.t. which expectations are taken. A *generalized* transform is introduced ($u = (u_1,...,u_n)^T$)

$$\Psi^{\chi}(u,X_t,t,T) = E^{\chi}\left[exp\left(-\int_t^T R(s,X_s)ds\right)e^{u\cdot X_T} \;\middle|\; \mathcal{F}_t\right] \tag{1.6}$$

where $u \in \mathbb{C}^n$ which, for affine processes, may be expressed in the familiar exponential-affine form (Duffie et al., 2000, Prop. 1):

$$\Psi^{\chi}(u,X_t,t,T) = e^{\alpha(t)+\beta(t)\cdot X_t} \tag{1.7}$$

where $\alpha(t)$ and each component $\beta_k(t)$ ($k = 1,...,n$) of $\beta(t)$ solve the set of equations:

$$\dot{\alpha}(t) = \rho_0 - K_0^{\top}\beta - \frac{1}{2}\beta^T H_0\beta - \lambda_0\left(\theta(\beta)-1\right) \tag{1.8}$$

$$\dot{\beta}_k(t) = \rho_1 - K_1^T\beta - \frac{1}{2}\sum_{i,j=1}^{n}\beta_i(H_1^{(k)})_{ij}\beta_j - \lambda_1\left(\theta(\beta)-1\right) \tag{1.9}$$

with terminal conditions:

$$\alpha(T) = 0 \tag{1.10}$$

$$\beta(T) = u \tag{1.11}$$

This can be proved by applying Ito's lemma to find $d\Psi^{\chi}(X_t)$, with dX_t given as in (1.1). Unless jump intensities are constant ($\lambda(t,X_t) \equiv \lambda_0$), equations (1.9) are coupled, with different components of β mixed. Therefore α and β will have the following dependencies in general:

$$\alpha = \alpha(t,T,u = (u_1,...,u_n)^T) \tag{1.12}$$

$$\beta_k = \beta_k(t,T,u = (u_1,...,u_n)^T) \tag{1.13}$$

Function $\theta(c)$, which is in fact the moment generating function of jump amplitudes Z, is called *jump transform*:

$$\theta(c) = \int_{\Omega} e^{c \cdot Z} d\nu(Z) \tag{1.14}$$

with $c = (c_1, c_2, ..., c_n)^T \in \mathbb{C}^n$, $\Omega \subseteq \mathbb{R}^n$ and $\nu(Z = (z_1, z_2..., z_n)^T)$ denoting the multivariate jump-size distribution under the measure associated to χ. The first component z_1 will usually denotes the jump-size of the log-price and c_1 its conjugated variable, whereas z_i and c_i, with $i > 1$, are associated with volatility factors.[1]

The *payoff function* $G_{a,b}(\cdot)$, $a, b \in \mathbb{R}^n$, $y \in \mathbb{R}$ is introduced as follows

$$G_{a,b}(y, X_t, t, T, \chi) = E^{\chi}\left[exp\left(-\int_t^T R(s, X_s)ds\right) e^{a \cdot X_T} \mathcal{I}_{b \cdot X_T \leq y}\right] \tag{1.15}$$

which has a clear pricing interpretation if the chosen measure is the risk-neutral one ($\chi = \chi_{\mathbb{Q}}$): $G_{a,b}(y, X_t, t, T, \chi_{\mathbb{Q}})$ is the price at time t of a claim which pays at time T the amount $e^{a \cdot X_T}$ if the claim is in-the-money at time T (that is if $b \cdot X_T \leq y$).

1.2 Pricing

From (1.15), it is clear that the risk-neutral evaluation of the price at time t of an European call option (of maturity T and strike: K) may be written in the log-price $x_t = \log S_t$ as ($\epsilon(1)_i = 1$ if $i = 1$ and 0 otherwise)

$$\begin{aligned} C(t, T, K) &= E^{\mathbb{Q}}\left[exp\left(-\int_t^T R(s, X_s)ds\right)(e^{x_T} - K)^+\right] \\ &= G_{\epsilon(1), -\epsilon(1)}(-\log K, X_t, T, \chi_{\mathbb{Q}}) - K G_{0, -\epsilon(1)}(-\log K, X_t, T, \chi_{\mathbb{Q}}) \end{aligned} \tag{1.16}$$

where $(x)^+ = max(x, 0)$.[2] Interestingly, they found a closed-form expression for $G_{a,b}(y)$ in terms of the Ψ^{χ} transform, via inversion of its Fourier transform $\mathcal{G}_{a,b}(z)$:

$$G_{a,b}(y, X_t, t, T, \chi) = \frac{\Psi^{\chi}(a, X_t, t, T)}{2} - \frac{1}{\pi}\int_0^{\infty} \frac{\text{Im}\left[e^{-izy}\Psi^{\chi}(a + izb, X_t, t, T)\right]}{z} dz \tag{1.17}$$

Proof. Given in (Duffie et al., 2000, App. A). □

[1] Unless a permutation of indexes has been performed.

[2] This expression must be changed in case permutations of the components of X_t apply: $\epsilon(1)$ have to be replaced by $\epsilon(i)$ if the i-th component of X_t is the log-price x_t.

This last expression allows to give a closed-form expression for the price of a large class of securities in which the state process is an AJD.
In this Section we will elaborate on the connection between the Duffie et al. (2000) generalized transform and payoff function on a side, and on the S-martingale and T-forward measures and characteristic functions of the general option pricing formula of Geman et al. (1994) on the other side. We start with a simple Lemma concerning change of numeraire transformations. We will state it as a Lemma to be self-contained in the present exposition, but it is in fact a manipulation of (Geman et al., 1994, Corollay 2 of Theorem 1) and the notation is borrowed from Björk (Bjork, 1998, Prop. 26.4).

Lemma 1. *Assume that there exist two equivalent (on $\mathcal{F}_T$) martingale measures $\mathbb{Q}^0$ and $\mathbb{Q}^1$, whose associated numeraire processes are S_0 and S_1, respectively. Then, the likelihood process $L_0^1(t)$ of the change of numeraire transformation $\mathbb{Q}^0 \to \mathbb{Q}^1$ verifies:*

$$\frac{S_0(t)}{S_0(T)} = \frac{S_1(t)}{S_1(T)} \cdot \frac{L_0^1(T)}{E^{\mathbb{Q}^0}\Big[L_0^1(T)|\mathcal{F}_t\Big]} \quad 0 \le t \le T \tag{1.18}$$

Proof. According to (Geman et al., 1994, Cor. 2), the likelihood process $L_0^1(t)$ defined in (Bjork, 1998, Eq. 26.18) and recalled here ($0 \le t \le T$) takes the form

$$L_0^1(t) = \frac{S_0(0)}{S_1(0)} \frac{S_1(t)}{S_0(t)} \tag{1.19}$$

Therefore

$$\frac{S_0(t)}{S_0(T)} = \frac{S_1(t)}{S_1(T)} \frac{L_0^1(T)}{L_0^1(t)} \tag{1.20}$$

and thus the thesis holds since $L_0^1(t)$, as defined in (1.19), is a $\mathbb{Q}^0$-martingale. □

We will make use of this Lemma in order to connect, via the Abstract Bayes' Formula (Bjork, 1998, Prop. B.41), expectations under a given $\mathbb{Q}^0$ measure with those under an *ad hoc* chosen $\mathbb{Q}^1$ measure. The general context of application is illustrated in the following $\mathbb{Q}^0$-compound expectation of the variable $\mathcal{X}$:

$$E^{\mathbb{Q}^0}\Big[\frac{S_0(t)}{S_0(T)} \cdot \mathcal{X}|\mathcal{F}_t\Big] = \frac{E^{\mathbb{Q}^0}\Big[\frac{S_1(t)}{S_1(T)} \cdot \mathcal{X} L_0^1(T)|\mathcal{F}_t\Big]}{E^{\mathbb{Q}^0}\Big[L_0^1(T)|\mathcal{F}_t\Big]} = E^{\mathbb{Q}^1}\Big[\frac{S_1(t)}{S_1(T)} \cdot \mathcal{X}|\mathcal{F}_t\Big] \tag{1.21}$$

We will specialize Lemma 1 to transformations of the risk-neutral measure $\mathbb{Q}^0 = \mathbb{Q}$, which is the martingale measure associated to the riskless money account

$$B(t) = B(0) exp\Big(\int_0^t R(s, X_s) ds\Big) \tag{1.22}$$

where we have defined the (possibly stochastic) short rate consistently with the AJD notation above. In particular, we will consider, as *ad hoc* $\mathbb{Q}^1$ measures, the following two equivalent martingale measures:

- *S-martingale measure,* $\mathbb{Q}^S$: whose associated numeraire is the price process $S(t)$ of the asset and, according to definition (1.19), the likelihood process $L^S(t)$, $0 \leq t \leq T$ of the change of numeraire transformation $\mathbb{Q} \to \mathbb{Q}^S$ is

$$L^S(t) = \frac{B(0)}{S(0)} \frac{S(t)}{B(t)} \tag{1.23}$$

- *T-forward measure,* $\mathbb{Q}^T$: whose associated numeraire is the price process of a zero-coupon bond maturing at time T

$$p(t,T) = E^{\mathbb{Q}}\Big[\frac{B(t)}{B(T)}|\mathcal{F}_t\Big] \tag{1.24}$$

  which is worth $p(T,T) = 1$ at maturity. Correspondingly, the likelihood process $L^T(t)$, $0 \leq t \leq T$ of the change of numeraire transformation $\mathbb{Q} \to \mathbb{Q}^T$ takes the form

$$L^T(t) = \frac{B(0)}{p(0,T)} \frac{p(t,T)}{B(t)} \tag{1.25}$$

Corollary 1. *Consider the risk-neutral measure ($\mathbb{Q}$) and the equivalent (on $\mathcal{F}_T$) martingale measures S-martingale ($\mathbb{Q}^S$) and T-forward ($\mathbb{Q}^T$). Then the discounting factor may be expressed as follows ($0 \leq t \leq T$):*

$$exp\Big(-\int_t^T R(s,X_s)ds\Big) = \begin{cases} \dfrac{S(t)}{S(T)} \cdot \dfrac{L^S(T)}{E^{\mathbb{Q}}[L^S(T)|\mathcal{F}_t]} & \text{if } \mathbb{Q} \to \mathbb{Q}^S \\ p(t,T) \cdot \dfrac{L^T(T)}{E^{\mathbb{Q}}[L^T(T)|\mathcal{F}_t]} & \text{if } \mathbb{Q} \to \mathbb{Q}^T \end{cases} \tag{1.26}$$

Proof. Straightforward from the definition of riskless money account (1.22) and specializing Lemma 1 to the likelihood processes $L^S(t)$ and $L^T(t)$ in (1.23) and (1.25). □

Corollary 1 will be needed in order to relate the risk-neutral specification $\Psi^{\chi_{\mathbb{Q}}}$ of the generalized transform[3] (defined in (1.6))

$$\Psi^{\chi_{\mathbb{Q}}}(u, X_t, t, T) = E^{\mathbb{Q}}\left[exp\left(-\int_t^T R(s,X_s)ds\right) e^{u \cdot X_T} \;\middle|\; \mathcal{F}_t\right] \tag{1.27}$$

[3]Under $\mathbb{Q}$, χ is $\chi_{\mathbb{Q}}$ and note that $E^{\chi_{\mathbb{Q}}}[\cdot]$ has exactly the same meaning of $E^{\mathbb{Q}}[\cdot]$, so we have preferred the latter notation, which is more familiar to every body.

of the state vector process X_t with its characteristic functions under the S-martingale and T-forward measures, as presented in the following Proposition 1. Let us first introduce the conditional characteristic functions of the log-price process x_t at time T under $\mathbb{Q}^S$ and $\mathbb{Q}^T$, respectively:

$$f_1(z;X_t) = E^{\mathbb{Q}^S}\left[e^{izx_T}|\mathcal{F}_t\right] \tag{1.28}$$

$$f_2(z;X_t) = E^{\mathbb{Q}^T}\left[e^{izx_T}|\mathcal{F}_t\right] \tag{1.29}$$

where the dependencies on the entire state vector process $X_t = (x_t, \sigma^2_{1,t}, \sigma^2_{2,t}, ...)^T$ is in general legitimate. These can be extended to the entire process n-dimensional X_t process (at time T) as follows:

$$F_1(z;X_t) = E^{\mathbb{Q}^S}\left[e^{iz\cdot X_T}|\mathcal{F}_t\right] \tag{1.30}$$

$$F_2(z;X_t) = E^{\mathbb{Q}^T}\left[e^{iz\cdot X_T}|\mathcal{F}_t\right] \tag{1.31}$$

We have not change notation as it should be clear by the context, but to be crystal-clear: in (1.28) and (1.29) the Fourier variable is $z \in \mathbb{R}$, whereas in the general versions (1.30) and (1.31) it is $z \in \mathbb{R}^n$.

Proposition 1. *Consider the risk-neutral measure ($\mathbb{Q}$) and the equivalent (on $\mathcal{F}_T$) martingale measures S-martingale ($\mathbb{Q}^S$) and T-forward ($\mathbb{Q}^T$). Then, the risk-neutral specification $\Psi^{\chi_\mathbb{Q}}$ (1.27) of the generalized transform Ψ^χ (1.6) may be expressed as follows ($u \in \mathbb{C}^n$):*

$$\Psi^{\chi_\mathbb{Q}}(u, X_t, t, T) = \begin{cases} S(t)E^{\mathbb{Q}^S}\left[\dfrac{e^{u\cdot X_T}}{S(T)}|\mathcal{F}_t\right] \\ p(t,T)E^{\mathbb{Q}^T}\left[e^{u\cdot X_T}|\mathcal{F}_t\right] \end{cases} \tag{1.32}$$

at any time $0 \le t \le T$. Moreover, expressing $u = \mathrm{Re}(u) + i\,\mathrm{Im}(u)$, with $\mathrm{Re}(u), \mathrm{Im}(u) \in \mathbb{R}^n$, we have in particular:

- *if the log-price x_t is the i-th component of X_t and if $\mathrm{Re}(u) = \epsilon(i)$, then $\Psi^{\chi_\mathbb{Q}}$ verifies:*

$$\Psi^{\chi_\mathbb{Q}}\Big(\epsilon(i) + i\,\mathrm{Im}(u), X_t, t, T\Big) = S(t)F_1\Big(\mathrm{Im}(u); X_t\Big) \tag{1.33}$$

  where the X_T conditional characteristic function (w.r.t. $\mathbb{Q}^S$) $F_1(z;X_t)$ is defined as in (1.30).

- *if evaluated on the pure-imaginary sub-space $u = i\,\mathrm{Im}(u)$, $\Psi^{\chi_{\mathbb{Q}}}$ verifies:*

$$\Psi^{\chi_{\mathbb{Q}}}\Big(i\,\mathrm{Im}(u), X_t, t, T\Big) = p(t,T)F_2\Big(\mathrm{Im}(u); X_t\Big) \tag{1.34}$$

where the X_T conditional characteristic function (w.r.t. $\mathbb{Q}^T$) $F_2(z; X_t)$ is defined as in (1.31).

These results are invariant under permutations of the components of the state vector X_t.

Proof. By definition (1.27) of $\Psi^{\chi_{\mathbb{Q}}}$, applying the first of (1.26), we get:

$$\begin{aligned}
\Psi^{\chi_{\mathbb{Q}}}(u, X_t, t, T) &= \frac{E^{\mathbb{Q}}\left[\frac{S(t)}{S(T)} e^{u\cdot X_T} L^S(T)|\mathcal{F}_t\right]}{E^{\mathbb{Q}}\Big[L^S(T)|\mathcal{F}_t\Big]} \\
&= E^{\mathbb{Q}^S}\left[\frac{S(t)}{S(T)} e^{u\cdot X_T}|\mathcal{F}_t\right] \\
&= S(t)E^{\mathbb{Q}^S}\left[\frac{e^{u\cdot X_T}}{S(T)}|\mathcal{F}_t\right]
\end{aligned} \tag{1.35}$$

which is the first of (1.32). Last equality holds since the asset price $S(t)$ at time t is $\mathcal{F}_t$-measurable. Concerning with the second of (1.32), considering again (1.27) and the second of (1.26), we get:

$$\begin{aligned}
\Psi^{\chi_{\mathbb{Q}}}(u, X_t, t, T) &= \frac{E^{\mathbb{Q}}\Big[p(t,T)e^{u\cdot X_T} L^T(T)|\mathcal{F}_t\Big]}{E^{\mathbb{Q}}\Big[L^T(T)|\mathcal{F}_t\Big]} \\
&= E^{\mathbb{Q}^T}\Big[p(t,T)e^{u\cdot X_T}|\mathcal{F}_t\Big] \\
&= p(t,T)E^{\mathbb{Q}^T}\Big[e^{u\cdot X_T}|\mathcal{F}_t\Big]
\end{aligned} \tag{1.36}$$

where last equality holds as the zero-coupon bond price $p(t,T)$ at time t is $\mathcal{F}_t$-measurable.
Equations (1.33) and (1.34) are particular cases of (1.32) and are obtained expressing $u \in \mathbb{C}^n$ as $u = \mathrm{Re}(u) + i\,\mathrm{Im}(u)$, exploiting conditions on real/imaginary parts and substituting definitions (1.30) and (1.31) into (1.42) and (1.43), respectively. The invariance under permutations is achieved since equations (1.32), as well as the condition resulting into the (1.34), concern only scalar products[4]; moreover

[4]The scalar product is unaffected by the same reshuffling of the components of the vectors involved in the product. If the reshuffled vectors have the form $x' = \pi x$, then since the *permutation* matrix π must be unitary (in the present Real context it is simply orthogonal):

$$x' \cdot y' = (\pi x)\cdot(\pi y) = (\pi^T \pi x)\cdot y = (\pi^{-1}\pi x)\cdot y = x \cdot y. \tag{1.37}$$

the condition $\mathrm{Re}(u) = \epsilon(i)$, resulting into the (1.33), accounts explicitly for any possible reshuffling of the components of X_t. □

Dealing with (risk-neutral) pricing evaluation of an European call option (1.16), we will have to evaluate the payoff function $G_{a,b}(y)$ with 1-dimensional specifications of vectors a and b. Thus the vector $u \in \mathbb{C}^n$ (on which the $\Psi^{\chi_{\mathbb{Q}}}$ transform have to be evaluated), will have only one nonzero component, the first one or - if permutations of X_t apply - the one corresponding to the log-price component x_t.

The following Corollary of Proposition 1 provides a match of the relevant-for-pricing evaluation of the generalized transform Ψ^{χ} of Duffie et al. (2000), with the conditional characteristic functions associated to the S-martingale and T-forward distributions of the log-price appearing in the general option pricing formula (Geman et al., 1994, Th. 2).

Corollary 2. *Consider the setting of Proposition (1) and in particular if the log-price x_t is the i-th component of X_t. Then:*

- *if $\mathrm{Re}(u) = \epsilon(i)$ and $\mathrm{Im}(u) = z\epsilon(i)$, then $\Psi^{\chi_{\mathbb{Q}}}$ verifies:*

$$\Psi^{\chi_{\mathbb{Q}}}\Big(\epsilon(i) + iz\epsilon(i), X_t, t, T\Big) = S(t) f_1(z; X_t) \tag{1.38}$$

  where the conditional characteristic function $f_1(z; X_t)$ (w.r.t. $\mathbb{Q}^S$) of the log-price x_T is defined as in (1.28).

- *if $\mathrm{Im}(u) = z\epsilon(i)$, then $\Psi^{\chi_{\mathbb{Q}}}$ verifies:*

$$\Psi^{\chi_{\mathbb{Q}}}\Big(iz\epsilon(i), X_t, t, T\Big) = p(t,T) f_2(z; X_t) \tag{1.39}$$

  where the conditional characteristic function $f_2(z; X_t)$ (w.r.t. $\mathbb{Q}^T$) of the log-price x_T is defined as in (1.29).

These results are invariant under permutations of the components of the state vector X_t.

Proof. From definitions (1.28) and (1.29) of the log-price characteristic functions, equations (1.38) and (1.39) are straightforward specializations of (1.32) (first and the second, respectively). The invariance w.r.t. permutations of the components of the state vector X_t is explicitly accounted in the $\epsilon(i)$ notation. □

The following Proposition for the risk-neutral specification of the payoff function

$$G_{a,b}(y, X_t, t, T, \chi_{\mathbb{Q}}) = E^{\mathbb{Q}}\left[exp\left(-\int_t^T R(s, X_s)ds\right) e^{a\cdot X_T} \mathcal{I}_{b\cdot X_T \leq y}\right] \tag{1.40}$$

parallels equations (1.32) of Proposition (1) for the generalized transform $\Psi^{\chi_{\mathbb{Q}}}$.

Proposition 2. *Consider the risk-neutral measure (Q) and the equivalent (on $\mathcal{F}_T$) martingale measures S-martingale (Q^S) and T-forward (Q^T). Then, the risk-neutral specification (1.40) of the payoff function (1.15) may be expressed as follows ($a, b \in \mathbb{R}^n$, $y \in \mathbb{R}$):*

$$G_{a,b}(y, X_t, t, T, \chi_{\mathbb{Q}}) = \begin{cases} S(t)E^{Q^S}\left[\dfrac{e^{a\cdot X_T}}{S(T)}\mathcal{I}_{b\cdot X_T \le y}|\mathcal{F}_t\right] \\ p(t,T)E^{Q^T}\left[e^{a\cdot X_T}\mathcal{I}_{b\cdot X_T \le y}|\mathcal{F}_t\right] \end{cases} \tag{1.41}$$

These results are invariant under permutations of the components of the state vector X_t.

Proof. The proof is an application of Lemma 1. From the risk-neutral specification (1.40) of $G_{a,b}$ and applying the first of (1.26), we get:

$$\begin{aligned} G_{a,b}(y, X_t, t, T, \chi_{\mathbb{Q}}) &= \frac{E^{\mathbb{Q}}\left[\frac{S(t)}{S(T)}e^{a\cdot X_T}\mathcal{I}_{b\cdot X_T \le y}L^S(T)|\mathcal{F}_t\right]}{E^{\mathbb{Q}}\left[L^S(T)|\mathcal{F}_t\right]} \\ &= E^{Q^S}\left[\frac{S(t)}{S(T)}e^{a\cdot X_T}\mathcal{I}_{b\cdot X_T \le y}|\mathcal{F}_t\right] \\ &= S(t)E^{Q^S}\left[\frac{e^{a\cdot X_T}}{S(T)}\mathcal{I}_{b\cdot X_T \le y}|\mathcal{F}_t\right] \end{aligned} \tag{1.42}$$

which is the first of (1.41). Last equality holds since the asset price $S(t)$ at time t is $\mathcal{F}_t$-measurable. Concerning with the second of (1.41), considering again (1.40) and the second of (1.26), we get:

$$\begin{aligned} G_{a,b}(y, X_t, t, T, \chi_{\mathbb{Q}}) &= \frac{E^{\mathbb{Q}}\left[p(t,T)e^{a\cdot X_T}\mathcal{I}_{b\cdot X_T \le y}L^T(T)|\mathcal{F}_t\right]}{E^{\mathbb{Q}}\left[L^T(T)|\mathcal{F}_t\right]} \\ &= E^{Q^T}\left[p(t,T)e^{a\cdot X_T}\mathcal{I}_{b\cdot X_T \le y}|\mathcal{F}_t\right] \\ &= p(t,T)E^{Q^T}\left[e^{a\cdot X_T}\mathcal{I}_{b\cdot X_T \le y}|\mathcal{F}_t\right] \end{aligned} \tag{1.43}$$

where last equality holds as the zero-coupon bond price $p(t,T)$ at time t is $\mathcal{F}_t$-measurable. The invariance under permutations holds since equations (1.41) involve only scalar products. □

From the risk-neutral evaluation (1.16) of the price of an European call, if the

log-price x_t is the i-th component of X_t, then it becomes:

$$\begin{aligned} C(t,T,K) &= E^{\mathbb{Q}}\left[exp\left(-\int_t^T R(s,X_s)ds\right)(S(T)-K)^+\right] \\ &= G_{\epsilon(i),-\epsilon(i)}(-\log K, X_t, T, \chi_{\mathbb{Q}}) - KG_{0,-\epsilon(i)}(-\log K, X_t, T, \chi_{\mathbb{Q}}) \end{aligned} \tag{1.44}$$

As it represents a price, whose numerical value must be independent from the specific evaluation setting, equation (1.44) must coincide with the general option pricing formula given in Theorem 2 of Geman et al. (1994)

$$C(t,T,K) = S(t)Q^S\Big(S(T)\geq K\Big) - Kp(t,T)Q^T\Big(S(T)\geq K\Big) \tag{1.45}$$

which is written in its general formulation, allowing for the possibility of a stochastic short rate R. The next Corollary to Proposition 8 closes the circle, as it states the correspondence between the risk-neutral pricing formula in the DPS setting and the general one of GKR. It parallels Corollary 2, which links the generalized transform under Q with the characteristic functions under Q^S and Q^T.

Proposition 3. *Consider the setting of Proposition (8). In particular if the log-price x_t is the i-th component of X_t. Then:*

$$G_{\epsilon(i),-\epsilon(i)}(-\log K, X_t, T, \chi_{\mathbb{Q}}) = S(t)Q^S\Big(S(T)\geq K\Big) \tag{1.46}$$

$$G_{0,-\epsilon(i)}(-\log K, X_t, T, \chi_{\mathbb{Q}}) = p(t,T)Q^T\Big(S(T)\geq K\Big) \tag{1.47}$$

These results are invariant under permutations of the components of the state vector X_t.

Proof. Equations (1.46) and (1.47) are straightforward specializations of (1.41) (first and the second, respectively). The invariance w.r.t. permutations of the components of the state vector X_t is explicitly accounted in the $\epsilon(i)$ notation.

In the context of GKR, once the characteristic functions (1.28) and (1.29) have been found, the pricing formula (1.45) can be explicitly (numerically) evaluated as follows:

$$Q^S\Big(S(T)\geq K\Big) = \frac{1}{2} + \frac{1}{\pi}\int_0^\infty \mathrm{Re}\left[\frac{e^{-iz\log(K)}f_1(z;X_t)}{iz}\right]dz \tag{1.48}$$

$$Q^T\Big(S(T)\geq K\Big) = \frac{1}{2} + \frac{1}{\pi}\int_0^\infty \mathrm{Re}\left[\frac{e^{-iz\log(K)}f_2(z;X_t)}{iz}\right]dz \tag{1.49}$$

whereas, recalling the expression in (1.17) for $G_{a,b}$, in the Duffie, Pan and Singleton setting the pricing formula (1.44) lead us to evaluate the following integrals (if

the log-price is the i-th component of X_t):

$$G_{\epsilon(i),-\epsilon(i)}(-\log K, X_t, T, \chi_{\mathbb{Q}}) = \frac{\Psi^{\chi_{\mathbb{Q}}}(\epsilon(i))}{2} - \frac{1}{\pi}\int_0^\infty \frac{\operatorname{Im}\left[e^{iz\log(K)}\Psi^{\chi_{\mathbb{Q}}}(\epsilon(i) - iz\epsilon(i))\right]}{z} dz \tag{1.50}$$

$$G_{0,-\epsilon(i)}(-\log K, X_t, T, \chi_{\mathbb{Q}}) = \frac{\Psi^{\chi_{\mathbb{Q}}}(\mathbf{0})}{2} - \frac{1}{\pi}\int_0^\infty \frac{\operatorname{Im}\left[e^{iz\log(K)}\Psi^{\chi_{\mathbb{Q}}}(-iz\epsilon(i))\right]}{z} dz \tag{1.51}$$

where $\mathbf{0}$ is a n-vector of zeros. In order to prove (1.46) and (1.47) we can demonstrate that the integral expressions (1.50) and (1.51) in fact coincides with (1.48) and (1.49) respectively. And this is indeed the case, thanks to Corollary 2. Observe that for any complex valued function[5] $g : \mathbb{C} \to \mathbb{C}$ we have $\operatorname{Im}(g(z)) = \operatorname{Re}(g(z)/i)$ and $\operatorname{Im}(z) = -\operatorname{Im}(z^*)\ \forall z \in \mathbb{C}$. Moreover, recalling the definition (1.6), under complex conjugation (denoted with the $*$):

$$\begin{aligned}
\Psi^{\chi*}(u, X_t, t, T) =& \Psi^{\chi*}(\operatorname{Re}(u) + i\operatorname{Im}(u), X_t, t, T) && (1.52)\\
=& \Psi^{\chi}(\operatorname{Re}(u) - i\operatorname{Im}(u), X_t, t, T) && (1.53)\\
=& \Psi^{\chi}(u^*, X_t, t, T) && (1.54)
\end{aligned}$$

This lead us to (only relevant dependencies written explicitly):

$$\begin{aligned}
G_{a,b}(y) &= \frac{\Psi^{\chi}(a)}{2} - \frac{1}{\pi}\int_0^\infty \frac{\operatorname{Im}\left[e^{-izy}\Psi(a+izb)\right]}{z} dz\\
&= \frac{\Psi^{\chi}(a)}{2} + \frac{1}{\pi}\int_0^\infty \frac{\operatorname{Im}\left[e^{izy}\Psi^*(a+izb)\right]}{z} dz\\
&= \frac{\Psi^{\chi}(a)}{2} + \frac{1}{\pi}\int_0^\infty \operatorname{Re}\left[\frac{e^{izy}\Psi^*(a+izb)}{iz}\right] dz\\
&= \frac{\Psi^{\chi}(a)}{2} + \frac{1}{\pi}\int_0^\infty \operatorname{Re}\left[\frac{e^{izy}\Psi(a-izb)}{iz}\right] dz
\end{aligned} \tag{1.55}$$

In addition we observe that:

$$\Psi^{\chi_{\mathbb{Q}}}(\epsilon(i), X_t, t, T) \overset{1.33}{=} S(t) \tag{1.56}$$

$$\Psi^{\chi_{\mathbb{Q}}}(\mathbf{0}, X_t, t, T) \overset{1.34}{=} p(t, T) \tag{1.57}$$

[5] and thus *a fortiori* this holds for a real-valued one

Therefore, beginning with (1.50), we have:

$$\begin{aligned}
G_{\epsilon(i),-\epsilon(i)}(-\log K, X_t, T, \chi_{\mathbb{Q}}) =& \frac{\Psi^{\chi_{\mathbb{Q}}}(\epsilon(i))}{2} - \frac{1}{\pi}\int_0^\infty \frac{\operatorname{Im}\left[e^{iz\log(K)}\Psi^{\chi_{\mathbb{Q}}}(\epsilon(i) - iz\epsilon(i))\right]}{z} dz \\
\overset{1.55}{=}& \frac{\Psi^{\chi_{\mathbb{Q}}}(\epsilon(i))}{2} + \frac{1}{\pi}\int_0^\infty \operatorname{Re}\left[\frac{e^{-iz\log(K)}\Psi^{\chi_{\mathbb{Q}}}(\epsilon(i) + iz\epsilon(i))}{iz}\right] dz \\
\overset{1.38,1.56}{=}& S(t)\left\{\frac{1}{2} + \frac{1}{\pi}\int_0^\infty \operatorname{Re}\left[\frac{e^{-iz\log(K)}f_1(x; X_t)}{iz}\right] dz\right\} \\
\overset{1.48}{=}& S(t)Q^S\Big(S(T) \geq K\Big)
\end{aligned} \tag{1.58}$$

and for (1.51) we have

$$\begin{aligned}
G_{0,-\epsilon(i)}(-\log K, X_t, T, \chi_{\mathbb{Q}}) =& \frac{\Psi^{\chi_{\mathbb{Q}}}(\mathbf{0})}{2} - \frac{1}{\pi}\int_0^\infty \frac{\operatorname{Im}\left[e^{iz\log(K)}\Psi^{\chi_{\mathbb{Q}}}(-iz\epsilon(i))\right]}{z} dz \\
\overset{1.55}{=}& \frac{\Psi^{\chi_{\mathbb{Q}}}(\mathbf{0})}{2} + \frac{1}{\pi}\int_0^\infty \operatorname{Re}\left[\frac{e^{-iz\log(K)}\Psi^{\chi_{\mathbb{Q}}}(iz\epsilon(i))}{iz}\right] dz \\
\overset{1.39,1.57}{=}& p(t,T)\left\{\frac{1}{2} + \frac{1}{\pi}\int_0^\infty \operatorname{Re}\left[\frac{e^{-iz\log(K)}f_2(x; X_t)}{iz}\right] dz\right\} \\
\overset{1.49}{=}& p(t,T)Q^T\Big(S(T) \geq K\Big)
\end{aligned} \tag{1.59}$$

□

Chapter 2

VIX and VIX derivatives

The growing demand for trading volatility and managing volatility risk has lead today to a liquid market for derivative securities whose payoff is explicitly determined by the volatility of some underlying. Derivatives of this kind are generically referred to as volatility derivatives and include, among many, variance swaps, futures and options written on a volatility index known as VIX (Carr and Lee, 2009).

Variance swaps were the first volatility derivatives traded in the over-the-counter (OTC) market, dating back to the first half of the 80s. These are swap contracts with zero upfront premium and a single payment at expiration in which the long side pays a positive dollar amount, the variance swap rate, agreed upon at inception. In front of this fixed payment, the short side agrees to pay the annualized average of squared daily logarithmic returns of an underlying index. The amount paid by the floating leg is usually called realized variance.

By the end of 1998, both practitioner and academic works had already suggested that variance swaps can be accurately replicated by a strip of out-of-the-money (OTM) vanilla options (Britten-Jones and Neuberger, 2000; Demeterfi et al., 1999). The high implied volatilities experienced in that years contributed to the definitive take off of these instruments, with hedge funds taking short positions in variance and banks, on the other side, buying it and contextually selling and delta-hedging the variance replicating strip.

With the 2000s, the OTC market for volatility kept increasing, with several innovative contracts introduced, such as options on realized variance, conditional and corridor variance swaps[1] in 2005, and timer options[2] in 2007.

[1] These are swaps in which the floating leg pays the variance realized only during days in which a condition is satisfied by the return process. The exact specification of the payout of these swaps differs from firm to firm (Allen et al., 2006; Carr and Lewis, 2004).

[2] Exotic options whose maturity is a random stopping time, corresponding to a known amount of

On the exchanges side of the market, the Chicago Board Options Exchange (CBOE) introduced in 1993 the VIX volatility index. In an early formulation, the volatility index - today known as VXO - was an average of the Black and Scholes (1973) implied volatility of eight near term OEX American options (calls and puts on the S&P100 index).

In 2003, CBOE completely revised the definition of VIX index under several aspects: the underlying index was switched to be the S&P500 (SPX) and the flat implied volatility methodology of Black and Scholes (1973) was left in favor of a robust replication of the variance swap rate Exchange (2009), in the footprints of results in the literature (Britten-Jones and Neuberger, 2000; Carr and Madan, 2001; Demeterfi et al., 1999). The market definition of VIX will be presented in the next Section.

Derivatives written on VIX index were introduced in the second half of 2000s: VIX futures in 2004 and VIX options in 2006. Their popularity stems from the well-known negative correlation between VIX and SPX index, which made these instruments a widely accepted asset class for trading, diversifying and hedging. In this respect, SPX and VIX indexes, together with options on both markets, provide a valuable source of information to better specify and understand the dynamics of volatility.

This has lead to the need of a framework for consistent pricing volatility derivatives and derivatives on the underlying, that is the need to design models able to fit the observed cross-section of option prices of both markets and properly price and hedge exotic products.

The present chapter is organized as follows: next Section introduces the CBOE VIX index, whereas derivatives written on it are presented in sections 2.1.2 and 2.1.3. Market definitions and the unique empirical properties of VIX futures and options, which make volatility a peculiar asset class, are therein discussed. Section 2.2 is an account of the academic and practitioner contributions to VIX and VIX derivatives literature. In particular, *standalone* and *consistent* approaches are distinguished and respectively reviewed in sections 2.2.1 an 2.2.2. The first approach models the VIX index as a separated independent process, whilst the latter derives it from a model for the S&P500 returns.

2.1 Markets: definitions and empirical facts

2.1.1 VIX Index

The VIX volatility index measures the 30-day expected volatility of the S&P500 index (Exchange, 2009). It is computed by CBOE as a model-free replication of

cumulated realized volatility being surpassed; product of this kind had been popularized by Société Générale Corporate and Investment Banking (SC BIC).

the realized variance over the following $T = 30$ days using a portfolio of short-maturity out-of-the-money options on the S&P500 index over a discrete grid of strike prices. At time t, the quantity

$$\sigma^2_{t,T} = \frac{2}{T-t}\sum_i \frac{\Delta K_i}{K_i^2} e^{r(T-t)} Q(K_i, t, T) - \frac{2}{T-t}\left(\frac{F(t,T)}{K_0} - 1\right)^2 \tag{2.1}$$

is computed and the corresponding VIX index value is

$$VIX_t = 100 \times \sigma_{t,T} \tag{2.2}$$

The sum runs over a set of strikes of OTM options of price $Q(K_i, t, T)$ with common expiry at time T, the risk-free rate r is the bond-equivalent yield of the U.S. T-bill maturing closest to the expiration date of the SPX options and K_i is the strike of the i-th option. $\Delta K_i = (K_{i+1} - K_i)/2$ is the interval between two consecutive strikes[3] and $F(t, T)$ denotes the time-t forward SPX index level deduced by put-call parity as

$$F(t,T) = K^* + e^{r(T-t)}\left[C(K^*, t, T) - P(K^*, t, T)\right]. \tag{2.3}$$

The strike K^* is the strike at which the price difference between an OTM call $C(K^*, t, T)$ and put $P(K^*, t, T)$ is minimum

$$\begin{aligned} K^* &= K_{i^*} \\ i^* &= \min_i |C(K_i, t, T) - P(K_i, t, T)| \end{aligned} \tag{2.4}$$

and K_0 is the first strike below the level of $F(t, T)$.

Since VIX_t is expressed in annualized terms, investors typically divide it by $\sqrt{256}$ in order to gauge the expected size of the daily movements in the stock markets implied by this index (Rhoads, 2011). Being an industry standard, several technical details apply to VIX calculation, for which we refer to the CBOE VIX white paper (Exchange, 2009). Among these, the time to expiration $T - t$ is measured in calendar days and in order to replicate the precision that is commonly used by professional option and volatility traders, each day is divided into minutes and the annualization is consistently referred to the minutes in the year.

Moreover, the components of the VIX calculation are near- and next-term put and call options with, respectively, more than $T_1 = 23$ days and less than $T_2 = 37$ days to expiration. For these two maturity buckets, formula (2.1) is applied with appropriate risk-free rates R_1, R_2, and forward SPX index levels $F(t, T_1), F(t, T_2)$,

[3]For the lowest (highest) strikes, ΔK_i is defined as the difference between that strike and next higher (lower) one.

computed as in (2.3). The volatility levels $\sigma_{t,T_1}, \sigma_{t,T_2}$ are then consistently obtained. The effective variance level $\sigma^2_{t,30}$ to be considered in VIX calculation is the weighted average of σ^2_{t,T_1} and σ^2_{t,T_2}

$$\sigma^2_{t,30} = \left[T_1 \sigma^2_{t,T_1} \left(\frac{N_{T_2} - N_{30}}{N_{T_2} - N_{T_1}} \right) + T_2 \sigma^2_{t,T_2} \left(\frac{N_{30} - N_{T_1}}{N_{T_2} - N_{T_1}} \right) \right] \times \frac{N_{365}}{N_{30}} \tag{2.5}$$

where N_T denotes the number of minutes to settlement of option in the near-/next-term maturity bucket and N_{30} (N_{365}) is the number of minutes in 30 (365) days. Finally, the VIX index value effectively computed is

$$VIX_t = 100 \times \sigma_{t,30} \tag{2.6}$$

CBOE began disseminating the price level information about VIX using the methodology exposed here from September 22, 2003, but price data are available, back-calculated, since 1990.

Figure 1 shows thirteen years of historical closing prices of S&P500 and VIX, in which is evident the inverse relation between the two indexes, with VIX spiking when the S&P500 index falls and then slowly mean-reverting toward lower levels. Figure 2 presents the empirical VIX closing price distribution obtained with data from 1990 to 2013. The distribution is positively skewed and leptokurtic, which is evidently in contrast with the negatively skewed distribution of returns, which is a stylized fact commonly found in market data.
The financial press has usually referred to VIX as the *fear gauge* and it is currently considered as a reliable barometer of investor sentiment and market volatility. The interest expressed by several investors in trading instruments related to the market's expectation of future volatility has lead CBOE to introduce futures and options written on VIX index, respectively in 2004 and 2006.

2.1.2 VIX Futures

The idea of a futures contract on VIX is to provide a pure play on the volatility level, independently of the direction of S&P500. These contracts are currently traded at the Chicago Futures Exchange (CFE), introduced in 2003 by the CBOE expressly to provide exchange-traded volatility derivatives.

VIX futures contracts settle on the Wednesday that is thirty days prior to the third Friday of the calendar month immediately following the month in which the applicable VIX futures contract expires. From figure 5, for example, the May 2004 (labelled as K4) contract settled on Wednesday, May 19, 2004.

The underlying is the VIX index and each contract is written on $1,000 times the VIX. The date-t settlement value $F_{VIX}(t,T)$ of a futures of tenor T is calculated with a so called Special Opening Quotation (SOQ) of VIX, which is obtained from

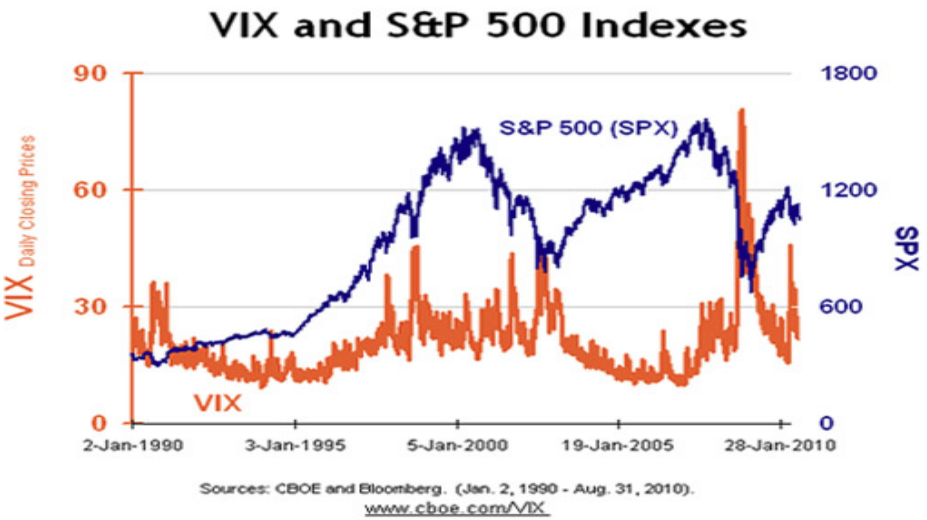

Figure 1: S&P500 and VIX index daily closing values from January 1990, to December 2003. Source: Bloomber and CBOE.

a sequence of opening prices of the SPX options considered for the VIX calculation at date T. An extensive discussion of the settlement procedures and market conventions of VIX futures can be found in the paper of Zhang et al. (2010).

From a pricing perspective, since the VIX index is not the price of any traded asset, but just a risk-neutral volatility forecast, there is no cost-of-carry relationship, arbitrage free, between VIX futures price $F_{VIX}(t,T)$ and the underlying VIX_t (Grünbichler and Longstaff, 1996; Zhang et al., 2010)

$$F_{VIX}(t,T) \neq VIX_t e^{r(T-t)} \tag{2.7}$$

and, differently from commodity futures, there is no convenience yield either. In absence of any other market information, the model price of futures (and options) on VIX have to be computed according the risk neutral evaluation formula

$$F_{VIX}(t,T) = E^{\mathbb{Q}}[VIX_T|\mathcal{F}_t] \tag{2.8}$$

where $\mathbb{Q}$ denotes the martingale pricing measure and the VIX_t dynamics is described by some model, either directly (*standalone* approach) or implied by the S&P500 dynamics (*consistent* approach), as will be discussed in the next section. The term structure of VIX Futures is the graph obtained as a map

$$T \Longrightarrow F_{VIX}(t,T) \tag{2.9}$$

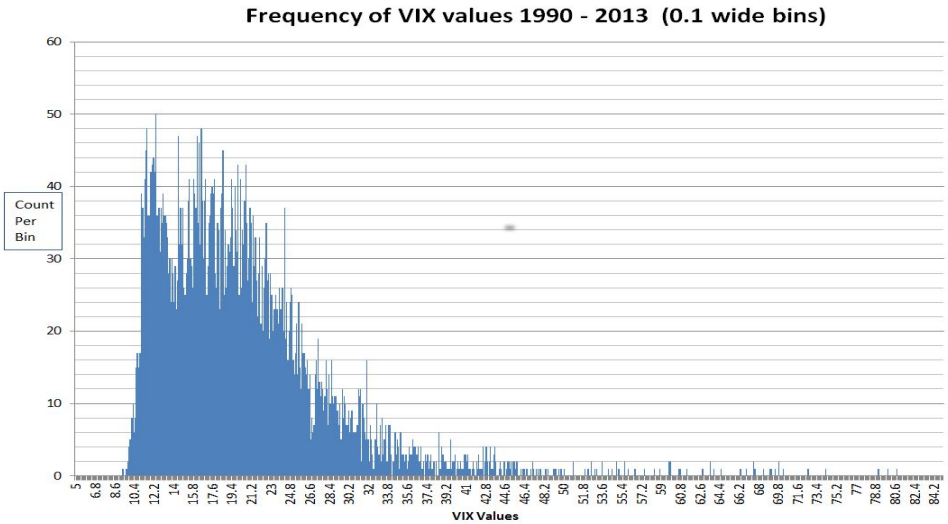

Figure 2: VIX closing price distribution. Sample is from January 1990 to March 2013. Source: Six Figure Investing blog.

and its shape provides interesting insights on market expectations. Figure 3 provides an example of *humped* term structure, in which a *contango* market for lower tenors, in which investors expect future VIX (and, therefore, volatility) to rise, is followed by a *backwardation* phase in which market expects volatility to calm down somehow in the future. In figure 4, the term structure of VIX futures is plotted against date between February 2006 and December 2010, spanning a period before, during and after the financial crisis. The level of prices remains low and the shape of the term structure upward sloping until mid-2007, suggesting a too low perceived value of the VIX index. The period of the crisis then raised the overall level of the prices, but the backwarding shapes suggests that market expected high volatility in the short-period, but not in the medium- to long- term. The sample period in figure 4 ends just before the beginning of the Greek debt crisis. By definition of futures contract, as date t approaches the settlement date T, the price of the futures converges to the spot VIX value and at settlement

$$F_{VIX}(T,T) = VIX_T \tag{2.10}$$

Figure 5 provides an example of this convergence with the price time series of four different contracts expiring between May and November 2004, starting from values relatively far from the corresponding VIX level and gradually converging to its level at expiration.

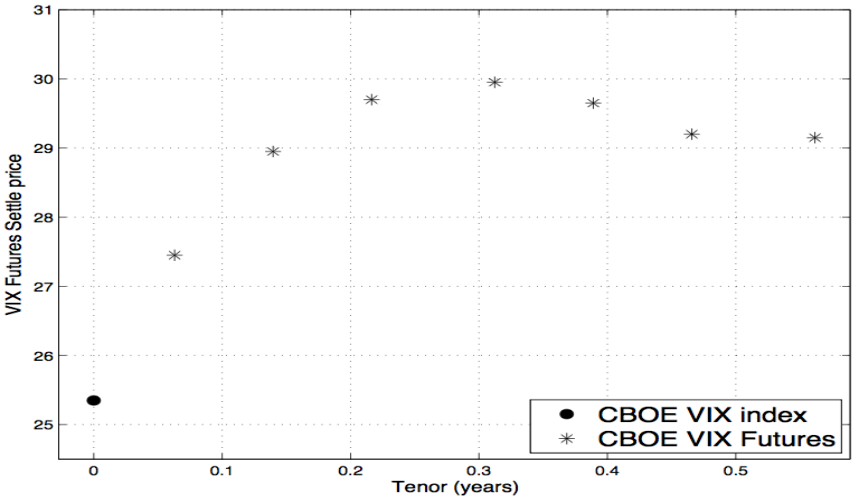

Figure 3: VIX futures term structure, as observed on Monday, 29 June 2009. VIX futures settle prices are in US$ and tenor T is expressed in years.

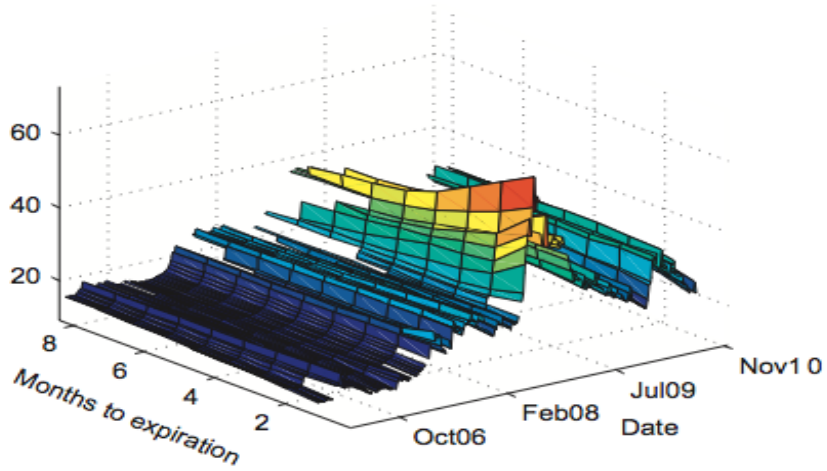

Figure 4: VIX futures term structure, as observed between February 2006 and December 2010. VIX futures settle prices are in US$. Source: Mencía and Sentana (2013).

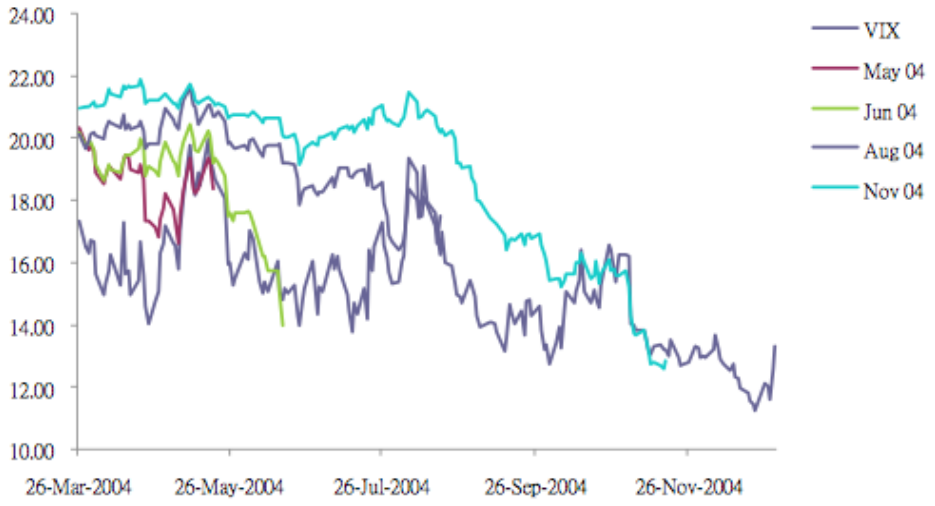

Figure 5: Pattern of VIX index value and four VIX futures settle prices: May 04, Jun 04, Aug 04 and Nov 04, settling respectively on 19 May, 16 June, 18 August and 17 November 2004. Source: *The New Market for Volatility Trading* (Zhang et al., 2010).

In light of the present analysis of displaced affine models, a consideration is useful for future reference: a hump in the term structure is hard to get reproduced by Heston-like affine models if calibrated consistently on both VIX futures, SPX and VIX options, unless the instantaneous volatility process σ_t is extended with the introduction of a so-called displacement ϕ_t, a positive deterministic function which acts as a lower bound for the volatility process, that we found able to dramatically increase the fit to the term structure of futures on VIX.

2.1.3 VIX Options

Call options on VIX with maturity T and strike K are European-style options paying the amount $(VIX_T - K)^+$ at maturity.Since they expire the same day of a futures on VIX and subsume the same volatility reference period of 30 days starting from the maturity date, from equation (2.10) they can be regarded as options on a VIX futures contract $F_{VIX}(t,T)$ sharing expiry date with the option. This implies that VIX call (put) prices $C_{VIX}(K,t,T)$ (P_{VIX}) can be priced according to

the risk-neutral evaluation[4]

$$\begin{aligned} C_{VIX}(K,t,T) &= e^{-r\tau} E^{\mathbb{Q}}\left[\left(F_{VIX}(T,T)-K\right)^{+} \middle| \mathcal{F}_t \right] \\ P_{VIX}(K,t,T) &= e^{-r\tau} E^{\mathbb{Q}}\left[\left(K-F_{VIX}(T,T)\right)^{+} \middle| \mathcal{F}_t \right] \end{aligned} \tag{2.11}$$

where $\tau = T - t$ and satisfy the following put-call parity relation (Lian and Zhu, 2013, eq. 25)

$$C_{VIX}(K,t,T) - P_{VIX}(K,t,T) = e^{-r(T-t)}\left(F_{VIX}(t,T)-K\right) \tag{2.12}$$

Moreover, no arbitrage conditions can be expressed with respect to VIX futures price (Lin and Chang, 2009)

$$\begin{aligned} \left(e^{-r(T-t)}\left(F_{VIX}(t,T)-K\right)\right)^{+} &\leq C_{VIX}(K,t,T) \leq e^{-r(T-t)} F_{VIX}(t,T) \\ \left(e^{-r(T-t)}\left(K-F_{VIX}(t,T)\right)\right)^{+} &\leq P_{VIX}(K,t,T) \leq e^{-r(T-t)} K \end{aligned} \tag{2.13}$$

Given the price of a call option on VIX, $C^{*}_{VIX}(K,t,T)$, the implied volatility $\sigma^{Blk}_{VIX}(K,T)$ at time t is inverted through the Black (1976) formula solving the equation (Papanicolaou and Sircar, 2014, Sec. 2.2)

$$C^{Blk}_{VIX}(K,t,T;F_{VIX}(t,T),r,\sigma^{Blk}_{VIX}(K,T)) = C^{*}_{VIX}(K,t,T) \tag{2.14}$$

where

$$\begin{aligned} C^{Blk}_{VIX}(K,t,T;F,r,\sigma) &= e^{-r(T-t)}\left(F\mathcal{N}(d_1) - K\mathcal{N}(d_2)\right) \\ d_1 &= \frac{\log\left(\frac{F}{K}\right) + \frac{1}{2}\sigma^2(T-t)}{\sigma\sqrt{T-t}} \\ d_2 &= d_1 - \sigma\sqrt{T-t} \end{aligned} \tag{2.15}$$

and $\mathcal{N}(\cdot)$ denotes the CDF of the standard normal distribution function.

The empirical observation of S&P500 vanilla and VIX option implied volatility surfaces conveys relevant informations on the different nature of the two markets. As an example of the most evident differences between the two markets, in figure 6 we plot the Black and Scholes (1973) implied volatility surface observed on Monday, 29 June 2009 and in figure 7 the VIX implied surface of call options observed on the same date.

Both options datasets have been filtered using standard procedures (Aït-Sahalia and Lo, 1998; Bakshi et al., 1997), as will be detailed for our empirical analysis in Chapter 4. Since VIX call options are fairly more liquid than put options, only the

[4] As it is usually assumed in the VIX derivative literature, the short rate r is held fixed and deterministic (Mencía and Sentana, 2013).

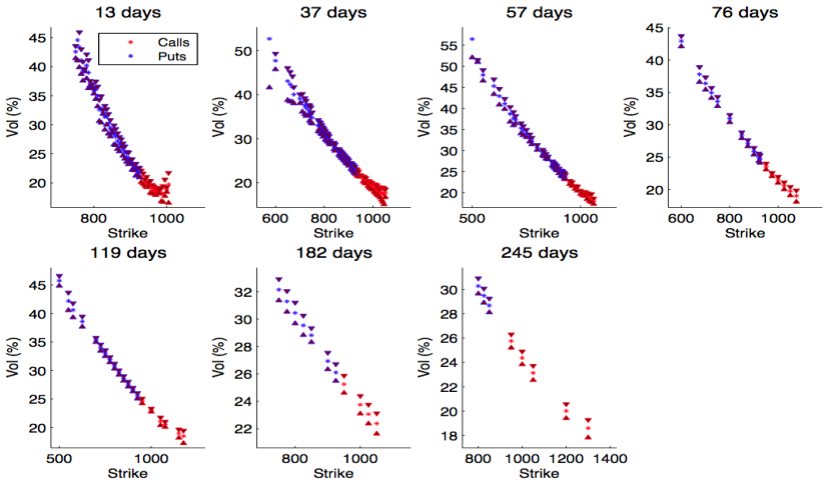

Figure 6: Black and Scholes (1973) implied volatility surface of european calls and puts on S&P500, as observed on Monday, 29 June 2009. Asterisk (triangle) markers are for mid (bid/ask) price implied vols. Maturities are expressed in days and volatilities are in % points.

former have been reported in figure 7, and the price of an illiquid in-the-money (ITM) call option has been inferred from the corresponding put price via put-call parity (2.12). The SPX implied volatility surface observed in figure 6 presents typical features: a negative skew more pronounced at lower maturities with OTM calls much more cheaper than corresponding puts. The VIX surface of figure 7 instead, shows rather peculiar characteristics: the implied volatility smile is upward sloping and the volatility level is overall higher compared to vanilla options. OTM call options on VIX are much more liquid (and are traded at higher premiums) than OTM puts, showing an opposite scenario with respect to options on S&P500, in which OTM puts are more expensive and heavily traded. A possible explanation for this dichotomy is the following: both puts on S&P500 and calls on VIX provide insurance from equity market downturns. On the buy-side, investors use OTM S&P500 put options to protect their portfolios against sharp decreases in stock prices and increases in volatility (Branger et al., 2014). On the sell-side, market makers that have net short positions on OTM S&P500 index puts require net long positions on OTM VIX calls to hedge their volatility risk (Chung et al., 2011). Moreover, by holding VIX derivatives investors can expose their portfolio to S&P500 volatility without need to delta hedge their option open positions with positions on the stock index. Due to this possibility, VIX options are the only asset in which open interests are highest for OTM call strikes (Rhoads, 2011).

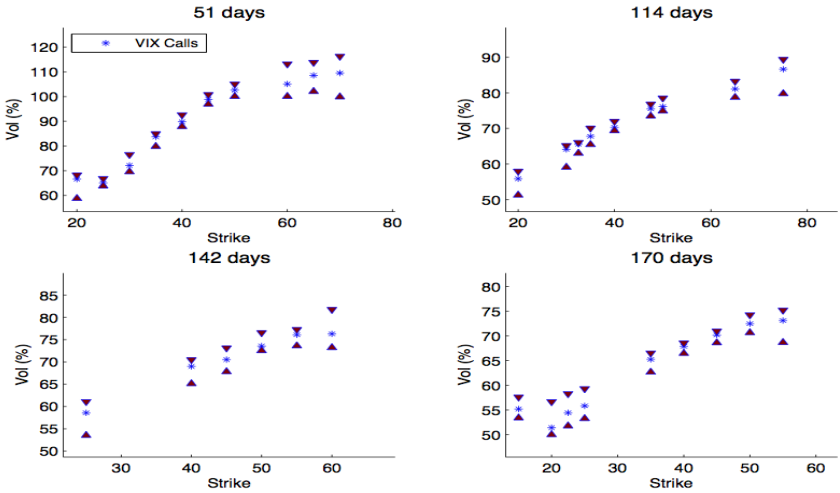

Figure 7: Black implied volatility surface Black (1976) of call options on VIX, as observed on Monday, 29 June 2009. Asterisk (triangle) markers are for mid (bid/ask) price implied vols. Maturities are expressed in days and volatilities are in % points.

2.2 Models: *standalone* and *consistent* approach

Theoretical approaches for VIX modeling can be broadly divided in two categories: a *consistent* and a *standalone* approach. The contributions considered most relevant for this thesis will be reviewed in this section.

2.2.1 Standalone models of VIX

In the earlier standalone approach, the volatility is directly modeled, separated from the underlying stock index process. This approach only focuses on pricing derivatives written on VIX index without considering SPX options. A risk-neutral dynamics for VIX_t is usually assumed and pricing formulas as well as calibration to VIX futures and options can be easily obtained. Within this stream of literature, theoretical contributions in modeling VIX index and pricing VIX derivatives appeared well before the opening of the corresponding markets.[5]

[5]In this Section we mostly follow the review of Mencía and Sentana (2013), though redefining the notation in order to normalize it to the rest of the thesis.

The GBM model of Whaley (1993)

In 1993, when VIX definition was still Black-Scholes based (i.e. VIX was what is today known as VXO), Whaley (1993) modeled VIX_t as a Geometric Brownian Motion (GBM) under the martingale measure $\mathbb{Q}$

$$\frac{dVIX_t}{VIX_t} = rdt + \sigma dW_t \tag{2.16}$$

The pricing formula for a VIX call option $C_{VIX}^{\mathsf{GBM}}(K,t,T)$ under the model (2.16) is the Black-76 formula Black (1976), as presented in equation (2.15) and that of a futures is

$$F_{VIX}^{\mathsf{GBM}}(t,T) = E^{\mathbb{Q}}[VIX_T|\mathcal{F}_t] = VIX_t e^{r(T-t)} \tag{2.17}$$

The GBM dynamics is both too simple to capture the dynamics of VIX, since it does not allow for mean-reversion, and to reproduce the positive implied skew of VIX options, since it yields a flat implied volatility.

The observed mean-reversion property of VIX was introduced in the subsequent models of Grünbichler and Longstaff (1996) and Detemple and Osakwe (2000).

The SQR model of Grünbichler and Longstaff (1996)

Grünbichler and Longstaff (1996) modeled the standard deviation of stock index returns as a square-root mean reverting model (Cox et al., 1985)

$$dVIX_t = \alpha\left(\beta - VIX_t\right)dt + \Lambda\sqrt{VIX_t}dW_t \tag{2.18}$$

where β is the long-term mean-reverting level, α the rate of mean-reversion and Λ the constant vol-of-vol parameter. Under the SQR model, the VIX index is proportional to a non-central χ^2 variable with $2q+2$ degrees of freedom and parameter of non-centrality $2u$, that is at any point in time the outcome of the volatility index process is distributed according to

$$2cVIX_T \overset{|\mathcal{F}_t}{\sim} \chi^2\left(2q+2, 2u\right) \tag{2.19}$$

with

$$\begin{aligned} c &= \frac{2\alpha}{\Lambda^2\left(1-e^{-\alpha\tau}\right)} \\ u &= cVIX_t e^{-\alpha\tau} \\ v &= cVIX_T \\ q &= \frac{2\alpha\beta}{\Lambda^2} - 1 \end{aligned} \tag{2.20}$$

The transition pdf of VIX_t is therefore known in closed form

$$p^{\mathbb{Q}}_{VIX}(VIX_T \mid VIX_t) = ce^{-u-v}\left(\frac{v}{u}\right)^{q/2} I_q(2\sqrt{uv}) \times \mathcal{I}\{VIX_T \geq 0\} \tag{2.21}$$

where $I_q(\cdot)$ is a modified Bessel function of the first kind of order q, $\tau = T - t$ and the indicator function is defined as $\mathcal{I}\{x \geq 0\} = 1$ if $x \geq 0$ and 0 otherwise. As a result, the price of a VIX futures is simply (Mencía and Sentana, 2013, eq. 4)

$$F^{\mathsf{SQR}}_{VIX}(t,T) = E^{\mathbb{Q}}[VIX_T|\mathcal{F}_t] = \beta + (VIX_t - \beta)\, e^{-\alpha\tau} \tag{2.22}$$

and options on VIX can be obtained in terms of the CDF $F_{NC\chi^2}(\cdot; k, \lambda)$ of a non-central χ^2 random variable with k degrees of freedom and non-centrality parameter λ (Mencía and Sentana, 2013, eq. 5)

$$\begin{aligned} C^{\mathsf{SQR}}_{VIX}(K,t,T) = {} & VIX_t e^{-(\alpha+r)\tau}\left[1 - F_{NC\chi^2}(2cK; 2q+6, 2u)\right] \\ & + \beta\left(1 - e^{-\alpha\tau}\right)\left[1 - F_{NC\chi^2}(2cK; 2q+4, 2u)\right] e^{-r\tau} \\ & - Ke^{-r\tau}\left[1 - F_{NC\chi^2}(2cK; 2q+2, 2u)\right] \end{aligned} \tag{2.23}$$

The LOU model of Detemple and Osakwe (2000)

Detemple and Osakwe (2000) modeled the $\log VIX_t$ as an Ornstein-Uhlenbeck process (LOU)

$$d\log VIX_t = \alpha\left(\beta - \log VIX_t\right) dt + \Lambda dW_t \tag{2.24}$$

which subsumes a log-normal conditional distribution for VIX_t,

$$VIX_T \overset{|\mathcal{F}_t}{\sim} Log\mathcal{N}\left(\mu(t,T), \phi^2(\tau)\right) \tag{2.25}$$

where

$$\begin{aligned} \mu(t,T) &= \beta + (\log VIX_t - \beta)\, e^{-\alpha\tau} \\ \phi^2(\tau) &= \frac{\Lambda^2}{2\alpha}\left(1 - e^{-2\alpha\tau}\right) \end{aligned} \tag{2.26}$$

and therefore, as in the SQR model, β and α are the long-run mean and mean-reversion parameters, respectively. Futures on VIX are easily priced as conditional mean of a $Log\mathcal{N}$ variable

$$F^{\mathsf{LOU}}_{VIX}(t,T) = E^{\mathbb{Q}}[VIX_T|\mathcal{F}_t] = e^{\mu(t,T)+\frac{1}{2}\phi^2(\tau)} \tag{2.27}$$

and the price of a call option on VIX can be expressed as a Black (1976) formula (Mencía and Sentana, 2013, eq. 7), given in (2.15)

$$C^{\mathsf{LOU}}_{VIX}(K,t,T) = C^{Blk}_{VIX}(K,t,T; F^{\mathsf{LOU}}_{VIX}(t,T), r, \phi(\tau)) \tag{2.28}$$

which presents a flat implied volatility across strikes, but depending on the maturity of the options, due to the time-dependent volatility parameter $\phi(\tau)$.

Both SQR and LOU have been extensively studied in literature: Zhang and Zhu (2006) analyzed the SQR pricing errors on VIX futures and Dotsis et al. (2007) studied the gains of adding jumps. The hedging effectiveness of SQR and LOU specifications have been tested by Psychoyios and Skiadopoulos (2006), and Wang and Daigler (2011) added options on VIX to the testing sample. Overall, as confirmed by the extensive analysis conducted by Mencía and Sentana (2013), who considered historical VIX and VIX derivatives data[6] from February 2006 (opening of VIX options market) to December 2010, the LOU dynamics yields lower pricing errors compared to the SQR. Their performance tends to deteriorate during the 2008-09 financial crisis and the underlying assumption of an exponentially fast rate of mean reversion towards the long-run mean, poses both SQR and LOU models at odds with the empirical evidence, especially during bearish stock markets when VIX takes long periods to revert from high levels. Moreover, both models are unable to reproduce the positive skew observed in VIX options, the LOU yielding a flat implied volatility w.r.t. strike (for each maturity), and the SQR a negative skew.

The SQR and LOU extensions of Mencía and Sentana (2013)

The restriction of an exponential rate of mean reversion in the SQR model, is relaxed introducing the concatenated CSQR model (Bates, 2012)

$$\begin{aligned} dVIX_t &= \alpha\left(\beta_t - VIX_t\right)dt + \Lambda\sqrt{VIX_t}dW_t^{VIX} \\ d\beta_t &= \bar{\alpha}\left(\bar{\beta} - \beta_t\right)dt + \bar{\Lambda}\sqrt{\beta_t}dW_t^{\beta} \end{aligned} \tag{2.29}$$

where $corr(dW_t^{VIX}, dW_t^{\beta}) = 0$. This extension features a stochastic mean reverting level β_t, which in turn reverts toward a long-rung level $\bar{\beta}$. The stochastic central tendency β_t directly affects the conditional mean of $E^{\mathbb{Q}}\left[VIX_T|\,\mathcal{F}_t\right]$, that is the futures price (Mencía and Sentana, 2013, eq. 10 and 11)

$$\begin{aligned} F_{VIX}^{\text{CSQR}}(t,T) &= \hat{\beta} + \delta(\tau)(\beta_t - \bar{\beta}) + (VIX_t - \beta_t)\,e^{-\alpha\tau} \\ \delta(\tau) &= \frac{\alpha}{\alpha - \bar{\alpha}}e^{-\bar{\alpha}\tau} - \frac{\bar{\alpha}}{\alpha - \bar{\alpha}}e^{-\alpha\tau} \end{aligned} \tag{2.30}$$

[6] They use also historical data on the VIX index itself in order to estimate SQR and LOU models under both under real and risk-neutral measures. Since in this thesis our focus is on derivative pricing, we do not consider explicitly real measure specifications.

but seems to be unable to reproduce the positive skew of VIX options, priced according to Amengual and Xiu Amengual and Xiu (2012)

$$\begin{aligned} C_{VIX}^{\mathsf{CSQR}}(K,t,T) &= \frac{e^{-r\tau}}{\pi}\int_0^\infty \mathrm{Re}\left[f_{VIX}^{\mathsf{CSQR}}(z;\tau)\frac{e^{-Kz}}{z^2}\right] d\,\mathrm{Im}(z) \\ \mathrm{Re}(z) &< \zeta_c(\tau) := \frac{2\alpha}{\Lambda^2}\frac{1}{1-e^{-\alpha\tau}} \end{aligned} \tag{2.31}$$

where $\tau = T - t$ and

$$f_{VIX}^{\mathsf{CSQR}}(z;\tau) = E^{\mathbb{Q}}\left[e^{izVIX_T}\middle|\,\mathcal{F}_t\right] \tag{2.32}$$

with $z = \mathrm{Re}(z) + i\,\mathrm{Im}(z) \in \mathbb{C}$, is the conditional characteristic function of VIX (Mencía and Sentana, 2013, App. B).

Extensions of the LOU model are first considered separately.

- A CTOU model extends the $\log VIX_t$ dynamics with a time-varying central tendency

$$\begin{aligned} d\log VIX_t &= \alpha\left(\beta_t - \log VIX_t\right)dt + \Lambda dW_t^{VIX} \\ d\beta_t &= \bar{\alpha}\left(\bar{\beta} - \beta_t\right)dt + \bar{\Lambda}dW_t^{\beta} \end{aligned} \tag{2.33}$$

  where $corr(dW_t^{VIX}, dW_t^{\beta}) = 0$.

- In the LOUJ model, compensated λ intense exponential jumps introduce non-normality in the conditional distribution of $\log VIX_t$

$$\begin{aligned} d\log VIX_t &= \alpha\left(\beta - \log VIX_t\right)dt + \Lambda dW_t^{VIX} + dM_t \\ dM_t &= cdN_t - \frac{\lambda}{\alpha\delta}dt \end{aligned} \tag{2.34}$$

  where N_t is an independent Poisson process and $c \sim \mathcal{E}xp(\delta)$.

- The constant spot volatility assumption is relaxed with the LOUSV

$$\begin{aligned} d\log VIX_t &= \alpha\left(\beta - \log VIX_t\right)dt + \omega_t^2 dW_t \\ d\omega_t^2 &= -\lambda\omega_t^2 dt + cdN_t \end{aligned} \tag{2.35}$$

  where N_t is an independent Poisson process, with intensity λ and $c \sim \mathcal{E}xp(\delta)$. The advantage of the chosen specification for the stochastic volatility ω_t^2, as compared for example with a square root dynamics, is that it allows to price futures and options on VIX_t by means of Fourier inversion of its conditional CF.

Then in combination.

- Combining time-varying central tendency and jumps, the CTOUJ model is obtained

$$\begin{aligned} d\log VIX_t &= \alpha\left(\beta_t - \log VIX_t\right)dt + \Lambda dW_t^{VIX} + dM_t \\ d\beta_t &= \bar{\alpha}\left(\bar{\beta} - \beta_t\right)dt + \bar{\Lambda} dW_t^{\beta} \\ dM_t &= cdN_t - \frac{\lambda}{\alpha\delta}dt \end{aligned} \tag{2.36}$$

  where $corr(dW_t^{VIX}, dW_t^{\beta}) = 0$ and jumps are as in the LOUJ model.

- If time-varying central tendency is combined with stochastic volatility, the CTOUSV model is obtained

$$\begin{aligned} d\log VIX_t &= \alpha\left(\beta_t - \log VIX_t\right)dt + \omega_t dW_t^{VIX} \\ d\beta_t &= \bar{\alpha}\left(\bar{\beta} - \beta_t\right)dt + \bar{\Lambda} dW_t^{\beta} \\ d\omega_t^2 &= -\lambda\omega_t^2 dt + cdN_t \end{aligned} \tag{2.37}$$

  where $corr(dW_t^{VIX}, dW_t^{\beta}) = 0$ and stochastic volatility ω_t^2 is as in the LOUSV model.

All the ·OU· extensions of the basic LOU model belong to the class of the AJD processes analyzed in Duffie et al. (2000), as shown in App. A of Mencía and Sentana (2013). As a consequence, VIX derivative prices can be obtained computing the conditional CF of the $\log VIX_t$ process

$$f_{\log VIX}^{\cdot OU\cdot}(z;t,T) = E^{\mathbb{Q}}\left[e^{iz\log VIX_T}\middle|\,\mathcal{F}_t\right] \tag{2.38}$$

detailed in App. C of Mencía and Sentana (2013) for all ·OU· specifications. Therefore, VIX futures are easily obtained as

$$F_{VIX}^{\cdot OU\cdot} = f_{\log VIX}^{\cdot OU\cdot}(-i;t,T) \equiv E^{\mathbb{Q}}\left[VIX_T\middle|\,\mathcal{F}_t\right] \tag{2.39}$$

and VIX options can be priced applying the results of Carr and Madan (1999)

$$C_{VIX}^{\cdot OU\cdot} = \frac{e^{-\alpha\log K}}{\pi}\int_0^{\infty} e^{-iu\log K}\psi_{\alpha}(u)du \tag{2.40}$$

where

$$\psi_{\alpha}(u) = \frac{e^{-r\tau}f_{\log VIX}^{\cdot OU\cdot}(u-(1+\alpha)i;t,T)}{\alpha^2+\alpha-u^2+i(1+2\alpha)u} \tag{2.41}$$

Their findings show that the time-varying central tendency has a deep impact in pricing futures, whereas the time-varying stochastic volatility of VIX reduces pricing errors on VIX options and the CTOUSV model yields the overall best fit

in both markets. They find that jumps almost do not change futures prices and provide a minor improvement for VIX options. In conclusion, they give empirical support to a model of spot (log) VIX featuring time-varying central tendency and stochastic volatility, needed to capture the level and shape of VIX futures term structure, as well as the positive slope of options on VIX.

2.2.2 Consistent models of S&P500 and VIX

Although closed-form expressions for VIX derivatives prices are readily obtainable with the standalone approach, the tractability comes at the expense of consistency with vanilla options. Since the same volatility process underlies both equity and volatility derivatives, a reasonable model should be able to consistently price both vanilla on S&P500 and derivatives on VIX. A feature that is difficult to test if the volatility dynamics is directly modeled. Moreover, VIX index itself is computed by CBOE with a portfolio of liquid out of the money SPX vanilla, but modeling it directly does not necessarily presumes the requested replicability.

Consistent approaches retain the inherent relationship between S&P500 and VIX index. Given a risk-neutral dynamics for the S&P500 index S_t, the expression for the VIX index in continuous time has been derived in a model-free way in terms of the risk neutral expectation of a log contract (Lin, 2007, App. A)

$$\left(\frac{VIX_t}{100}\right)^2 = -\frac{2}{\bar{\tau}} E^{\mathbb{Q}}\left[\log\left(\frac{S_{t+\bar{\tau}}}{F(t,t+\bar{\tau})}\right)\middle|\mathcal{F}_t\right] \tag{2.42}$$

where $\bar{\tau} = 30/365$ and $F(t,t+\bar{\tau}) = S_t e^{(r-q)\bar{\tau}}$ denotes the forward price of the underlying SPX (Duan and Yeh, 2010; Zhang et al., 2010). This expression links the SPX dynamics with that of the VIX volatility index and will be at the base of VIX derivatives pricing. Assuming a stochastic volatility affine specification $\cdot\mathsf{SV}\cdot$,[7] as it is predominant within this stream of literature, the expression (2.42) takes a simple form: it is an affine function of the stochastic volatility factors $\sigma^2_{i,t}$ driving the dynamics of S_t

$$\left(\frac{VIX_t^{\cdot\mathsf{SV}\cdot}}{100}\right)^2 = \frac{1}{\bar{\tau}}\left(\sum_{i=1}^{n} a_i \sigma^2_{i,t} + b_i\right) \tag{2.43}$$

where (a_i, b_i) depend on the risk neutral drift of the volatility factors in the $[t, t+\bar{\tau}]$ time interval and, eventually, on the presence of jumps (both in S_t and/or in $\sigma^2_{i,t}$), but not on the specification of the martingale component of the factors (Egloff et al., 2010; Leippold et al., 2007, Corollary 1).[8]

[7] SV is for Stochastic Volatility, the dots are to synthetically include the generalization of the basic SV model of Heston (1993) that will be considered in the following.

[8] The expression in (3.15) can be derived for any $\cdot\mathsf{SV}\cdot$ model, given the dynamics of S_t. It will be

Consistent models of VIX futures

Early contributions focused on the replication of the term structure of VIX futures. Zhang and Zhu (2006), assumed a risk-neutral Heston (1993) stochastic volatility SV model for the SPX dynamics S_t

$$\begin{aligned} dS_t &= rS_t dt + S_t \sigma_t dW_t^S \\ d\sigma_t^2 &= \alpha(\beta - \sigma_t^2)dt + \Lambda \sigma_t dW_t^\sigma \end{aligned} \tag{2.44}$$

where $corr\left(dW_t^S, dW_t^\sigma\right) = \rho dt$. Zhu and Zhang (2007), extended the (2.44) dynamics allowing for a time-dependent mean reverting level β_t which can be calibrated to the term structure of the forward variance

$$E^{\mathbb{Q}}\left[V_T \middle| \mathcal{F}_t\right] = V_t e^{-\alpha(T-t)} + \alpha \int_t^T e^{-\alpha(T-s)} \beta_s ds \tag{2.45}$$

The time-varying mean reverting level β_t is made stochastic in the SMRSV model of Zhang et al. (2010), where

$$d\beta_t = \bar{\Lambda} dW_t^\beta \tag{2.46}$$

with $corr(dW_t^\sigma, dW_t^\beta) = 0$ and can be calibrated to the observed VIX futures term structure observed in a given day. The effect of jumps in the S&P500 and volatility dynamics has been analyzed by Lin (2007), who considered the SVCJ model[9] for $x_t = \log S_t$, introduced in Duffie et al. (2000)

$$\begin{aligned} dx_t &= \left(r - q - \lambda\bar{\mu} - \frac{1}{2}\sigma_t^2\right) dt + \sigma_t dW_t^S + c_x dN_t \\ d\sigma_t^2 &= \alpha(\beta - \sigma_t^2)dt + \Lambda \sigma_t dW_t^\sigma + c_\sigma dN_t \end{aligned} \tag{2.47}$$

where $corr\left(dW_t^S, dW_t^\sigma\right) = \rho dt$. The SVCJ model features correlated co-jumps, driven by the compound Poisson process N_t, with state-dependent intensity $\lambda = \lambda_0 + \lambda_1 \sigma_t^2$, exponentially distributed volatility jumps $c_\sigma \sim \mathcal{E}xp(\mu_{co,\sigma})$, jumps in price conditionally normally distributed $c_x \sim \mathcal{N}(\mu_{co,x} + \rho_J c_\sigma, \delta_{co,x}^2) \mid c_\sigma$. The characteristic function of the jump size is given by

$$\theta^{co}(z_x, z_\sigma) = E^{\mathbb{Q}}\left[e^{ic_x z_x + ic_\sigma z_\sigma}\right] = \frac{e^{i\mu_{co,x} z_x - \frac{1}{2}\delta_{co,x}^2 z_x^2}}{1 - i\mu_{co,\sigma}\left(z_\sigma + \rho_J z_x\right)} \tag{2.48}$$

and the compensator process is $\lambda\bar{\mu}t$, with $\bar{\mu} = E^{\mathbb{Q}}\left[e^{c_x} - 1\right] = \theta^{co}(-i, 0)$. In these models the VIX squared is as in (3.15), where

given for any model reviewed here, will be explicitly deduced for our 2-SVCVJ++ model in Chapter 3 and will be generalized to a broad class of affine models for volatility derivatives in Proposition 10.

[9] SVCJ is for Stochastic Volatility with Correlated Jumps in price and volatility.

- under the SV model in Zhang and Zhu (2006):

$$\begin{aligned} a(\bar{\tau}) &= \frac{1-e^{-\bar{\tau}\alpha}}{\alpha} \\ b(\bar{\tau}) &= \beta\Big(\bar{\tau} - a(\bar{\tau})\Big) \end{aligned} \tag{2.49}$$

- under the time-dependent mean-reverting model MRSV in Zhu and Zhang (2007)

$$\begin{aligned} a(\bar{\tau}) &= \frac{1-e^{-\bar{\tau}\alpha}}{\alpha} \\ b(t, t+\bar{\tau}) &= \int_t^{t+\bar{\tau}} \left(1 - e^{-(t+\bar{\tau}-s)}\right) \beta_s ds \end{aligned} \tag{2.50}$$

- under the stochastic mean-reverting model SMRSV in Zhang et al. (2010), the VIX index depends on the instantaneous mean-reverting level β_t

$$\begin{aligned} a(\bar{\tau}) &= \frac{1-e^{-\bar{\tau}\alpha}}{\alpha} \\ b(t, \bar{\tau}) &= \beta_t\Big(\bar{\tau} - a(\bar{\tau})\Big) \end{aligned} \tag{2.51}$$

- under the SVCJ model in Lin (2007), the VIX index will depend also on the jump sizes and correlation[10]

$$\begin{aligned} a(\bar{\tau}) &= \frac{1-e^{-\bar{\tau}\alpha}}{\alpha} \\ b(\bar{\tau}) &= \frac{\alpha\beta + \lambda\mu_{co,\sigma}}{\alpha}\Big(\bar{\tau} - a(\bar{\tau})\Big) + 2\lambda\Big[\bar{\mu} - (\mu_{co,x} + \rho_J\mu_{co,\sigma})\Big] \end{aligned} \tag{2.52}$$

As already noted for the SQR standalone model, outcomes of a CIR process (Cox et al., 1985) are proportional to a non-central χ^2 random variable. Therefore, knowing the transition function $p^{\mathbb{Q}}_{\sigma}(\sigma^2_T|\sigma^2_t)$ (which has the same functional form as the $p^{\mathbb{Q}}_{VIX}(VIX_T|VIX_t)$ in (2.21)), VIX futures prices under the SV model of Zhang and Zhu (2006) can be computed taking the expected value of the VIX at expiration

$$F^{\mathsf{SV}}_{VIX}(t,T) = E^{\mathbb{Q}}\left[VIX_T|\,\mathcal{F}_t\right] = 100 \times \int_0^{\infty} \sqrt{a(\bar{\tau}) + b(\bar{\tau})y}\; p^{\mathbb{Q}}_{\sigma}(y|x)dy \tag{2.53}$$

[10]For reasons of brevity, and as this will the specification with which we will mostly work with, we report only the expressions for $\lambda = \lambda_0$ and $\lambda_1 = 0$. The complete expressions with $\lambda_1 > 0$ can be found in (Lin, 2007, eq 7).

where (a, b) are given in (2.49). In the same way can be priced futures under the MRSV in Zhu and Zhang (2007), but $p_\sigma^{\mathbb{Q}}(\sigma_T^2|\sigma_t^2)$ has to be evaluated Fourier-inverting its conditional CF $f_\sigma(z; \sigma_t^2, t, T)$

$$p_\sigma^{\mathbb{Q}}(y|x) = \frac{1}{\pi}\int_0^\infty e^{-izy} f_\sigma(z; x, t, T)dz \tag{2.54}$$

Zhang et al. (2010) and Lin (2007) adopted approximated expressions.[11] In the SMRSV model in (2.46), they approximated β_T with β_t under the expectation $F_{VIX}(t,T) = E^{\mathbb{Q}}[VIX_T|\mathcal{F}_t]$, omitting $\mathcal{O}(\bar{\Lambda}^2)$ terms, and then made a third order expansion around $E^{\mathbb{Q}}\left[\sigma_T^2\middle|\mathcal{F}_t\right]$, leveraging on the availability of closed-form expressions for the moments of the CIR model. For the SVCJ in (2.47), Lin proposed a convexity adjustment to overcome the non linear relation between squared VIX, which is a known affine function of the stochastic volatility σ_t^2 according to (2.52), and VIX futures price (Lin, 2007, eq. 8 and 9)

$$\begin{aligned} F_{VIX}^{\text{SVCJ}}(t,T) &= E^{\mathbb{Q}}[VIX_T|\mathcal{F}_t] \\ &\approx \sqrt{E^{\mathbb{Q}}[VIX_T^2|\mathcal{F}_t]} - \frac{var[VIX_T^2|\mathcal{F}_t]}{8(E^{\mathbb{Q}}[VIX_T^2|\mathcal{F}_t])^{3/2}} \end{aligned} \tag{2.55}$$

With calibration performed on VIX futures data from May 2004 to November 2008, Zhang et al. (2010) find reasonable good in sample results and, with the mean-reverting level β_t calibrated on the term structure observed in date t, the SMRSV model predicts one day lag $t+1$ out-of-sample changes in the term structure rather reliably (out-of-sample period ending on February 2009). The SVCJ model of Lin (2007) evidenced that contribution of jumps in S_t is determinant (with respect to a SV specification) in pricing the medium- to long-term structure of futures (sample from May 2004 to April 2006), while the inclusion of jumps in volatility σ_t^2 (possibly with a state-dependent intensity) reduce the out-of-sample pricing error on short-term dated futures on VIX.

Nevertheless, the two approximations proposed in Lin (2007) and Zhang et al. (2010) have been criticized by Zhu and Lian (2012), who showed that those approximations could be often inaccurate. Moreover, they found an exact analytical pricing formula for futures on VIX which is applicable to any model as long as the conditional CF $f_\sigma(z; \sigma_t^2, t, T)$ is computable. Taking as example the SVCJ model (with constant $\lambda = \lambda_0$), the Zhu and Lian (2012) VIX futures pricing formula is[12]

$$\begin{aligned} F_{VIX}^{\text{SVCJ}}(t,T) &= E^{\mathbb{Q}}[VIX_T|\mathcal{F}_t] \\ &= 100 \times \frac{1}{2\sqrt{\pi}}\int_0^\infty \frac{1 - e^{-sb(\bar{\tau})/\bar{\tau}} f_\sigma(isa(\bar{\tau})/\bar{\tau}; \sigma_t^2, t, T)}{s^{3/2}} ds \end{aligned} \tag{2.56}$$

[11] We refer to the papers for detailed derivations.

[12] Recalling the identity $\sqrt{x} = \frac{1}{2\sqrt{\pi}}\int_0^\infty \frac{1-e^{-sx}}{s^{3/2}} ds$ (Zhu and Lian, 2012, eq. A9) and Fubini theorem.

where (a, b) are given in (2.52) and $(\tau = T - t)$

$$f_{\sigma}^{\text{SVCJ}}(z; \sigma_t^2, t, T) = E^{\mathbb{Q}}\left[e^{iz\sigma_T^2} \middle| \mathcal{F}_t \right] = e^{A^{\sigma}(z;\tau) + B^{\sigma}(z;\tau)\sigma_t^2 + C_{co}^{\sigma}(z;\tau)} \tag{2.57}$$

is the conditional CF of σ_t^2 (Zhu and Lian, 2012, eq. A3), with coefficients A^{σ}, B^{σ} and C_{co}^{σ} satisfying the following set of ODEs (Zhu and Lian, 2012, eq. A4)

$$\begin{aligned}
\frac{\partial A^{\sigma}(z;\tau)}{\partial \tau} &= \alpha\beta B^{\sigma}(z;\tau) \\
\frac{\partial B^{\sigma}(z;\tau)}{\partial \tau} &= \frac{1}{2}\Lambda^2 \left(B^{\sigma}(z;\tau)\right)^2 - \alpha B^{\sigma}(z;\tau) \\
\frac{\partial C_{co}^{\sigma}(z;\tau)}{\partial \tau} &= \lambda\Big(\theta^{co}\left(0, -iB^{\sigma}(z,\tau)\right) - 1\Big)
\end{aligned} \tag{2.58}$$

with initial conditions $A^{\sigma}(z;0) = C_{co}^{\sigma}(z;0) = 0,\ B^{\sigma}(z;0) = iz$, and closed form solutions (Zhu and Lian, 2012, eq. A6)

$$\begin{aligned}
A^{\sigma}(z;\tau) &= -\frac{2\alpha\beta}{\Lambda^2}\log\left(1 - iz\frac{\Lambda^2}{2\alpha}\left(1 - e^{-\alpha\tau}\right)\right) \\
B^{\sigma}(z;\tau) &= \frac{ize^{-\alpha\tau}}{1 - iz\frac{\Lambda^2}{2\alpha}\left(1 - e^{-\alpha\tau}\right)} \\
C_{co}^{\sigma}(z;\tau) &= \lambda\Theta(z;\tau,\mu_{co,\sigma}) \\
\Theta(z;\tau,\mu) &= -\frac{2\mu}{\Lambda^2 - 2\alpha\mu}\log\left(1 - \frac{iz}{1 - iz\mu}\frac{\Lambda^2 - 2\alpha\mu}{2\alpha}\left(1 - e^{-\alpha\tau}\right)\right)
\end{aligned} \tag{2.59}$$

Consistent introduction of VIX options

On the wave of the increasing demand for volatility trading in the years of the financial crisis, the academic interest has moved consistently toward the rather new market of options written on the volatility process of stock indexes, mostly focusing on the widespread CBOE options on VIX. However, the transition was not easy at all and even today there is ongoing debate about which specification is better at capturing the structural novelties presented by the volatility surface implied by VIX options: an upward sloping smile, more pronounced for shorter maturities and flattening at the longer, with considerable time-variation on daily scales.

A clear-cut observation, which evidenced the deep distinction between SPX vanilla options and those written on its VIX volatility index, was made by Gatheral (2008). He pointed out that VIX options truly constitute a discriminant for stochastic volatility models: even though Heston (1993) model performs fairly well to price S&P500 option, it totally fails to price VIX options, usually producing a negatively

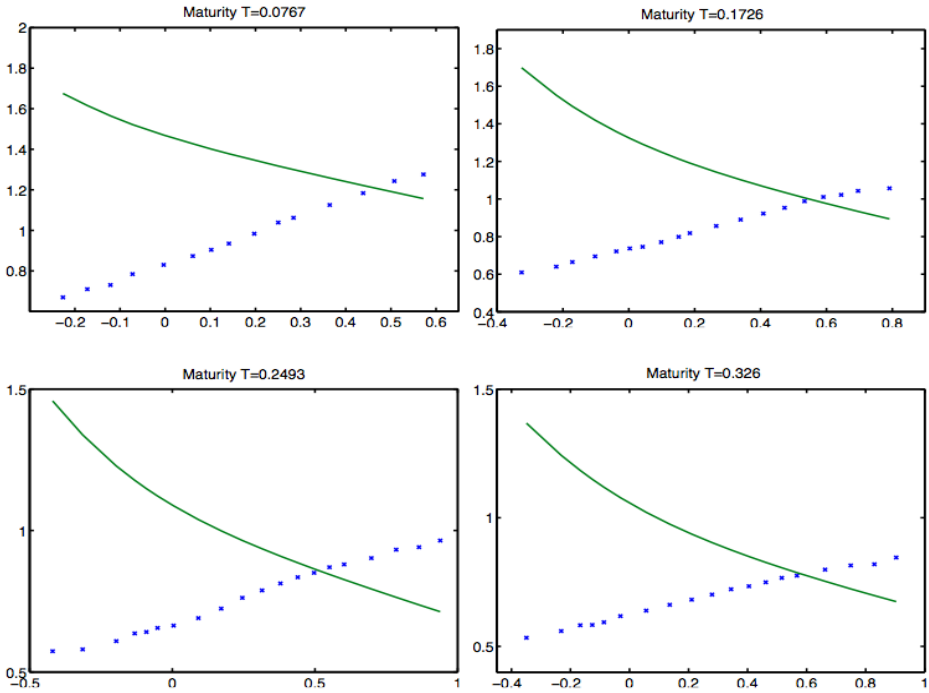

Figure 8: Market and SV model Heston (1993) implied volatilities for VIX options (four maturities) on October 20th, 2010 (date t) plotted with respect to log-moneyness $\log(K/F_{VIX}(t,T))$. Maturities T are in year fractions. The market (resp. model) implied volatilities are represented by the blue crosses (resp. the solid green line). These fits are obtained by minimizing relative errors between market implied volatilities and the Heston model implied volatility. Source: *Inferring volatility dynamics and risk premia from the S&P 500 and VIX markets* (Bardgett et al., 2013, version of July 21st, 2013).

skewed surface. (an example is presented in figure 8).

From the technical perspective, the transition from the linear payoffs of VIX futures, toward the piecewise linear one of options on VIX, together with the widespread lack of known transition pdf of volatility $p_\sigma^{\mathbb{Q}}$ featured by the newly introduced models,[13] has strongly pushed the mathematical development and numerical implementation of sophisticated techniques, commonly based on the Fourier inversion (Carr and Madan, 1999; Lewis, 2000, 2001) or series development (Bardgett et al., 2013; Fang and Oosterlee, 2008) of the conditional charac-

[13]The dynamics of which is far richer than that of a SV model Heston (1993).

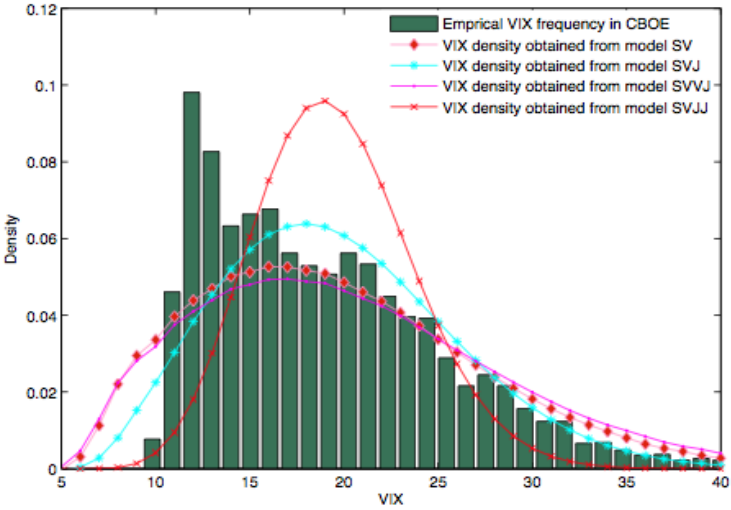

Figure 9: A Comparison of the VIX steady-state density distributions obtained with SV, SVJ, SVVJ and SVCJ models and empirical VIX frequency. The SV model is the Heston (1993) model considered by Zhang and Zhu (2006) and defined in (2.44). The SVCJ model (here denoted with the alternative label SVJJ) is the one-factor correlated co-jump model introduced in Duffie et al. (2000), considered in (Lin, 2007, setting $\lambda_1 \equiv 0$), Zhu and Lian (2012) and Lian and Zhu (2013) and defined in (2.47). The SVJ model features jumps in price only, is considered in the equity pricing literature in (Bakshi et al., 1997; Bates, 1996, among many), is defined in equation (2.67) and is nested in the SVCJ model taking $c_\sigma \equiv 0$. The SVVJ model features jumps in variance only, is introduced in Duffie et al. (2000) as nested in the SVCJ model taking $c_x \equiv 0$ and is nested in the model of Sepp (2008b), defined in equation (2.71), setting to the constant 1 the local volatility term ψ_t. The model implied steady-state distribution is taken from the transition density $p^{\mathbb{Q}}_{VIX'}(y|x)/100$ in (2.63) (or equivalently (Zhu and Lian, 2012, eq. 8)) in the limit $\tau = T - t \to \infty$. Data sample: VIX close levels between March 2004 and July 2008. Sampling frequency: daily. Model parameters: taken from (Zhu and Lian, 2012, Table 2). Source: *An analytical formula for VIX futures and its applications* Zhu and Lian (2012).

teristic function of volatility f_σ, which, for the wide class of affine models has a closed form expression (Chen and Joslin, 2012; Duffie et al., 2000).
Elaborating on the observation of Gatheral (2008) and on the empirical properties of the VIX options' surface it can be concluded that the $p^{\mathbb{Q}}_\sigma$ volatility distribution implied by VIX options has more mass at high volatility and less mass at lower volatility levels than the non-central χ^2 pdf of a SV Heston (1993) model (an example is given in figure 9).
Right skewness can be primarily induced by jumps in the volatility factor σ_t^2,

as essentially proposed with the SVVJ model[14] by Sepp (2008a,b) and as featured (together with correlated co-jumps in returns) by the SVCJ model in Duffie et al. (2000), considered in the VIX option pricing context by (Lian and Zhu, 2013, among many).
Alternatively, one can model the S&P500 index dynamics with stochastic volatility σ_t^2 and a stochastic volatility of volatility ω_t^2 positively correlated to the SPX volatility dynamics. This model is likely to produce a positive sloping skew in VIX options as it implies that low values of the S&P500 index (market downturns) are followed by high values of its volatility and, in turn, of its volatility of volatility. This possibility has been considered by Branger et al. (2014), with the 2-SVSVJ model,[15] which features stochastic volatility of variance, together with Gamma distributed jumps in variance.
Multi-factor specifications, as the 2-SV model proposed by Christoffersen et al. (2009), were already found relevant in the context of equity pricing: e.g. providing stochastic leverage correlation between the return and variance processes, better capturing the volatility term structure and enhancing the model ability to fit maturity-dependent smiles (Andersen et al., 2002; Kaeck and Alexander, 2012; Mencía and Sentana, 2013, among many). Additional factors have been added in various ways:

- as an additional independent volatility factor $\sigma_{2,t}^2$ in the 2-SVCJ model of Chen and Poon (2013) and Lo et al. (2013);

- as a stochastic volatility of variance factor ω_t^2 in the 2-SVSVJ of Branger et al. (2014);

- as a stochastically mean-reverting level β_t in the 2-SMRSVCJ[16] of Bardgett et al. (2013).

These affine specifications, together with some non-affine models proposed, will be reviewed in what follows. We will first focus on models focused (and calibrated) in reproducing the empirical properties of VIX options, then we will consider the few truly consistent models that tackle the problem of jointly calibrating the S&P500 and VIX options surfaces. We anticipate that, with the exclusion of Kokholm et al. (2015),[17] we are the first to include also VIX futures in the joint calibration of the 2-SVCVJ++ model, to be introduced in the next chapter.

[14] SVVJ is for Stochastic Volatility with Jumps in its stochastic Volatility.

[15] 2-SVSVJ is for Stochastic Variance of Stochastic Volatility with Jumps in volatility.

[16] 2-SMRSVCJ is for 2-factors Stochastic Mean-Reversion of Stochastic Volatility with Correlated Jumps in price and volatility.

[17] Whose most specified model is a one factor SVCJ model which yields not satisfactory results, thus claiming for more flexibility.

Consistent models of VIX options

Lian and Zhu (2013): a general (simple) pricing formulas for SVCJ (SV) model

Lian and Zhu (2013), considered a SVCJ model given in equation (2.47), as in Zhu and Lian (2012) and Lin (2007)[18]

$$\begin{aligned} dx_t &= \left(r - q - \lambda\bar{\mu} - \frac{1}{2}\sigma_t^2\right)dt + \sigma_t dW_t^S + c_x dN_t \\ d\sigma_t^2 &= \alpha(\beta - \sigma_t^2)dt + \Lambda\sigma_t dW_t^\sigma + c_\sigma dN_t \end{aligned} \tag{2.60}$$

and derive a closed-form expression (derived in Appendix of Lian and Zhu (2013)) for futures $F_{VIX}^{\mathsf{SVCJ}}(t,T)$ and call options $C_{VIX}^{\mathsf{SVCJ}}(K,t,T)$ on VIX ($VIX_t = x, K' = K/100, \bar{\tau} = 30/365, \tau = T - t$)

$$\begin{aligned} \frac{F_{VIX}^{\mathsf{SVCJ}}}{100} &= \frac{\bar{\tau}}{2a\sqrt{\pi}}\int_0^\infty \mathrm{Re}\left[e^{izb/a} f_\sigma\left(-iz; \frac{\bar{\tau}x^2 - b}{a}, t, T\right)\frac{1}{(iz\bar{\tau}/a)^{3/2}}\right] d\,\mathrm{Re}(z) \\ \frac{C_{VIX}^{\mathsf{SVCJ}}}{100} &= \frac{\bar{\tau}e^{-r\tau}}{2a\sqrt{\pi}}\int_0^\infty \mathrm{Re}\left[e^{izb/a} f_\sigma\left(-iz; \frac{\bar{\tau}x^2 - b}{a}, t, T\right)\frac{1 - erf(K'\sqrt{iz\bar{\tau}/a})}{(iz\bar{\tau}/a)^{3/2}}\right] d\,\mathrm{Re}(z) \end{aligned} \tag{2.61}$$

where $z = \mathrm{Re}(z) + i\,\mathrm{Im}(z) \in \mathbb{C}$. The integrals are performed along a straight line parallel to the $\mathrm{Re}(z)$ axis, selecting $0 < \mathrm{Im}(z) < \zeta_c(\tau)$, where the critical value is

$$\zeta_c(\tau) = \min\left(\frac{1}{\mu_{co,\sigma}}, \frac{1}{\frac{\Lambda^2}{2\alpha}(1 - e^{-\alpha\tau}) + \mu_{co,\sigma}e^{-\alpha\tau}}\right) \tag{2.62}$$

as given in (Lian and Zhu, 2013, eq. A7). Moreover, (a,b) are as in (2.52), f_σ is the conditional characteristic function on σ_t^2, defined in (2.57), and $erf(z) = \frac{2}{\sqrt{\pi}}\int_0^z e^{-s^2}ds$ is the complex error function. The formula leverages on the fact that - for one factor models - the transition pdf $p_{VIX'}^{\mathbb{Q}}$ of the scaled index $VIX' = VIX/100$ is in one-to-one correspondence with $p_\sigma^{\mathbb{Q}}$ and thus with f_σ, by Fourier-inversion. From VIX expression (3.15), if $n = 1$,

$$\begin{aligned} p_{VIX'}^{\mathbb{Q}}(y \mid x) &= \frac{2\bar{\tau}y}{a} p_\sigma^{\mathbb{Q}}\left(\frac{\bar{\tau}y^2 - b}{a}\,\middle|\,\frac{\bar{\tau}x^2 - b}{a}\right) \\ &= \frac{\bar{\tau}y}{a\pi}\int_{\mathbb{R}} e^{-iz\left(\frac{\bar{\tau}y^2 - b}{a}\right)} f_\sigma\left(z; \frac{\bar{\tau}x^2 - b}{a}, t, T\right) dz \\ &= \frac{2\bar{\tau}y}{a\pi}\int_0^\infty \mathrm{Re}\left[e^{-iz\left(\frac{\bar{\tau}y^2 - b}{a}\right)} f_\sigma\left(z; \frac{\bar{\tau}x^2 - b}{a}, t, T\right)\right] d\,\mathrm{Re}(z) \end{aligned} \tag{2.63}$$

[18] If $\lambda_1 \equiv 0$.

as detailed in eq. 7 and Appendix of Lian and Zhu (2013)). This one-to-one relation is lost in multi-factor models (consider again equation (3.15) if $n \geq 2$), and thus the formula proposed by Lian and Zhu cannot be extended directly to multi-factor affine models Lian and Zhu (2013).

If the SVCJ model is restricted to the Heston SV dynamics in (2.44), leveraging on (2.63) and on the fact that, under CIR diffusion Cox et al. (1985),

$$2c\sigma_T^2 \overset{|\mathcal{F}_t}{\sim} \chi^2\left(2q+2, 2u\right) \tag{2.64}$$

with c, q and u given in (2.20) (with $VIX_{\cdot}$ replaced by $\sigma_{\cdot}^2$) and transition density $p_\sigma^{\mathbb{Q}}(\sigma_T^2|\sigma_t^2)$ given by

$$p_\sigma^{\mathbb{Q}}(y \mid x) = ce^{-u-v}\left(\frac{v}{u}\right)^{q/2} I_q(2\sqrt{uv}) \times \mathcal{I}\left\{y \geq 0\right\} \tag{2.65}$$

as in (2.21), they show that the price of futures and options on VIX can be computed by direct integration of their payoff[19]

$$\begin{aligned} F^{\mathsf{SV}}(t,T) &= 100 \times \int_{\sqrt{b(\bar{\tau})/\bar{\tau}}}^{\infty} y\, p_{VIX'}^{\mathbb{Q}}(y \mid x)dy \\ C^{\mathsf{SV}}(K,t,T) &= 100 \times e^{-r\tau} \int_{max(K', \sqrt{b(\bar{\tau})/\bar{\tau}})}^{\infty} (y-K')^+\ p_{VIX'}^{\mathbb{Q}}(y \mid x)dy \end{aligned} \tag{2.66}$$

where $\cdot' = \cdot/100$ and $(x)^+ = max(x, 0)$ and the integration domain has been restricted, considering the effective support of the integrands.

Kokholm et al. (2015): a simple pricing formula for the SVJ model

In a recent publication, Kokholm et al. (2015) extend the last kind of pricing formulas to the SVJ model[20] (Bakshi et al., 1997; Bates, 1996)

$$\begin{aligned} dx_t &= \left(r - q - \lambda\bar{\mu} - \frac{1}{2}\sigma_t^2\right)dt + \sigma_t dW_t^S + c_x dN_t \\ d\sigma_t^2 &= \alpha(\beta - \sigma_t^2)dt + \Lambda\sigma_t dW_t^\sigma \end{aligned} \tag{2.67}$$

where $corr\left(dW_t^S, dW_t^\sigma\right) = \rho dt$. The SVJ model features idiosyncratic jumps in price only, driven by the compound Poisson process N_t, with constant intensity λ. Jump sizes are normally distributed $c_x \sim \mathcal{N}(\mu_x, \delta_x^2)$. The characteristic function of the jump size is given by

$$\theta^x(z_x) = E^{\mathbb{Q}}\left[e^{ic_x z_x}\right] = e^{i\mu_x z_x - \frac{1}{2}\delta_x^2 z_x^2} \tag{2.68}$$

[19] The formula for VIX futures is analogous to (2.53), as given in Zhang and Zhu (2006).

[20] SVJ is for Stochastic Volatility with Jumps in price.

and the compensator process is $\lambda\bar{\mu}t$, with $\bar{\mu}_{\mathsf{SVJ}} = E^{\mathbb{Q}}\left[e^{c_x} - 1\right] = \theta^x(-i) - 1$. The SVJ model is nested in the SVCJ model in (2.47), imposing $c_\sigma \equiv 0$. The proposed pricing formula leverage on the observation of Baldeaux and Badran (2014) that the introduction of jumps in returns imply a simple translation of the distribution of VIX_t, in particular:

$$p^{\mathbb{Q},\mathsf{SVJ}}_{VIX'}(y \mid x; b^{\mathsf{SVJ}}(\bar{\tau})) = p^{\mathbb{Q},\mathsf{SV}}_{\sigma}\left(y \mid x; b^{\mathsf{SV}}(\bar{\tau}) + 2\lambda\left(\theta^x(-i) - 1 - \mu_x\right)\right) \quad \text{in (2.65)} \tag{2.69}$$

where we have explicitly written model dependencies and $b^{\mathsf{SV}}(\bar{\tau})$ has been defined in (2.49). To conclude, also if the S_t dynamics features jumps, we have for the SVJ model:

$$\left.\begin{aligned} F^{\mathsf{SVJ}}(t,T) &= F^{\mathsf{SV}}(t,T) \\ C^{\mathsf{SVJ}}(K,t,T) &= C^{\mathsf{SV}}(K,t,T) \end{aligned}\right| b(\bar{\tau}) \Longrightarrow b(\bar{\tau}) + 2\lambda\left(\theta^x(-i) - 1 - \mu_x\right) \tag{2.70}$$

with $F^{\mathsf{SV}}, C^{\mathsf{SV}}$ given in (2.66). These expressions are evidently simpler to implement and faster to execute than the corresponding general formulas in (2.61) implemented with $c_\sigma \equiv 0$, that is reducing the SVCJ model to the SVJ.

They perform a calibration on few days quotes of SPX and VIX options and VIX futures term structures. Their results are unsatisfactory, especially considering the ability of the SVCJ model of capturing the different shapes of the term structure (Kokholm et al., 2015, figure 8). We conclude that they are probably facing the need of an additional volatility factor.

Sepp (2008b): the SVVJ model with jumps in variance only and deterministic ATM volatility term structure

Sepp (2008b) proposes a one factor SVVJ model in which the stochastic volatility features positive upward jumps with the aim of better capture the right skewness of the VIX distribution.[21]

$$\begin{aligned} dx_t &= \left[r - q - \lambda\bar{\mu} - \frac{1}{2}\left(\psi_t\sigma_t^2\right)\right]dt + \sqrt{\psi_t\sigma_t^2}dW_t^S \\ d\sigma_t^2 &= \alpha(\beta - \sigma_t^2)dt + \Lambda\sigma_t dW_t^\sigma + c_\sigma dN_t \end{aligned} \tag{2.71}$$

The risk-neutral correlation is constant $corr(dW_t^S, dW_t^\sigma) = \rho dt$ and jumps in variance are driven by the compound Poisson process with constant intensity λ and the sizes distributed according to an exponential distribution $c_\sigma \sim \mathcal{E}xp(\mu_\sigma)$, whose

[21] To compare with the original notation in (Sepp, 2008b, eq. 2) ψ_t corresponds to $\sigma^2(t)$ and the volatility dynamics $dV(t)$ corresponds to $d\sigma_t^2$ if $\beta = 1$ and $\sigma_0^2 = 1$. Other variables are simply renamed.

characteristic function is given by

$$\theta^{\sigma}(z_{\sigma}) = \frac{1}{1 - i\mu_{\sigma} z_{\sigma}} \tag{2.72}$$

Since VIX derivatives are not driven directly by returns dynamics, but mostly by their volatility dynamics,[22] the dynamics of the asset price process is left purely continuous. In this model, the istantaneous variance is a time-dependent affine function of the volatility level

$$V_c(\sigma_t^2) = \psi_t \sigma_t^2 \tag{2.73}$$

Given the continuous dynamics of $x_t = \log S_t$, the VIX volatility index coincides with the annualized expected diffusive quadratic variation (alternatively named expected realized variance) (Sepp, 2008b, eq. 3,4 and 8,9)

$$\begin{aligned} \left(\frac{VIX_t}{100}\right)^2 &= \frac{1}{\bar{\tau}} E^{\mathbb{Q}}\left[\int_t^{t+\bar{\tau}} V_c(\sigma_s^2) ds \middle| \mathcal{F}_t\right] \\ &= \frac{1}{\bar{\tau}} \int_t^{t+\bar{\tau}} \psi_s \left[1 + \frac{\lambda \mu_{\sigma}}{\alpha}\left(1 - e^{-\alpha(s-t)}\right)\right] ds \times \sigma_t^2 \\ &= a(t, t+\bar{\tau}; \psi_{[t,t+\bar{\tau}]}) + b(t, t+\bar{\tau}; \psi_{[t,t+\bar{\tau}]})\sigma_t^2 \end{aligned} \tag{2.74}$$

where $(a(t), b(t))$ are $(m_1(t), m_2(t))$ given in (Sepp, 2008b, eq. 8). Futures on VIX can be therefore expressed as a t-expectation of the (square root of) forward realized variance[23] (Sepp, 2008b, eq. 10)

$$\begin{aligned} \frac{F_{VIX}^{\mathsf{SVVJ}}(t,T)}{100} &= E^{\mathbb{Q}}\left[\sqrt{\left(\frac{VIX_T}{100}\right)^2} \middle| \mathcal{F}_t\right] \\ &= E^{\mathbb{Q}}\left[a(T, T+\bar{\tau}; \psi_{[T,T+\bar{\tau}]}) + b(T, T+\bar{\tau}; \psi_{[T,T+\bar{\tau}]})\sigma_T^2 \middle| \mathcal{F}_t\right] \end{aligned} \tag{2.75}$$

Function ψ_t is a piece-wise constant deterministic function that Sepp interprets coherently as an at-the-money volatility. Indeed, from the last equation, ψ_t can be calibrated to any observed VIX futures term structure $F_{VIX}^*(t,T)$. We anticipate here that the SVVJ model is a model that evidently belongs to our general

[22] We will come back to this point in Section 3.2.2 (in particular in Proposition 11) when we will present our pricing formulas (which hold for a general affine displaced volatility framework) in which it will be clear that the price of VIX derivatives is essentially driven by the volatility distribution, through the characteristic function of the volatility state vector.

[23] Which is denoted with $\bar{I}(t,T) = E^{\mathbb{Q}}\left[\int_t^T \sigma^2(t')V(t')dt' \middle| \mathcal{F}_t\right]$ in the original notation of the paper (Sepp, 2008b, eq. 3).

framework of Section (3.2) for affine models featuring a continuous spot variance $V_c(X_t)$ which is an affine function

$$V_c(X_t) = \Psi_t^\top X_t + \Phi_t \tag{2.76}$$

of the possibly multi-factor volatility state vector $X_t \in \mathbb{R}^n$. Here $X_t = \sigma_t^2$ and V_c is as in (2.73). In this perspective, the expression for the VIX / realized variance of equation (2.74) is a particular case of Proposition (8), equation (3.63) and Proposition (10). Moreover, Sepp (2008b) presents a pricing formula for a general class of derivatives written on volatility (Sepp, 2008b, eq. 5,6). We skip it from the present discussion as it is mathematically strictly related[24] to the general pricing formula for VIX derivatives that will be presented in Proposition 6 for our 2-SVCJ++ model and, more in general, in Proposition 11 for our displaced affine framework for volatility.

Lo et al. (2013) and Chen and Poon (2013): ***Is it better to add jumps to σ_t^2 or a second $\sigma_{2,t}^2$ factor?***

The contribution of the working paper Lo et al. (2013) is twofold: it proposes efficient numerical approximations to compute the price of VIX derivatives under the 2-SVCJ model and then, relying separately on VIX futures and options data, examines the relative contribution of jumps in volatility and of an additional volatility factor. The 2-SVCJ model combines the SVCJ model of Duffie et al. (2000) with the 2-SV model of Christoffersen et al. (2009)

$$\begin{aligned}
dx_t &= \left[r - q - \lambda\bar{\mu} - \frac{1}{2}\left(\sigma_{1,t}^2 + \sigma_{2,t}^2\right)\right]dt + \sigma_{1,t}dW_{1,t}^S + \sigma_{2,t}dW_{2,t}^S + c_x dN_t \\
d\sigma_{1,t}^2 &= \alpha_1(\beta_1 - \sigma_{1,t}^2)dt + \Lambda_1\sigma_{1,t}dW_{1,t}^\sigma + c_\sigma dN_t \\
d\sigma_{2,t}^2 &= \alpha_2(\beta_2 - \sigma_{2,t}^2)dt + \Lambda_2\sigma_{2,t}dW_{2,t}^\sigma
\end{aligned} \tag{2.77}$$

where the jump structure is the same of the SVCJ model in (2.47) and the two volatility factors are mutually independent and correlated with the returns process as follows

$$\begin{aligned}
&corr(dW_{i,t}^S, dW_{i,t}^\sigma) = \rho_i dt \quad \text{for } i = 1, 2 \\
&corr(dW_{i,t}^S, dW_{j,t}^\sigma) = 0 \quad \text{if } i \neq j
\end{aligned} \tag{2.78}$$

In this model, the squared VIX of (3.15) is given by

$$\left(\frac{VIX_t^{\text{2-SVCJ}}}{100}\right)^2 = \frac{1}{\bar{\tau}}\left(\sum_{i=1}^{2} a_i\sigma_{i,t}^2 + b_i\right) \tag{2.79}$$

[24]Thought slightly more general, since formulas (Sepp, 2008b, eq. 5,6) are not restricted to derivatives written directly on volatility, but e.g. on the realized variance too.

with

$$
\begin{aligned}
a_i(\bar{\tau}) &= \frac{1-e^{-\bar{\tau}\alpha_i}}{\alpha_i} \quad \text{for } i=1,2 \\
b_1(\bar{\tau}) &= \frac{\alpha_1\beta_1+\lambda\mu_{co,\sigma}}{\alpha_1}\Big(\bar{\tau}-a_1(\bar{\tau})\Big)+2\lambda\Big[\bar{\mu}-(\mu_{co,x}+\rho_J\mu_{co,\sigma})\Big] \\
b_2(\bar{\tau}) &= \beta_2\Big(\bar{\tau}-a_1(\bar{\tau})\Big)
\end{aligned}
\tag{2.80}
$$

Their approximation is based on the following identity ($\cdot' = \cdot/100$)

$$
\begin{aligned}
\frac{C_{VIX}^{\text{2-SVCJ}}(K,t,T)}{100} &= e^{-r\tau}E^{\mathbb{Q}}\left[(VIX_T'-K)^+\middle|\mathcal{F}_t\right] \\
&= e^{-r\tau}E^{\mathbb{Q}}\left[\left(\sqrt{B+V_T}-K'\right)^+\middle|\mathcal{F}_t\right] \\
&= e^{-r\tau}\left[\tilde{G}(K')-K'G_{0,-1}\left(B-K'^2\right)\right]
\end{aligned}
\tag{2.81}
$$

where

$$
\begin{aligned}
B &= \left(b_1(\bar{\tau})+b_2(\bar{\tau})\right)/\bar{\tau} \\
V_t &= \left(a_1(\bar{\tau})\sigma_{1,t}^2+b_2(\bar{\tau})\sigma_{2,t}^2\right)/\bar{\tau}
\end{aligned}
\tag{2.82}
$$

and

$$
\begin{aligned}
\tilde{G}(K) &= E^{\mathbb{Q}}\left[\sqrt{B+V_T}\,\mathcal{I}\left\{V_T\geq K^2-B\right\}\middle|\mathcal{F}_t\right] \\
G_{a,b}(y) &= E^{\mathbb{Q}}\left[e^{aV_T}\,\mathcal{I}\left\{bV_T\leq y\right\}\middle|\mathcal{F}_t\right]
\end{aligned}
\tag{2.83}
$$

The expression in (2.81) is exact and similar to the standard representation of European options payoff, due to Duffie, Pan and Singleton (Duffie et al., 2000, eq. 1.6), except for the non linear function $\tilde{G}(\cdot)$ of the V_t process (which is a linear combination of the variance factors $\sigma_{i,t}^2$). Their idea is to reconnect $\tilde{G}(K)$ to a $G_{a,b}(y)$ function approximating the non-linear payoff with an exponential curve fitted in the (k,N) interval $[V_0^{(k)},V_N^{(k)}]$ covering k standard deviation around the mean $E^{\mathbb{Q}}[V_T|\mathcal{F}_t]$. The approximation is based on a series expansion in terms of the form $G_{c_n,-1}(-V_n^{(k)})$ with $n=0,...,N$ and is given in eq. 15 of Lo et al. (2013). The VIX call option is given in their Proposition 1 and it is exact in the limit $(k,N)\to\infty$. Futures are priced setting $K=r=0$ in the corresponding call option formula. We refer to the paper for details and the lengthy expressions.

Moreover, together with nested specifications, they consider the SVCJ model as a representative of discontinuous volatility dynamics, and the 2-SV model as representative of multi-factor specification. Their dataset is made of daily VIX futures settle prices and VIX options end-of-the-day quotes from January 2007 to December 2010. Under their approximated pricing setting, they perform

separately the calibration on the data of the two markets. Their results pointed out that one-factor specifications significantly under-perform (compared to two-factors model), in reproducing *humped* VIX futures term structures (an is example given in figure 3). The intuition they provide for this is that (approximately) the term structure $F_{VIX}(t, t+\tau)$ produced by one-factor models can only be monotonically increasing (decreasing) in the horizon $\tau = T - t$ when σ_t^2 is smaller (greater) than the long-run effective mean (Lo et al., 2013, Lemma in App. B)

$$\beta_{eff} = \beta + \lambda \frac{\mu_{co,\sigma}}{\alpha} \tag{2.84}$$

Moreover, one-factor models like the SVCJ model can only generate monotonic daily changes between term structures $F_{VIX}(t, \cdot)$ and $F_{VIX}(t+1, \cdot)$ (Lo et al., 2013, Prop. 2 in App. B). Coming to the pricing of VIX options, using the nested SVJ model in (2.67) as benchmark, they find that adding jumps in σ_t^2 provide only a minor improvement in terms of pricing error, whereas the introduction of an additional factor produces remarkably lower RMSEs. From the experience of this thesis, we think that the conclusions in this paper showing an almost negligible impact of jumps in variance are likely to be biased from the separate use of the two VIX derivatives datasets and since the authors do not consider at all options on S&P500, thought the strong need for a multi-factor structure in volatility is perfectly in line with literature (Andersen et al., 2002; Kaeck and Alexander, 2012; Mencía and Sentana, 2013, among many).

The 2-SVCJ model (along with nested specifications) have been considered also by Chen and Poon (2013). They concentrate on the term structure of the correlation between VIX futures $F(t, T)$ of different maturities, which is stantaneously

$$\rho_t^{1,2} = \frac{E^{\mathbb{Q}}\left[dF(t,T_1)dF(t,T_2)\middle|\,\mathcal{F}_t\right]}{\sqrt{E^{\mathbb{Q}}\left[dF(t,T_1)dF(t,T_1)\middle|\,\mathcal{F}_t\right]E^{\mathbb{Q}}\left[dF(t,T_2)dF(t,T_2)\middle|\,\mathcal{F}_t\right]}} \tag{2.85}$$

where, under the 2-SVCJ, $F(t, T)$ solve the SDE in (Chen and Poon, 2013, Sec. 4.2.2). This has a direct implication on the effectiveness of hedging strategies, as it is possible to hedge a futures contract on VIX with other futures contracts of different maturities, and futures contracts on VIX are the somehow natural hedging tool for options on VIX, being their underlying. Their study analytically shows that one-factor models always imply a perfect correlation $\rho_t^{1,2} \approx 1$ between VIX futures of different maturities (at odds with the market), whereas the addition of another volatility factor is able to enrich considerably the possible shapes of correlation term structure produced by the model.

Branger et al. (2014): the stochastic volatility of variance 2-SVSVJ model

In their analysis, Branger et al. (2014) propose an affine framework to price volatility derivatives and specialize it considering a model with stochastic volatility of variance and gamma distributed jumps in variance. We will come back on their general framework in Section 3.2, when we will introduce our displaced affine framework. The volatility dynamics of the 2-SVSVJ model is

$$\begin{aligned} d\sigma_t^2 &= \alpha(\beta - \sigma_t^2)dt + \Lambda\omega_t dW_{1,t}^{\sigma} + c_\sigma dN_t \\ d\omega_t^2 &= \alpha_\omega(\beta_\omega - \omega_t^2)dt + \Lambda_\omega \omega_t dW_t^{\omega} \end{aligned} \tag{2.86}$$

where the risk neutral correlation between variance σ_t^2 and its stochastic volatility ω_t^2 is described by

$$corr(dW_t^{\sigma}, dW_t^{\omega}) = \rho_{\sigma\omega}dt \tag{2.87}$$

and jumps in variance are driven by the compound Poisson process with intensity affine $\lambda = \lambda_{0,\sigma} + \lambda_{1,\sigma}\sigma_t^2$ and the sizes are distributed according to Gamma distribution of shape ν and mean μ_σ

$$c_\sigma \sim \Gamma\left(\nu, \frac{\mu_\sigma}{\nu}\right) \tag{2.88}$$

whose characteristic function is given by

$$\theta^{\sigma}(z_\sigma) = \frac{1}{\left(1 - i\frac{\mu_\sigma}{\nu}z_\sigma\right)^{\nu}} \tag{2.89}$$

In their empirical analysis, the authors state that the returns $\log S_t$ dynamics lacks of jumps, but leave it otherwise deliberately unspecified.[25] They test the 2-SVSVJ model on the average VIX option implied volatility surface of the period from February 2006 to December 2011.

Their results show that both variance jumps and a stochastic volatility of variance are important to reconcile empirical regularities with the theoretical models. Positive shocks to the instantaneous variance increase both its mean and volatility, contributing both to increase the overall level of the surface, and to make the skew upward sloping. In terms of VIX distribution, jumps in variance introduce right skewness. This is particularly pronounced[26] since the Gamma distribution with shape parameter $\nu < 1$ has higher variance, skewness and kurtosis compared to the nested exponential distribution (which is a Gamma with $\nu \equiv 1$).

[25] The correlation structure between the Wieners W_t^S and W_t^{σ} is not required in an analysis based on VIX derivatives only. We will come back on the role of the correlation structure of the model in Appendix A.7.

[26] As compared for example to a SVCJ model, which features exponentially distributed jumps in σ_t^2.

Moreover, the presence of stochastic volatility of variance factor ω_t^2 increases the persistency of the effect of the shocks due to jumps, which has an impact on the long-term options and overally contributing to increasing the kurtosis of the VIX distribution (more weight on both tails of the pdf, compared to a model with $\omega_t^2 = \sigma_t^2$). Finally, the strong positive correlation $\rho_{\sigma\omega}$ between variance σ_t^2 and its stochastic volatility ω_t^2 (they find $\rho_{\sigma\omega} = 0.88$) makes OTM options on VIX rather expensive,[27] in turn contributing to the upward sloping smile.

Bardgett et al. (2013): the stochastic mean-reverting level of volatility 2-SMRSVCJ model

Bardgett et al. (2013) leverage on the widespread literature results that have shown the inadequate limitations to the volatility dynamics induced by one-factor models and that adding an additional factor to the Heston (1993) model, thought increasing the complexity of the model, is a need to provide an accurate description of the volatility dynamics (Andersen et al., 2002; Bates, 2012; Egloff et al., 2010; Kaeck and Alexander, 2012; Mencía and Sentana, 2013, among many). They overcome the limitations of one-factor models in their two-factor model 2-SMRSVCJ (Bardgett et al., 2013, Sec. 2.1)

$$\begin{aligned} dx_t &= \left(r - q - \lambda\bar{\mu} - \frac{1}{2}\sigma_t^2\right)dt + \sigma_t dW_t^S + c_x dN_t \\ d\sigma_t^2 &= \alpha(\beta_t - \sigma_t^2)dt + \Lambda\sigma_t dW_t^\sigma + c_\sigma dN_t \\ d\beta_t &= \bar{\alpha}(\bar{\beta} - \beta_t)dt + \bar{\Lambda}\sqrt{\beta_t}dW_t^\beta + c_\beta dN_t' \end{aligned} \tag{2.90}$$

The only nonzero correlation is $corr(dW_t^S, dW_t^\sigma) = \rho dt$ and jumps are driven by the two independent compound Poisson processes N_t and N_t' with affine intensities $\lambda = \lambda_0 + \lambda_1\sigma_t^2 + \lambda_2\beta_t$ and $\lambda' = \lambda_0' + \lambda_1'\beta_t$, respectvely. The sizes are independent and distributed according to $c_x \sim \mathcal{N}(\mu_{co,x}, \delta_{co,x}^2)$, $c_\sigma \sim \mathcal{E}xp(\mu_{co,\sigma})$ and $c_\beta \sim \mathcal{E}xp(\mu_\beta)$. The characteristic function of gaussian price jumps, $\theta^x(z_{co,x})$, was already given for the SVJ model in (2.68) (the compensator term is $\bar{\mu} = \theta^x(-i) - 1$), whereas exponential jumps in volatility are described by the same jump characteristic function of the SVVJ model of Sepp (2008b), given in (2.72).

They leverage on the Fourier Cosine Expansion, introduced by Fang and Oosterlee (2008), to develop in Fourier series the VIX call option payoff, in such a way

[27] In particular more expensive compared to their benchmark Black (1976) prices, as computed with a Whaley (1993) model (2.16) with comparable volatility of VIX_t. This is somehow the specular of the phenomenon observed in equity options in which a negative correlation ρ between returns $\log S_t$ and stochastic volatility σ_t^2 in a Heston (1993) model makes the prices of ITM equity options higher than the benchmark Black and Scholes (1973) prices with comparable returns volatility.

that under their model (Bardgett et al., 2013, eq. 15)

$$C_{VIX}^{\text{2-SMRSVCJ}}(K,t,T) = 100 \times e^{-r\tau}\left(\frac{1}{2}A_0U_0 + \sum_{n=1}^{N} A_nU_n\right) \tag{2.91}$$

Coefficients A_n depend marginally on the jump structure of returns, through the affine expression of the squared VIX index (Bardgett et al., 2013, eq. 9,10), and strongly on the conditional CF of the volatility state vector $(\sigma_t^2, \beta_t)^\top$

$$f_{\sigma,\beta}(z_\sigma, z_\beta; \sigma_t^2, \beta_t, t, T) = E^{\mathbb{Q}}\left[e^{iz_\sigma\sigma_T^2 + iz_\beta\beta_T}\middle|\mathcal{F}_t\right] \tag{2.92}$$

where $z_\sigma, z_\beta \in \mathbb{C}$. $f_{\sigma,\beta}$ is computable in closed-form and takes the usual exponential-affine form (Bardgett et al., 2013, Prop. 2.2 and App. A and C). Coefficients U_n are Cosine transforms of the rescaled payoff ($x = VIX' = VIX/100, k = K' = K/100$)

$$\frac{w_C(x^2)}{100} = \left(\sqrt{x^2} - k\right)^+ \tag{2.93}$$

which have the functional form

$$\begin{aligned} U_n &= \int_a^b (\sqrt{x}-k)^+ cos(\omega_n(x-a))dx \\ &= \frac{2}{b-a}\,\mathrm{Re}\left\{e^{-i\omega_n a}\left[\frac{\sqrt{b}e^{-i\omega_n b}}{i\omega_n} + \sqrt{\pi}\frac{erf(\sqrt{-i\omega_n b}) - erf(k\sqrt{-i\omega_n})}{2(-i\omega_n)^{3/2}}\right]\right\} \end{aligned} \tag{2.94}$$

if $n \geq 1$ and similarly for U_0. The parameters $\omega_n = n\pi/b - a$ are angular frequencies and the expansion interval $[a, b]$ is a support interval for the distribution $p^{\mathbb{Q}}_{VIX'}$ of VIX'_T that have to be selected. The pricing formula is exact in the limits of $N, a, b \to \infty$. For details and derivation refer to their Proposition 2.3 and Appendix B.

For their empirical analysis they consider a continuous β_t factor ($c_\beta \equiv 0$). The dataset for daily calibrations consists of closing prices of European SPX and VIX options from March 2006 to October 2010. They jointly calibrate the 2-SMRSVCJ, together with several nested specifications, to the cross Section of prices in some chosen dates.[28] From their analysis it can be concluded that jumps in the return $\log S_t$ and variance σ_t^2 processes are needed to better reproduce the right tail of the variance distribution and short-maturity options. Moreover, the introduction

[28] Their analysis goes far beyond a simple calibration exercise. They make jointly use also of times series data of the S&P500 and VIX indexes and estimate real $\mathbb{P}$ and risk-neutral $\mathbb{Q}$ parameters, along with equity and variance risk-premia, adopting a particle-filtering methodology (Pitt and Shephard, 1999). Ours is a deliberately partial review of their contribution.

of a stochastic level of reversion β_t for the variance helps to better represent the tails of the returns distribution and the term structure of S&P 500 and VIX option prices.

Consistent non-affine models

We will now give an account of the main non-affine models aiming at reproducing the peculiar properties of the VIX options surface and/or at jointly calibrating the two SPX and VIX markets. We usually refer to the original papers for the details concerning the pricing formulas as are usually involved and often require rather sophisticated Monte-Carlo techniques.to get implemented.

Gatheral (2008) and Bayer et al. (2013): the double mean-erverting CEV model DMR

Gatheral (2008) proposes a double mean-reverting model, in which each volatility factor follows a CEV dynamics

$$\begin{aligned} \frac{dS_t}{S_t} &= \sigma_t dW_t^S \\ d\sigma_t^2 &= \alpha(\beta_t - \sigma_t^2)dt + \Lambda(\sigma_t^2)^{\gamma_1} dW_t^\sigma \\ d\beta_t &= \bar{\alpha}(\bar{\beta} - \beta_t)dt + \bar{\Lambda}(\beta_t)^{\gamma_2} dW_t^\beta \end{aligned} \tag{2.95}$$

where the Wieners are allowed to be correlated. The DMR model features a short term variance level σ_t^2 that reverts to a moving level β_t at rate α. β_t reverts to the long term level $\bar{\beta}$ at the slower rate $\bar{\alpha} < \alpha$. This model reduces to the 2-SV model of Christoffersen et al. (2009) if $\gamma_1 = \gamma_2 = 0.5$ and to a double log-normal model if $\gamma_1 = \gamma_2 = 1$. Testing calibrations performed on daily SPX and VIX surfaces suggest that $\gamma_1 \approx 1$, which is consistent with the stylized fact that volatility should be roughly log-normally distributed and that the implied VIX distribution of the 2-SV model presents too few right skew and a too fat left tail around 0.

Closed-form pricing expressions are not available and the calibration of the DMR model is rather involved: parameters $(\alpha, \bar{\alpha}, \bar{\beta})$ are calibrated interpolating/extrapolating/integrating the t-time series of option strips that replicate the fair value $SW_{t,T}$ of variance swaps (check the variance swap rate replication in (3.58)), which, under the diffusive dynamics S_t, can be expressed as the realized variance

$$SW_{t,T} = \frac{1}{T-t}[\log S]_{t,T}^c = \frac{1}{T-t} E^{\mathbb{Q}} \left[\int_t^T \sigma_s^2 ds \middle| \mathcal{F}_t \right] \tag{2.96}$$

which can be easily computed as under the DMR model (Bayer et al., 2013, eq. 2.3). This allows also to estimate the volatility state variables σ_t^2, β_t with a linear regression of $SW_{t,T}$. While the elasticity parameters (γ_1, γ_2) can be estimated

through a SABR calibration, the other parameters (vol-of-vol $\lambda, \bar{\lambda}$ and correlations between Wieners) are Monte-Carlo estimated.

Cont and Kokholm (2013): a consistent framework for index options and volatility derivatives

We give an extremely partial and untechnical review of their work Cont and Kokholm (2013). The fundamental object of their framework is the Forward Variance Swap rate V_t^i, seen at time t for the forward interval $[T_i, T_{i+1}]$. In continuous time it is the time-t expected value of the forward total quadratic variation $[\log S]_{T_i,T_{i+1}}$ of the returns process S_t in the $[T_i, T_{i+1}]$ interval[29]

$$V_t^i = \frac{1}{T_{i+1} - T_i} E^{\mathbb{Q}} \left[[\log S]_{T_i,T_{i+1}} \middle| \mathcal{F}_t \right] \tag{2.97}$$

Imposing a Lévy specification for the dynamics of $V_t^i = V_0^i e^{X_t^i}$, this in turn imposes restrictions on the compatible dynamics of the return process $\log S_t$. Having directly modeled a quantity related to volatility, this enables closed form solutions for futures and options on VIX, as long as the conditional characteristic function of the exponent X_t^i is available (it is given for various jump specifications in their Appendix). Options on the underlying S_t index instead, need Monte-Carlo simulations of the path of V_t^i to be priced (Cont and Kokholm, 2013, eq. 3.17).

Papanicolaou and Sircar (2014): sharp regime-shifts make Heston smiling

Papanicolaou and Sircar (2014) extend the familiar Heston (1993) model adding sharp-regime shifts to the realized volatility which has also impact on jumps in price, featuring a regime-dependent jump structure.

$$\begin{aligned} dx_t &= \left(r - \frac{1}{2} f^2(\theta_t)\sigma_t^2 - \delta\nu(\theta_{t-}) \right) dt + f(\theta_t)\sigma_t dW_t^S - \lambda(\theta_t) c_x dN_t \\ d\sigma_t^2 &= \alpha(\beta - \sigma_t^2)dt + \Lambda\sigma_t dW_t^\sigma \end{aligned} \tag{2.98}$$

The discrete variable $\theta_t \in \{1, 2, 3\}$ represents the state (low, medium and high) of volatility and is driven by a Markov-Chain Q_{mn} with δ-slow time scale

$$\frac{d}{dt} p_\theta^{\mathbb{Q}}(\theta_t = n) = \sum_{m=1}^{3} Q_{mn} p_\theta^{\mathbb{Q}}(\theta_t = m) \quad n = 1, 2, 3 \tag{2.99}$$

[29] See also equation (3.34), in which we defined the *spot* variance swap rate $SW_{t,T}$ (which is obtained from V_t^i if $T_i = t, T_{i+1} = T$), and discussion in Section 3.2.1.

These changes of state enters in the returns' dynamics via the purely discontinuous process $dN_t = \mathcal{I}\{\theta_t \neq \theta_{t-}\}$ and modulate the realized variance through function $f(\theta_t)$. Jump sizes are driven, both in amplitude and in direction, by function $\lambda(\theta_t)$, which modulates positive exponential jumps $c_x \sim \infty$. Function $\delta\nu(\theta_{t-})$ compensate jumps.

The tractability of their model arise from the fact that options prices P can be approximated around the original Heston price P_0 by a power series of the small δ time scale (Papanicolaou and Sircar, 2014, eq. 9)

$$P \approx P_0 + \delta P_1 + \delta^2 P_2 \tag{2.100}$$

Stock options are easily in power series of the price Fourier transform $\hat{P}$ (Papanicolaou and Sircar, 2014, eq. 12 and 13)

$$\hat{P} \approx \hat{P}_0 + \delta \hat{P}_1 + \delta^2 \hat{P}_2 \tag{2.101}$$

To price options on VIX, it is possible to write down explicitly the transition density of the effective volatility process which is, as a density, the product of two independent densities: the pdf $p^{\mathbb{Q}}_{\sigma}$ of the diffusion σ^2_t and the Markov Chain transition density $p^{\mathbb{Q}}_{\theta}$ of the state process θ_t (Papanicolaou and Sircar, 2014, Sec. 4.2)

$$p^{\mathbb{Q}}_{\sigma}\left(\sigma^2_T = y \middle| \, \sigma^2_T = y\right) \times p^{\mathbb{Q}}_{\theta}\left(\theta_T = m \middle| \, \theta_T = n\right) \tag{2.102}$$

This pdf, integrated against the payoff of the option w.r.t. y and summed over the final possible states $m = 1, 2, 3$, gives the conditional expected value of the payoff, that is the price.

A joint SPX and VIX option calibration performed on few selected dates, shows that regime shifts helps capturing the positive sloping skew of options on VIX, consistently with the SPX negative one.

To conclude, other model which is ought to mention are:

- the affine Lévy model of Kallsen et al. (2011) which allows to joint price derivatives on the underlying and it volatility;
- the 3/2 consistent stochastic volatility model of Baldeaux and Badran (2014) which is able to capture the upward sloping smile of VIX options and, augmented with jumps in price, is able to consistently fit short-term vanilla options too;
- the standalone analysis of Goard and Mazur (2013) which test the 3/2 diffusion as a direct specification for the VIX index dynamics, in which the changes in vol-of-vol are more sensible to the actual level of the index.

Chapter 3

The Heston++ model

The empirical evidences and the results of the literature, discussed and reviewed in the previous Chapter, enable us to design and motivate our model, whose first objective is the consistently pricing of both vanilla S&P500 options and VIX derivatives. We make the following requirements to our candidate model:

- **Reliability**: it should be able to express an outstanding ability in matching market prices and to guarantee it in several different market scenarios.

- **Consistency**: being *reliable*, it should be able to accommodate consistently and in a financially convincing way the rather different features of the equity and volatility markets.

- **Tractability**: being *consistent* with both markets, it should still preserve the tractability usually featured by models designed for pricing equity only and extend it to the class of volatility derivatives.

The consistency requirement induces us to exclude the *standalone* models presented in Section 2.2.1 as we primarily require an adequate description and control of the S&P500 dynamics. In this, models that directly specify the dynamics of VIX_t are not necessarily incompatible with the SPX vanilla surface (Mencía and Sentana, 2013). Nevertheless, the requested replicability of the VIX index in terms of vanilla options is not guaranteed modeling directly its dynamics (Branger et al., 2014). We therefore decided to opt for a *consistent* model for the underlying S&P500 index dynamics S_t. This in turn induces a dynamics for the VIX_t index which is by default consistent with the market definition of VIX.[1]

[1] Or at least with its continuous time limit, as discussed in Section 3.2.1.

As discussed in Section 2.2.2, the academic (and practitioner) interest around consistent models is primarily concerned with accommodating the rather new features presented by derivatives written on VIX with models designed for the equity market. The several different term structures experienced by futures, the high implied volatility of options on VIX and the upward sloping smile of their implied surface, severely challenged the consistency and reliability of often standard and benchmark models such as the Heston model (Gatheral, 2008). One-factor models pose too strict limitation to the volatility dynamics and an additional volatility factor is likely to provide a more accurate description (Andersen et al., 2002; Bates, 2012; Egloff et al., 2010; Kaeck and Alexander, 2012; Mencía and Sentana, 2013, among many).

Multi-factor models have been found able to better capture the different shapes and correlation of the VIX term structure (Chen and Poon, 2013; Lo et al., 2013) and a second factor, added to a Heston dynamics, has been introduced as a stochastic volatility of variance factor (Branger et al., 2014) or as a stochastic mean reverting level (Bardgett et al., 2013). The enhanced specification of the volatility of volatility provided by the additional factor is likely to produce the upward sloping smile of the VIX implied surface and/or to better capture its term structure.

Moreover, the distribution of VIX has been found empirically more skewed than a χ^2 like distribution induced by the CIR dynamics of the stochastic volatility factor of a Heston model and a direct channel to increase the right skewness of the model distribution of VIX can be represented by the addition of jumps in the volatility dynamics (Sepp, 2008b).

Our model is in the line of the *consistent* approach. We specify a single dynamics for the price process, and use this dynamics to price vanilla options together with VIX futures and options and employ an affine multi-factor specification with jumps.

We augment the time homogeneous dynamics of the model with a deterministic shift extension ϕ_t (also called a *displacement*) to the stochastic volatility σ_t^2, as already introduced by (Pacati et al., 2014), so that the effective instantaneous volatility V_t driving the model is given by

$$V_t = \sigma_t^2 + \phi_t \tag{3.1}$$

The class of models obtained with the extension is labelled Heston++, since it parallels the structure of the CIR++ model of Brigo and Mercurio (2001), in which a deterministic function ϕ_t is added to a time-homogeneous spot-rate model x_t, such that the instantaneous short rate described by the model is

$$r_t = x_t + \phi_t \tag{3.2}$$

and the extension is meant to fit the term structure of interest rates. Pacati et al. (2014) show that the deterministic shift can dramatically improve the calibration

of the term structure of at-the-money vanilla options, thus improving sensibly the fit of the whole surface of vanilla.

In this paper, we extend their model (by adding jumps in volatility) and show that the deterministic shift ϕ_t provides the necessary flexibility to describe the term structure of VIX futures and the surface of VIX options, without compromising the fit on vanilla options, which makes our model eventually *reliable*. Moreover, this flexibility comes at no additional expense in terms of both analytical and numerical complexity, compared to a non-displaced specification, which makes it also *tractable*.

Further, the success of our proposed specification to jointly fit the vanilla and VIX surfaces (two "smiles" at once) also allows to exploit the additional information content provided by variance derivatives to learn about the features of the price dynamics. Overall, we provide strong support for the contemporaneous presence of two kinds of jumps in volatility, the first being correlated with jumps in the index (typically, accounting for market downturns accompanied by a spike in volatility, as also empirically supported by Todorov and Tauchen (2011) and Bandi and Renò (2015)), and the second being independent from price movements and accounting for spikes in volatility not accompanied by changes in the index. Our empirical findings suggest then that traders in option markets hedge against both sources of risk. In particular, idiosyncratic jumps in volatility appear to be particularly relevant for the pricing of VIX options.

The Chapter is structured as follows. In Section 3.1 we specify the model adopted in our empirical investigations together with the closed-form pricing expressions for SPX vanilla options and VIX index and derivatives. In Section 3.2 we introduce a general affine framework which allows for a general affine transformation of the instantaneous volatility.

3.1 Pricing VIX derivatives with the Heston++ model

In this Section we introduce the Heston++ model for the dynamics of the underlying price. It is an affine model with a deterministic shift extension in the spirit of Brigo and Mercurio (2001). We then provide pricing formulas for equity and VIX futures and options.

3.1.1 Model specification

We consider a filtered probability space $(\Omega, \mathcal{F}, \{\mathcal{F}_t\}_{t\geq 0}, \mathbb{Q})$, satisfying usual assumptions. Under the risk-neutral measure $\mathbb{Q}$, we specify the evolution of the

logarithmic price of the underlying $x_t = \log S_t$ as follows

$$\begin{aligned} dx_t &= \left[r - q - \lambda\bar{\mu} - \frac{1}{2}\left(\sigma_{1,t}^2 + \phi_t + \sigma_{2,t}^2\right)\right]dt + \sqrt{\sigma_{1,t}^2 + \phi_t}\, dW_{1,t}^S + \sigma_{2,t} dW_{2,t}^S + c_x dN_t \\ d\sigma_{1,t}^2 &= \alpha_1(\beta_1 - \sigma_{1,t}^2)dt + \Lambda_1\sigma_{1,t} dW_{1,t}^\sigma + c_\sigma dN_t + c'_\sigma dN'_t \\ d\sigma_{2,t}^2 &= \alpha_2(\beta_2 - \sigma_{2,t}^2)dt + \Lambda_2\sigma_{2,t} dW_{2,t}^\sigma \end{aligned} \tag{3.3}$$

where r is the short rate, q is the continuously compounded dividend yield rate, and in which the risk-neutral dynamics of the index is driven by continuous and discontinuous shocks, modeled by the Wiener processes $W_{1,2}^S, W_{1,2}^\sigma$ and the independent Poisson processes N, N' respectively. The short rate and the dividend rate are kept constant for simplicity, but could be easily be made time-varying, for example as in Bakshi et al. (1997). The first volatility factor is *displaced*, as in Pacati et al. (2014), by a sufficiently regular deterministic function ϕ_t which verifies:

$$\phi_t \geq 0 \text{ and } \phi_0 = 0, \tag{3.4}$$

and $\alpha_i, \beta_i, \Lambda_i$ are non-negative constants. In this (and following) Chapter we generically label this model as Heston++. Alternatively, we refer to it also as 2-SVCVJ++ model, stressing its dynamical properties[2] and eventually to distinguish from the several nested specifications that will be discussed in Section 3.1.2 and will be as well part of the empirical analysis presented in the next Chapter. The corresponding dynamics of the index S_t is, by Itō's lemma:

$$\frac{dS_t}{S_{t-}} = (r - q - \lambda\bar{\mu})\, dt + \sqrt{\sigma_{1,t}^2 + \phi_t} dW_{1,t}^S + \sigma_{2,t} dW_{2,t}^S + (e^{c_x} - 1)\, dN_t \tag{3.5}$$

All correlations among Wiener processes are zero, with the exception of the following ones, which are defined as

$$corr(dW_{1,t}^S, dW_{1,t}^\sigma) = \rho_1 \sqrt{\frac{\sigma_{1,t}^2}{\sigma_{1,t}^2 + \phi_t}} dt \tag{3.6}$$

$$corr(dW_{2,t}^S, dW_{2,t}^\sigma) = \rho_2 dt \tag{3.7}$$

where $\rho_1, \rho_2 \in [-1, 1]$ are constants. This choice guarantees that the model is affine according to the specification analysis of Dai and Singleton (2002), extended by (Cheridito et al., 2010; Collin-Dufresne et al., 2008). Indeed, with this correlation structure imposed, it is possible to write the diffusion matrix $\sigma(t, \sigma_{1,t}^2, \sigma_{2,t}^2)$ in the

[2] 2-factor Stochastic Volatility model with Co-jumps between price and volatility and idiosyncratic Volatility jumps.

extended canonical form:

$$\begin{aligned}
&\sigma(t,\sigma_{1,t}^2,\sigma_{2,t}^2) = \Sigma\sqrt{V(t,\sigma_{1,t}^2,\sigma_{2,t}^2)} \\
&= \begin{pmatrix} \Lambda_1 & 0 & 0 & 0 \\ 0 & 0 & \Lambda_2 & 0 \\ \rho_1 & \sqrt{1-\rho_1^2} & \rho_2 & \sqrt{1-\rho_2^2} \end{pmatrix} \begin{pmatrix} \sqrt{\sigma_{1,t}^2} & 0 & 0 & 0 \\ 0 & \sqrt{\sigma_{1,t}^2 + \frac{\phi_t}{1-\rho_1^2}} & 0 & 0 \\ 0 & 0 & \sqrt{\sigma_{2,t}^2} & 0 \\ 0 & 0 & 0 & \sqrt{\sigma_{2,t}^2} \end{pmatrix}
\end{aligned} \tag{3.8}$$

Appendix A.7, under the extended displaced affine framework introduced in Section 3.2, elaborates on the meaning of the restrictions in the correlation structure, such as (3.6), to be imposed in displaced affine models in order to preserve and extend the affinity of the un-displaced model toward the displaced specification.

The Poisson processes N_t and N_t' are independent (between them) and also independent from all the Wiener processes. Their intensities are given by the constant parameters λ and λ' respectively. They drive jumps in price and jumps in volatility. The first Poisson process N_t is responsible for correlated jumps, occurring simultaneously in price and volatility, with sizes c_x and c_σ respectively. The second Poisson process N_t' is instead responsible for idiosyncratic jumps in volatility, with size c_σ', independent from all other shocks. Jumps in volatility are exponentially distributed, with parameters $\mu_{co,\sigma}$ and $\mu_{id,\sigma}$ expressing the mean of correlated and idiosyncratic jumps respectively. Jumps in price are conditionally (to jumps in volatility) normally distributed with conditional mean $\mu_x + \rho_J c_\sigma$ and variance δ_x^2. The characteristic functions of the jump sizes are thus given by:

$$\begin{aligned}
\theta^{co}(z_x, z_\sigma) &= E^{\mathbb{Q}}\left[e^{ic_x z_x + ic_\sigma z_\sigma}\right] = \frac{e^{i\mu_x z_x - \frac{1}{2}\delta_x^2 z_x^2}}{1 - i\mu_{co,\sigma}\left(z_\sigma + \rho_J z_x\right)} \\
\theta^{id}(z_\sigma') &= E^{\mathbb{Q}}\left[e^{ic_\sigma' z_\sigma'}\right] = \frac{1}{1 - i\mu_{id,\sigma} z_\sigma'}
\end{aligned} \tag{3.9}$$

where $z_x, z_\sigma, z_\sigma' \in \mathbb{C}$. Jumps characteristic functions in equation (3.9) can be extended to the complex plane as long as, respectively

$$\begin{aligned}
\mathrm{Im}(z_\sigma + \rho_J z_x) &> -1/\mu_{co,\sigma} \\
Im(z_\sigma') &> -1/\mu_{id,\sigma}
\end{aligned} \tag{3.10}$$

This lead to the parameter restriction $\rho_J < 1/\mu_{co,\sigma}$ which is assumed throughout the present analysis and which is often *a fortiori* satisfied by market calibrated correlation parameter, as it is usually found $\rho_J \leq 0$. We define $\bar{\mu} = E^{\mathbb{Q}}\left[e^{c_x} - 1\right] = \theta^{co}(-i, 0) - 1$, so that the price jump compensator is $\lambda\bar{\mu}t$.

3.1.2 Nested models

The Heston++ model (3.3) belongs to the affine class of (Duffie et al., 2000). In case of no displacement ($\phi_t \equiv 0$), the model nests several models already analyzed in the literature and introduced in Section 2.2.1.
Imposing $\sigma_{2,t} \equiv 0$, several one-factor specifications can be obtained: the standard Heston SV model of (2.44) if $N_t \equiv N'_t \equiv 0$ is additionally imposed; if $N'_t \equiv z_\sigma \equiv 0$ (i.e. allowing for log-normal jumps in price only) the SVJ model in (2.67) is recovered, which is considered for example by (Bakshi et al., 1997; Bates, 1996) and introduced by Duffie et al. (2000) as a nested specification of the SVCJ model in (2.47), which features correlated co-jumps in price and volatility.
The SVCJ model, extensively studied in the equity pricing literature (Broadie et al., 2007; Eraker, 2004; Eraker et al., 2003, among many), is obtained by switching off the N'_t Poisson process and imposing $\sigma_{2,t} \equiv 0$. This model is considered for the pricing of futures and options on VIX by Kokholm et al. (2015); Lian and Zhu (2013); Lin (2007); Zhu and Lian (2012).
If $N_t \equiv \sigma_{2,t} \equiv 0$, we obtain the SVVJ model of equation (2.71) which features idiosyncratic jumps in volatility and is introduced in Duffie et al. (2000) as nested in the SVCJ model switching off jumps in price. The SVVJ model is adopted by Sepp (2008b) for VIX option pricing extended with a local volatility term.
Two-factor specifications can be obtained letting $\sigma_{2,t} > 0$: the double Heston 2-SV model of Christoffersen et al. (2009) is obtained imposing no jumps $N_t \equiv N'_t \equiv 0$. If $N'_t \equiv z_\sigma \equiv 0$, the 2-SVJ of Bates (2000) with constant jump intensity is obtained. Finally if $N'_t \equiv 0$ we obtain the 2-SVCJ model of equation (2.95) considered by Chen and Poon (2013); Lo et al. (2013) for VIX derivatives pricing. The corresponding displaced models are obtained letting $\phi_t \geq 0$ and are labelled as their $\phi_t \equiv 0$ counterparts, with the suffix ++. Without restrictions, we label the model by 2-SVCVJ. The unrestricted model has in total 17 parameters, that can be schematically described as follows

$$
\begin{aligned}
S_t: &\qquad \overbrace{(\mu_x, \delta_x^2)}^{\mathcal{N}\ jumps} \quad \underbrace{(\lambda, \rho_J)} \\
\sigma_{1,t}^2: &\quad \underbrace{(\alpha_1, \beta_1, \Lambda_1, \sigma_{1,0}^2)}_{\mathsf{SV}factor} \qquad \underbrace{\overbrace{\mu_{co,\sigma}}^{co-} \quad \overbrace{(\lambda', \mu_{id,\sigma})}^{idiosync-}}_{\mathcal{E}xp\ jumps} \\
\sigma_{2,t}^2: &\quad \overbrace{(\alpha_2, \beta_2, \Lambda_2, \sigma_{2,0}^2)}
\end{aligned}
$$

plus the function ϕ_t.

3.1.3 SPX and VIX derivatives pricing

In this Section we generically label with $\mathcal{H}$ the model 2-SVCVJ and its nested specifications described in the previous Section and with $\mathcal{H}$++ the 2-SVCVJ++ model in (3.3) and its nested specifications ($\mathcal{H}$ models with $\phi_t \geq 0$). The analytical tractability of the displaced models $\mathcal{H}++$ directly stems from the properties of non-displaced specifications $\mathcal{H}$. The following Lemma summarizes the relation among the log-price and volatility characteristic functions of the $\mathcal{H}$ and $\mathcal{H}++$ models. All proofs and mathematical detailes are contained in Appendix A.1.

Lemma 2. *Under the $\mathcal{H}$++ models, the conditional characteristic function of the price returns $f_x^{\mathcal{H}++}(z) = E^{\mathbb{Q}}\left[e^{izx_T}\middle|\mathcal{F}_t\right]$ and of the two stochastic volatility factors $f_\sigma^{\mathcal{H}++}(z_1,z_2) = E^{\mathbb{Q}}\left[e^{iz_1\sigma_{1,T}^2+iz_2\sigma_{2,T}^2}\middle|\mathcal{F}_t\right]$ are given by:*

$$\begin{aligned} f_x^{\mathcal{H}++}(z;x_t,\sigma_{1,t}^2,\sigma_{2,t}^2,t,T,\phi) &= f_x^{\mathcal{H}}(z;x_t,\sigma_{1,t}^2,\sigma_{2,t}^2,\tau)e^{-\frac{1}{2}z(i+z)I_\phi(t,T)} \\ f_\sigma^{\mathcal{H}++}(z_1,z_2;\sigma_{1,t}^2,\sigma_{2,t}^2,\tau) &= f_\sigma^{\mathcal{H}}(z_1,z_2;\sigma_{1,t}^2,\sigma_{2,t}^2,\tau) \end{aligned} \tag{3.11}$$

where $\tau = T-t$, $z, z_1, z_2 \in \mathbb{C}$ and $I_\phi(t,T) = \int_t^T \phi_s ds$.

We can thus provide closed-form pricing formulas for vanilla options and VIX derivatives for any of the $\mathcal{H}$++ model based on the conditional characteristic functions of the log-index and volatility factors under the corresponding $\mathcal{H}$ model. For both classes of derivatives, we use the results of Lewis (2000, 2001) which turn out to be convenient for numerical implementation.

Proposition 4. *Under the $\mathcal{H}$++ models, the arbitrage-free price at time t of a European call option on the underlying S_t, with strike price K and time to maturity $\tau = T-t$, is given by*

$$C_{SPX}^{\mathcal{H}++}(K,t,T) = S_t e^{-q\tau} - \frac{1}{\pi}\sqrt{S_t K}e^{-\frac{1}{2}(r+q)\tau}\int_0^\infty \mathrm{Re}\left[e^{iuk}f_x^{\mathcal{H}}\left(u-\frac{i}{2}\right)\right]\frac{e^{-\left(u^2+\frac{1}{4}\right)I_\phi(t,T)}}{u^2+\frac{1}{4}}du \tag{3.12}$$

where $k = \log\left(\frac{S_t}{K}\right) + (r-q)\tau$.

The price dynamics under the $\mathcal{H}$++ models also determines the dynamics of the volatility index. In practice, as will be discussed in Section 3.2.1, the VIX quotation at time t is computed by CBOE as a model-free replication of the integrated variance over the following 30 days. In the present analysis we will adopt a standard definition for the volatility index, expressed as the risk-neutral expectation of a log-contract, as given in equation (2.42), which we rewrite for convenience (Duan and Yeh, 2010; Lin, 2007; Zhang et al., 2010):

$$\left(\frac{VIX_t}{100}\right)^2 = -\frac{2}{\bar{\tau}}E^{\mathbb{Q}}\left[\log\left(\frac{S_{t+\bar{\tau}}}{F(t,t+\bar{\tau})}\right)\middle|\mathcal{F}_t\right] \tag{3.13}$$

where $F_{t,t+\bar{\tau}} = e^{(r-q)\bar{\tau}} S_t$ denotes the forward index quotation. For the CBOE VIX, $\bar{\tau} = 30$ days. The following Proposition gives the expression of VIX_t under the $\mathcal{H}$ models and the effect of the displacement ϕ_t on the index dynamics.

Proposition 5. *Under the $\mathcal{H}$++ models,*

$$\left(\frac{VIX_t^{\mathcal{H}++}}{100}\right)^2 = \left(\frac{VIX_t^{\mathcal{H}}}{100}\right)^2 + \frac{1}{\bar{\tau}} I_\phi(t, t+\bar{\tau}) \tag{3.14}$$

where $(VIX_t^{\mathcal{H}}/100)^2$ is the corresponding quotation under $\mathcal{H}$ models, which is an affine function of the volatility factors $\sigma_{1,t}^2$ and $\sigma_{2,t}^2$

$$\left(\frac{VIX_t^{\mathcal{H}}}{100}\right)^2 = \frac{1}{\bar{\tau}} \left(\sum_{k=1,2} a_k \sigma_{k,t}^2 + b_k \right) \tag{3.15}$$

where $I_\phi(t, t+\bar{\tau}) = \int_t^{t+\bar{\tau}} \phi_s ds$ and the exact forms of $a_k(\bar{\tau})$ and $b_k(\bar{\tau})$ are provided in Appendix A.3.

Pricing of VIX derivatives is complicated by the non affinity of VIX with respect to volatility process. As discussed in Section 2.1.2, the arbitrage-free price $F_{VIX}(t,T)$ at time t of a futures contract with tenor T written on it cannot be derived as a simple cost-of-carry relationship, but has to be evaluated as the risk neutral expectation of the VIX at settlement (Bardgett et al., 2013; Zhang et al., 2010)

$$F_{VIX}(t,T) = E^{\mathbb{Q}} \left[VIX_T \middle| \mathcal{F}_t \right] \tag{3.16}$$

Call options on VIX with maturity T and strike K are European-style options paying the amount $(VIX_T - K)^+$ at maturity. As discussed in Section 2.1.3, they can be regarded as options on VIX futures price process and can be priced according to standard risk-neutral evaluation

$$C_{VIX}(K,t,T) = e^{-r\tau} E^{\mathbb{Q}} \left[(VIX_T - K)^+ \middle| \mathcal{F}_t \right] \tag{3.17}$$

We solve the complications related to the non-linear relation between VIX and volatility by taking advantage of the analytical tractability of the conditional characteristic function of the volatility factors $f^{\mathcal{H}++}(z_1, z_2)$ in Lemma 2, and on the generalized Fourier transform techniques of Chen and Joslin (2012); Lewis (2000, 2001). We provide an explicit pricing formula for futures and options on VIX for $\mathcal{H}++$ models in the following Proposition. Similar results can be found in the literature (Branger et al., 2014; Lian and Zhu, 2013; Sepp, 2008a,b).

Proposition 6. *Under $\mathcal{H}$++ models, the time t value of a futures on VIX_t settled at time T and the arbitrage-free price at time t of a call option on VIX_t, with strike price*

K and time to maturity $\tau = T - t$ are given respectively by (not relevant dependencies suppressed and $\bar{\tau} = 30/365$)

$$\frac{F^{\mathcal{H}++}_{VIX}(t,T)}{100} = \frac{1}{2\sqrt{\pi}} \int_0^\infty \mathrm{Re}\left[f^{\mathcal{H}}_{\sigma}\left(-z\frac{a_1}{\bar{\tau}}, -z\frac{a_2}{\bar{\tau}} \right) \frac{e^{-iz\left(\sum_{k=1,2} b_k + I_\phi(T,T+\bar{\tau})\right)/\bar{\tau}}}{(-iz)^{3/2}} \right] d\,\mathrm{Re}(z) \tag{3.18}$$

and

$$\frac{C^{\mathcal{H}++}_{VIX}(K,t,T)}{100} = \frac{e^{-r\tau}}{2\sqrt{\pi}} \times \int_0^\infty \mathrm{Re}\left[f^{\mathcal{H}}_{\sigma}\left(-z\frac{a_1}{\bar{\tau}}, -z\frac{a_2}{\bar{\tau}} \right) \frac{e^{-iz\left(\sum_{k=1,2} b_k + I_\phi(T,T+\bar{\tau})\right)/\bar{\tau}} \left(1 - erf(K/100\sqrt{-iz})\right)}{(-iz)^{3/2}} \right] d\,\mathrm{Re}(z) \tag{3.19}$$

where $z = \mathrm{Re}(z) + i\,\mathrm{Im}(z) \in \mathbb{C}$, $0 < \mathrm{Im}(z) < \zeta_c(\tau)$, $\zeta_c(\tau)$ is given in Appendix A.4, and $erf(z) = \frac{2}{\sqrt{\pi}} \int_0^z e^{-s^2} ds$ is the error function with complex argument (Abramowitz and Stegun, 1965).

We have analyzed the effect of the choice of the upper bound $\zeta_c(\tau)$ on the integrand behavior and pricing performance. Figure 10 reports, for the 2-SVCVJ model, the shape of the two integrands of Proposition 6 on the imaginary z axis $\mathrm{Re}(z) = 0$ and the effect on VIX Options and Futures model prices when $\mathrm{Im}(z)$ is set to different values within the strip of regularity $0 < \mathrm{Im}(z) < \zeta_c(\tau)$ in equation (A.21). Figure 11 reports the effect of the $\mathrm{Im}(z)$ running in the 2-SVCVJ++ model in correspondence of different ranges of the displacement integral $I_\phi(T, T+\bar{\tau})$ in Proposition 6. In our empirical analysis we have found convenient to chose $\mathrm{Im}(z) = \zeta_c(\tau)/2$.

We conclude this Section by observing that we are not assuming any explicit functional form for the displacement function ϕ_t, but we use it as an analytically tractable correction for the corresponding pricing formulas for the non-displaced models $\mathcal{H}$. The only degrees of freedom of ϕ_t determined by SPX and VIX derivatives are its integrals over the life of the options on price, $I_\phi(t,T)$, and those over the fixed forward volatility horizon of $\bar{\tau}$ from the expiry of VIX futures/options onward $I_\phi(T, T+\bar{\tau})$. These are the quantities that will be effectively calibrated to market data. Moreover, calibrated integrals are constrained by the non-negativity of ϕ_t. For example, if we observe two consecutive SPX vanilla maturities T_1^{SPX}, T_2^{SPX} and an intermediate VIX option expiration T^{VIX} ordered as

$$t < T_1^{SPX} < T^{VIX} < T^{VIX} + \bar{\tau} < T_2^{SPX} \ , \tag{3.20}$$

the only ordering in the integrals compatible with $\phi_t \geq 0$ is

$$I_\phi(t, T_2^{SPX}) - I_\phi(t, T_1^{SPX}) \geq I_\phi(T^{VIX}, T^{VIX} + \bar{\tau}) \geq 0 \ . \tag{3.21}$$

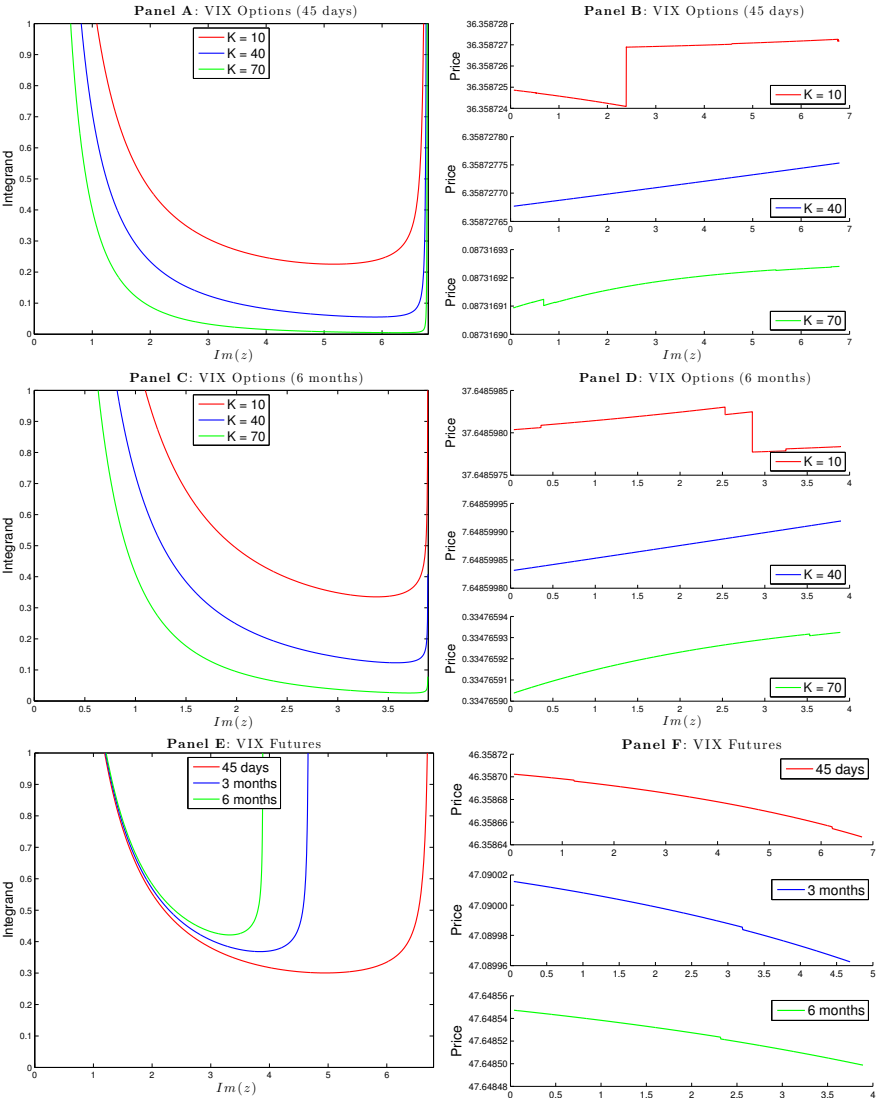

Figure 10: Left panels A, C and E report the shape of the VIX Options and Futures integrands in the pricing formulas of Proposition 6 for the 2-SVCVJ model as a function of $\mathrm{Im}(z)$ ranging in the strip of regularity $0 < \mathrm{Im}(z) < \zeta_c(\tau)$ and setting $Re(z) = 0$. Model parameters are taken from the last column of table 6, interest rate is set to $r = 0$ and there is no displacement ($\phi_t \equiv 0$). In panel A (C) we consider VIX options with a maturity of 45 days (6 months), i.e. $\tau = 45/365$ ($\tau = 0.5$), and strikes $K = 10, 40$ and 70, whereas in panel E VIX Futures with tenors of 45 days, 3 and 6 months, i.e. $\tau = 45/365, 0.25$ and 0.5 (corresponding $\zeta_c(\tau)$ bounds are $6.80, 4.69$ and 3.89, respectively). Right panels B and D (F) present VIX options (Futures) 2-SVCVJ model prices as a function of $0 < \mathrm{Im}(z) < \zeta_c(\tau)$ for maturities corresponding to the right panels A and B (E). Integrals are calculated with the Matlab function quadgk, with default error tolerance (AbsTol $= 10^{-10}$ and RelTol $= 10^{-6}$).

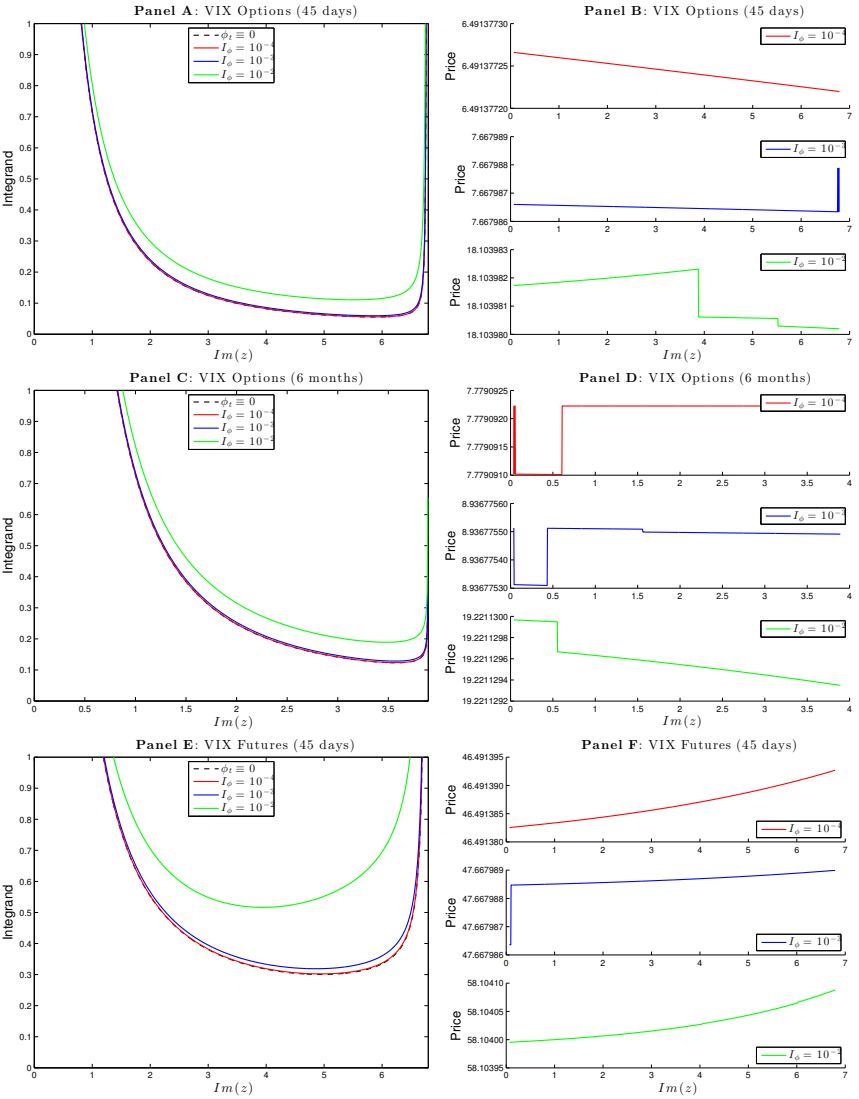

Figure 11: Left panels A, C and E report the shape of the VIX Options and Futures integrands in the pricing formulas of Proposition 6 for the 2-SVCVJ++ model as a function of $\mathrm{Im}(z)$ ranging in the strip of regularity $0 < \mathrm{Im}(z) < \zeta_c(\tau)$ and setting $Re(z) = 0$. Model parameters are taken from the last column of table 6, interest rate is set to $r = 0$ and displacement parameter $I_\phi(T, T+\bar{\tau})$ is set to $I_\phi = 10^{-4}, 10^{-3}$ and 10^{-2}. In panel A (C) we consider VIX options with a maturity of 45 days (6 months), i.e. $\tau = 45/365$ ($\tau = 0.5$), and strikes $K = 40$, whereas in panel E VIX Futures with tenors of 45 days, i.e. $\tau = 45/365$ (corresponding $\zeta_c(\tau)$ bound is 6.80). Right panels B and D (F) present VIX options (Futures) 2-SVCVJ++ model prices as a function of $0 < \mathrm{Im}(z) < \zeta_c(\tau)$ for maturities corresponding to the right panels A and B (E). Integrals are calculated with the Matlab function quadgk, with default error tolerance (AbsTol $= 10^{-10}$ and RelTol $= 10^{-6}$).

3.2 A general displaced affine framework for volatility

We will now introduce a general framework, which embeds the $\mathcal{H}$++ models,[3] that allows for a more general description of the istantaneous volatility. The ϕ_t-displaced (eventually multi-factor) dynamics of the spot volatility is further extended with a second deterministic displacement function ψ_t, which modules the amplitude of the volatility process, which seems to be a feature already noticed and appreciated in literature (Papanicolaou and Sircar, 2014; Sepp, 2008b; Zhao, 2013). The general framework describes in a mathematical compact way these possible general deterministic extensions of the volatility process, still preserving the *affinity* of the specification.

Our analytical approach builds on the general characterization of affine models introduced by Duffie et al. (2000), the affine model for variance swaps of Egloff et al. (2010); Leippold et al. (2007) and on the affine model of VIX derivatives of Branger et al. (2014). We consider a class of displaced AJD models in which the risk-neutral dynamics of the S&P500 index features several diffusive and jump risk sources and two general forms of displacement characterize the dynamics of the instantaneous variance process, which is affine in the state vector of volatility factors.

Consider a filtered probability space $(\Omega, \mathcal{F}, \{\mathcal{F}_t\}_{t\geq 0}, \mathbb{Q})$, where $\{\mathcal{F}_t\}_{t\geq 0}$ represents the history of the market up to time t and $\mathbb{Q}$ denotes the pricing measure. The dynamics of the volatility factor state vector $X_t = (\sigma^2_{1,t}, ..., \sigma^2_{n,t})^\top \in \mathbb{R}^n$ is described by the affine jump diffusion

$$dX_t = \mu(t, X_t)dt + \sigma(t, X_t)dW^X_t + \sum_{j=1}^{m_X} dZ_{j,t} \tag{3.22}$$

where W^X_t is an n-dim standard Wiener process and each $Z_{j,t}$ is a n-dim compound Poisson process. The affine structure of the process is the following:

Drift vector: $\mu(t, X) = K_0 + K_1 X_t$ where $K_0 \in \mathbb{R}^n$ and $K_1 \in \mathbb{R}^{n\times n}$;

Variance-covariance matrix: $(\sigma(t, X)\sigma^\top(t, X))_{ij} = (H_0)_{ij} + (H_1)_{ij} \cdot X_t = (H_0)_{ij} + \sum_{k=1}^n (H_1^{(k)})_{ij} X_{k,t}$ where H_0 and each $H_1^{(k)}$ are symmetric $n \times n$ real matrices;

Jump intensities: $\lambda_j(X_t) = \lambda_{0,j} + \lambda^\top_{1,j} X_t$ where $\lambda_{0,j} \in \mathbb{R}$ and $\lambda_{1,j} \in \mathbb{R}^n$ for each $j = 1, ..., m_X$;

[3] That is, the 2-SVCVJ++ model introduced in the previous Section together with all its nested specifications discussed in Section 3.1.2.

Jump sizes: random $Z_j^X \in \mathbb{R}^{n}$[4] distributed according to the risk-neutral jump measure ν_j of finite variation and independent of jump timing for each $j = 1, ..., m_X$. The corresponding moment generating function (MGF) is

$$\theta_j(u) = \int_{\mathbb{R}^n} e^{u^\top Z_j^X} d\nu_j(Z_j^X) = E^{\mathbb{Q}}[e^{u^\top Z_j^X}] \tag{3.23}$$

where $u \in \mathbb{C}^n$.

Under pricing measure $\mathbb{Q}$, the S&P500 index returns process $\log S_t$ features n diffusive risk factor contributions and m_S jump risk sources, as follows:

$$\begin{aligned} d\log S_t = &\left(r - q - \frac{1}{2}\sum_{i=1}^{n}\left(\psi_{i,t}\sigma_{i,t}^2 + \phi_{i,t}\right) - \sum_{j=1}^{m_S}\bar{\mu}_{j,t}\hat{\lambda}_{j,t}\right) dt \\ &+ \sum_{i=1}^{n}\sqrt{\psi_{i,t}\sigma_{i,t}^2 + \phi_{i,t}}dW_{i,t}^S + \sum_{j=1}^{m_S} c_j dN_{j,t} \end{aligned} \tag{3.24}$$

where r and q are the constant short-rate and continuously compounded dividend yield rate, respectively. Each $W_{i,t}^S$ is a scalar standard Wiener process and each $c_j N_{j,t}$ is a scalar compound Poisson process characterized by:

Jump intensities: affine in the volatility factor state vector: $\hat{\lambda}_{j,t} = \hat{\lambda}_{0,j} + \hat{\lambda}_{1,j}^\top X_t$;

Jump sizes: random c_j, with jump measure $\hat{\nu}_j$ of finite variation and independent from the jump timing for each $j = 1, ..., m_S$. The MGF is

$$\hat{\theta}_j(u) = \int_{\mathbb{R}} e^{uc_j} d\hat{\nu}_j(c_j) = E^{\mathbb{Q}}[e^{uc_j}] \tag{3.25}$$

where $u \in \mathbb{C}$ and compensator process

$$\bar{\mu}_{j,t} = E^{\mathbb{Q}}[e^{c_j} - 1|\mathcal{F}_t] = \hat{\theta}_j(1) - 1. \tag{3.26}$$

The multiplicative $\psi_{i,t}$ and additive $\phi_{i,t}$ displacement functions are deterministic non-negative functions

$$\psi_{i,t} \geq 0 \text{ and } \phi_{i,t} \geq 0 \tag{3.27}$$

initially set to $\psi_{i,0} = 1$ and $\phi_{i,0} = 0$ for each $i = 1, ..., n$. The present setting is different with respect to the setting in Leippold et al. (2007) and Egloff et al. (2010),

[4]That is $Z_{i,j}^X \in \mathbb{R}$ is the random jump size of the i-th volatility factor, induced by the j-th kind of jump.

since it allows for uncompensated jumps in the stochastic volatility factors dynamics. Moreover, it features a time-varying affine structure of the instantaneous diffusive variance

$$V_c(X_t) = \sum_{i=1}^{n} V_{c,i}(\sigma_{i,t}^2) = \sum_{i=1}^{n} \psi_{i,t}\sigma_{i,t}^2 + \phi_{i,t} = \Psi_t^\top X_t + \mathbf{1}^\top \Phi_t \tag{3.28}$$

where we have denoted with $\mathbf{1} \in \mathbb{R}^n$ a vector of ones. A similar setup is presented also in Branger et al. (2014), but the affinity structure of the diffusive spot variance is restricted to be constant in time

$$V_c(X_t) = \Psi^\top X_t. \tag{3.29}$$

As observed by Zhao (2013), multi-factor affine models, mostly with constant coefficients, are extensively employed in modeling interest rate dynamics (Duffie and Kan, 1996; Duffie et al., 2000), volatility dynamics (Christoffersen et al., 2009; Egloff et al., 2010) and default rate dynamics (Duffie and Singleton, 1999). Models with a time-varying affinity structure of spot variance are less common. In the context of variance derivatives, a $n = 2$ factor model with

$$V_c(\sigma_{1,t}^2, \sigma_{2,t}^2) = \psi_{1,t}\sigma_{1,t}^2 + \psi_{2,t}\sigma_{2,t}^2 \tag{3.30}$$

has been considered by Zhao (2013) in order to fit the term structure of variance, interpolating between the initial and steady-state mean variance, with $\psi_{2,t} \propto 1 - \psi_{1,t}$ playing a role of a damping function. Another $n = 1$ factor model with time-dependent multiplicative displacement, calibrated on futures and options on VIX, with

$$V_c(\sigma_t^2) = \psi_t \sigma_t^2 \tag{3.31}$$

has been considered by Sepp (2008b) where the function ψ_t is calibrated to the term structure of VIX futures. Our 2-SVCVJ++ model, introduced in Section 3.1.1, is a particular instance of the present setting, with $n = 2$ factors and a lower bounded spot variance

$$V_c(\sigma_{1,t}^2, \sigma_{2,t}^2) = \sigma_{1,t}^2 + \phi_t + \sigma_{2,t}^2 \tag{3.32}$$

where the function $\phi_t \geq 0$ improves considerably the fit of the VIX futures term structure, while preserving the other degrees of freedom of the model for the consistent fit of options on S&P500 and VIX.

The jump structure outlined above allows for the dynamics of X_t and $\log S_t$ to feature both independent *idiosyncratic jumps* and simultaneous correlated *co-jumps*. For example, in order to model the fact the k-th kind of jump is a correlated co-jump between the price process S_t and the i-th volatility factor $X_{i,t}$, one may consider a common Poisson process $N_{k,t}$, driving synchronized jumps in both processes and correlated jump sizes $(c_k, Z_{i,k}^X)$. This is the case of our 2-SVCVJ++

model, in which the first factor $\sigma_{1,t}^2$ features two kind of jumps, one idiosyncratic and the other one correlated and syncronized with the underlying S&P500 index process. This rich jump specification increases the volatility of variance, that is the *vol-of-vol*, and dramatically improves the ability of the model to fit the positive skew of the VIX options surface.
The jump contribution to the instantaneous variance is given by

$$V_d(X_t) = \sum_{j=1}^{m_S} E^{\mathbb{Q}}[c_j^2] \left(\hat{\lambda}_{0,j} + \hat{\lambda}_{1,j}^\top X_t \right) \tag{3.33}$$

and therefore the overall spot variance is the sum of the two contributions $V_c(X_t) + V_d(X_t)$. Correspondingly, the total quadratic variation of the index returns between time t and T, $[\log S]_T - [\log S]_t$, which we will denote as $[\log S]_{t,T}$, is the sum of the diffusive and jump contributions:

$$[\log S]_{t,T} = \int_t^T V_c(X_s)ds + \int_t^T V_d(X_s)ds = [\log S]_{t,T}^c + [\log S]_{t,T}^d \tag{3.34}$$

where we have defined the diffusive and jumps contributions

$$[\log S]_{t,T}^c = \int_t^T \Psi_s^\top X_s + \mathbf{1}^\top \Phi_s ds \tag{3.35}$$

$$[\log S]_{t,T}^d = \sum_{j=1}^{m_S} E^{\mathbb{Q}}[c_j^2] \left(\hat{\lambda}_{0,j}\tau + \hat{\lambda}_{1,j}^\top \int_t^T X_s ds \right) \tag{3.36}$$

where $\tau = T - t$. As will be discussed in Section 3.2.1, the fair price $SW_{t,T}$ of a variance swap contract is the (annualized) risk-neutral expected value of the total quadratic variation at the time t at which the contract is made:

$$\begin{aligned} SW_{t,T} &= \frac{1}{\tau} E^{\mathbb{Q}} \left[[\log S]_{t,T} \middle| \mathcal{F}_t \right] \\ &= \frac{1}{\tau} E^{\mathbb{Q}} \left[[\log S]_{t,T}^c \middle| \mathcal{F}_t \right] + \frac{1}{\tau} E^{\mathbb{Q}} \left[[\log S]_{t,T}^d \middle| \mathcal{F}_t \right] \end{aligned} \tag{3.37}$$

We need therefore to compute in the present setting the expected values of the diffusive and jump contributions (3.35) and (3.36). We will follow (Egloff et al., 2010; Leippold et al., 2007) and begin introducing the conditional characteristic function (CF) of the diffusive quadratic variation (3.35).

Proposition 7. *Under general integrability conditions,*[5] *the conditional characteristic function of the diffusive quadratic variation (3.35) takes the following exponential affine form:*

$$E^{\mathbb{Q}} \left[e^{iz[\log S]_{t,T}^c} \middle| \mathcal{F}_t \right] = e^{\alpha_c + \beta_c^\top X_t} \tag{3.38}$$

[5] See (Duffie et al., 2000, Prop. 1).

with $z \in \mathbb{R}$ and coefficients $\alpha_c(z,t,T) \in \mathbb{R}$ and $\beta_c(z,t,T) \in \mathbb{R}^n$ satisfying the following ordinary and Riccati differential equations, respectively

$$\begin{aligned}\dot{\alpha_c}(z,t,T) &= -K_0^\top \beta_c - \frac{1}{2}\beta_c^\top H_0 \beta_c - iz\mathbf{1}^\top \Phi(t) - \sum_{j=1}^{m_X} \lambda_{0,j}\left(\theta_j(\beta_c) - 1\right) \\ \dot{\beta}_c(z,t,T) &= -K_1^\top \beta_c - \frac{1}{2}\beta_c^\top H_1 \beta_c - iz\Psi(t) - \sum_{j=1}^{m_X} \lambda_{1,j}\left(\theta_j(\beta_c) - 1\right)\end{aligned} \tag{3.39}$$

and the terminal conditions $\alpha_c(z,T,T) = 0$ and $\beta_c(z,T,T) = 0$.

Proof. See Proposition 1 of Egloff et al. (2010), though with a slightly different notation. The proof is analogous to the one in (Mortensen, 2005, App. A.2), thought in the context of intesity-based credit risk models and is derived in the footsteps of Proposition 1 of Duffie et al. (2000), which provides the standard transform analysis for CF-like expectations in affine models. In particular, the closed-form expression of the CF of an integrated affine process can be found in (Duffie and Singleton, 2012, App. A.5) and (Duffie and Garleanu, 2001, App. A) in the credit risk context and in Duffie and Kan (1996), in the general analysis of interest rates models. □

From the characteristic function (3.38), its expectation is easily obtained by differentiation w.r.t. z

$$E^{\mathbb{Q}}\left[[\log S]^c_{t,T}|\mathcal{F}_t\right] = -i\left[\frac{\partial \alpha_c}{\partial z} + \left(\frac{\partial \beta_c}{\partial z}\right)^\top X_t\right]\Bigg|_{z=0} \tag{3.40}$$

and partial derivatives may be computed in closed form, as presented in the next Proposition.

Proposition 8. *Under the setting described above, the conditional expectation of the diffusive quadratic variation in (3.35) is the following affine function of the volatility factor state vector X_t:*

$$E^{\mathbb{Q}}\left[[\log S]^c_{t,T}|\mathcal{F}_t\right] = A_c + B_c^\top X_t + \mathbf{1}^\top \int_t^{t+\bar{\tau}} \Phi_s ds \tag{3.41}$$

where $A_c \in \mathbb{R}$ and $B_c \in \mathbb{R}^n$ can be expressed in integral terms[6]

$$\begin{aligned}A_c(t,T;\Psi_{[t,T]}) &= \int_t^T B_c^\top(s,T;\Psi_{[s,T]})ds \left(K_0 + \sum_{j=1}^{m_X} \lambda_{0,j}\nabla\theta_j(0)\right) \\ B_c(t,T;\Psi_{[t,T]}) &= \int_t^T e^{\left(K_1^\top + \sum_{j=1}^{m_X} \lambda_{1,j}\nabla\theta_j^\top(0)\right)(s-t)}\Psi(s)ds\end{aligned} \tag{3.42}$$

[6] From definition (3.23), $\nabla\theta_j(0)$ stands for $\nabla\theta_j(u)|_{u=0} = E^{\mathbb{Q}}[Z_j^X]$.

Proof. Start from the equations for (α, β) in (3.39) and follow the same arguments of the proof of Proposition 2 in Leippold et al. (2007). □

In the case of constant affinity structure of spot variance, as it is commonly assumed in literature, we get the following Corollary.

Corollary 3. *If the multiplicative displacement vector is constant $\Psi_t \equiv \Psi$, the functions A_c and B_c are time homogeneous*

$$\begin{aligned} A_c(\tau) &= \left[B_c^\top(\tau) - \Psi^\top \tau\right] \left(K_1^\top + \sum_{j=1}^{m_X} \lambda_{1,j} \nabla \theta_j^\top(0)\right)^{-1} \left(K_0 + \sum_{j=1}^{m_X} \lambda_{0,j} \nabla \theta_j(0)\right) \\ B_c(\tau) &= \left[e^{\left(K_1^\top + \sum_{j=1}^{m_X} \lambda_{1,j} \nabla \theta_j^\top(0)\right)\tau} - Id_n\right] \left(K_1^\top + \sum_{j=1}^{m_X} \lambda_{1,j} \nabla \theta_j^\top(0)\right)^{-1} \Psi \end{aligned} \tag{3.43}$$

where $\tau = T - t$ and $Id_n \in \mathbb{R}^{n \times n}$ is the identity matrix.

If jumps in volatility are compensated, that is if we make the following substitution

$$\sum_{j=1}^{m_X} dZ_{j,t} \Longrightarrow \sum_{j=1}^{m_X} \left(dZ_{j,t} - \lambda_j(X_t) E^{\mathbb{Q}}[Z_j^X] dt\right) \tag{3.44}$$

in (3.22) and if both multiplicative Ψ_t and additive Φ_t displacements are constant functions of time, expression (3.41) for the expected integrated variance $E^{\mathbb{Q}}\left[[\log S]_{t,T}^c | \mathcal{F}_t\right]$ consistently reduces to the corresponding expression given by Proposition 2 of Leippold et al. (2007).
We conclude this Section deriving the expected value of the jump-induced contribution $[\log S]_{t,T}^d$ in (3.36) to the total quadratic variation, which is a linear function of the volatility state vector X_t integrated between time t and T.

Proposition 9. *Under general integrability conditions,[7] the conditional expectation of the jump quadratic variation is a linear function of the integrated volatility state vector X_t*

$$E^{\mathbb{Q}}\left[[\log S]_{t,T}^d | \mathcal{F}_t\right] = \sum_{j=1}^{m_S} E^{\mathbb{Q}}[c_j^2] \left(\hat{\lambda}_{0,j}\tau + \hat{\lambda}_{1,j}^\top E^{\mathbb{Q}}\left[\int_t^T X_s ds \middle| \mathcal{F}_t\right]\right) \tag{3.45}$$

where

$$E^{\mathbb{Q}}\left[\int_t^T X_s ds \middle| \mathcal{F}_t\right] = A_x(\tau) + B_x(\tau) X_t \tag{3.46}$$

[7] See (Duffie et al., 2000, Prop. 1).

and the time homogeneous functions $A_x \in \mathbb{R}^n$ and $B_x \in \mathbb{R}^{n\times n}$ are as follows:

$$\begin{aligned} A_x(\tau) &= [B_x(\tau) - Id_n\tau]\left(K_1 + \sum_{j=1}^{m_X} \nabla\theta_j(0)\lambda_{1,j}^\top\right)^{-1}\left(K_0 + \sum_{j=1}^{m_X} \lambda_{0,j}\nabla\theta_j(0)\right) \\ B_x(\tau) &= \left[e^{\left(K_1+\sum_{j=1}^{m_X}\nabla\theta_j(0)\lambda_{1,j}^\top\right)\tau} - Id_n\right]\left(K_1 + \sum_{j=1}^{m_X} \nabla\theta_j(0)\lambda_{1,j}^\top\right)^{-1} \end{aligned} \tag{3.47}$$

Proof. This expectation has been carried out in a similar setting in (Branger et al., 2014, eq. 6), though no proof can be found. A proof can be easily derived in the following way, from the results in Proposition 7:

1. Consider the conditional CF of the affine process $X_t \in \mathbb{R}^n$ integrated in $[t, T]$

$$F_x(Z; X_t, \tau) = E^{\mathbb{Q}}\left[e^{iZ^\top \int_t^T X_s ds}\middle|\mathcal{F}_t\right] \tag{3.48}$$

   where $Z \in \mathbb{R}^n$.

2. The CF F_x can be easily derived from the conditional CF of the diffusive quadratic variation $[\log S]^c_{t,T}$, given in equation (3.38), since:

$$\begin{aligned} f_c(z; X_t, \Psi_t, \Phi_t) &= E^{\mathbb{Q}}\left[e^{iz[\log S]^c_{t,T}}\middle|\mathcal{F}_t\right] \\ &= E^{\mathbb{Q}}\left[e^{iz\int_t^T \Psi_s^\top X_s + \mathbf{1}^\top\Phi_s ds}\middle|\mathcal{F}_t\right] \end{aligned} \tag{3.49}$$

   and therefore

$$F_x(Z; X_t, \tau) = f_c(1; X_t, Z, \mathbf{0}) \tag{3.50}$$

   where $\mathbf{0} \in \mathbb{R}^n$ is the zero vector.

3. Finally, take the gradient of F_x w.r.t Z and evaluate it at $Z = \mathbf{0}$:

$$\begin{aligned} E^{\mathbb{Q}}\left[\int_t^T X_s ds\middle|\mathcal{F}_t\right] &= -i\nabla_Z F_x(Z; X_t, \tau)|_{Z=\mathbf{0}} \\ &= A_x(\tau) + B_x(\tau)X_t \end{aligned} \tag{3.51}$$

In appendix A.5 we apply a different approach, applying the concept of functional derivative and deriving the expectation of $\int_t^T X_s ds$ directly from the integral $\int_t^T \Psi_s^\top X_s ds$ (part of $[\log S]^c_{t,T}$ in (3.35)), considering it as a functional of the function Ψ_t. □

3.2.1 Affine modeling of VIX index

In this Section we will consider variance swaps and the VIX volatility index and study the relation among them. We will first introduce standard literature results concerning the replication of variance swaps, then we will step back to the VIX market definition discussed in Section 2.1 and connect it to a variance swap replication strategy. Finally, we will present the expression for both instruments under the affine framework outlined in the previous Section.
Variance swaps are annualized forward contracts written on the annualized realized variance $RV_{t,T}$ of daily (less often, weekly) logarithmic returns over a time grid $t = t_0 < t_1 < ... < t_k = T$ spanning the fixed interval of time $[t, T]$ into the future (Bossu et al., 2005; Demeterfi et al., 1999), which following Cont and Kokholm (2013) can be written as

$$RV_{t,T} = \frac{1}{\tau} \sum_{i=1}^{k} \left(\log \frac{S_{t_i}}{S_{t_{i-1}}} \right)^2 \tag{3.52}$$

where $\tau = T - t$ and S_t is a price process of the underlying that, for derivative pricing, we model on a filtered $(\Omega, \mathcal{F}, \{\mathcal{F}_t\}_{t \geq 0}, \mathbb{Q})$. At maturity, the payoff of the long side of the swap is equal to the difference between the realized variance $RV_{t,T}$ and a constant called *variance swap rate* $SW_{t,T}$, determined at inception t (Carr and Wu, 2009, eq. 1)

$$N \left(RV_{t,T} - SW_{t,T} \right) \tag{3.53}$$

and where N is the notional of the contract. For any semi-martingale, as the time-grid gets finer (i.e. as $\sup_{i=1,...,k} |t_i - t_{i-1}| \to 0$), the realized variance $RV_{t,T}$ in (3.52) converges to the annualized total quadratic variation $[\log S]_{t,T}$ defined in equation (3.34)

$$RV_{t,T} = \frac{1}{\tau} [\log S]_{t,T} \tag{3.54}$$

Therefore, in the limit of continuous monitoring,[8] variance swaps are contingent claims on the annualized total quadratic variation $[\log S]_{t,T}$ of the log price in that interval (Cont and Kokholm, 2013; Todorov and Tauchen, 2011). No arbitrage implies zero net value of the contract at the time of initiation. Therefore, the variance swap rate fair value

$$SW_{t,T} = E^{\mathbb{Q}} \left[RV_{t,T} \middle| \mathcal{F}_t \right] \tag{3.55}$$

[8]The approximation $RV_{t,T} \approx \frac{1}{\tau} [\log S]_{t,T}$ is still acceptable when the sampling frequency is daily (Broadie and Jain, 2008).

for a variance swap signed at time t and maturing at time T is the annualized time-t conditional quadratic variation (3.34) between time t and T

$$\begin{aligned} SW_{t,T} &= \frac{1}{\tau} E^{\mathbb{Q}} \left[[\log S]_{t,T} \middle| \mathcal{F}_t \right] \\ &= \frac{1}{\tau} E^{\mathbb{Q}} \left[[\log S]^c_{t,T} \middle| \mathcal{F}_t \right] + \frac{1}{\tau} E^{\mathbb{Q}} \left[[\log S]^d_{t,T} \middle| \mathcal{F}_t \right] \end{aligned} \tag{3.56}$$

Under the affine model introduced in the previous Section, we therefore have:

$$\begin{aligned} SW_{t,T} = \frac{1}{\tau} \left(E^{\mathbb{Q}} \left[\int_t^T \Psi_s^\top X_s ds \middle| \mathcal{F}_t \right] + \mathbf{1}^\top \int_t^T \Phi_s^\top ds \right) \\ + \frac{1}{\tau} \sum_{j=1}^{m_S} E^{\mathbb{Q}}[c_j^2] \left(\hat{\lambda}_{0,j} \tau + \hat{\lambda}_{1,j}^\top E^{\mathbb{Q}} \left[\int_t^T X_s ds \middle| \mathcal{F}_t \right] \right) \end{aligned} \tag{3.57}$$

Carr and Wu showed that the variance swap rate $SW_{t,T}$ can be replicated by a portfolio of out-of-the-money options $Q(K,t,T)$ maturing at the same time T of the contract with an infinite continuum of strikes K plus an error term $\epsilon(t,T)$ of third order in jump sizes[9]

$$SW_{t,T} = \frac{2}{\tau} e^{r\tau} \int_0^\infty \frac{Q(K,t,T)}{K^2} dK + \epsilon(t,T) \tag{3.58}$$

The error term is induced by jumps in the S_t process and, under our affine framework, can be written as

$$\epsilon(t,T) = -\frac{2}{\tau} \sum_{j=1}^{m_S} E^{\mathbb{Q}} \left[e^{c_j} - 1 - c_j - \frac{c_j^2}{2} \right] \left(\hat{\lambda}_{0,j} \tau + \hat{\lambda}_{1,j}^\top E^{\mathbb{Q}} \left[\int_t^T X_s ds \middle| \mathcal{F}_t \right] \right) \tag{3.59}$$

Consider the market definition of VIX, as presented in Section 2.1. In the limit of an infinite continuum of strike prices,[10] the square of the VIX index given in (2.1) and (2.2) approaches the first summand in (3.58)[11] (Carr and Wu, 2006; Cont and Kokholm, 2013)

$$\lim_{\substack{\Delta K \to 0 \\ K_{max} \to +\infty \\ K_{min} = 0}} \left(\frac{VIX_t}{100} \right)^2 = \frac{2}{\bar{\tau}} e^{r\bar{\tau}} \int_0^\infty \frac{Q(K,t,t+\bar{\tau})}{K^2} dK \tag{3.60}$$

[9] See eq. 5 in Carr and Wu (2009) and (Carr and Madan, 2001; Demeterfi et al., 1999; Jiang and Tian, 2007).

[10] And neglecting also the error induced by the interpolation between T_1 and T_2 option maturity buckets.

[11] The second term in (2.1), $\left(\frac{F(t,T)}{K_0} - 1 \right)^2$, is due to the use of the put-call parity in order to substitute an ITM call option at K_0 with an OTM put at the same strike and it is lost in the limit of a continuum of strikes, as we assume in the present analysis (Carr and Wu, 2006, App. B).

where $\bar{\tau} = 30/365$ denotes the annualized 30 days horizon inherent in VIX definition. We can therefore express the square of the VIX index at time t as

$$\begin{aligned}\left(\frac{VIX_t}{100}\right)^2 &= SW_{t,t+\bar{\tau}} - \epsilon(t, t+\bar{\tau}) \\ &= \frac{1}{\bar{\tau}} E^{\mathbb{Q}}\left[\left[\log S\right]_{t,t+\bar{\tau}} \middle| \mathcal{F}_t\right] - \epsilon(t, t+\bar{\tau}) \\ &= \frac{1}{\bar{\tau}} E^{\mathbb{Q}}\left[\left[\log S\right]^c_{t,t+\bar{\tau}} \middle| \mathcal{F}_t\right] + \left(\frac{1}{\bar{\tau}} E^{\mathbb{Q}}\left[\left[\log S\right]^d_{t,t+\bar{\tau}} \middle| \mathcal{F}_t\right] - \epsilon(t, t+\bar{\tau})\right)\end{aligned} \tag{3.61}$$

If we switch off jumps, VIX index and variance swap rate over the same horizon consistently coincide

$$\left(\frac{VIX_t}{100}\right)^2 \equiv SW_{t,t+\bar{\tau}} \Bigg| \; S_t \text{ has continuous paths} \tag{3.62}$$

but if we allow the price process S_t to jump, the effect on the discontinuity on the variance swap rate is different from its effect on the VIX. Equation (3.61) is commonly adopted as a continuous-time definition of VIX (Zhao, 2013). Comparing to VIX CBOE calculations in (2.1), (2.2) and (2.5), formula (3.61) is exact up to the discretization error due to $\Delta K > 0$, the truncation errors due to a finite number of strikes $K_{max} < +\infty, K_{min} > 0$ and the error introduced ignoring the linear interpolation/extrapolation between the two maturity buckets at T_1 and T_2. In our affine framework, comparing the expression in (3.61) with the one for variance swap rates in (3.57), the VIX index squared at time t can be explicitly written as

$$\begin{aligned}\left(\frac{VIX_t}{100}\right)^2 = \frac{1}{\tau}\Bigg(&E^{\mathbb{Q}}\left[\int_t^T \Psi_s^\top X_s ds \middle| \mathcal{F}_t\right] + \mathbf{1}^\top \int_t^T \Phi_s^\top ds\Bigg) \\ &+ \frac{2}{\bar{\tau}} \sum_{j=1}^{m_S} E^{\mathbb{Q}}\left[e^{c_j} - 1 - c_j\right]\left(\hat{\lambda}_{0,j}\bar{\tau} + \hat{\lambda}_{1,j}^\top E^{\mathbb{Q}}\left[\int_t^{t+\bar{\tau}} X_s ds \middle| \mathcal{F}_t\right]\right)\end{aligned} \tag{3.63}$$

and we can see that the difference between VIX and variance swap rate induced by jumps is consistently of third orders in jumps size (Branger et al., 2014, App. B.1)

$$\left(\frac{VIX_t}{100}\right)^2 - SW_{t,t+\bar{\tau}} = -\epsilon(t, t+\bar{\tau}) = \mathcal{O}\left(E^{\mathbb{Q}}\left[c^3\right]\right) \tag{3.64}$$

which shows that, under our continuous time affine framework, the error induced approximating the VIX (squared and scaled) with the variance swap rate is of third order in the jump sizes.

With the results in propositions 8 and 9 we can price instruments which directly depend on the dynamics of volatility. In particular, the VIX index can be written as an affine function of the volatility factor state vector.

Proposition 10. *Under the affine framework of Section 3.2, from definition (3.63), the VIX index squared at time t is*

$$\left(\frac{VIX_t}{100}\right)^2 = \frac{1}{\bar{\tau}}\left(a + b^\top X_t + \mathbf{1}^\top \int_t^{t+\bar{\tau}} \Phi_s ds\right) \tag{3.65}$$

where functions $a \in \mathbb{R}$ and $b \in \mathbb{R}^n$ can be expressed as:

$$\begin{aligned} a(t, t+\bar{\tau}; \Psi_{[t,t+\bar{\tau}]}) &= A_c(t, t+\bar{\tau}; \Psi_{[t,t+\bar{\tau}]}) + 2\sum_{j=1}^{m_S} E^{\mathbb{Q}}\left[e^{c_j} - 1 - c_j\right]\left(\hat{\lambda}_{0,j}\bar{\tau} + \hat{\lambda}_{1,j}^\top A_x(\bar{\tau})\right) \\ b(t, t+\bar{\tau}; \Psi_{[t,t+\bar{\tau}]}) &= B_c(t, t+\bar{\tau}; \Psi_{[t,t+\bar{\tau}]}) + 2\sum_{j=1}^{m_S} E^{\mathbb{Q}}\left[e^{c_j} - 1 - c_j\right] B_x^\top(\bar{\tau})\hat{\lambda}_{1,j} \end{aligned} \tag{3.66}$$

Proof. Straightforward application of definition (3.63), where the affinity coefficients $(A_c, B_c) \in \mathbb{R} \times \mathbb{R}^n$ of the diffusive quadratic variation have been defined in (3.42) and the corresponding coefficients $(A_x, B_x) \in \mathbb{R}^n \times \mathbb{R}^{n\times n}$ of the integrated volatility factor state vector have been defined in (3.47). □

If the multiplicative displacement vector is constant $\Psi_t \equiv \Psi$, the expected diffusive quadratic variation of proposition 8 is affine in the expectation of the integrated volatility factor state vector X_t of proposition 9 and the following corollary summarizes how the affinity structure of VIX squared simplifies

Corollary 1. *If the multiplicative displacement vector is constant $\Psi_t \equiv \Psi$, the VIX squared affinity coefficients $(a, b) \in \mathbb{R} \times \mathbb{R}^n$ are time homogeneous functions*

$$\begin{aligned} a(\bar{\tau}) &= \Psi^\top A_x(\bar{\tau}) + 2\sum_{j=1}^{m_S} E^{\mathbb{Q}}\left[e^{c_j} - 1 - c_j\right]\left(\hat{\lambda}_{0,j}\bar{\tau} + \hat{\lambda}_{1,j}^\top A_x(\bar{\tau})\right) \\ b(\bar{\tau}) &= B_x^\top(\bar{\tau})\left(\Psi + 2\sum_{j=1}^{m_S} E^{\mathbb{Q}}\left[e^{c_j} - 1 - c_j\right]\hat{\lambda}_{1,j}\right) \end{aligned} \tag{3.67}$$

Under the same setting, from (3.56), the variance $SW_{t,t+\bar{\tau}}$ at time t, over the same 30-day horizon of the VIX_t, can be obtained replacing

$$2E^{\mathbb{Q}}\left[e^{c_j} - 1 - c_j\right] \tag{3.68}$$

with

$$E^{\mathbb{Q}}[c_j^2] \tag{3.69}$$

everywhere in (3.66) and (3.67).

3.2.2 Affine modeling of VIX derivatives

The payoff of a VIX futures contract settled at time T and of a call option on VIX of strike K and maturing at T are linear functions of the VIX index value at settle VIX_T, respectively $w_F(VIX_T) = VIX_T$ and $w_C(VIX_T) = (VIX_T - K)^+$. As it is clear from Proposition 10, the index VIX has a non linear (square-root) relation with the volatility vector X_t. To overcome this issue, together with the other mentioned above, we rewrite the payoffs as non-linear functions of the scaled squared VIX index

$$\begin{aligned} w_F(VIX'^2_T) &= 100 \times \sqrt{VIX'^2_T} \\ w_C(VIX'^2_T) &= 100 \times \left(\sqrt{VIX'^2_T} - K'\right)^+ \end{aligned} \tag{3.70}$$

where $VIX'_t = VIX_t/100$ and $K' = K/100$ are, respectively, the index and strike values expressed in percentage points. The Fourier transforms for these payoffs are available in closed form

$$\begin{aligned} \hat{w}_F(z) &= \int_0^\infty e^{izVIX'^2_T} w_F(VIX'^2_T) dVIX'^2_T \\ &= 100 \times \frac{\sqrt{\pi}}{2} \frac{1}{(-iz)^{3/2}} \\ \hat{w}_C(z) &= \int_{-\infty}^\infty e^{izVIX'^2_T} w_C(VIX'^2_T) dVIX'^2_T \\ &= 100 \times \frac{\sqrt{\pi}}{2} \frac{1 - erf(K'\sqrt{-iz})}{(-iz)^{3/2}} \end{aligned} \tag{3.71}$$

with $z = \mathrm{Re}(z) + i\,\mathrm{Im}(z) \in \mathbb{C}$ and are single-valued regular functions in the upper half of the complex plane $\mathrm{Im}(z) > 0$. Following the approach in (Lewis, 2000, 2001), in the next Proposition we will derive a closed-form expression for the VIX derivative prices in terms of the complex Fourier transform of futures and options payoffs and the complex CF of the volatility factor state vector X_t.

Proposition 11. *Under the affine framework described above, the time t value of a futures on VIX settled at time T and the arbitrage-free price at time t of a call option with strike price K and time to maturity $\tau = T - t$ are given respectively by (not relevant dependencies suppressed and $\bar{\tau} = 30/365$)*

$$F_{VIX}(t,T) = 100 \times \frac{1}{2\sqrt{\pi}} \int_0^\infty \mathrm{Re}\left[f_\sigma\left(-z\frac{b}{\bar{\tau}}\right) \frac{e^{-iz\left(a + \mathbf{1}^\top I_\Phi(T, T+\bar{\tau})\right)/\bar{\tau}}}{(-iz)^{3/2}} \right] d\,\mathrm{Re}(z) \tag{3.72}$$

and

$$C_{VIX}(K,t,T) = 100 \times \frac{e^{-r\tau}}{2\sqrt{\pi}} \times \int_0^\infty \mathrm{Re}\left[f_\sigma\left(-z\frac{b}{\bar{\tau}}\right) \frac{e^{-iz\left(a+\mathbf{1}^\top I_\Phi(T,T+\bar{\tau})\right)/\bar{\tau}}\left(1-erf(K/100\sqrt{-iz})\right)}{(-iz)^{3/2}} \right] d\,\mathrm{Re}(z) \tag{3.73}$$

where $z = \mathrm{Re}(z) + i\,\mathrm{Im}(z) \in \mathbb{C}$ *and the integrals are performed along a line parallel to the* $\mathrm{Re}(z)$ *axis selecting* $\mathrm{Im}(z)$ *such that* $0 < \mathrm{Im}(z) < \zeta_c(t,T)$*. The complex valued* $erf(z) = \frac{2}{\sqrt{\pi}}\int_0^z e^{-s^2} ds$ *is the error function with complex argument, the integrated additive displacement vector is*

$$I_\Phi(T, T+\bar{\tau}) = \int_T^{T+\bar{\tau}} \Phi_s ds \tag{3.74}$$

and the VIX index affinity coefficients $a \in \mathbb{R}$ *and* $b \in \mathbb{R}^n$ *are given in Proposition 10 and have to be evaluated at time* T*.*[12] *Finally, the function*

$$f_\sigma(Z; X_t, t, T) = E^{\mathbb{Q}}\left[e^{iZ^\top X_T} \middle| \mathcal{F}_t \right] \tag{3.75}$$

with $Z = \mathrm{Re}(Z) + i\,\mathrm{Im}(Z) \in \mathbb{C}^n$*, is the risk-neutral conditional characteristic function of* $X_t \in \mathbb{R}^n$*.*

Proof. See Appendix A.6. □

The upper bound $\zeta_c(t,T)$ depends on the CF f_σ of the specific model considered and is derived explicitly for our 2-SVCVJ++ model in Appendix A.4. Similar results can be found in the literature (Branger et al., 2014; Lian and Zhu, 2013; Sepp, 2008a,b). The previous Proposition is completely specified once the conditional CF of the stochastic volatility process X_t is known. As shown in Duffie et al. (2000) and as will be presented in the next Proposition, an affine process X_t always has a CF and its functional form is exponential affine in X_t.

Proposition 12. *Under the affine framework described above and under technical regularity conditions*[13]*, the risk-neutral conditional characteristic function of* $X_t \in \mathbb{R}^n$ *is the following exponential affine function of* X_t

$$f_\sigma(Z; X_t, t, T) = e^{A_\sigma + B_\sigma^\top X_t} \tag{3.76}$$

[12] That is their explicit dependencies in the pricing formulas are $a(T, T+\bar{\tau}; \Psi_{[T,T+\bar{\tau}]})$ and $b(T, T+\bar{\tau}; \Psi_{[T,T+\bar{\tau}]})$.

[13] Refer to (Duffie et al., 2000, Prop. 1).

where the functions $A_\sigma(Z;t,T) \in \mathbb{C}$ and $B_\sigma(Z;t,T) \in \mathbb{C}^n$ satisfy the following ordinary and Riccati differential equations, respectively[14]

$$\begin{aligned}
\dot{A}_\sigma(Z,t,T) &= -K_0^\top B_\sigma - \frac{1}{2} B_\sigma^\top H_0 B_\sigma - \sum_{j=1}^{m_X} \lambda_{0,j} \left(\theta_j(B_\sigma) - 1\right) \\
\dot{B}_\sigma(Z,t,T) &= -K_1^\top B_\sigma - \frac{1}{2} B_\sigma^\top H_1 B_\sigma - \sum_{j=1}^{m_X} \lambda_{1,j} \left(\theta_j(B_\sigma) - 1\right)
\end{aligned} \tag{3.77}$$

with $Z = \mathrm{Re}(Z) + i\,\mathrm{Im}(Z) \in \mathbb{C}^n$ and the terminal conditions $A_\sigma(Z,T,T) = 0$ and $B_\sigma(Z,T,T) = iZ$.

Proof. This proposition is a particular case of (Duffie et al., 2000, Prop. 1). □

The ODE for A_σ is integrable once the Riccati equations for B_σ has been solved. These last often do not have a closed-form analytical solution, mostly because model parameters in K_1 and H_1 may be time-dependent or in case of co-jumps between volatility factors, modeled through the jump MGF $\theta_j(B_{i,\sigma}, B_{k,\sigma})$ which eventually couples the two Riccati for $B_{i,\sigma}$, and $B_{k,\sigma}$, making them not separately integrable.

[14] Here $x^\top H_1 x \in \mathbb{C}^n$ is the complex vector whose k-th component is $\sum_{i,j=1}^n x_i (H_1^{(k)})_{ij} x_j$ and $H_1^{(k)} \in \mathbb{R}^{n\times n}$.

Chapter 4

The Heston++ model: empirical analysis

In our empirical analysis we jointly fit S&P500 options - together with VIX futures and options - using the Heston++ model. We study the contribution of the various features of the model analyzing their impact on the pricing performance over a sample period of two years.

Our study endorses the results from literature concerning the need of a multi-factor specification of the volatility dynamics (Andersen et al., 2002; Bates, 2012; Egloff et al., 2010; Kaeck and Alexander, 2012; Mencía and Sentana, 2013) and of a discontinuous returns process (Bakshi et al., 1997; Bates, 1996; Eraker, 2004; Pan, 2002). We therefore choose as a benchmark model for our analysis the 2-SVJ model of Section 3.1.2, which features two Heston stochastic volatility factors and normal jumps in the returns dynamics. We then analyze the different contributions of jumps in volatility inserting two sources of exponential jumps in one of the two volatility factors. We first add them separately as an idiosyncratic source of discontinuity (2-SVVJ model) and then correlated and synchronized with jumps in price (2-SVCJ model). Then, we let the two discontinuity components act together in the 2-SVCVJ model.

At the same time, we make a displacement transformation on the volatility dynamics of each $\mathcal{H}$ model considered and analyze the performance of the corresponding $\mathcal{H}++$ model. In addition, we repeat the analysis restricting the freedom of factor parameters imposing the Feller condition (Andersen and Piterbarg, 2007; Cox et al., 1985; Duffie and Kan, 1996).

Our analysis shows that the Heston++ model - calibrated consistently on the three markets - works remarkably well, with an overall absolute (relative) estimation error below 2.2% (4%). The key feature of the model is a deterministic

displacement of the instantaneous volatility, in addition to the usual multi-factor affine structure. Our empirical results show a decisive improvement in the pricing performance over non-displaced models, and also provide clear empirical support for the presence of both price-volatility co-jumps and idiosyncratic jumps in the volatility dynamics.

The chapter is structured as follows: Section 4.1 describes the financial data adopted for the empirical analysis and the descriptive statistics. Section 4.2 discusses the results and Section 4.2.2 describes the impact of restricting the volatility dynamics imposing the Feller condition. Section 4.3 concludes.

4.1 Empirical analysis

Our sample period spans two years, ranging from January 7, 2009 to December 29, 2010. The sampling frequency is weekly and the observation day is Wednesday. In total, we have 104 weekly surfaces and term structures. Closing prices of S&P500 vanilla and VIX options are adopted, together with settlement prices of VIX futures.

Commonly adopted exclusion filters are applied to data (Aït-Sahalia and Lo, 1998; Bakshi et al., 1997; Bardgett et al., 2013). We exclude option quotes with negative bid-ask spreads, zero bids and filter out observations not satisfying standard no-arbitrage conditions.[1] Potential liquidity and asynchronicity biases are reduced considering only options with maturity between one week and one year and excluding contracts not traded on a given date. Following Bardgett et al. (2013), the analysis is carried out only with liquid OTM options for the S&P500 market and only with liquid call options for the VIX market. If a VIX ITM call lacks of liquidity, we use the put-call parity in equation (2.12) to infer the liquid price of the call from a more liquid VIX OTM put. [2] We compute moneyness as the option exercise price divided by the current index level for SPX options and as the ratio of the option strike and the VIX futures settle price for options on VIX.[3] We further exclude glaring outliers (for a total of three market prices of VIX options) and eliminate SPX (VIX) maturity slices made of less than 6 (3) options quoted.
The final sample is made of a total of 24,279 vanilla options (233 per day), 2,767 VIX options (27 per day), and 792 VIX futures (8 per day). OTM vanilla (VIX call options) span on average 7 (5) maturity slices, ranging from 1 (4) weeks-to-maturity to 12 (6) months and from 0.5 (0.4) to 1.4 (3.3) in the moneyness dimension. The term structure of VIX futures ranges from roughly 7 days to 10 months.

[1] For example, we eliminate VIX options on the basis of the appropriate parity relations discussed in Section 2.1.3.

[2] We consider as *liquid* a contract, either option or futures, which has both positive Volume and Open Interests.

[3] Therefore, OTM calls (puts), either vanilla or VIX options, are options of moneyness > 1 (< 1).

Vanilla options range in the entire filtered time-frame from one week to the year, whereas VIX options range from 4 weeks to 6 months.

Summary statistics for S&P500 index options, are presented in Table 1 and sample characteristics of VIX derivatives are presented in Table 2.

The complementarity of SPX and VIX options markets reflects in the opposite relative liquidities of calls and puts. Put (call) options on S&P500 (VIX) index are more heavily traded than calls (puts), accounting for 59% (68%) of the total observations, with OTM puts (calls) more than double than OTM calls (puts). As discussed in Section 2.1.3, a possible explanation for this dichotomy is the fact that both vanilla puts and VIX call options provide insurance from equity market downturns.

Implied volatilities (IVs) of VIX options are generally higher than those for SPX options, the latter averaging around 23% (respectively 32%) in the case of calls (resp. puts) quotes, while the first averaging around 76% (resp. 70%).

The opposite sign of the skewness of S&P500 and VIX distributions, translates in the opposite slopes of IV skews. They decrease with moneyness for S&P500 options, ranging on average from about 30% to 20% going from ITM to OTM calls (respectively from about 36% to 21% going from OTM to ITM puts). The opposite is instead observed in the VIX options market, with average IV skews ranging from levels of 66% to 82% going from ITM to OTM calls (respectively from levels of 61% to 85% going from OTM to ITM puts).

Moreover, based on our sample of data, the ATM term structure of S&P500 IVs does not display a clear trend, ranging roughly between 23% for options of maturities below 45 days and 26% for those expiring in more than 90 days. Nevertheless, this is not the case for VIX options, where we observe a downward trend of about 20 volatility points on average (going from approximately an ATM IV of 82% for options in the nearest maturity bucket, to approximately 60% for options in the farthest one), a fact compatible with a volatility-of-volatility decreasing with time to maturity, which is in turn consistent with the mean-reverting nature of volatility.

Tables 1 and 2 provide further details about the implied volatility surfaces of the two markets along the moneyness-maturity dimensions.

4.2 Calibration results

For each day in sample, we jointly calibrate each $\mathcal{H}$ and $\mathcal{H}$++ model described in the Section 3.1 to daily SPX and VIX option market surfaces and VIX futures term structure.

Table 1: Sample characteristics of S&P500 options. The table reports the average prices, bid-ask spreads (BA), Black and Scholes (1973) implied volatilities (IV), bid-ask implied volatility spreads (IV BA), trading volume, open interests (OI), the total number of (and in percentage of the total) observations (Obs) for each moneyness-maturity category of call (Panel A) and put (Panel B) options on S&P500 index. The sample period is from January 7, 2009 to December 29, 2010 and the sampling frequency is weekly (Wednesdays). *Maturity* is defined as the number of days to expiration. *Moneyness* is defined as the ratio of the option exercise price to the current index level. ITM (OTM), ATM and OTM (ITM) categories for calls (puts) are defined by *Moneyness* < 0.95, $0.95 - 1.05$, and > 1.05, respectively.

Maturity	**Moneyness**							
	Panel A: Calls				Panel B: Puts			
	ITM	**ATM**	**OTM**	**All**	**OTM**	**ATM**	**ITM**	**All**
< 45 Days								
Price	90.84	24.61	2.02	30.12	2.99	24.54	81.08	15.77
BA	2.83	1.81	0.59	1.64	0.72	1.90	2.93	1.27
IV	30.43	22.92	20.14	23.48	36.35	23.39	20.19	30.92
IV BA	7.37	2.17	1.91	3.04	2.90	2.32	7.40	3.04
Volume	351.36	3378.77	2445.77	2557.84	2300.30	3394.44	108.86	2498.61
OI	19734.07	25392.34	17186.77	21987.46	23523.10	22979.02	9930.25	22350.05
Obs	863	2507	1373	4743	4232	2316	517	7065
Obs (% of TOT)	6.63	19.26	10.55	36.43	22.35	12.23	2.73	37.32
$45 - 90$ Days								
Price	114.58	36.67	5.64	29.27	8.51	39.45	112.74	21.76
BA	2.91	2.32	1.09	1.79	1.28	2.44	3.08	1.68
IV	30.37	23.97	19.93	22.65	35.79	24.78	21.21	32.13
IV BA	2.99	1.47	1.65	1.70	2.31	1.53	3.86	2.17
Volume	279.63	1914.14	923.79	1282.75	1314.92	2479.65	215.41	1577.75
OI	20349.71	16199.80	10566.55	13897.48	18797.49	17432.34	11966.58	18107.94
Obs	459	2034	2295	4788	4710	1862	324	6896
Obs (% of TOT)	3.53	15.62	17.63	36.78	24.88	9.83	1.71	36.42
> 90 Days								
Price	149.66	64.52	17.69	48.92	24.24	71.85	168.24	46.99
BA	3.45	3.06	1.96	2.51	2.10	3.11	3.48	2.45
IV	30.20	25.35	21.16	23.64	34.77	25.90	22.24	31.67
IV BA	1.69	1.13	1.23	1.25	1.56	1.16	2.25	1.52
Volume	264.54	1313.80	884.30	959.23	1270.31	1794.78	457.17	1330.29
OI	23226.76	24169.13	24861.13	24436.20	32406.18	22356.63	20350.24	29061.33
Obs	403	1190	1895	3488	3396	1181	395	4972
Obs (% of TOT)	3.10	9.14	14.56	26.79	17.94	6.24	2.09	26.26
All								
Price	110.90	37.18	8.85	34.84	10.95	40.15	117.23	26.15
BA spread	3.00	2.25	1.27	1.93	1.31	2.36	3.14	1.73
IV	30.36	23.80	20.40	23.22	35.70	24.43	21.12	31.56
IV BA spread	4.88	1.70	1.57	2.07	2.31	1.79	4.82	2.32
Volume	311.99	2430.18	1285.98	1660.61	1640.63	2724.07	248.10	1856.39
OI	20713.86	21875.81	17069.84	19668.26	24164.15	20914.65	13794.06	22567.39
Obs	1725	5731	5563	13019	12338	5359	1236	18933
Obs (% of TOT)	13.25	44.02	42.73	100.00	65.17	28.31	6.53	100.00

Table 2: Sample characteristics of VIX options and VIX futures. The table reports the average prices, bid-ask spreads (BA), Black (1976) implied volatilities (IV), bid-ask implied volatility spreads (IV BA), trading volume, open interests (OI), the total number of (and in percentage of the total) observations (Obs) for each moneyness-maturity category of call (Panel A) and put (Panel C) options on VIX index. Panel B reports VIX futures settle prices, trading volume, open interests and observations for each maturity bucket. The sample period is from January 7, 2009 to December 29, 2010 and the sampling frequency is weekly (Wednesdays). *Maturity* is defined as the number of days to expiration. *Moneyness* for an option of maturity T is defined as the ratio of the option exercise price to the current VIX futures price expiring at T. ITM (OTM), ATM and OTM (ITM) for calls (puts) are defined by *Moneyness* < 0.95, $0.95 - 1.05$, and > 1.05, respectively.

Maturity	**Moneyness**								
	Panel A: Calls				Panel B:	Panel C: Puts			
	ITM	**ATM**	**OTM**	**All**	Futures	**OTM**	**ATM**	**ITM**	**All**
< 45 Days									
Price	6.76	2.55	0.62	2.64	28.24	0.62	2.40	8.63	4.71
BA	0.36	0.19	0.11	0.19		0.11	0.18	0.34	0.23
IV	93.14	82.50	109.75	101.77		74.31	82.42	100.93	88.29
IV BA	41.02	6.81	9.64	18.53		7.92	6.79	24.45	15.47
Volume	748.47	4256.80	3918.95	3026.72	5008.29	6154.98	5738.87	1133.00	3720.95
OI	10959.08	27865.80	46552.45	33978.53	24226.57	42227.53	65398.43	27405.76	39504.99
Obs	209	81	422	712	144	154	81	208	443
Obs (%)	6.68	2.59	13.48	22.74	18.18	10.29	5.41	13.89	29.59
$45 - 90$ Days									
Price	7.03	3.51	1.03	2.77	29.71	1.03	3.51	10.55	4.37
BA	0.40	0.26	0.16	0.23		0.15	0.26	0.39	0.24
IV	66.65	68.55	85.93	79.38		63.89	71.07	80.68	70.23
IV BA	15.81	5.21	6.39	8.59		5.45	5.33	12.35	7.55
Volume	616.66	1705.28	1521.56	1317.62	1698.15	1874.18	1761.46	252.97	1356.71
OI	9259.12	17392.99	19378.60	16679.62	11052.12	24158.37	26138.52	5647.18	18781.01
Obs	188	79	496	763	144	215	66	125	406
Obs (%)	6.00	2.52	15.84	24.37	18.18	14.36	4.41	8.35	27.12
> 90 Days									
Price	7.60	4.12	1.68	3.70	29.99	1.36	3.91	9.40	3.45
BA	0.53	0.39	0.27	0.36		0.24	0.38	0.50	0.32
IV	54.84	59.38	68.87	63.70		55.27	60.99	65.04	58.26
IV BA	13.97	5.60	5.55	8.07		5.68	5.74	8.24	6.22
Volume	167.82	372.16	437.14	349.97	279.97	634.48	874.23	131.62	572.71
OI	2588.51	4694.07	4182.87	3758.77	2629.10	6236.55	5368.43	1337.81	5081.06
Obs	495	170	991	1656	504	403	112	133	648
Obs (%)	15.81	5.43	31.65	52.89	63.64	26.92	7.48	8.88	43.29
All									
Price	7.28	3.59	1.28	3.23	29.62	1.12	3.34	9.37	4.07
BA spread	0.46	0.31	0.21	0.29		0.19	0.29	0.40	0.27
IV	66.30	67.25	82.34	76.18		61.47	70.26	85.26	70.39
IV BA spread	20.70	5.81	6.67	10.58		6.06	5.96	16.58	9.32
Volume	398.47	1644.80	1488.58	1194.48	1397.51	2080.97	2621.70	611.14	1716.98
OI	5955.69	13421.72	17497.20	13779.56	8087.37	18407.28	29435.06	14129.24	18983.52
Obs	892	330	1909	3131	792	772	259	466	1497
Obs (%)	28.49	10.54	60.97	100.00	100.00	51.57	17.30	31.13	100.00

Joint calibration is performed minimizing for each date in sample the following normalized sum of squared relative errors

$$\begin{aligned} L = & \sum_{i=1}^{N_{SPX}} \left(\frac{IV_{i,SPX}^{MKT} - IV_{i,SPX}^{mdl}}{IV_{i,SPX}^{MKT}} \right)^2 \\ & + \frac{N_{SPX}}{N_{Fut}} \sum_{j=1}^{N_{Fut}} \left(\frac{F_j^{MKT} - F_j^{mdl}}{F_j^{MKT}} \right)^2 \\ & + \frac{N_{SPX}}{N_{VIX}} \sum_{k=1}^{N_{VIX}} \left(\frac{IV_{k,VIX}^{MKT} - IV_{k,VIX}^{mdl}}{IV_{k,VIX}^{MKT}} \right)^2 \end{aligned} \tag{4.1}$$

where N_{SPX} (N_{VIX}) are the number of S&P500 (VIX) options quotes observed in a given date, IV^{MKT} (IV^{mdl}) the corresponding market (model) implied volatilities and F^{MKT} (F^{mdl}) the market (model) VIX futures prices term structure, made of N_{Fut} points. The use of relative errors is suggested by the different range of implied volatility values of SPX and VIX options and normalizing factors N_{SPX}/N_{VIX} and N_{SPX}/N_{Fut} adjust for the difference in the number of quotes, which would otherwise severely penalize the fit of the term structure of VIX futures. All $\mathcal{H}$ and $\mathcal{H}$++ models are nested with respect to the metrics in (4.1). We compare the pricing performance of each model separately on each market in terms of the absolute errors

$$\begin{aligned} RMSE_{SPX} &= \sqrt{\frac{1}{N_{SPX}} \sum_{i=1}^{N_{SPX}} \left(IV_{i,SPX}^{MKT} - IV_{i,SPX}^{mdl} \right)^2} \\ RMSE_{Fut} &= \sqrt{\frac{1}{N_{Fut}} \sum_{j=1}^{N_{Fut}} \left(F_j^{MKT} - F_j^{mdl} \right)^2} \\ RMSE_{VIX} &= \sqrt{\frac{1}{N_{VIX}} \sum_{k=1}^{N_{VIX}} \left(IV_{k,VIX}^{MKT} - IV_{k,VIX}^{mdl} \right)^2} \end{aligned} \tag{4.2}$$

and relative errors

$$\begin{aligned} RMSRE_{SPX} &= \sqrt{\frac{1}{N_{SPX}} \sum_{i=1}^{N_{SPX}} \left(\frac{IV_{i,SPX}^{MKT} - IV_{i,SPX}^{mdl}}{IV_{i,SPX}^{MKT}} \right)^2} \\ RMSRE_{Fut} &= \sqrt{\frac{1}{N_{Fut}} \sum_{j=1}^{N_{Fut}} \left(\frac{F_j^{MKT} - F_j^{mdl}}{F_j^{MKT}} \right)^2} \\ RMSRE_{VIX} &= \sqrt{\frac{1}{N_{VIX}} \sum_{k=1}^{N_{VIX}} \left(\frac{IV_{k,VIX}^{MKT} - IV_{k,VIX}^{mdl}}{IV_{k,VIX}^{MKT}} \right)^2} \end{aligned} \tag{4.3}$$

Moreover, we evaluate the overall calibration performance with the aggregate errors

$$RMSE_{All} = \sqrt{\frac{1}{N}\sum_{i}^{N}\left(Q_i^{MKT} - Q_i^{mdl}\right)^2}$$
$$RMSRE_{All} = \sqrt{\frac{1}{N}\sum_{i}^{N}\left(\frac{Q_i^{MKT} - Q_i^{mdl}}{Q_i^{MKT}}\right)^2} \tag{4.4}$$

where $N = N_{SPX} + N_{Fut} + N_{VIX}$ and we have denoted synthetically with Q^{MKT} (Q^{mdl}) the market (model) quotes of the SPX (VIX) implied volatilities IV^{MKT} (IV^{mdl}) and VIX futures prices F^{MKT} (F^{mdl}). In $RMSE_{All}$ definition we have divided by 100 each VIX futures price F in order to make it comparable with the implied volatility levels IV_{SPX} and IV_{VIX}.

Figures from 12 to 18 show, in chronological order, the calibration results and calibrated parameters of the 2-SVCVJ++ and of the nested 2-SVCVJ models for some selected dates and different market situations.

Figures 14 and 16 provide examples of days in which the VIX futures term structure displays a hump. These figures show, quite clearly, that taking advantage of the added flexibility provided by the deterministic shift ϕ_t in fitting the term structure of VIX futures, the 2-SVCVJ++ model (solid red line) is able to calibrate the vanilla and VIX options jointly without particular difficulty. The 2-SVCVJ model (dashed blue line), missing such a flexibility, cannot reproduce the prices of the two market even with the high (17) number of parameters employed. Moreover, the fit of the two surfaces comes at expenses of the fit of the term structure of VIX futures, where the non-displaced model is not able to reproduce the hump, with a relative error $RMSRE_{Fut}$ more than 5 (9) times the corresponding error of the displaced 2-SVCVJ++ model on July 8 (respectively September 2), 2009, which is remarkably low: 0.21% (resp. 0.42%).

Figures 12 and 18 show two rather common and different market situations. The first date, March 4, 2009 (respectively the second one, August 11, 2010), displays a decreasing (resp. roughly increasing) VIX futures term structure. Also in this case, though with two jump sources, the 2-SVCVJ model has some difficulty in reproducing adequately the VIX options skew. To make this clear, consider the term structure of the $K = 40$ strike in the VIX option surface of figure 18. We see that the level of the surface goes from the 180 volatility points (vps) at the nearest maturity of 7 days, to the roughly 60 vps at the longest maturity of 161 days. Nevertheless, the amplitude of the skew, which is of roughly 80 vps at 7 days, is still considerable at the longest maturity (approximately 25 vps). This phenomenon requires a model which is able to recreate the positive sloping skew of the VIX implied surface, not only for the shortest maturities, but for the entire term structure. The increased degrees of freedom introduced by the displacement

Table 3: Calibration errors (in %). This table reports the sample average (max in sample) of the Root Mean Squared Error (Panel A) and Root Mean Squared Relative Error (Panel B) of all the $\mathcal{H}$ and $\mathcal{H}$++ models calibrated jointly to S&P500 options, VIX futures and VIX options market data. The sample period is from January 7, 2009 to December 29, 2010 and the sampling frequency is weekly (Wednesdays). For each date in sample, the fit is performed minimizing the distance L in equation 4.1. Here we report the absolute (relative) errors on (S&P500 and VIX options) implied volatility surfaces $RMSE_{SPX}$ and $RMSE_{VIX}$ ($RMSRE_{SPX}$ and $RMSRE_{VIX}$) in percentage points and errors on the VIX futures term structures in US$. Performance measures are defined in equations (4.2) to (4.3). Overall pricing errors $RMSE_{All}$ and $RMSRE_{All}$ are expressed in percentage points and defined in equation (4.4).

	2-SVJ	2-SVJ++	2-SVCJ	2-SVCJ++	2-SVVJ	2-SVVJ++	2-SVCVJ	2-SVCVJ++
Panel A: RMSE								
$RMSE_{SPX}$	1.17	0.99	1.04	0.86	0.99	0.77	0.90	0.65
	(6.01)	(3.75)	(4.11)	(2.42)	(4.28)	(3.15)	(4.28)	(1.64)
$RMSE_{Fut}$	0.70	0.49	0.59	0.34	0.59	0.31	0.53	0.22
	(3.49)	(1.85)	(1.62)	(1.32)	(1.66)	(1.19)	(1.50)	(1.07)
$RMSE_{VIX}$	5.73	3.82	4.12	2.45	4.06	2.32	3.39	1.64
	(27.91)	(17.58)	(17.66)	(9.03)	(15.55)	(8.76)	(14.70)	(4.03)
$RMSE_{All}$	2.20	1.56	1.70	1.16	1.64	1.07	1.42	0.82
	(8.80)	(4.84)	(5.44)	(3.14)	(7.12)	(3.97)	(4.57)	(2.11)
Panel B: RMSRE								
$RMSRE_{SPX}$	4.06	3.30	3.55	2.73	3.42	2.51	3.07	2.02
	(16.79)	(9.29)	(10.93)	(6.04)	(11.31)	(8.25)	(11.31)	(3.95)
$RMSRE_{Fut}$	2.32	1.61	2.01	1.13	1.98	1.02	1.81	0.74
	(9.11)	(5.01)	(6.48)	(3.73)	(6.14)	(2.92)	(6.13)	(2.60)
$RMSRE_{VIX}$	7.38	4.66	5.69	3.12	5.59	2.88	4.78	2.04
	(28.32)	(16.50)	(25.14)	(13.11)	(23.66)	(12.98)	(23.56)	(4.34)
$RMSRE_{All}$	4.63	3.51	3.91	2.80	3.77	2.56	3.34	2.01
	(15.75)	(9.90)	(10.54)	(6.15)	(10.70)	(7.94)	(10.70)	(3.94)

ϕ_t help a lot also in these situations, with the 2-SVCVJ++ making a relative error $RMSRE_{VIX}$ of 2.55% (resp. 3.26%) on the *backwarding* (resp. *contango*) volatility market of March 4, 2009 (resp. August 11, 2010), which is almost 3.9 (resp. 3.4) times lower than the corresponding $RMSRE_{VIX}$ made by the undisplaced model 2-SVCVJ.

Tables 3 reports the summary statistics on the root mean squared errors for the $\mathcal{H}$ and $\mathcal{H}$++ models averaged over the three markets. Tables 4 and 5 report the same summary statistics dissected on the three markets. Table 6 reports average parameter estimates together with their in-sample standard deviation.

Our results clearly show that the addition of the deterministic shift is crucial for the joint fit of the three markets. The 2-SVCVJ, which is the richer non-displaced model considered, performs very well on average with a sample mean relative error of 3.1% on SPX vanilla options, 1.8% on VIX futures and 4.8% on VIX

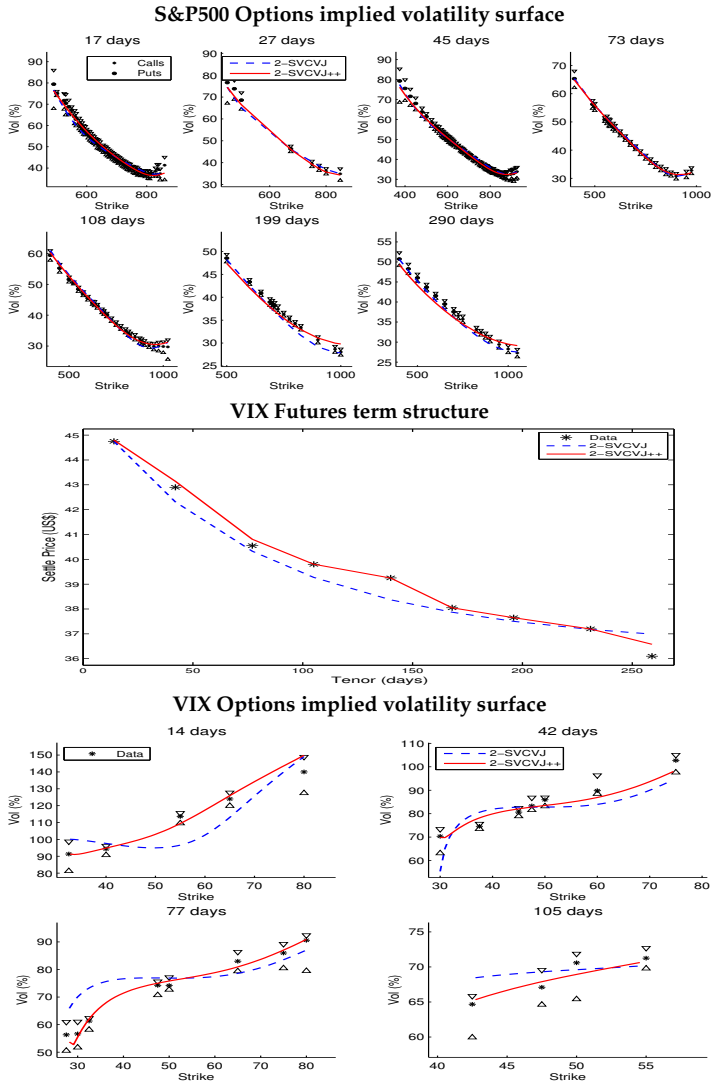

Figure 12: Fit results on March 4, 2009. This figure reports market and model implied volatilities for S&P500 (plot at the top) and VIX (plot at the bottom) options, together with the term structure of VIX futures (plot in the middle) on March 4, 2009 obtained calibrating jointly on the three markets the 2-SVCVJ (blue dashed line) and 2-SVCVJ++ (red line). Maturities and tenors are expressed in days and volatilities are in % points and VIX futures settle prices are in US$. Relative errors 2-SVCVJ++ (2-SVCVJ) model: $RMSRE_{SPX} = 2.04\%$ (2.74%), $RMSRE_{Fut} = 0.53\%$ (1.31%), $RMSRE_{VIX} = 2.55\%$ (9.83%). Absolute errors 2-SVCVJ++ (2-SVCVJ) model: $RMSE_{SPX} = 0.95\%$ (1.30%), $RMSE_{Fut} = 0.20\ US\$$ (0.51 $US\$$), $RMSE_{VIX} = 2.74\%$ (7.62%).

March 4, 2009	2-SVCVJ	2-SVCVJ++
α_1	3.3240	3.0912
$\sqrt{\beta_1}$ (%)	31.9752	24.0894
Λ_1	1.0679	1.1152
ρ_1	-0.8431	-0.9690
$\sigma_{1,0}$ (%)	42.9752	34.5792
α_2	93.7102	43.2533
$\sqrt{\beta_2}$ (%)	17.1913	25.2210
Λ_2	46.1993	8.7081
ρ_2	-0.5685	-0.5891
$\sigma_{2,0}$ (%)	30.6615	34.8718
λ	0.0012	0.0016
$E[c_x]$	-4.3743	-2.2030
$\sqrt{Var[c_x]}$	0.5652	0.6053
$\mu_{co,\sigma}$	18.6006	68.4667
$corr(c_x, c_\sigma)$	0.8477	-0.8799
λ	0.0051	0.0025
$\mu_{id,\sigma}$	17.3522	57.6487

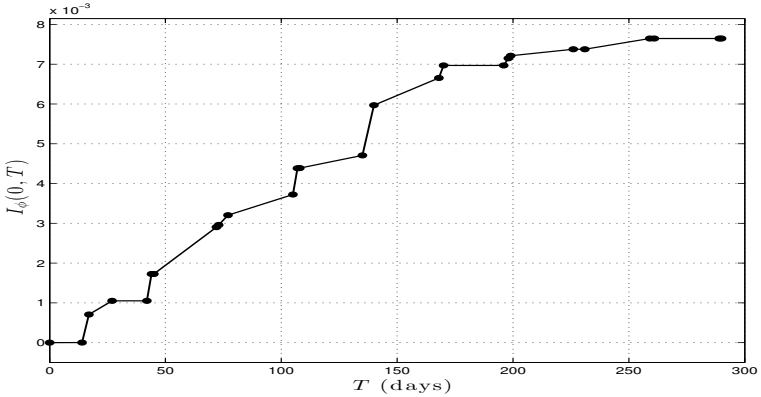

Figure 13: Calibrated parameters on March 4, 2009 of 2-SVCVJ and 2-SVCVJ++ models and $I_\phi(0,T)$ displacement integrals of 2-SVCVJ++ model. Fit results are shown in Figure 12.

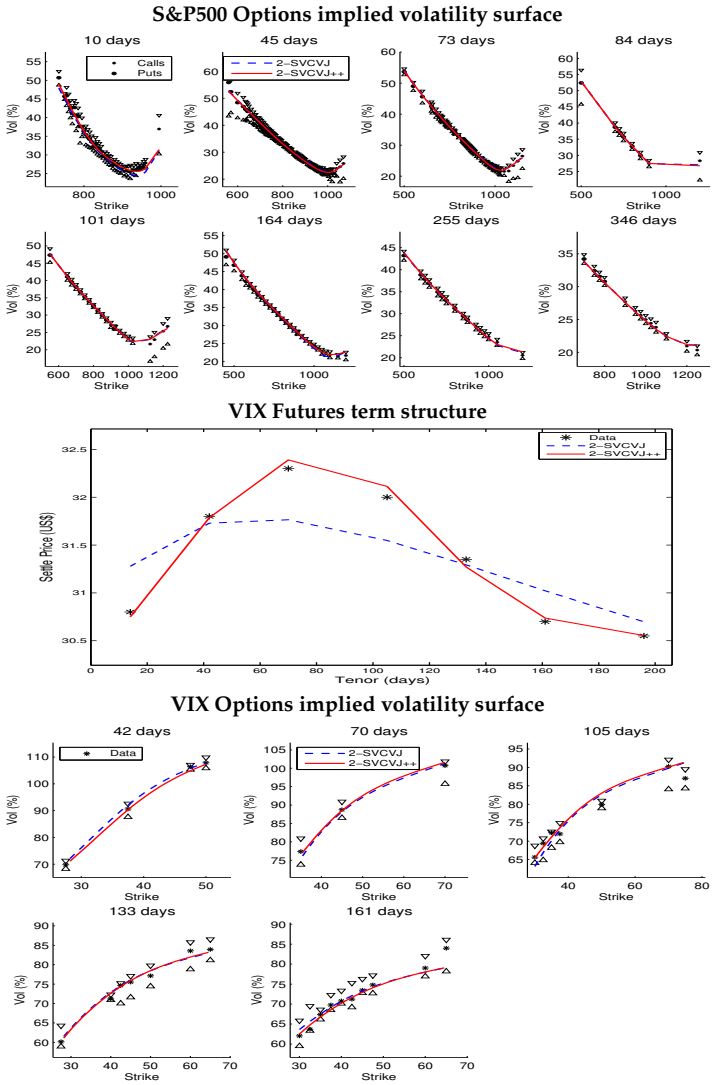

Figure 14: Fit results on July 8, 2009. This figure reports market and model implied volatilities for S&P500 (plot at the top) and VIX (plot at the bottom) options, together with the term structure of VIX futures (plot in the middle) on July 8, 2009 obtained calibrating jointly on the three markets the 2-SVCVJ (blue dashed line) and 2-SVCVJ++ (red line). Maturities and tenors are expressed in days and volatilities are in % points and VIX futures settle prices are in US$. Relative errors 2-SVCVJ++ (2-SVCVJ) model: $RMSRE_{SPX} = 1.77\%$ (2.29%), $RMSRE_{Fut} = 0.21\%$ (1.11%), $RMSRE_{VIX} = 1.89\%$ (2.24%). Absolute errors 2-SVCVJ++ (2-SVCVJ) model: $RMSE_{SPX} = 0.59\%$ (0.73%), $RMSE_{Fut} = 0.07\,US\$$ (0.35 $US\$$), $RMSE_{VIX} = 1.55\%$ (1.73%).

July 8, 2009	2-SVCVJ	2-SVCVJ++
α_1	2.1364	1.8702
$\sqrt{\beta_1}$ (%)	10.4533	9.1898
Λ_1	0.3900	0.4164
ρ_1	-0.8850	-0.9054
$\sigma_{1,0}$ (%)	23.0944	22.2989
α_2	6.3082	6.5529
$\sqrt{\beta_2}$ (%)	27.1845	26.7377
Λ_2	2.3147	2.4890
ρ_2	-0.9194	-0.9265
$\sigma_{2,0}$ (%)	12.7423	10.4210
λ	0.4065	0.5185
$E[c_x]$	-0.0732	-0.0778
$\sqrt{Var[c_x]}$	0.1637	0.1577
$\mu_{co,\sigma}$	0.0019	0.0006
$corr(c_x, c_\sigma)$	0.0357	0.0044
λ	0.0009	0.0006
$\mu_{id,\sigma}$	124.5221	147.0826

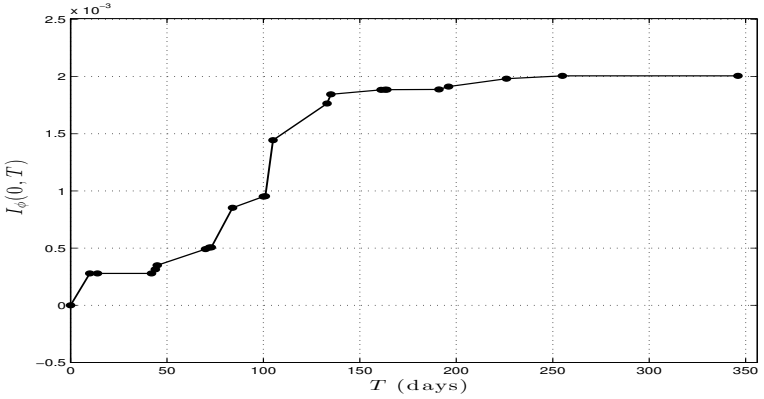

Figure 15: Calibrated parameters on July 8, 2009 of 2-SVCVJ and 2-SVCVJ++ models and $I_\phi(0,T)$ displacement integrals of 2-SVCVJ++ model. Fit results are shown in Figure 14.

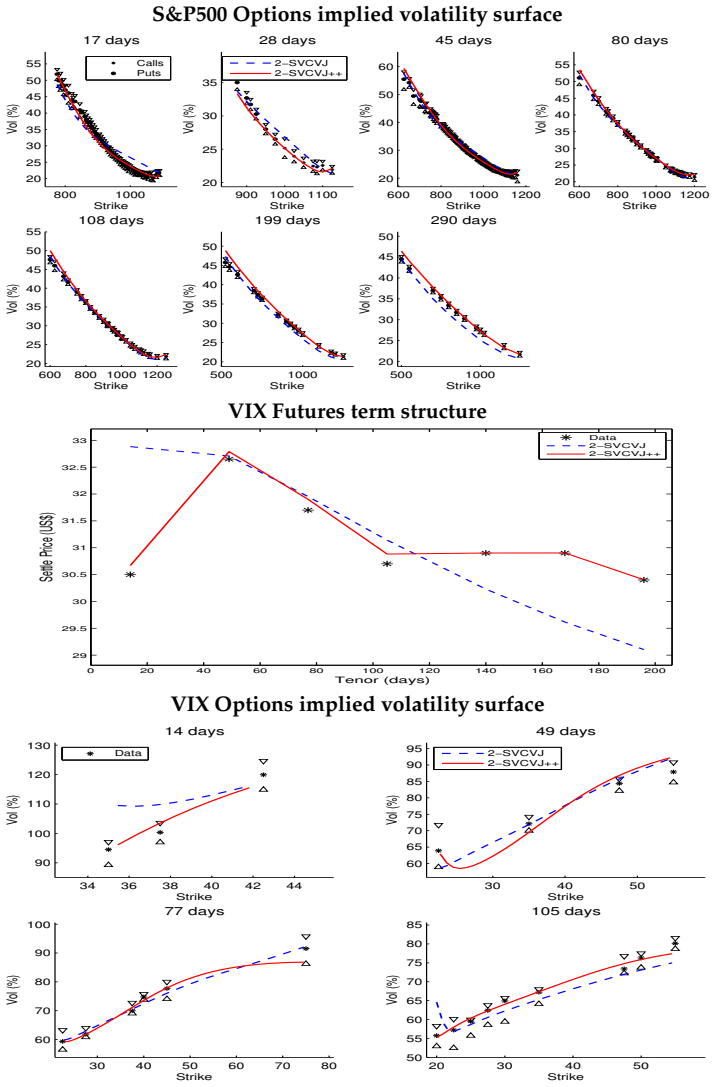

Figure 16: Fit results on September 2, 2009. This figure reports market and model implied volatilities for S&P500 (plot at the top) and VIX (plot at the bottom) options, together with the term structure of VIX futures (plot in the middle) on September 2, 2009 obtained calibrating jointly on the three markets the 2-SVCVJ (blue dashed line) and 2-SVCVJ++ (red line). Maturities and tenors are expressed in days and volatilities are in % points and VIX futures settle prices are in US$. Relative errors 2-SVCVJ++ (2-SVCVJ) model: $RMSRE_{SPX} = 2.74\%$ (5.65%), $RMSRE_{Fut} = 0.42\%$ (3.85%), $RMSRE_{VIX} = 2.31\%$ (6.11%). Absolute errors 2-SVCVJ++ (2-SVCVJ) model: $RMSE_{SPX} = 0.91\%$ (1.56%), $RMSE_{Fut} = 0.13\ US\$$ (1.18 $US\$$), $RMSE_{VIX} = 2.01\%$ (4.87%).

September 2, 2009	2-SVCVJ	2-SVCVJ++
α_1	11.7166	0.8281
$\sqrt{\beta_1}$ (%)	23.3745	1.3579
Λ_1	2.7121	0.3948
ρ_1	-0.5227	-0.9446
$\sigma_{1,0}$ (%)	0.0000	21.4092
α_2	2.5723	8.5742
$\sqrt{\beta_2}$ (%)	0.0336	23.5188
Λ_2	0.4933	2.6570
ρ_2	-1.0000	-0.7593
$\sigma_{2,0}$ (%)	25.2973	7.4480
λ	0.0080	0.0384
$E[c_x]$	-2.3407	-0.5350
$\sqrt{Var[c_x]}$	0.4612	0.6800
$\mu_{co,\sigma}$	10.1579	0.0002
$corr(c_x, c_\sigma)$	-0.9971	0.0851
λ	0.0000	0.0243
$\mu_{id,\sigma}$	1.0000	0.0001

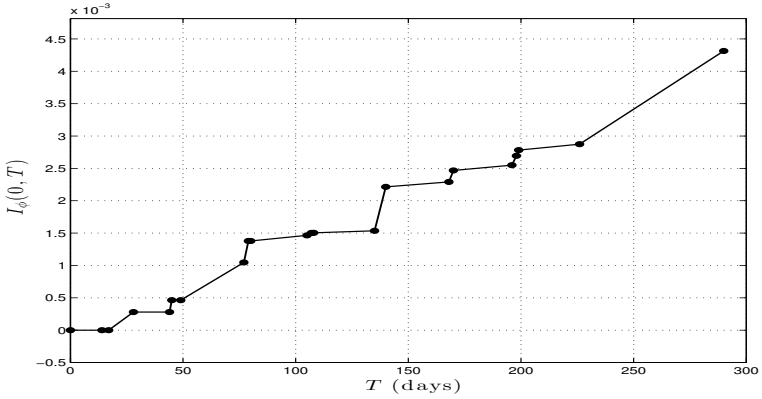

Figure 17: Calibrated parameters on September 2, 2009 of 2-SVCVJ and 2-SVCVJ++ models and $I_\phi(0,T)$ displacement integrals of 2-SVCVJ++ model. Fit results are shown in Figure 16.

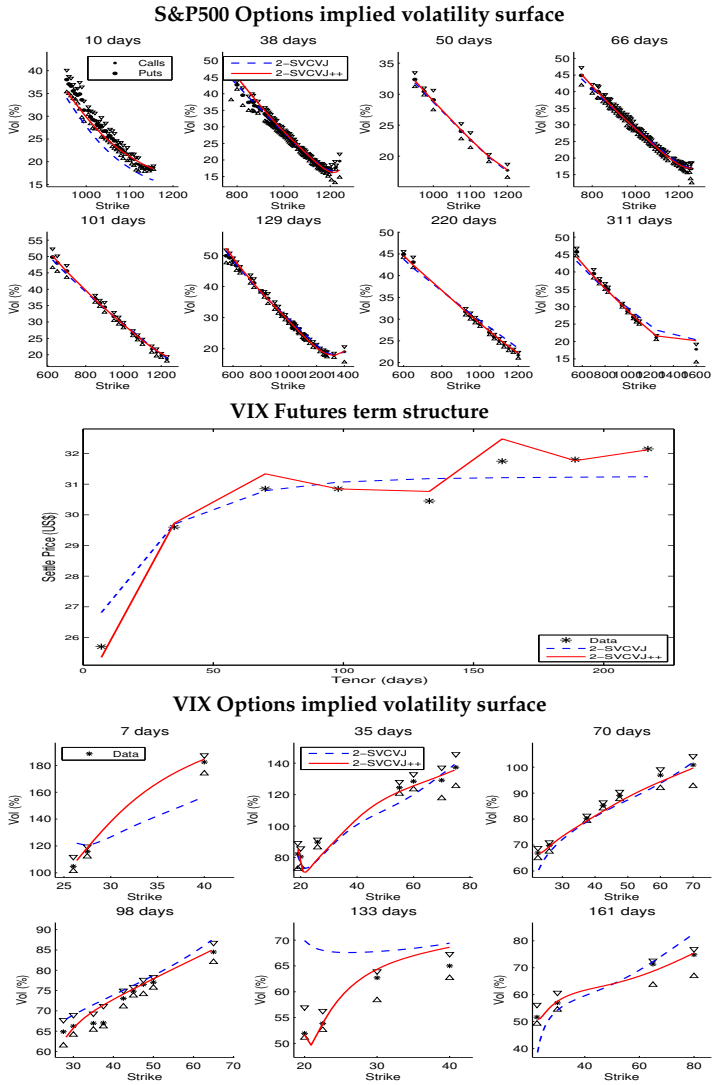

Figure 18: Fit results on August 11, 2010. This figure reports market and model implied volatilities for S&P500 (plot at the top) and VIX (plot at the bottom) options, together with the term structure of VIX futures (plot in the middle) on August 11, 2010 obtained calibrating jointly on the three markets the 2-SVCVJ (blue dashed line) and 2-SVCVJ++ (red line). Maturities and tenors are expressed in days and volatilities are in % points and VIX futures settle prices are in US$. Relative errors 2-SVCVJ++ (2-SVCVJ) model: $RMSRE_{SPX} = 2.88\%$ (5.60%), $RMSRE_{Fut} = 1.17\%$ (2.21%), $RMSRE_{VIX} = 3.26\%$ (11.03%). Absolute errors 2-SVCVJ++ (2-SVCVJ) model: $RMSE_{SPX} = 0.86\%$ (1.47%), $RMSE_{Fut} = 0.35\ US\$$ (0.64 $US\$$), $RMSE_{VIX} = 2.76\%$ (8.39%).

August 11, 2010	2-SVCVJ	2-SVCVJ++
α_1	0.0369	0.1349
$\sqrt{\beta_1}$ (%)	13.8529	44.9580
Λ_1	0.3882	0.5256
ρ_1	-0.6825	-0.9648
$\sigma_{1,0}$ (%)	16.4115	16.4905
α_2	12.0826	15.1604
$\sqrt{\beta_2}$ (%)	26.8442	22.7877
Λ_2	2.4498	3.6664
ρ_2	-0.9913	-1.0000
$\sigma_{2,0}$ (%)	4.3691	7.4445
λ	0.0444	0.0013
$E[c_x]$	-0.2200	-1.1115
$\sqrt{Var[c_x]}$	0.0270	1.9305
$\mu_{co,\sigma}$	0.0003	36.4290
$corr(c_x, c_\sigma)$	-0.9993	-0.7037
λ	0.0010	36.7457
$\mu_{id,\sigma}$	171.2908	0.0000

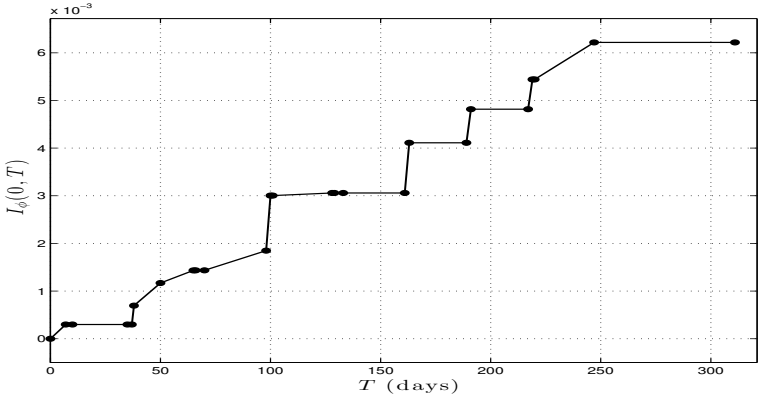

Figure 19: Calibrated parameters on August 11, 2010 of 2-SVCVJ and 2-SVCVJ++ models and $I_\phi(0,T)$ displacement integrals of 2-SVCVJ++ model. Fit results are shown in Figure 18.

Table 4: Calibration RMSE (in %) on VIX futures by Tenor category. This table reports the sample average of the Root Mean Squared Relative Error for different Tenor categories of futures on VIX for all the $\mathcal{H}$ (Panel A) and $\mathcal{H}$++ (Panel B) models. Refer to main text and Table 3 for calibration details. Here we report the relative errors on VIX futures term structures $RMSE_{Fut}$, as defined in the second of (4.3), conditioned to the Tenor category considered, measured in days. Errors are expressed in percentage points and the sample average is weighted by the number of daily observations in each tenor category. Overall errors are reported in Table 3.

	Tenor (days)						
	Panel A: $\mathcal{H}$ models				Panel B: $\mathcal{H}++$ models		
	< 45	$45-90$	> 90		< 45	$45-90$	> 90
2-SVJ	0.39	0.25	1.49	2-SVJ++	0.29	0.17	1.04
2-SVCJ	0.38	0.24	1.19	2-SVCJ++	0.19	0.13	0.70
2-SVVJ	0.36	0.22	1.22	2-SVVJ++	0.17	0.13	0.64
2-SVCVJ	0.35	0.21	1.07	2-SVCVJ++	0.12	0.13	0.44
Observations				Observations (% of TOT = 792)			
	144	144	504		18.18	18.18	63.64

options, as, shown in 3 (Panel A, 7th column). Nevertheless, as shown in Figures 14 and 16, it often fails in reproducing a humped VIX futures term structure and, as confirmed by Table 4 (Panel A), it tends to perform poorly at longer tenors. Moreover, as shown by Figures 12 and 18, the change of the slope of call options on VIX observed at low strikes and the skew term-structure is sometimes hardly fitted and, as confirmed by Table 5 (Panel C), pricing errors tends to concentrate at low values of moneyness and at intermediate maturities.

As shown in Table 5 (Panel A), the calibration error on vanilla options on S&P500 is remarkably low and tends to increase, in absolute terms, at short and long maturities and at higher strikes.

With the simple introduction of the displacement ϕ_t, which is costless from a computational perspective, the overall errors of 2-SVCVJ model, mentioned above, collapse to the 2-SVCVJ++ model errors: 2.0%, 0.7%, and 2.0% (respectively on SPX vanilla, VIX futures and VIX options), which is roughly half of the average relative error without the extension (see Table 3, Panel A, last two columns). It is particularly striking that the *maximum* error in this case becomes 3.9%, 2.6% and 4.3%, which is comparable with the *average* error obtained without displacement (on VIX options, the maximum error with displacement is less than the average error without displacement). From Table 3, the mean (maximum) overall relative pricing error $RMSRE_{All}$ is 3.34% (10.70%) for the 2-SVCVJ model and 2.01% (3.94%) for the displaced 2-SVCVJ++ model.

From Table 6, calibrated parameters are overall in line with typical values found in the literature (Bates, 2000; Christoffersen et al., 2009; Duffie et al., 2000) for two-factor stochastic volatility models. We observe a *fast* mean-reverting factor $\sigma^2_{2,t}$, coupled with a *slow* factor $\sigma^2_{1,t}$. Considering the 2-SVCVJ++ model, the fast (respectively slow) factor shows a half-life $\log(2)/\alpha$ of approximately 5 weeks

Table 5: Calibration RMSE (in %) on SPX and VIX options by Moneyness - Maturity category. This table reports the sample average of the Root Mean Squared Relative Error for different Moneyness and time-to-Maturity categories of options on SPX (respectively VIX) for all the $\mathcal{H}$ models in Panel A (resp. C) and $\mathcal{H}$++ models in Panel B (resp. D). Refer to main text and Table 3 for calibration details. Here we report the relative errors on VIX implied volatility surfaces $RMSE_{VIX}$, as defined in the third of (4.3), conditioned to the Moneyness - Maturity category considered. Time to *Maturity* is measured in days and *Moneyness* for an option of maturity T is defined as the ratio of the option exercise price to the current index level for S&P500 optionts and of the exercise price to the current VIX futures price expiring at T for VIX options. For each category, errors are expressed in percentage points and the sample average is weighted by the number of daily observations in each category.

Maturity	**Moneyness** of SPX options								
	Panel A: $\mathcal{H}$ models					Panel B: $\mathcal{H}++$ models			
	< 0.95	$0.95 - 1.05$	> 1.05	**All**		< 0.95	$0.95 - 1.05$	> 1.05	**All**
< 45 Days									
2-SVJ	3.92	4.59	5.21	4.57	2-SVJ++	3.31	3.07	3.96	3.51
2-SVCJ	3.69	3.99	4.63	4.12	2-SVCJ++	2.98	2.62	3.36	3.04
2-SVVJ	3.33	4.04	4.67	3.95	2-SVVJ++	2.54	2.45	3.50	2.78
2-SVCVJ	3.00	3.68	4.34	3.60	2-SVCVJ++	2.23	2.12	3.06	2.42
$45 - 90$ Days									
2-SVJ	2.42	2.16	3.21	2.71	2-SVJ++	2.17	1.75	2.50	2.26
2-SVCJ	2.11	1.84	2.64	2.31	2-SVCJ++	1.98	1.24	1.96	1.90
2-SVVJ	2.02	1.83	2.70	2.25	2-SVVJ++	1.73	1.27	2.13	1.81
2-SVCVJ	1.88	1.68	2.27	2.01	2-SVCVJ++	1.62	0.90	1.64	1.53
> 90 Days									
2-SVJ	2.61	3.99	6.39	4.40	2-SVJ++	2.51	3.54	5.20	3.80
2-SVCJ	2.42	3.50	5.34	3.82	2-SVCJ++	2.28	2.67	3.89	3.02
2-SVVJ	2.14	3.43	5.30	3.66	2-SVVJ++	1.92	2.50	3.66	2.73
2-SVCVJ	2.11	3.16	4.48	3.27	2-SVCVJ++	1.65	1.43	2.40	1.93
All Days									
2-SVJ	3.21	3.91	5.22		2-SVJ++	2.81	2.98	4.16	
2-SVCJ	2.96	3.37	4.40		2-SVCJ++	2.54	2.39	3.25	
2-SVVJ	2.69	3.41	4.40		2-SVVJ++	2.18	2.24	3.22	
2-SVCVJ	2.49	3.10	3.83		2-SVCVJ++	1.93	1.67	2.40	
Observations					Observations (% of TOT)				
< 45 Days	4232	2642	1373	8247	< 45 Days	17.43	10.88	5.66	33.97
$45 - 90$ Days	4704	2368	2292	9364	$45 - 90$ Days	19.37	9.75	9.44	38.57
> 90 Days	3369	1418	1881	6668	> 90 Days	13.88	5.84	7.75	27.46
All Days	12305	6428	5546	24279	**All** Days	50.68	26.48	22.84	100.00

Maturity	**Moneyness** of VIX options								
	Panel C: $\mathcal{H}$ models					Panel D: $\mathcal{H}++$ models			
	< 0.95	$0.95 - 1.05$	> 1.05	**All**		< 0.95	$0.95 - 1.05$	> 1.05	**All**
< 45 Days									
2-SVJ	10.66	9.50	7.54	9.13	2-SVJ++	4.95	6.73	5.43	5.88
2-SVCJ	7.59	5.74	4.47	5.92	2-SVCJ++	2.79	3.77	3.07	3.25
2-SVVJ	8.45	6.54	4.30	6.25	2-SVVJ++	2.23	3.31	3.29	3.24
2-SVCVJ	6.20	4.95	3.32	4.67	2-SVCVJ++	1.61	2.27	1.98	2.08
$45 - 90$ Days									
2-SVJ	11.10	6.60	4.71	7.46	2-SVJ++	4.99	5.00	3.51	4.37
2-SVCJ	9.32	4.51	3.93	6.25	2-SVCJ++	2.88	2.72	2.96	3.11
2-SVVJ	9.02	4.56	3.54	5.79	2-SVVJ++	2.43	2.70	2.66	2.77
2-SVCVJ	8.31	3.60	3.01	5.19	2-SVCVJ++	1.80	1.89	2.08	2.11
> 90 Days									
2-SVJ	8.89	4.50	4.26	6.07	2-SVJ++	3.64	3.03	3.31	3.53
2-SVCJ	7.61	3.86	3.54	5.15	2-SVCJ++	2.72	2.55	2.65	2.78
2-SVVJ	7.70	3.67	3.10	4.96	2-SVVJ++	2.33	2.40	2.45	2.52
2-SVCVJ	7.25	3.66	2.99	4.73	2-SVCVJ++	1.64	2.13	2.01	2.00
All Days									
2-SVJ	10.78	6.83	5.45		2-SVJ++	4.82	4.67	4.11	
2-SVCJ	8.88	4.87	4.03		2-SVCJ++	3.09	3.06	2.96	
2-SVVJ	8.93	4.94	3.64		2-SVVJ++	2.53	2.85	2.82	
2-SVCVJ	8.02	4.31	3.20		2-SVCVJ++	1.81	2.26	2.10	
Observations					Observations (% of TOT)				
< 45 Days	135	59	390	584	< 45 Days	4.88	2.13	14.09	21.11
$45 - 90$ Days	190	57	477	724	$45 - 90$ Days	6.87	2.06	17.24	26.17
> 90 Days	384	137	938	1459	> 90 Days	13.88	4.95	33.90	52.73
All Days	709	253	1805	2767	**All** Days	25.62	9.14	65.23	100.00

Table 6: Calibrated parameters. This table reports the sample median (median absolute deviation) of joint SPX, VIX futures and VIX options calibrated parameters for all the $\mathcal{H}$ and $\mathcal{H}$++ models considered in the empirical analysis. The sample period is from January 7, 2009 to December 29, 2010 and the sampling frequency is weekly (Wednesdays). Panel A (B) reports 1^{st} (2^{nd}) volatility factor diffusive parameters. Panel C reports intensity and unconditional mean and standard deviation of normal jumps in price, where $E[c_x] = \mu_x$ and $Var[c_x] = \delta_x^2$ under 2-SVJ, 2-SVVJ models (respectively $\mu_x + \rho_J \mu_{co,\sigma}$ and $\delta_x^2 + \rho_J^2 \mu_{co,\sigma}^2$ under 2-SVCJ, 2-SVCVJ) and analogously under the corresponding displaced specifications. Panel D reports the correlated co-jumps parameters. The unconditional correlation between jump sizes is $corr(c_x, c_\sigma) = \rho_J \mu_{co,\sigma} / \sqrt{Var[c_x]}$ under models 2-SVCJ, 2-SVCVJ and corresponding displaced specifications. Panel E reports the idiosyncratic jumps parameters.

	2-SVJ	2-SVJ++	2-SVCJ	2-SVCJ++	2-SVVJ	2-SVVJ++	2-SVCVJ	2-SVCVJ++
Panel A: 1^{st} Factor								
α_1	2.714	2.444	2.262	2.097	2.140	2.084	1.967	1.676
	(1.564)	(1.544)	(1.347)	(1.150)	(1.279)	(1.310)	(1.334)	(1.070)
$\sqrt{\beta_1}$ (%)	21.419	20.878	19.157	19.275	20.399	20.353	17.819	18.219
	(5.460)	(5.629)	(6.282)	(6.300)	(8.181)	(7.495)	(9.162)	(6.079)
Λ_1	0.637	0.554	0.481	0.491	0.433	0.492	0.445	0.504
	(0.341)	(0.225)	(0.227)	(0.159)	(0.204)	(0.173)	(0.219)	(0.115)
ρ_1	−0.871	−0.884	−0.876	−0.891	−0.879	−0.891	−0.865	−0.964
	(0.122)	(0.105)	(0.121)	(0.095)	(0.117)	(0.102)	(0.121)	(0.036)
$\sigma_{1,0}$ (%)	16.679	16.691	16.977	16.484	16.307	16.047	16.250	16.376
	(6.885)	(5.927)	(4.845)	(4.615)	(4.349)	(4.850)	(4.677)	(4.837)
Panel B: 2^{nd} Factor								
α_2	7.740	6.583	8.058	6.998	8.240	7.346	8.451	6.488
	(3.005)	(2.035)	(3.190)	(2.577)	(4.221)	(3.458)	(3.420)	(2.477)
$\sqrt{\beta_2}$ (%)	20.642	20.795	21.658	21.536	22.181	21.084	22.950	21.531
	(2.707)	(2.602)	(3.401)	(2.826)	(4.456)	(4.258)	(4.308)	(3.158)
Λ_2	2.207	2.194	2.196	2.219	1.992	2.156	2.050	2.115
	(1.036)	(0.615)	(0.870)	(0.728)	(0.778)	(0.606)	(0.738)	(0.576)
ρ_2	−0.939	−0.997	−0.996	−1.000	−0.995	−1.000	−0.997	−1.000
	(0.061)	(0.003)	(0.004)	(0.000)	(0.005)	(0.000)	(0.003)	(0.000)
$\sigma_{2,0}$ (%)	10.085	7.461	9.024	8.387	7.895	7.634	8.683	7.984
	(6.680)	(5.627)	(6.912)	(6.050)	(5.583)	(4.176)	(6.309)	(4.640)
Panel C: Price jumps								
λ	0.038	0.040	0.040	0.045	0.041	0.079	0.079	0.064
	(0.035)	(0.037)	(0.034)	(0.040)	(0.038)	(0.061)	(0.053)	(0.055)
$E[c_x]$	−0.377	−0.362	−0.398	−0.371	−0.265	−0.262	−0.240	−0.280
	(0.281)	(0.256)	(0.257)	(0.227)	(0.189)	(0.176)	(0.151)	(0.183)
$\sqrt{Var[c_x]}$	0.520	0.512	0.554	0.521	0.269	0.245	0.318	0.413
	(0.291)	(0.282)	(0.347)	(0.335)	(0.184)	(0.151)	(0.215)	(0.255)
Panel D: CO-jumps								
$\mu_{co,\sigma}$	-	-	0.153	0.090	-	-	0.039	0.065
	-	-	(0.153)	(0.090)	-	-	(0.039)	(0.065)
$corr(c_x, c_\sigma)$	-	-	−0.428	−0.341	-	-	−0.363	−0.520
	-	-	(0.428)	(0.346)	-	-	(0.366)	(0.458)
Panel E: Idiosyncratic jumps								
λ'	-	-	-	-	0.003	0.002	0.002	0.013
	-	-	-	-	(0.003)	(0.002)	(0.002)	(0.012)
$\mu_{id,\sigma}$	-	-	-	-	5.510	10.091	1.213	0.052
	-	-	-	-	(5.500)	(10.084)	(1.213)	(0.052)

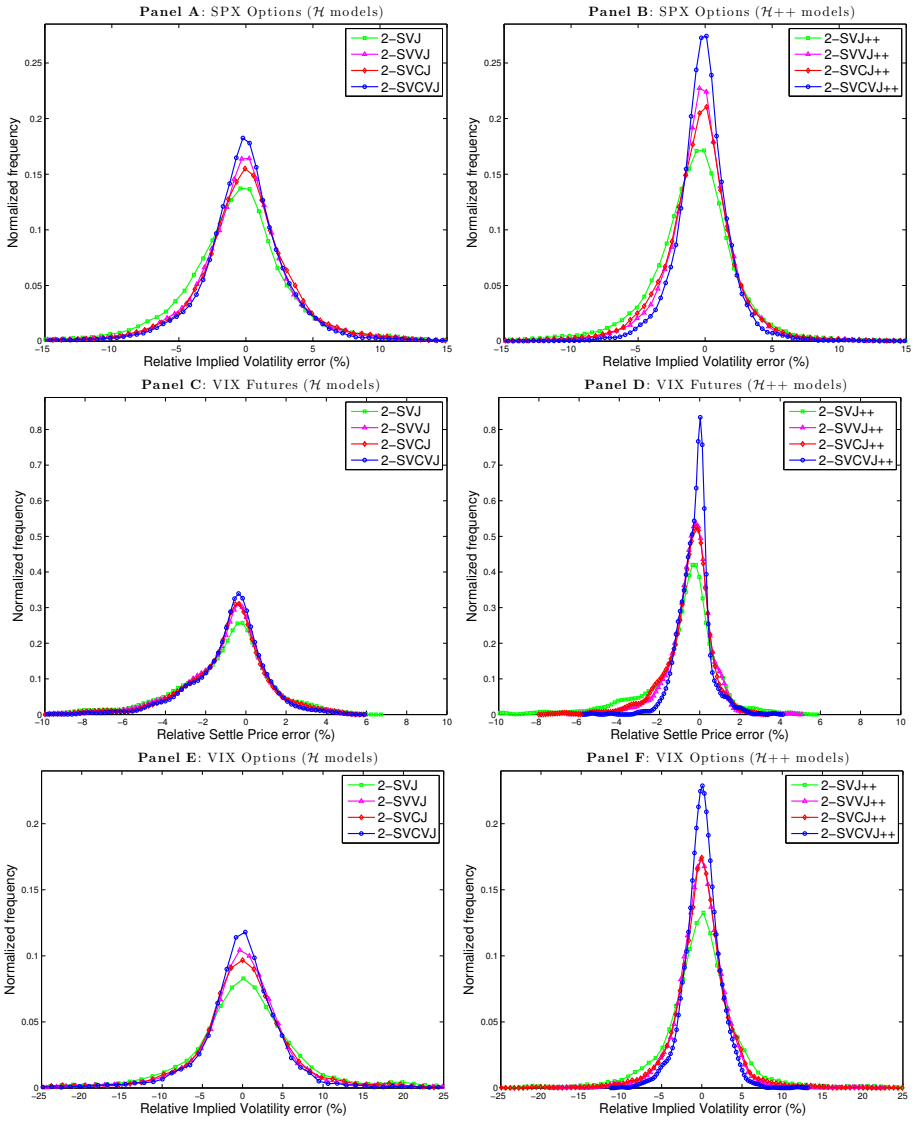

Figure 20: Relative error distribution. This figure reports the relative pricing error for all calibrated $\mathcal{H}$ and $\mathcal{H}++$ models, computed for each of the 24279 S&P500 implied volatilities, each of the 792 VIX Futures settle prices, and each of the 2767 VIX implied volatilities distributed along the 104 Wednesdays in the sample period, from January 7, 2009 to December 29, 2010. Refer to main text and Table 3 for calibration details. In Panel A (B) we plot the error distribution of $\mathcal{H}$ ($\mathcal{H}$++) models on SPX implied volatilities. In Panel C (D) we plot the error distribution of $\mathcal{H}$ ($\mathcal{H}$++) models on VIX Futures settle prices. In Panel E (F) we plot the error distribution of $\mathcal{H}$ ($\mathcal{H}$++) models on VIX implied volatilities. All errors are expressed in percentage points.

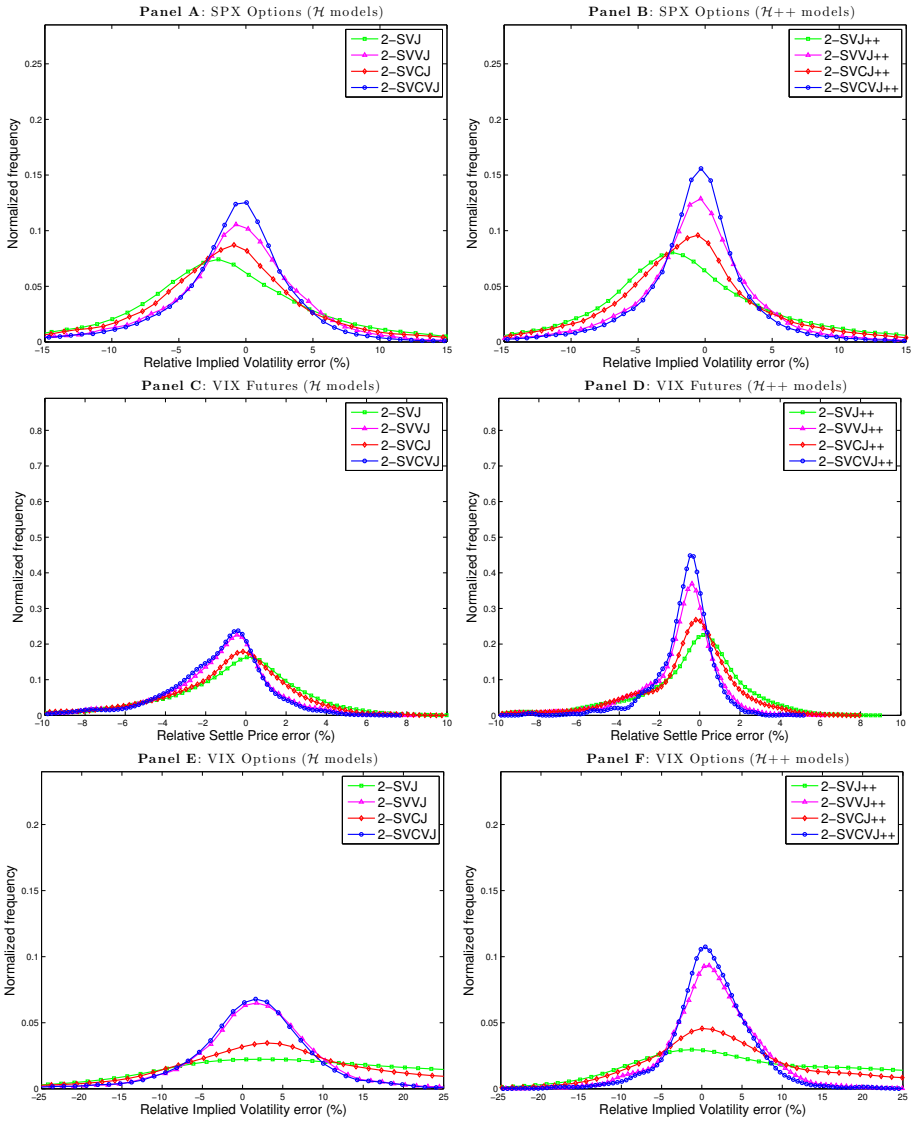

Figure 21: Relative error distribution with Feller condition imposed. This figure reports the relative pricing error for all calibrated $\mathcal{H}$ and $\mathcal{H}++$ models, as in figure 20, but with the Feller condition $2\alpha_i\beta_i \geq \Lambda_i^2$ imposed on both stochastic volatility factors ($\sigma_{i,t}^2$ $i = 1, 2$). Refer to Section 4.2.2 and Table 8 for calibration details. All errors are expressed in percentage points.

(resp. 5 months) and contributes with roughly 18 vps[4] (resp. 22 vps) to the long-term volatility level $\sqrt{\beta}$. The low values of jump-intensities confirm that jumps are *rare* events. The average number of jumps per year $252 \times \lambda$ is estimated around 16 for *co-jumps* and less (approximately 3) in the case of *idiosyncratic* jumps. These numbers are respectively slightly above[5] (resp. below) the 8/9 (resp. 13) per annum estimated by Bandi and Renò, 2015 with an extensive econometric analysis. Co-jumps (respectively idiosyncratic jumps) contribute to an increase of approximately 5% (resp. 2%) of the long-term volatility level, which is approximately evaluated as $\sqrt{\lambda \mu_{co,\sigma}/\alpha_1}$ (resp. $\sqrt{\lambda' \mu_{id,\sigma}/\alpha_1}$) for the case of co-jumps (resp. idiosyncratic jumps).

Figure 20 shows, visually, the distribution of relative signed pricing errors

$$\frac{Q_i^{MKT} - Q_i^{mdl}}{Q_i^{MKT}} \tag{4.5}$$

with Q_i definitions depending on the considered market (as described for equation 4.4), on all the $24,279$ S&P500 options, $2,767$ VIX options and 792 VIX Futures implied volatilities observed in the 104 days considered in the sample. The advantage of the extension over the traditional specification is large and clearly displayed. If the 2-SVCVJ model is used for consistent calibration of the three markets, the 10.7% (1.8%) of S&P500 options implied volatilities (respectively the 2.8% (0.3%) of VIX futures settle prices and 21.4% (6.2%) of VIX options implied volatilies) are priced with a relative error greater than 5% (10%).

The displacement increases remarkably the pricing performance, especially in reproducing the term structure of VIX futures and the VIX implied volatility surface. Indeed, when the 2-SVCVJ++ model is used, only the 3.3% (0.4%) of S&P500 options implied volatilities (respectively the 0.1% (0.0%) of VIX futures settle prices and 3.5% (0.1%) of VIX options implied volatilities) are priced with a relative error greater than 5% (10%).

4.2.1 Impact of the short-term

Using vanilla options data on DAX, EuroStoxx50 and FTSE indexes, Da Fonseca and Grasselli (2011) analyze the theoretical properties and calibration performance of several competitive option pricing models, focusing on the SV Heston (1993) model, the 2-SV Christoffersen et al. (2009) model and both single asset and multi-asset Wishart specifications: the Wishart Multidimensional Stochasti Volatility model (WMSV hereafter, introduced by Da Fonseca et al. (2008)) and the Wishart Affine Stochastic Correlation model (WASC hereafter, introduced by

[4] Volatility points.

[5] But inside the 95% confidence interval.

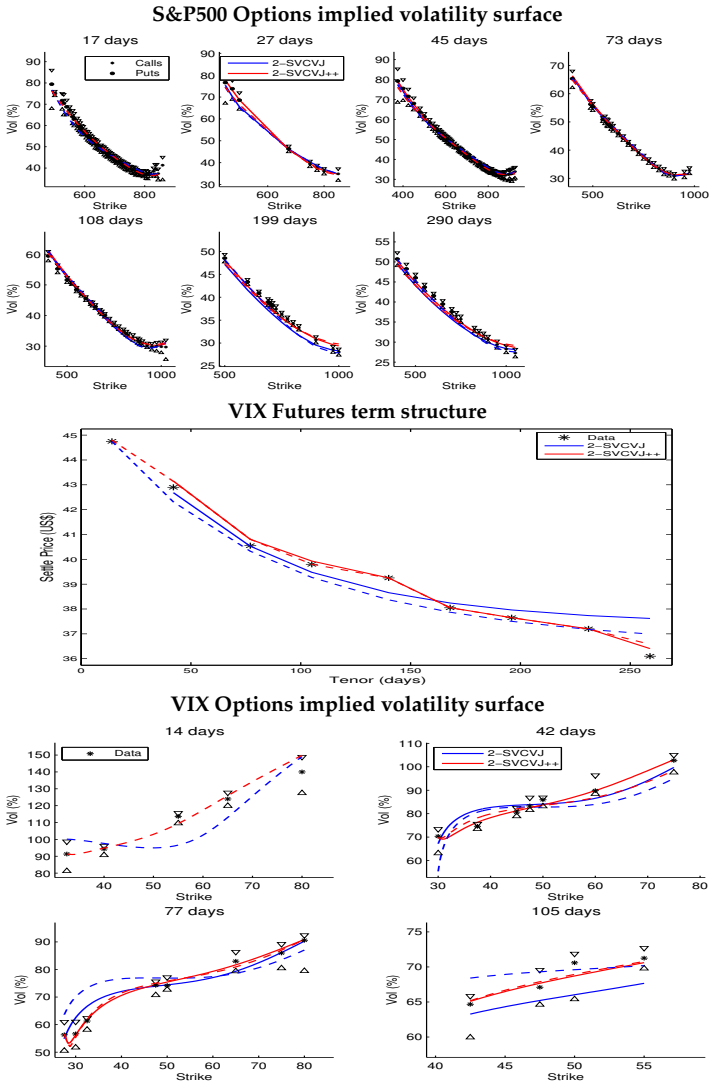

Figure 22: Impact of the short-term: fit results on March 4, 2009. This figure reports market and model implied volatilities for S&P500 (plot at the top) and VIX (plot at the bottom) options, together with the term structure of VIX futures (plot in the middle) on March 4, 2009 obtained calibrating jointly on the three markets the 2-SVCVJ (blue dashed line) and 2-SVCVJ++ (red dashed line). Maturities and tenors are expressed in days and volatilities are in % points and VIX futures settle prices are in US$. Superimposed (continuous lines) is the corresponding fit obtained with same models but excluding from the calibrating sample all contracts with maturity below 3 weeks.

March 4, 2009	2-SVCVJ		2-SVCVJ++	
minimum term	1 week	3 weeks	1 week	3 weeks
α_1	3.3240	4.5873	3.0912	3.2527
$\sqrt{\beta_1}$ (%)	31.9752	31.1138	24.0894	26.4659
Λ_1	1.0679	1.1687	1.1152	1.0705
ρ_1	−0.8431	−0.7720	−0.9690	−0.9601
$\sigma_{1,0}$ (%)	42.9752	44.0075	34.5792	33.7362
α_2	93.7102	76.7253	43.2533	36.0825
$\sqrt{\beta_2}$ (%)	17.1913	18.0654	25.2210	25.2725
Λ_2	46.1993	44.2530	8.7081	10.4823
ρ_2	−0.5685	−0.7326	−0.5891	−0.6765
$\sigma_{1,0}$ (%)	30.6615	24.4879	34.8718	34.1177
λ	0.0012	0.0013	0.0016	0.0015
$E[c_x]$	−4.3743	−5.9784	−2.2030	−0.9576
$\sqrt{Var[c_x]}$	0.5652	2.6655	0.6053	0.4291
$\mu_{co,\sigma}$	18.6006	23.7498	68.4667	62.3184
$corr(c_x, c_\sigma)$	0.8477	−0.7592	−0.8799	−0.8443
λ'	0.0051	0.0068	0.0025	0.0015
$\mu_{id,\sigma}$	17.3522	17.4651	57.6487	56.0874

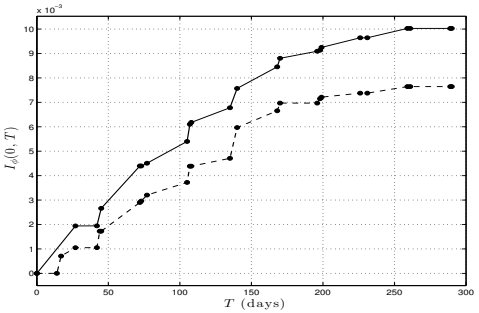

Figure 23: Impact of the short-term: calibrated parameters on March 4, 2009 of 2-SVCVJ and 2-SVCVJ++ models and $I_\phi(0,T)$ displacement integrals of 2-SVCVJ++ model: dashed (respectively continuous) line if short-term contracts are (resp. are not) included. Fit results are shown in Figure 22.

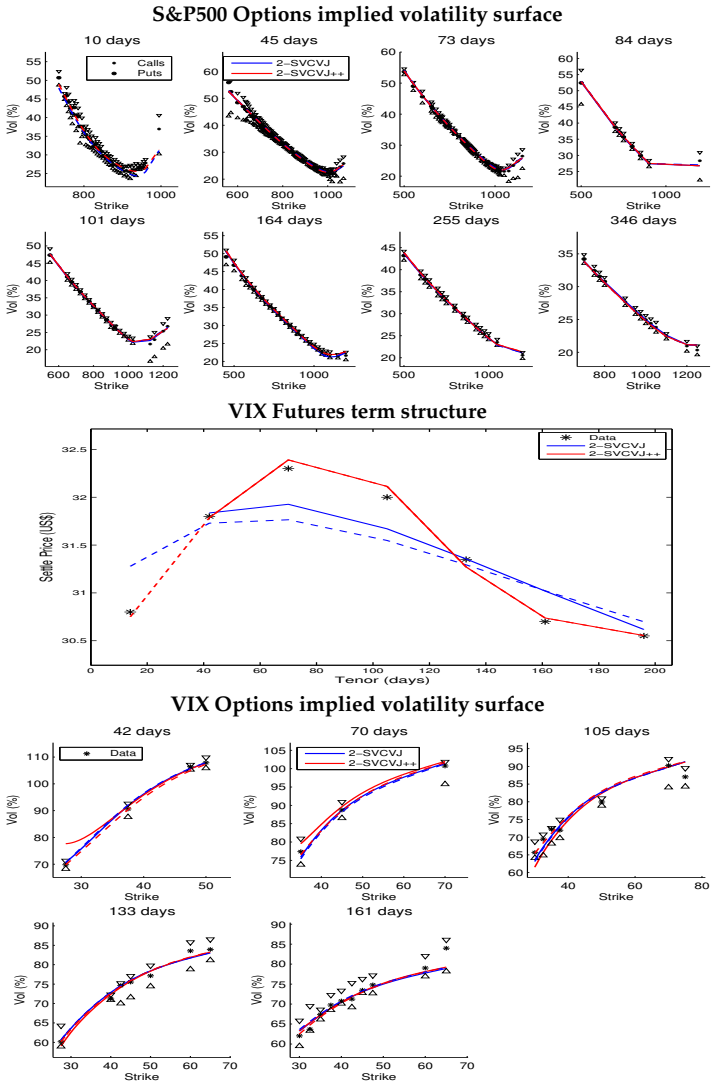

Figure 24: Impact of the short-term: fit results on July 8, 2009. This figure reports market and model implied volatilities for S&P500 (plot at the top) and VIX (plot at the bottom) options, together with the term structure of VIX futures (plot in the middle) on March 4, 2009 obtained calibrating jointly on the three markets the 2-SVCVJ (blue dashed line) and 2-SVCVJ++ (red dashed line). Maturities and tenors are expressed in days and volatilities are in % points and VIX futures settle prices are in US$. Superimposed (continuous lines) is the corresponding fit obtained with same models but excluding from the calibrating sample all contracts with maturity below 3 weeks.

July 8, 2009	2-SVCVJ		2-SVCVJ++	
minimum term	1 week	3 weeks	1 week	3 weeks
α_1	2.1364	1.9274	1.8702	1.8702
$\sqrt{\beta_1}$ (%)	10.4533	7.7945	9.1898	9.1898
Λ_1	0.3900	0.3741	0.4164	0.4164
ρ_1	-0.8850	-0.8886	-0.9054	-0.9054
$\sigma_{1,0}$ (%)	23.0944	22.8217	22.2989	22.2989
α_2	6.3082	7.2736	6.5529	6.5529
$\sqrt{\beta_2}$ (%)	27.1845	27.4401	26.7377	26.7377
Λ_2	2.3147	2.5024	2.4890	2.4890
ρ_2	-0.9194	-0.8755	-0.9265	-0.9265
$\sigma_{1,0}$ (%)	12.7423	10.4250	10.4210	10.4210
λ	0.4065	0.3682	0.5185	0.5185
$E[c_x]$	-0.0732	-0.0902	-0.0778	-0.0778
$\sqrt{Var[c_x]}$	0.1637	0.1662	0.1577	0.1577
$\mu_{co,\sigma}$	0.0019	0.0001	0.0006	0.0006
$corr(c_x, c_\sigma)$	0.0357	0.3155	0.0044	0.0044
λ'	0.0009	0.0009	0.0006	0.5185
$\mu_{id,\sigma}$	124.5221	109.0204	147.0826	147.0826

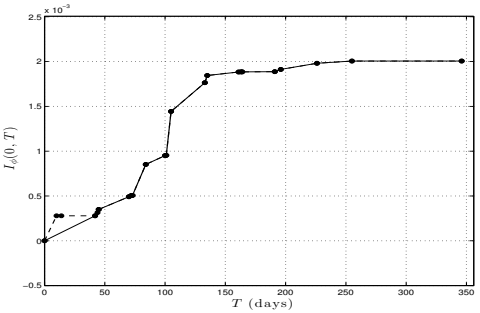

Figure 25: Impact of the short-term: calibrated parameters on July 8, 2009 of 2-SVCVJ and 2-SVCVJ++ models and $I_\phi(0,T)$ displacement integrals of 2-SVCVJ++ model: dashed (respectively continuous) line if short-term contracts are (resp. are not) included. Fit results are shown in Figure 24.

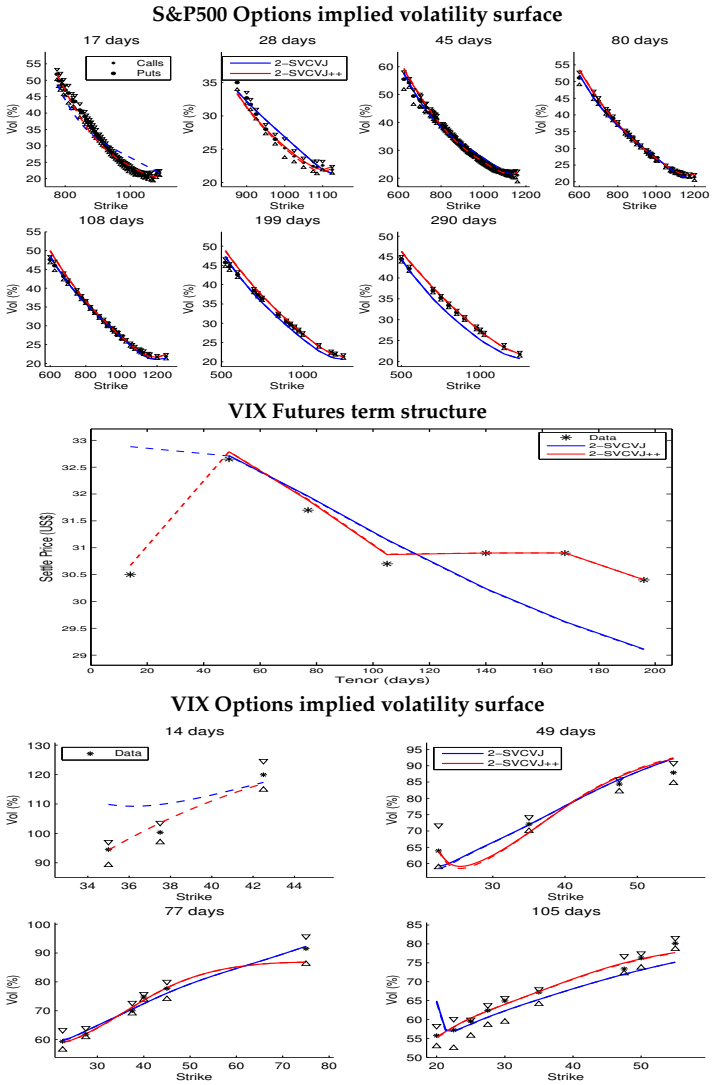

Figure 26: Impact of the short-term: fit results on September 2, 2009. This figure reports market and model implied volatilities for S&P500 (plot at the top) and VIX (plot at the bottom) options, together with the term structure of VIX futures (plot in the middle) on March 4, 2009 obtained calibrating jointly on the three markets the 2-SVCVJ (blue dashed line) and 2-SVCVJ++ (red dashed line). Maturities and tenors are expressed in days and volatilities are in % points and VIX futures settle prices are in US$. Superimposed (continuous lines) is the corresponding fit obtained with same models but excluding from the calibrating sample all contracts with maturity below 3 weeks.

September 2, 2009	2-SVCVJ		2-SVCVJ++	
minimum term	1 week	3 weeks	1 week	3 weeks
α_1	11.7166	11.7166	0.8281	1.0315
$\sqrt{\beta_1}$ (%)	23.3745	23.3752	1.3579	1.5546
Λ_1	2.7121	2.7121	0.3948	0.3961
ρ_1	−0.5227	−0.5227	−0.9446	−0.8938
$\sigma_{1,0}$ (%)	0.0000	0.1068	21.4092	22.2138
α_2	2.5723	2.5723	8.5742	8.3877
$\sqrt{\beta_2}$ (%)	0.0336	0.0336	23.5188	23.6298
Λ_2	0.4933	0.4933	2.6570	2.6278
ρ_2	−1.0000	−1.0000	−0.7593	−0.8246
$\sigma_{1,0}$ (%)	25.2973	25.2983	7.4480	6.7962
λ	0.0080	0.0080	0.0384	0.0374
$E[c_x]$	−2.3407	−2.3407	−0.5350	−0.4986
$\sqrt{Var[c_x]}$	0.4612	0.4612	0.6800	0.6866
$\mu_{co,\sigma}$	10.1579	10.1579	0.0002	0.0002
$corr(c_x, c_\sigma)$	−0.9971	−0.9971	0.0851	0.0723
λ'	0.0000	0.0000	0.0243	0.0374
$\mu_{id,\sigma}$	1.0000	1.0000	0.0001	0.0001

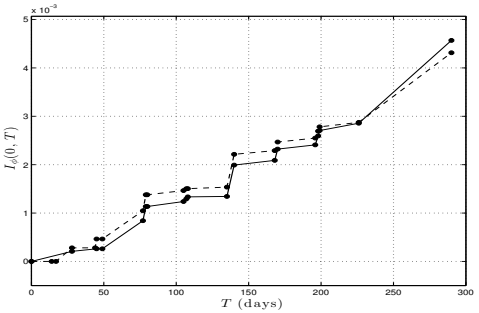

Figure 27: Impact of the short-term: calibrated parameters on September 2, 2009 of 2-SVCVJ and 2-SVCVJ++ models and $I_\phi(0,T)$ displacement integrals of 2-SVCVJ++ model: dashed (respectively continuous) line if short-term contracts are (resp. are not) included. Fit results are shown in Figure 24.

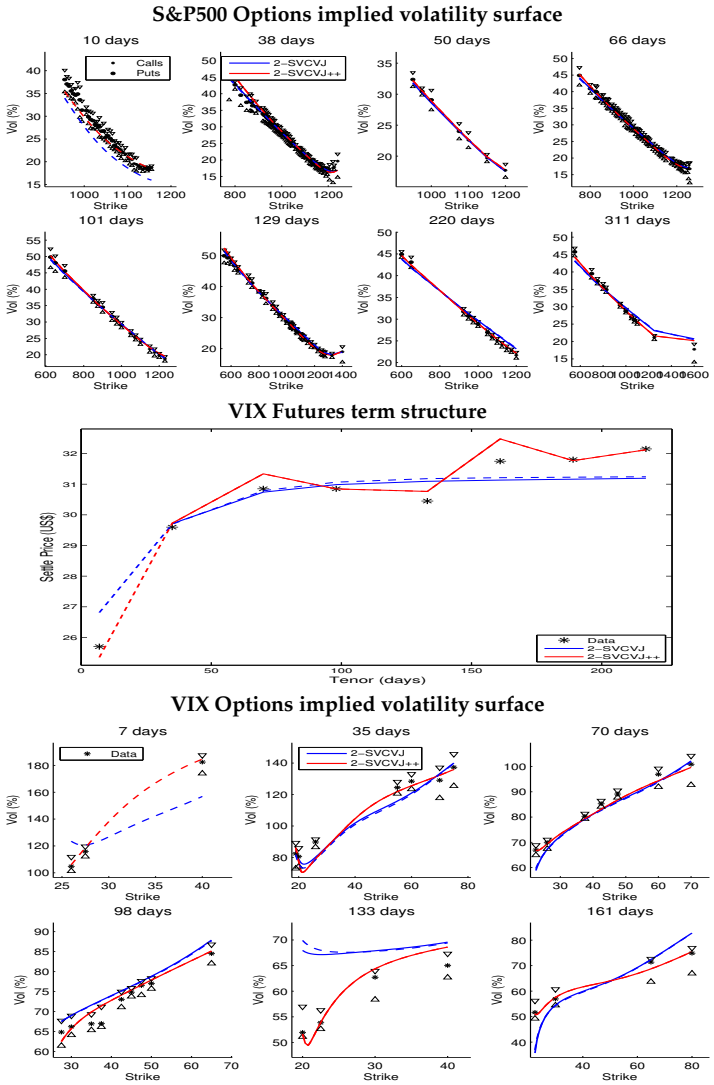

Figure 28: Impact of the short-term: fit results on August 11, 2010. This figure reports market and model implied volatilities for S&P500 (plot at the top) and VIX (plot at the bottom) options, together with the term structure of VIX futures (plot in the middle) on March 4, 2009 obtained calibrating jointly on the three markets the 2-SVCVJ (blue dashed line) and 2-SVCVJ++ (red dashed line). Maturities and tenors are expressed in days and volatilities are in % points and VIX futures settle prices are in US$. Superimposed (continuous lines) is the corresponding fit obtained with same models but excluding from the calibrating sample all contracts with maturity below 3 weeks.

Auguest 11, 2010	2-SVCVJ		2-SVCVJ++	
minimum term	1 week	3 weeks	1 week	3 weeks
α_1	0.0369	0.0190	0.1349	0.1349
$\sqrt{\beta_1}$ (%)	13.8529	29.0256	44.9580	44.9580
Λ_1	0.3882	0.4012	0.5256	0.5256
ρ_1	-0.6825	-0.6891	-0.9648	-0.9648
$\sigma_{1,0}$ (%)	16.4115	16.6534	16.4905	16.4905
α_2	12.0826	13.0322	15.1604	15.1604
$\sqrt{\beta_2}$ (%)	26.8442	26.6842	22.7877	22.7877
Λ_2	2.4498	2.6060	3.6664	3.6664
ρ_2	-0.9913	-0.9913	-1.0000	-1.0000
$\sigma_{1,0}$ (%)	4.3691	0.4348	7.4445	7.4445
λ	0.0444	0.0107	0.0013	0.0013
$E[c_x]$	-0.2200	-0.2258	-1.1115	-1.1115
$\sqrt{Var[c_x]}$	0.0270	0.1759	1.9305	1.9305
$\mu_{co,\sigma}$	0.0003	0.0968	36.4290	36.4290
$corr(c_x, c_\sigma)$	-0.9993	0.8893	-0.7037	-0.7037
λ'	0.0010	0.0011	36.7457	0.0013
$\mu_{id,\sigma}$	171.2908	161.2064	0.0000	0.0000

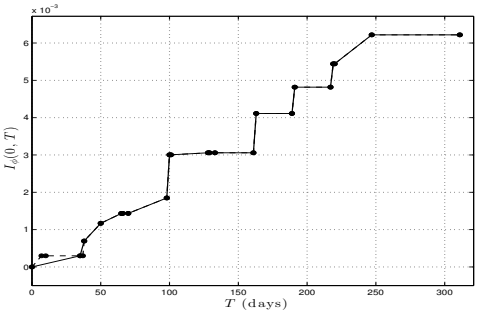

Figure 29: Impact of the short-term: calibrated parameters on August 11, 2010 of 2-SVCVJ and 2-SVCVJ++ models and $I_\phi(0,T)$ displacement integrals of 2-SVCVJ++ model: dashed (respectively continuous) line if short-term contracts are (resp. are not) included. Fit results are shown in Figure 24.

Table 7: Impact of the short term: calibrated parameters. This table reports the sample median (median absolute deviation) of joint SPX, VIX futures and VIX options calibrated parameters for the 2-SVCVJ and 2-SVCVJ++ models considered in the empirical analysis. The columns corresponding to the minimum term of 1 week are the last two columns of Table 6 and the others report the calibrated parameters of the same models calibrated excluding short-term contracts (less than 3 weeks to expiration) from the calibration sample. The sample period is from January 7, 2009 to December 29, 2010 and the sampling frequency is weekly (Wednesdays). Panel A (B) reports 1^{st} (2^{nd}) volatility factor diffusive parameters. Panel C reports intensity and unconditional mean and standard deviation of normal jumps in price, where $E[c_x] = \mu_x$ and $Var[c_x] = \delta_x^2$ under 2-SVJ, 2-SVVJ models (respectively $\mu_x + \rho_J \mu_{co,\sigma}$ and $\delta_x^2 + \rho_J^2 \mu_{co,\sigma}^2$ under 2-SVCJ, 2-SVCVJ) and analogously under the corresponding displaced specifications. Panel D reports the correlated co-jumps parameters. The unconditional correlation between jump sizes is $corr(c_x, c_\sigma) = \rho_J \mu_{co,\sigma} / \sqrt{Var[c_x]}$ under models 2-SVCJ, 2-SVCVJ and corresponding displaced specifications. Panel E reports the idiosyncratic jumps parameters.

	2-SVCVJ		2-SVCVJ++	
minimum term	1 week	3 weeks	1 week	3 weeks
Panel A: 1^{st} Factor				
α_1	1.9674	1.9705	1.6757	1.6774
	(1.3339)	(1.3713)	(1.0702)	(0.9609)
$\sqrt{\beta_1}$ (%)	17.8186	17.8029	18.2188	18.8151
	(9.1623)	(9.5317)	(6.0793)	(6.8431)
Λ_1	0.4445	0.4443	0.5040	0.4977
	(0.2186)	(0.2163)	(0.1151)	(0.1150)
ρ_1	−0.8651	−0.8681	−0.9641	−0.9616
	(0.1208)	(0.1269)	(0.0359)	(0.0384)
$\sigma_{1,0}$ (%)	16.2501	16.3388	16.3763	16.1583
	(4.6771)	(4.7309)	(4.8365)	(4.7190)
Panel B: 2^{nd} Factor				
α_2	8.4510	8.3306	6.4882	6.4963
	(3.4202)	(3.2965)	(2.4770)	(2.3888)
$\sqrt{\beta_2}$ (%)	22.9496	22.8742	21.5312	21.5067
	(4.3081)	(4.3159)	(3.1581)	(3.1416)
Λ_2	2.0495	2.0237	2.1152	2.0869
	(0.7383)	(0.6456)	(0.5764)	(0.5803)
ρ_2	−0.9972	−0.9967	−1.0000	−1.0000
	(0.0028)	(0.0033)	(0.0000)	(0.0000)
$\sigma_{1,0}$ (%)	8.6832	8.7519	7.9841	8.3909
	(6.3088)	(6.7075)	(4.6395)	(4.5115)
Panel C: Price jumps				
λ	0.0791	0.0759	0.0644	0.0658
	(0.0532)	(0.0524)	(0.0546)	(0.0542)
$E[c_x]$	−0.2404	−0.2449	−0.2795	−0.2728
	(0.1508)	(0.1497)	(0.1834)	(0.1797)
$\sqrt{Var[c_x]}$	0.3176	0.3152	0.4135	0.3889
	(0.2155)	(0.2162)	(0.2546)	(0.2291)
Panel D: CO-jumps				
$\mu_{co,\sigma}$	0.0393	0.0578	0.0650	0.0600
	(0.0393)	(0.0578)	(0.0650)	(0.0600)
$corr(c_x, c_\sigma)$	−0.3633	−0.5991	−0.5202	−0.5490
	(0.3660)	(0.4009)	(0.4578)	(0.4458)
Panel E: Idiosyncratic jumps				
λ'	0.0021	0.0023	0.0125	0.0111
	(0.0021)	(0.0023)	(0.0123)	(0.0110)
$\mu_{id,\sigma}$	1.2128	1.1341	0.0515	0.0211
	(1.2126)	(1.1340)	(0.0515)	(0.0211)

Da Fonseca et al. (2007)). We refer to Bru (1991) for a theoretical introduction to Wishart processes and to Gourieroux and Sufana (2004, 2010); Gruber et al. (2010); Leippold and Trojani (2008) for their application to derivative pricing. Da Fonseca and Grasselli (2011) analyze the different structural properties of the SV, 2-SV and WMSV models[6] in terms of the degrees of freedom relevant in describing the empirical features of the vanilla options surface and the model reaction to its changes (level and skew risks). As a setup for the comparison of the different models, they consider the model implied leverage correlation[7] and compare the short-term volatility-of-volatility expansions of the call price and implied volatility (Lewis, 2000), providing clear relations between the model implied skew and the parameters. Their analysis in particular confirms that multi factor models are needed to replicate a stochastic skew, as it is usually observed in market data. Furthermore, the WMSV model features and additional degree of freedom[8] w.r.t. the 2-SV model, which directly affects the skew of the surface, though it leaves unaltered the level of the surface. Our analysis, conducted calibrating multi-factor jump-diffusion models on vanilla, VIX futures and VIX options data, qualitatively confirms their calibration results for the 2-SV model, which can be obtained from our SVCVJ model switching off jumps (as detailed in Section 3.1.2). In particular, as detailed in Table 6 and reported on a daily basis in Figures from 13 to 19, we can see a *two-regime* property in our 2-factor models, with a fast factor, associated with the short-term smile, featuring a high volatility of volatility[9]. Nevertheless, our calibrated risk-neutral dynamics for the fast factor often degenerates to perfect anti-correlation. Interestingly, authors observe that the addition of jumps would lead to a lack of sensitivity of the skew term structure of the vanilla surface w.r.t. correlation parameters ρ_1 and ρ_2. In our setting, the instantaneous leverage correlation of the simplest displaced model that we consider in this thesis (the 2-SVJ++ model)

$$corr\left(\frac{dS_t}{S_{t-}}, d(\sigma_{1,t}^2+\sigma_{2,t}^2)\right) = \frac{\rho_1\Lambda_1\sigma_{1,t}^2+\rho_2\Lambda_2\sigma_{2,t}^2}{\sqrt{\sigma_{1,t}^2+\sigma_{2,t}^2+\lambda(\delta_x^2+\mu_x^2)+\phi_t}\sqrt{\Lambda_1\sigma_{1,t}^2+\Lambda_2\sigma_{2,t}^2}}dt \tag{4.6}$$

would suggest that this could be the case, as part of the skew is jump-induced. It is therefore interesting to test whether this observation can be extended to the present analysis in which three distinct market data sources are used to calibrate the models and if the presence of the displacement has an impact. We therefore

[6] In the present analysis we consider only the single-asset case of the analysis in Da Fonseca and Grasselli (2011).

[7] Which is the correlation between asset returns and the stochastic volatility. This quantity mainly drives the slope of the implied volatility surface (the skew), as it is clearly related to the skewness of returns distribution.

[8] The, possibly more than one, non-diagonal elements of the Σ state matrix.

[9] Which is in turns compatible with a more convex short-term smile of vanilla options.

get inspiration from their Section 2 and compare the calibration already performed with a new one in which all contracts with expirations less than 3 weeks are excluded. This analysis has been carried on for the 2-SVCVJ and 2-SVCVJ++ models and calibration results, as well as calibrated parameters (compared with those obtained including the short-term contracts) are displayed in Figures from 22 to 29 for the same days displayed before.

At least to the extent of the present analysis, from Table 7 and for the 4 days displayed,[10] we cannot see any evident difference, in terms of calibrated parameters (neither of the undisplaced, nor of the displaced models), as a consequence of the exclusion of the short term contracts. In particular, we can still see a clear *two-regime* property of the 2-factor calibrated models. We argue that this is in line with the value added by VIX derivatives on the specification of the model. Even if the addition of jumps introduces a mixing effect between the role of the correlation parameters and jump parameters, which would make less clear the effect of the previous on the skew of the vanilla surface (as the leverage correlation depends also on jumps), the introduction of volatility derivatives in the calibration sample helps to identify the latter (and in turns preserving the specification of the former): positive jumps in volatility, which we model partly correlated with those in price and partly idiosyncratic, mainly contribute to enhance the right skewness of the volatility distribution (which translates into the positive slopes of the VIX options surface).

4.2.2 Analysis with Feller condition imposed

As customary in the empirical S&P500 and VIX options pricing literature (Bardgett et al., 2013; Branger et al., 2014; Chen and Poon, 2013), a Feller condition is usually imposed on the volatility factors dynamics which restricts the mutual range of variability of drift and vol-of-vol parameters. The analysis of the preceding Section has been carried on without imposing such condition. As discussed in Pacati et al. (2015a), assuming a logarithmic generating process for volatility - which is increasingly found to provide an accurate description of the true volatility dynamics (Andersen et al., 2002; Bandi and Renò, 2015) - a square root diffusion which approximates the statistical properties of the generating process violates the Feller condition. To empirically assess the impact of the Feller condition on the present analysis, we have repeated the same calibration of the previous Section imposing

$$\nu = \frac{2\alpha_i\beta_i}{\Lambda_i^2} \geq 1 \quad i = 1, 2 \tag{4.7}$$

[10]The whole handbook with fit and calibrated paramters for both the complete analysis and this new analysis is available upon request.

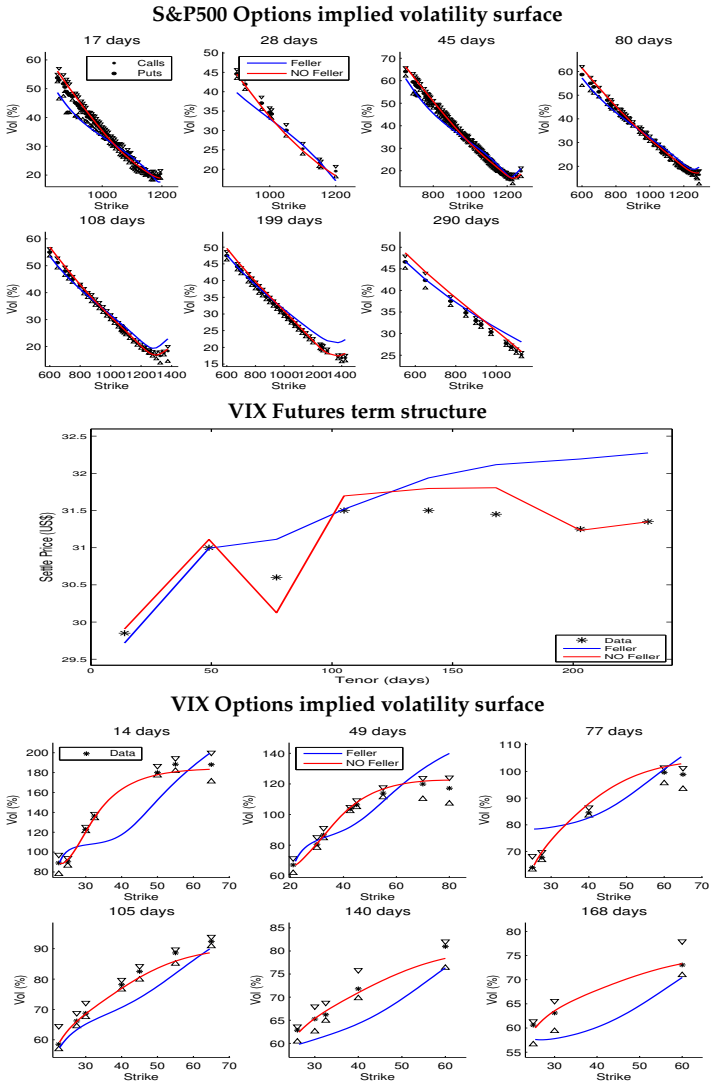

Figure 30: Impact of the Feller condition. This figure reports market and model implied volatilities for S&P500 (plot at the top) and VIX (plot at the bottom) options, together with the term structure of VIX futures (plot in the middle) on June 06, 2010 obtained calibrating jointly on the three markets the 2-SVCVJ++ model with Feller condition imposed (blue line) $2\alpha_i\beta_i \geq \Lambda_i^2$ on both stochastic volatility factors ($\sigma_{i,t}^2$ $i = 1, 2$) and with NO Feller condition imposed (red line). Maturities and tenors are expressed in days and volatilities are in % points and VIX futures settle prices are in US$. Relative errors without (with) Feller condition imposed: $RMSRE_{SPX} = 2.62\%$ (7.81%), $RMSRE_{Fut} = 0.80\%$ (1.84%), $RMSRE_{VIX} = 2.18\%$ (9.77%). Absolute errors without (with) Feller condition imposed: $RMSE_{SPX} = 0.94\%$ (2.33%), $RMSE_{Fut} = 0.25\,US\$$ ($0.58\,US\$$), $RMSE_{VIX} = 2.47\%$ (10.78%).

separately on each volatility factor, as discussed in (Andersen and Piterbarg, 2007; Duffie and Kan, 1996). Overall, the $\mathcal{H}$ and $\mathcal{H}$++, with or without Feller condition imposed (which, considering the positivity of drift and vol-of-vol parameters, corresponds respectively to the conditions $\nu \geq 1$ and $\nu > 0$), satisfy the following consistency conditions with respect to the metric induced by the loss function L of equation (4.1). In words:

1. each $\mathcal{H}$++ model *is better than* the corresponding $\mathcal{H}$ model;

2. each $\mathcal{H}$ or $\mathcal{H}$++ model with $\nu > 0$ *is better than* the same model with $\nu \geq 1$.

Table 8 (which corresponds to Table 3) reports the summary statistics on the root mean squared errors for the $\mathcal{H}$ and $\mathcal{H}$++ models averaged over the three markets, while Tables 9 and 11 , report the same summary statistics dissected on the three markets (Tables 9 and 11 are the analogous of Tables 4 and 5, respectively).

Figure 21 shows visually the distribution of the signed relative errors in equation (4.5) when the calibrations are performed imposing the Feller condition. Considering the 2-SVCVJ++ model, the 17.9% (4.7%) of S&P500 options implied volatilities (respectively the 1.9% (0.1%) of VIX futures settle prices and 26.0% (5.8%) of VIX options implied volatilies) are priced with a relative error greater than 5% (10%), which are values comparable with those of the undisplaced 2-SVCVJ model with Feller condition not imposed. Moreover, by visual inspection of the flattening of the error distribution of the 2-SVJ model, especially in the VIX options market, we see that the imposition of the Feller condition penalizes more the models which do not have jumps in volatility. A possible explanation could be the following: the Feller condition acts primarily as a binding on the vol-of-vol parameters Λ_i, that become constrained to be smaller than $\sqrt{2\alpha_i\beta_i}$. Then, if the model does not have another *channel* to increase the skewness of the volatility/VIX distribution - such as jumps in volatility - which is needed to reproduce the positive sloping smile of VIX options, it ends up to be more affected by such restriction w.r.t. a model, like the 2-SVVJ, 2-SVCJ and 2-SVCVJ which features discontinuous volatility dynamics.

Figure 30 shows a visual comparison between a typical calibration performed with 2-SVCVJ++ model when the Feller condition is imposed (blue line) and when it is not. It suggests that the restriction imposed prevents the model from capturing the convexity of the skew of VIX options - while still reproducing its positive slope - and from fitting long-term futures.

The visual results of figure 30 are confirmed comparing tables 9 (Panel B) and 11 (Panel D) with their no-Feller counterparts 4 and 5 (same Panels), where we see that the greatest increase in absolute pricing errors of 2-SVCVJ++ model when the Feller condition is imposed is on futures of long tenors, passing from 0.44% to 0.98% and, overall, on VIX options of short maturities, where the average absolute

Table 8: Calibration errors (in %) with Feller condition imposed. This table reports the sample average (max in sample) of the Root Mean Squared Error (Panel A) and Root Mean Squared Relative Error (Panel B) of all the $\mathcal{H}$ and $\mathcal{H}$++ models calibrated jointly to S&P500 options, VIX futures and VIX options market data with the Feller condition imposed $2\alpha_i\beta_i \geq \Lambda_i^2$ separately for $i = 1, 2$. The sample period is from January 7, 2009 to December 29, 2010 and the sampling frequency is weekly (Wednesdays). For each date in sample, the fit is performed minimizing the distance L in equation (4.1). Here we report the absolute (relative) errors on (S&P500 and VIX options) implied volatility surfaces $RMSE_{SPX}$ and $RMSE_{VIX}$ ($RMSRE_{SPX}$ and $RMSRE_{VIX}$) in percentage points and errors on the VIX futures term structures in US$. Performance measures are defined in equations (4.2) to (4.3). Overall pricing errors $RMSE_{All}$ and $RMSRE_{All}$ are expressed in percentage points and defined in equation (4.4).

	2-SVJ	2-SVJ++	2-SVCJ	2-SVCJ++	2-SVVJ	2-SVVJ++	2-SVCVJ	2-SVCVJ++
Panel A: RMSE								
$RMSE_{SPX}$	2.19	2.12	1.93	1.81	1.62	1.46	1.40	1.21
	(9.61)	(5.95)	(7.94)	(6.17)	(8.37)	(4.83)	(7.90)	(4.41)
$RMSE_{Fut}$	0.88	0.72	0.85	0.65	0.80	0.57	0.75	0.42
	(3.52)	(2.45)	(3.39)	(2.34)	(3.03)	(2.68)	(2.03)	(2.14)
$RMSE_{VIX}$	16.07	15.21	13.27	12.03	6.20	4.56	5.77	4.02
	(33.93)	(33.73)	(34.00)	(33.88)	(27.78)	(14.85)	(16.38)	(12.02)
$RMSE_{All}$	5.57	5.28	4.64	4.21	2.57	2.05	2.33	1.76
	(15.12)	(13.18)	(13.21)	(13.31)	(8.91)	(6.36)	(8.69)	(5.88)
Panel B: RMSRE								
$RMSRE_{SPX}$	7.09	6.56	6.30	5.71	5.65	4.95	4.89	4.03
	(28.37)	(12.40)	(22.20)	(11.99)	(23.35)	(12.90)	(22.09)	(11.71)
$RMSRE_{Fut}$	2.93	2.40	2.85	2.18	2.64	1.86	2.47	1.38
	(9.18)	(6.88)	(8.85)	(6.57)	(8.29)	(7.01)	(5.79)	(5.56)
$RMSRE_{VIX}$	17.87	16.23	14.79	12.70	7.96	5.24	7.32	4.42
	(35.47)	(27.94)	(29.88)	(27.94)	(25.44)	(14.00)	(25.39)	(12.05)
$RMSRE_{All}$	8.84	8.08	7.65	6.75	5.96	4.97	5.23	4.05
	(29.13)	(14.68)	(21.00)	(14.73)	(21.98)	(12.61)	(20.92)	(11.63)

error increases from roughly 2.1 vps[11] to more than 6 vps, and high strikes, where it increases from roughly 2 to 5 volatility points.

[11] Volatility points.

Table 9: Calibration RMSE (in %) on VIX futures by Tenor category with Feller condition imposed. This table reports the sample average of the Root Mean Squared Relative Error for different Tenor categories of futures on VIX for all the $\mathcal{H}$ (Panel A) and $\mathcal{H}$++ (Panel B) models. Refer to Section 4.2.2 and Table 8 for calibration details. Here we report the relative errors on VIX futures term structures $RMSE_{Fut}$, as defined in the second of (4.3), conditioned to the Tenor category considered, measured in days. Errors are expressed in percentage points and the sample average is weighted by the number of daily observations in each tenor category. Overall errors are reported in Table 8.

	Tenor (days)						
	Panel A: $\mathcal{H}$ models				Panel B: $\mathcal{H}++$ models		
	< 45	$45-90$	> 90		< 45	$45-90$	> 90
2-SVJ	0.51	0.38	1.76	2-SVJ++	0.40	0.28	1.53
2-SVCJ	0.45	0.34	1.79	2-SVCJ++	0.32	0.23	1.46
2-SVVJ	0.33	0.28	1.80	2-SVVJ++	0.19	0.18	1.35
2-SVCVJ	0.32	0.25	1.67	2-SVCVJ++	0.16	0.14	0.98
Observations				Observations (% of TOT = 792)			
	144	144	504		18.18	18.18	63.64

Figure 31: Scatter plot of the 2-SVCVJ++ mean-reversion parameters of $\sigma^2_{2,t}$: $\log_{10}(\alpha_2)$ Vs $\log_{10}(\sqrt{\beta_2})$ obtained in the daily calibration imposing the Feller condition $2\alpha_i\beta_i \geq \Lambda_i^2$ on both stochastic volatility factors ($\sigma^2_{i,t}$ $i = 1, 2$). α_2 is the rate of mean-reversion and $\sqrt{\beta_2}$ is the long-term volatility level.

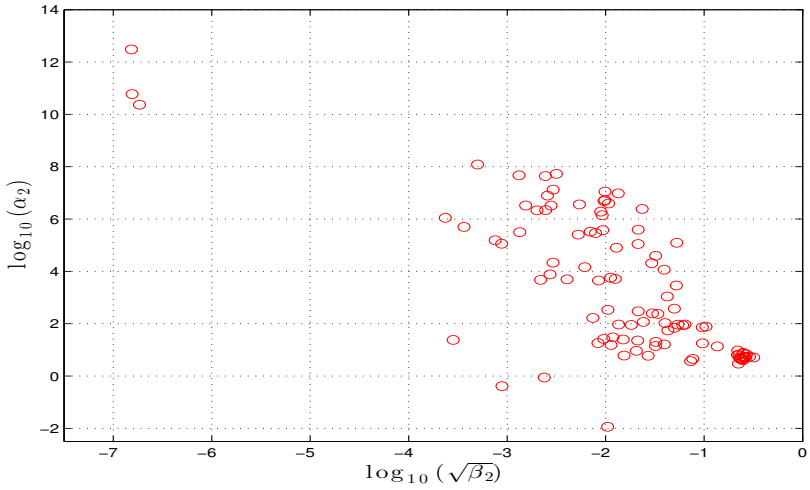

Table 10: Calibrated parameters with Feller condition imposed. This table reports the sample median (median absolute deviation) of joint SPX, VIX futures and VIX options calibrated parameters for all the $\mathcal{H}$ and $\mathcal{H}$++ models considered in the empirical analysis when the Feller condition $2\alpha_i\beta_i \geq \Lambda_i^2$ is imposed on both stochastic volatility factors ($\sigma_{i,t}^2$ $i = 1, 2$). The sample period is from January 7, 2009 to December 29, 2010 and the sampling frequency is weekly (Wednesdays). Panel A (B) reports 1^{st} (2^{nd}) volatility factor diffusive parameters. Panel C reports intensity and unconditional mean and standard deviation of normal jumps in price, where $E[c_x] = \mu_x$ and $Var[c_x] = \delta_x^2$ under 2-SVJ, 2-SVVJ models (respectively $\mu_x + \rho_J\mu_{co,\sigma}$ and $\delta_x^2 + \rho_J^2\mu_{co,\sigma}^2$ under 2-SVCJ, 2-SVCVJ) and analogously under the corresponding displaced specifications. Panel D reports the correlated co-jumps parameters. The unconditional correlation between jump sizes is $corr(c_x, c_\sigma) = \rho_J\mu_{co,\sigma}/\sqrt{Var[c_x]}$ under models 2-SVCJ, 2-SVCVJ and corresponding displaced specifications. Panel E reports the idiosyncratic jumps parameters.

	2-SVJ	2-SVJ++	2-SVCJ	2-SVCJ++	2-SVVJ	2-SVVJ++	2-SVCVJ	2-SVCVJ++
Panel A: 1^{st} Factor								
α_1	5.662	5.413	5.408	5.230	5.163	4.579	5.002	4.411
	(0.960)	(1.050)	(1.224)	(1.100)	(1.300)	(1.160)	(1.357)	(0.962)
$\sqrt{\beta_1}$ (%)	31.322	31.882	29.244	29.480	26.030	26.683	25.971	26.240
	(3.169)	(3.085)	(3.167)	(3.272)	(3.969)	(4.332)	(4.686)	(3.929)
Λ_1	1.069	1.039	0.950	0.942	0.791	0.756	0.775	0.752
	(0.172)	(0.184)	(0.175)	(0.170)	(0.240)	(0.185)	(0.231)	(0.158)
ρ_1	−0.861	−0.900	−0.880	−0.906	−0.973	−0.995	−0.987	−0.996
	(0.083)	(0.082)	(0.097)	(0.076)	(0.027)	(0.005)	(0.013)	(0.004)
$\sigma_{1,0}$ (%)	20.727	19.009	20.318	19.185	14.592	14.698	14.612	16.912
	(6.616)	(5.879)	(6.944)	(6.834)	(6.440)	(6.398)	(7.167)	(7.055)
Panel B: 2^{nd} Factor								
α_2	36408.4	2412.0	10561.0	19777.9	276.4	819.4	58.7	241.9
	(36399.8)	(24103.0)	(10557.9)	(19773.3)	(276.4)	(818.8)	(54.7)	(238.5)
$\sqrt{\beta_2}$ (%)	0.404	0.511	0.656	0.702	2.056	1.427	3.106	1.679
	(0.376)	(0.425)	(0.638)	(0.636)	(2.004)	(1.379)	(2.948)	(1.540)
Λ_2	0.313	0.365	0.418	0.399	0.405	0.435	0.578	0.683
	(0.285)	(0.360)	(0.383)	(0.354)	(0.401)	(0.416)	(0.405)	(0.577)
ρ_2	0.393	0.353	0.290	0.225	−0.702	−0.573	−0.554	−0.393
	(0.544)	(0.478)	(0.677)	(0.638)	(0.298)	(0.427)	(0.446)	(0.607)
$\sigma_{2,0}$ (%)	34.976	51.811	12.342	16.251	21.087	21.308	14.692	13.913
	(34.535)	(50.943)	(12.159)	(16.116)	(20.523)	(18.232)	(13.370)	(12.189)
Panel C: Price jumps								
λ	0.006	0.006	0.013	0.011	0.011	0.012	0.040	0.046
	(0.005)	(0.005)	(0.009)	(0.010)	(0.009)	(0.010)	(0.028)	(0.028)
$E[c_x]$	−0.404	−0.295	−0.242	−0.214	−0.912	−0.973	−0.364	−0.380
	(0.438)	(0.331)	(0.286)	(0.228)	(0.544)	(0.481)	(0.200)	(0.198)
$\sqrt{Var[c_x]}$	0.258	0.224	0.271	0.231	0.414	0.396	0.353	0.297
	(0.204)	(0.171)	(0.190)	(0.151)	(0.271)	(0.239)	(0.213)	(0.146)
Panel D: CO-jumps								
$\mu_{co,\sigma}$	-	-	0.000	0.000	-	-	0.601	0.674
	-	-	(0.000)	(0.000)	-	-	(0.601)	(0.602)
$corr(c_x, c_\sigma)$	-	-	−0.101	−0.019	-	-	−0.774	−0.878
	-	-	(0.253)	(0.236)	-	-	(0.226)	(0.122)
Panel E: Idiosyncratic jumps								
λ	-	-	-	-	0.110	0.131	0.082	0.134
	-	-	-	-	(0.066)	(0.076)	(0.081)	(0.112)
$\mu_{id,\sigma}$	-	-	-	-	0.931	0.687	0.554	0.443
	-	-	-	-	(0.521)	(0.340)	(0.390)	(0.266)

From inspection of Panel B of tables 5 and 11, the increasing trend of the errors is similar also on SPX options, passing from roughly 2 to 4.7 vps on the long-maturity bucket and from 2.4 to more than 6 vps on the high strikes bucket.

With this restriction imposed, table 8 shows that the average (maximum) relative pricing error of 2-SVCVJ++ increase to 4% (11.7%) on S&P500 options, 4.4% (12%) on VIX options and 1.4% (5.6%) on VIX futures, while for the 2-SVCVJ model we obtained 4.9% (22.1%) on S&P500 options, 7.3% (25.4%) on VIX options and 2.5% (5.8%) on VIX futures. Overall, when the Feller condition is imposed, the mean (maximum) overall relative pricing error $RMSRE_{All}$ grows up to 5.23% (20.92%) for the 2-SVCVJ model and 4.05% (11.63%) for the 2-SVCVJ++ model.

Table 10 shows the calibrated parameters of all $\mathcal{H}$ and $\mathcal{H}$++ models when the Feller condition is imposed on each factor $\sigma^2_{i,t}$. Considering the 2-SVCVJ++ model, calibrated parameters still show the different role played by the two volatility factors, with $\sigma^2_{1,t}$ still representing the *slow* mean-reverting factor, with a half life of almost 2 months. Nevertheless, while with Feller condition not imposed the two factors contribute to a comparable fraction of the long-term volatility level (table 6, last column), when the condition is imposed, the long-term level is driven almost exclusively by the slow factor. Figure 31 shows a scatter plot of the order of magnitude of the daily calibrated rate of mean reversion α_2 with respect to the calibrated $\sqrt{\beta_2}$ for the *fast* factor $\sigma^2_{2,t}$. As it is clear, insensately high values of α_2 are coupled with so small values of β_2 that - as a consequence - the factor[12] results to be simply unspecified. Consistently, the restriction imposed by the Feller condition on the vol-of-vol parameters $\Lambda_i \leq \sqrt{2\alpha_i\beta_i}$, induces the jump parameters to compensate for it, showing an increase in their mean value of roughly one order of magnitue $\mu_{co,\sigma} = 0.67, \mu_{id,\sigma} = 0.44$, whereas from table 6 they would have been $\mu_{co,\sigma} = 0.07, \mu_{id,\sigma} = 0.05$ if the Feller condition would have not been imposed. Moreover, the long-term level of the 2-SVCVJ++ models

$$\beta_{eff} = \beta_1 + \beta_2 + \lambda\frac{\mu_{co,\sigma}}{\alpha_1} + \lambda'\frac{\mu_{id,\sigma}}{\alpha_1} \tag{4.8}$$

results to be rather similar with or without the imposition of the Feller condition: $\sqrt{\beta_{eff}}$ is respectively 31.6% and 29.0%; a fact that is in line with the intuition that models with jumps in volatility are able, to some extent, to generate the necessary volatility-of-volatility - as required to reproduce the positive sloping skew of VIX options - leveraging on an increase of the contribution of jumps.

4.3 Conclusions

Our empirical results show a decisive improvement in the pricing performance over non-displaced models, and also provide strong empirical support for the

[12] Which, strictly speaking, would have a half-life of roughly one day.

Table 11: Calibration RMSE (in %) on SPX and VIX options by Moneyness - Maturity category with Feller condition imposed This table reports the sample average of the Root Mean Squared Relative Error for different Moneyness and time-to-Maturity categories of options on SPX (respectively VIX) for all the $\mathcal{H}$ models in Panel A (resp. C) and $\mathcal{H}$++ models in Panel B (resp. D). Refer to Section 4.2.2 and Table 8 for calibration details. Here we report the relative errors on VIX implied volatility surfaces $RMSE_{VIX}$, as defined in the third of (4.3), conditioned to the Moneyness - Maturity category considered. Time to *Maturity* is measured in days and *Moneyness* for an option of maturity T is defined as the ratio of the option exercise price to the current index level for S&P500 optionts and of the exercise price to the current VIX futures price expiring at T for VIX options.For each category, errors are expressed in percentage points and the sample average is weighted by the number of daily observations in each category. Overall errors are reported in Table 8.

Maturity	**Moneyness** of SPX options								
	Panel A: $\mathcal{H}$ models					Panel B: $\mathcal{H}++$ models			
	< 0.95	$0.95 - 1.05$	> 1.05	**All**		< 0.95	$0.95 - 1.05$	> 1.05	**All**
< 45 Days									
2-SVJ	8.11	7.91	9.51	8.69	2-SVJ++	8.38	6.51	7.91	7.99
2-SVCJ	6.99	7.51	8.55	7.75	2-SVCJ++	6.93	5.95	7.19	6.90
2-SVVJ	5.58	6.04	7.71	6.37	2-SVVJ++	5.25	4.60	5.97	5.38
2-SVCVJ	4.53	5.46	7.39	5.60	2-SVCVJ++	4.17	3.87	5.43	4.44
$45 - 90$ Days									
2-SVJ	4.32	5.27	6.08	5.25	2-SVJ++	4.27	5.03	5.37	4.89
2-SVCJ	3.82	4.60	5.34	4.59	2-SVCJ++	3.60	4.36	4.68	4.21
2-SVVJ	2.87	3.20	5.37	3.84	2-SVVJ++	2.72	2.39	4.59	3.35
2-SVCVJ	2.58	2.85	4.50	3.35	2-SVCVJ++	2.29	2.06	3.78	2.79
> 90 Days									
2-SVJ	3.79	7.33	9.53	6.73	2-SVJ++	3.71	7.06	8.78	6.34
2-SVCJ	3.47	6.33	8.23	5.91	2-SVCJ++	3.29	6.11	7.79	5.63
2-SVVJ	2.63	4.69	10.12	6.16	2-SVVJ++	2.38	3.95	9.74	5.79
2-SVCVJ	2.52	4.31	8.18	5.22	2-SVCVJ++	2.18	3.45	7.56	4.68
All Days									
2-SVJ	5.90	7.20	8.57		2-SVJ++	6.00	6.34	7.56	
2-SVCJ	5.17	6.61	7.65		2-SVCJ++	5.04	5.68	6.79	
2-SVVJ	4.08	5.12	8.31		2-SVVJ++	3.84	4.00	7.36	
2-SVCVJ	3.46	4.68	7.19		2-SVCVJ++	3.13	3.41	6.02	
Observations					Observations (% of TOT)				
< 45 Days	4232	2642	1373	8247	< 45 Days	17.43	10.88	5.66	33.97
$45 - 90$ Days	4704	2368	2292	9364	$45 - 90$ Days	19.37	9.75	9.44	38.57
> 90 Days	3369	1418	1881	6668	> 90 Days	13.88	5.84	7.75	27.46
All Days	12305	6428	5546	24279	**All** Days	50.68	26.48	22.84	100.00

Maturity	**Moneyness** of VIX options								
	Panel C: $\mathcal{H}$ models					Panel D: $\mathcal{H}++$ models			
	< 0.95	$0.95 - 1.05$	> 1.05	**All**		< 0.95	$0.95 - 1.05$	> 1.05	**All**
< 45 Days									
2-SVJ	14.26	16.24	21.44	20.39	2-SVJ++	8.57	12.00	20.97	18.62
2-SVCJ	13.06	13.30	18.21	17.63	2-SVCJ++	7.82	9.83	17.16	15.35
2-SVVJ	9.96	7.77	8.00	9.12	2-SVVJ++	3.95	5.47	7.20	6.64
2-SVCVJ	8.76	7.19	7.90	8.57	2-SVCVJ++	3.49	4.67	6.64	6.06
$45 - 90$ Days									
2-SVJ	12.87	8.31	20.74	18.73	2-SVJ++	6.17	7.00	20.29	16.97
2-SVCJ	11.78	7.30	15.73	14.83	2-SVCJ++	5.33	5.72	15.17	12.81
2-SVVJ	10.72	5.65	6.06	8.02	2-SVVJ++	3.39	3.43	5.29	4.96
2-SVCVJ	9.95	4.83	5.73	7.47	2-SVCVJ++	2.75	2.75	4.87	4.39
> 90 Days									
2-SVJ	14.70	7.10	18.19	17.02	2-SVJ++	9.54	6.31	17.71	15.37
2-SVCJ	13.14	5.48	13.63	13.56	2-SVCJ++	7.32	4.92	13.06	11.51
2-SVVJ	10.45	4.35	5.49	7.34	2-SVVJ++	4.01	3.27	4.79	4.61
2-SVCVJ	10.20	4.44	5.14	7.07	2-SVCVJ++	3.14	3.15	4.07	3.90
All Days									
2-SVJ	15.21	10.63	19.95		2-SVJ++	9.32	8.36	19.48	
2-SVCJ	13.81	8.62	15.56		2-SVCJ++	7.51	6.74	14.85	
2-SVVJ	11.38	5.95	6.45		2-SVVJ++	4.19	4.10	5.69	
2-SVCVJ	10.71	5.61	6.17		2-SVCVJ++	3.36	3.65	5.08	
Observations					Observations (of TOT)				
< 45 Days	135	59	390	584	< 45 Days	4.88	2.13	14.09	21.11
$45 - 90$ Days	190	57	477	724	$45 - 90$ Days	6.87	2.06	17.24	26.17
> 90 Days	384	137	938	1459	> 90 Days	13.88	4.95	33.90	52.73
All Days	709	253	1805	2767	**All** Days	25.62	9.14	65.23	100.00

presence of both price-volatility co-jumps and idiosyncratic jumps in the volatility dynamics.

The displacement contributes to dramatically increase the fit of the term structure of VIX futures, even when it displays humps. Moreover, the addition of the rich jump structure of the Heston++ model makes it able to capture the positive sloping smile of the VIX options surface and its term structure. Based on our results, the *maximum* errors of the 2-SVCVJ++ model are comparable with the *average* errors of the non-displaced 2-SVCVJ model.

The imposition of the Feller condition penalizes more the models with a poorer volatility specification, while models featuring jumps are able, to some extent, to compensate for the restrictions imposed on the vol-of-vol parameters leveraging on an increased contribution of jumps. Nevertheless, despite capturing the positive sloping skew of VIX options, the 2-SVCVJ++ model with Feller condition imposed seems unable to reproduce the correct convexity of the smile.

The pricing errors of displaced models with Feller condition imposed are roughly comparable with those of non-displaced models without Feller condition imposed. Overall, the imposition of the Feller condition does not compromise the superiority of the ϕ_t-displaced models over those non-displaced.

A model which consistently prices both equity and volatility market is a reasonable starting point in order to infer both equity and variance risk-premia from the data. In a possible research agenda we would leverage on the enhanced ability of displaced models in capturing the risk-neutral dynamics of the S&P500 and VIX indexes in order to try to infer their true dynamics. This route goes through the definition of a suitable change of measure between the *risk-neutral* and *physical* probability measure in this displaced jump-diffusion setup (Broadie et al., 2007; Pan, 2002). A proper methodology has to be designed in order to filter out unobserved latent variables, such as the volatility process and jumps. In this respect, standard Kalman filter-based methodologies already employed to estimate equity and variance risk-premia (Bates, 2000; Gruber et al., 2015) cannot be directly employed, due to the presence of non-normal innovations in the latent processes. Therefore, more refined non-standard filtering techniques will be required, such as the Auxiliary Particle filter introduced by Pitt and Shephard (1999) and already successfully employed for risk-premia estimation by Bardgett et al. (2013).

Future developments could lead toward the investigation and the deeper understanding of the meaning and role of the displacement ϕ_t, which seems to play a crucial role in the option pricing context. In particular, from a mathematical point of view, could be interesting to interpret displaced models as a kind of affine approximation of an unknown non-affine process. Moreover, from a financial point of view could be interesting to investigate whether, and to what extent, the displacement deterministic function can be interpreted as an additional volatility state vector.

Appendix A

Mathematical proofs and *addenda*

A.1 Conditional characteristic functions of $\mathcal{H}$ models

As the 2-SVCVJ is an affine model, ordinary calculations following Duffie et al. (2000) lead to characteristic functions which are exponentially affine in the state variables. For the logarithmic price and volatility factors we obtain, respectively:

$$\begin{aligned}\log f_x^{\text{2-SVCVJ}}(z;\tau) &= i(x_t + (r-q)\tau)z + \sum_{k=1,2}\left(A_k^x(z;\tau) + B_k^x(z;\tau)\sigma_{k,t}^2\right) + C_{co}^x(z;\tau) + C_{id}^x(z;\tau)\\ \log f_\sigma^{\text{2-SVCVJ}}(z_1,z_2;\tau) &= \sum_{k=1,2}\left(A_k^\sigma(z_k;\tau) + B_k^\sigma(z_k;\tau)\sigma_{k,t}^2\right) + C_{co}^\sigma(z_1;\tau) + C_{id}^\sigma(z_1;\tau)\end{aligned} \tag{A.1}$$

where coefficients satisfy the following sets of ODEs:

$$\begin{aligned}\frac{\partial A_k^x(z;\tau)}{\partial\tau} &= \alpha_k\beta_k B_k^x(z;\tau)\\ \frac{\partial B_k^x(z;\tau)}{\partial\tau} &= \frac{1}{2}\Lambda_k^2\left(B_k^x(z;\tau)\right)^2 - \left(\alpha_k - iz\rho_k\Lambda_k\right)B_k^x(z;\tau) - \frac{1}{2}z(i+z)\\ \frac{\partial C_{co}^x(z;\tau)}{\partial\tau} &= \lambda\Big(\theta^{co}\left(z,-iB_1^x(z,\tau)\right) - 1 - i\bar{\mu}z\Big)\\ \frac{\partial C_{id}^x(z;\tau)}{\partial\tau} &= \lambda'\Big(\theta^{id}\left(-iB_1^x(z,\tau)\right) - 1\Big)\end{aligned}$$

with null initial conditions at $\tau = 0$, and

$$\begin{aligned}
\frac{\partial A_k^\sigma(z_k;\tau)}{\partial \tau} &= \alpha_k \beta_k B_k^\sigma(z_k;\tau) \\
\frac{\partial B_k^\sigma(z_k;\tau)}{\partial \tau} &= \frac{1}{2}\Lambda_k^2 \left(B_k^\sigma(z_k;\tau)\right)^2 - \alpha_k B_k^\sigma(z_k;\tau) \\
\frac{\partial C_{co}^\sigma(z_1;\tau)}{\partial \tau} &= \lambda\Big(\theta^{co}\left(0, -iB_1^\sigma(z_1,\tau)\right) - 1\Big) \\
\frac{\partial C_{id}^\sigma(z_1;\tau)}{\partial \tau} &= \lambda'\Big(\theta^{id}\left(-iB_1^\sigma(z_1,\tau)\right) - 1\Big)
\end{aligned} \tag{A.2}$$

with initial conditions $A_k^\sigma(z_k;0) = C_{co}^\sigma(z_1;0) = C_{id}^\sigma(z_1;0) = 0$ and $B_k^\sigma(z_k;0) = iz_k$. Explicit solutions can be found. For the $f_x^{\text{2-SVCVJ}}$ coefficients, we have:

$$\begin{aligned}
A_k^x(z;\tau) &= \frac{\alpha_k\beta_k}{\Lambda_k^2}\left[(c_k - d_k)\tau - 2\log\left(\frac{1 - g_k e^{-d_k\tau}}{1 - g_k}\right)\right] \\
B_k^x(z,\tau) &= \frac{c_k - d_k}{\Lambda_k^2}\frac{1 - e^{-d_k\tau}}{1 - g_k e^{-d_k\tau}} \\
C_{co}^x(z;\tau) &= \lambda\tau\Big(\Theta^{co}(z;\tau) - 1 - i\bar{\mu}z\Big) \\
\Theta^{co}(z;\tau) &= exp\left\{i\mu_x z_x - \frac{1}{2}\delta_x^2 z_x^2\right\} \\
&\quad \times \frac{1}{G_{co}^-}\left[1 - \frac{2}{\tau}\frac{\mu_{co,\sigma}}{\Lambda_1^2}\frac{1}{G_{co}^+}\log\left(\frac{G_{co}^- - g_1 G_{co}^+ e^{-d_1\tau}}{(1-g_1)(1 - iz\rho_J\mu_{co,\sigma})}\right)\right] \\
C_{id}^x(z;\tau) &= \lambda'\tau\Big(\Theta^{id}(z;\tau) - 1\Big) \\
\Theta^{id}(z;\tau) &= \frac{1}{G_{id}^-}\left[1 - \frac{2}{\tau}\frac{\mu_{id,\sigma}}{\Lambda_1^2}\frac{1}{G_{id}^+}\log\left(\frac{G_{id}^- - g_1 G_{id}^+ e^{-d_1\tau}}{1 - g_1}\right)\right]
\end{aligned}$$

where we have defined the auxiliary parameters:

$$\begin{aligned}
c_k &= \alpha_k - iz\rho_k\Lambda_k \\
d_k &= \sqrt{c_k^2 + z(i+z)\Lambda_k^2} \\
g_k &= \frac{c_k - d_k}{c_k + d_k} \\
G_{co}^\pm &= 1 - iz\rho_J\mu_{co,\sigma} - \frac{\mu_{co,\sigma}}{\Lambda_1^2}(c_1 \pm d_1) \\
G_{id}^\pm &= 1 - \frac{\mu_{id,\sigma}}{\Lambda_1^2}(c_1 \pm d_1)
\end{aligned}$$

For the $f_\sigma^{\text{2-SVCVJ}}$ coefficients, we have:

$$\begin{aligned}
A_k^\sigma(z_k;\tau) &= -\frac{2\alpha_k\beta_k}{\Lambda_k^2}\log\left(1 - iz_k\frac{\Lambda_k^2}{2\alpha_k}\left(1-e^{-\alpha_k\tau}\right)\right)\\
B_k^\sigma(z_k;\tau) &= \frac{iz_k e^{-\alpha_k\tau}}{1 - iz_k\frac{\Lambda_k^2}{2\alpha_k}\left(1-e^{-\alpha_k\tau}\right)}\\
C_{co}^\sigma(z_1;\tau) &= \lambda\Theta(z_1;\tau,\mu_{co,\sigma})\\
C_{id}^\sigma(z_1;\tau) &= \lambda'\Theta(z_1;\tau,\mu_{id,\sigma})\\
\Theta(z_1;\tau,\mu) &= -\frac{2\mu}{\Lambda_1^2 - 2\alpha_1\mu}\log\left(1 - \frac{iz_1}{1-iz_1\mu}\frac{\Lambda_1^2-2\alpha_1\mu}{2\alpha_1}\left(1-e^{-\alpha_1\tau}\right)\right)
\end{aligned} \tag{A.3}$$

Characteristic functions of the other nested $\mathcal{H}$ models can be obtained applying the appropriate simplifications to the corresponding expressions just presented for the 2-SVCVJ model, as discussed in section (3.1.1), see Lian and Zhu (2013) and Kokholm et al. (2015) for the case of the SVCJ model of Duffie et al. (2000) and Chen and Poon (2013) for the case of the 2-SVCJ model with two volatility factors with correlated co-jumps between the first one and the price process. We present here the expressions for the nested models adopted in the empirical analysis. For ease of exposition we begin with the results for the two factor continuous 2-SV model of Christoffersen et al. (2009):

$$\begin{aligned}
\log f_x^{\text{2-SV}}(z;\tau) &= i(x_t + (r-q)\tau)z + \sum_{k=1,2}\left(A_k^x(z;\tau) + B_k^x(z;\tau)\sigma_{k,t}^2\right)\\
\log f_\sigma^{\text{2-SV}}(z_1,z_2;\tau) &= \sum_{k=1,2}\left(A_k^\sigma(z_k;\tau) + B_k^\sigma(z_k;\tau)\sigma_{k,t}^2\right)
\end{aligned} \tag{A.4}$$

For the 2-SVJ model, with log-normal jumps in price only we obtain:

$$\begin{aligned}
\log f_x^{\text{2-SVJ}}(z;\tau) &= \log f_x^{\text{2-SV}}(z;\tau) + C_{co}^x(z;\tau)|_{\mu_{co,\sigma}=0}\\
\log f_\sigma^{\text{2-SVJ}}(z_1,z_2;\tau) &= \log f_\sigma^{\text{2-SV}}(z_1,z_2;\tau)
\end{aligned} \tag{A.5}$$

For the 2-SVVJ model, with log-normal jumps in price and idiosyncratic jumps in $\sigma_{1,t}^2$ we obtain:

$$\begin{aligned}
\log f_x^{\text{2-SVVJ}}(z;\tau) &= \log f_x^{\text{2-SVJ}}(z;\tau) + C_{id}^x(z;\tau)\\
\log f_\sigma^{\text{2-SVVJ}}(z_1,z_2;\tau) &= \log f_\sigma^{\text{2-SV}}(z_1,z_2;\tau) + C_{id}^\sigma(z_1;\tau)
\end{aligned} \tag{A.6}$$

For the 2-SVCJ model, with correlated co-jumps in price and $\sigma_{1,t}^2$ we obtain:

$$\begin{aligned}
\log f_x^{\text{2-SVCJ}}(z;\tau) &= \log f_x^{\text{2-SV}}(z;\tau) + C_{co}^x(z;\tau)\\
\log f_\sigma^{\text{2-SVCJ}}(z_1,z_2;\tau) &= \log f_\sigma^{\text{2-SV}}(z_1,z_2;\tau) + C_{co}^\sigma(z_1;\tau)
\end{aligned} \tag{A.7}$$

Relations (3.11) are easily derived since each $\mathcal{H}$++ model is an affine model nesting the corresponding undisplaced $\mathcal{H}$ model.

A.2 Proof of Proposition 4: $C_{SPX}^{\mathcal{H}++}(K,t,T)$

The pricing formula is easily obtained from the first of (3.11) and from a straightforward application of results of Lewis (2000, 2001).

A.3 Proof of Proposition 5: $VIX_t^{\mathcal{H}++}$

Applying Itō's Lemma to the process $\log(S_{t+\bar{\tau}}/F_{t,t+\bar{\tau}})$, under the dynamics of the 2-SVCVJ++ in (3.3), the VIX definition in (3.13) may be rewritten as

$$\left(\frac{VIX_t}{100}\right)^2 = \frac{1}{\bar{\tau}}\sum_{k=1,2} E^{\mathbb{Q}}\left[\int_t^{t+\bar{\tau}} \sigma_{k,s}^2 ds \middle| \mathcal{F}_t\right] + 2\lambda E^{\mathbb{Q}}\Big[e^{c_x} - 1 - c_x\Big] + \frac{1}{\bar{\tau}} I_\phi(t, t+\bar{\tau}) \quad \text{(A.8)}$$

where we have also used the fact that ϕ_t is a deterministic function. The integrated volatilities and the co-jumps contribution can be computed in closed form (see for example Lin (2007) and Duan and Yeh (2010) for similar computations)

$$\begin{aligned}
E^{\mathbb{Q}}\left[\int_t^{t+\bar{\tau}} \sigma_{1,s}^2 ds \middle| \mathcal{F}_t\right] &= \frac{1-e^{-\bar{\tau}\alpha_1}}{\alpha_1}\sigma_{1,t}^2 + \frac{\alpha_1\beta_1 + \lambda\mu_{co,\sigma} + \lambda'\mu_{id,\sigma}}{\alpha_1}\left(\bar{\tau} - \frac{1-e^{-\bar{\tau}\alpha_1}}{\alpha_1}\right) \\
E^{\mathbb{Q}}\left[\int_t^{t+\bar{\tau}} \sigma_{2,s}^2 ds \middle| \mathcal{F}_t\right] &= \frac{1-e^{-\bar{\tau}\alpha_2}}{\alpha_2}\sigma_{2,t}^2 + \beta_2\left(\bar{\tau} - \frac{1-e^{-\bar{\tau}\alpha_2}}{\alpha_2}\right) \\
E^{\mathbb{Q}}\Big[e^{c_x} - 1 - c_x\Big] &= \bar{\mu} - (\mu_x + \rho_J\mu_{co,\sigma})
\end{aligned} \quad \text{(A.9)}$$

and therefore we have that the coefficients of affinity in (3.15) are

$$\begin{aligned}
a_k(\bar{\tau}) &= \frac{1-e^{-\bar{\tau}\alpha_k}}{\alpha_k} \quad , \quad k = 1,2 \\
b_1(\bar{\tau}) &= \frac{\alpha_1\beta_1 + \lambda\mu_{co,\sigma} + \lambda'\mu_{id,\sigma}}{\alpha_1}\Big(\bar{\tau} - a_1(\bar{\tau})\Big) + 2\lambda\Big[\bar{\mu} - (\mu_x + \rho_J\mu_{co,\sigma})\Big] \\
b_2(\bar{\tau}) &= \beta_2\Big(\bar{\tau} - a_2(\bar{\tau})\Big)
\end{aligned} \quad \text{(A.10)}$$

Relation (3.14) readily comes from the nesting of 2-SVCVJ model into 2-SVCVJ++ if $\phi_t \equiv 0$.

A.4 Proof of Proposition 6: $F_{VIX}^{\mathcal{H}++}(t,T)$ and $C_{VIX}^{\mathcal{H}++}(K,t,T)$

The payoffs of a VIX futures contract settled at time T and of a call option on VIX of strike K maturing at T are linear functions of the VIX index value at settle VIX_T, respectively VIX_T and $(VIX_T - K)^+$. As stated in Proposition 5, under $\mathcal{H}++$ models, VIX_T is non-linearly related to the value of volatility factor processes at time T, whose conditional

characteristic function is known in closed form as shown in Lemma 2. To overcome this issue we rewrite the payoffs as non-linear functions of the squared index

$$\begin{aligned}\frac{w_F(VIX_T'^2)}{100} &= \sqrt{VIX_T'^2} \\ \frac{w_C(VIX_T'^2)}{100} &= \left(\sqrt{VIX_T'^2} - K'\right)^+\end{aligned} \tag{A.11}$$

where $VIX_t' = VIX_t/100$ and $K' = K/100$ are, respectively, the index and strike values expressed in percentage points. Fourier transforms for these payoffs are available in closed form

$$\begin{aligned}\frac{\hat{w}_F(z)}{100} &= \frac{\sqrt{\pi}}{2}\frac{1}{(-iz)^{3/2}} \\ \frac{\hat{w}_C(z)}{100} &= \frac{\sqrt{\pi}}{2}\frac{1 - erf(K'\sqrt{-iz})}{(-iz)^{3/2}}\end{aligned} \tag{A.12}$$

and are single-valued regular functions in the upper half of the complex plane

$$\mathbb{S}_w = \{z \in \mathbb{C} : \mathrm{Im}(z) > 0\} \tag{A.13}$$

Denote with $f^{\text{2-SVCVJ++}}_{VIX'^2}$ the time t conditional characteristic function $E^{\mathbb{Q}}\left[e^{izVIX_T'^2}\middle|\mathcal{F}_t\right]$ of the squared index process $VIX_t'^2$ at time T under the 2-SVCVJ++ model. From Proposition 5 (with $\tau = T - t$)

$$\begin{aligned}f^{\text{2-SVCVJ++}}_{VIX'^2}(z;\tau) &= e^{izI_\phi(T,T+\bar{\tau})/\bar{\tau}} f^{\text{2-SVCVJ}}_{VIX'^2}(z;\tau) \\ &= e^{iz\left(\sum_{k=1,2} b_k(\bar{\tau}) + I_\phi(T,T+\bar{\tau})\right)/\bar{\tau}} f^{\text{2-SVCVJ}}_{\sigma}(za_1(\bar{\tau})/\bar{\tau}, za_2(\bar{\tau})/\bar{\tau};\tau)\end{aligned} \tag{A.14}$$

Following the approach of Lewis (2000, 2001), the value at time t of the call option on VIX under the 2-SVCVJ++ model is given by

$$\begin{aligned}C^{\text{2-SVCVJ++}}_{VIX}(K,t,T) &= e^{-r\tau}E^{\mathbb{Q}}\left[(VIX_T - K)^+\middle|\mathcal{F}_t\right] \\ &= e^{-r\tau}E^{\mathbb{Q}}\left[w_C(VIX_T'^2)\middle|\mathcal{F}_t\right] \\ &= \frac{e^{-r\tau}}{2\pi}\int_{i\,\mathrm{Im}(z)-\infty}^{i\,\mathrm{Im}(z)+\infty} f^{\text{2-SVCVJ++}}_{VIX'^2}(-z;\tau)\hat{w}_C(z)dz\end{aligned} \tag{A.15}$$

and similarly for futures

$$\begin{aligned}F^{\text{2-SVCVJ++}}_{VIX}(t,T) &= E^{\mathbb{Q}}\left[VIX_T\middle|\mathcal{F}_t\right] \\ &= E^{\mathbb{Q}}\left[w_F(VIX_T'^2)\middle|\mathcal{F}_t\right] \\ &= \frac{1}{2\pi}\int_{i\,\mathrm{Im}(z)-\infty}^{i\,\mathrm{Im}(z)+\infty} f^{\text{2-SVCVJ++}}_{VIX'^2}(-z;\tau)\hat{w}_F(z)dz\end{aligned} \tag{A.16}$$

from which the results in Proposition 6 follow since the real (imaginary) part is an even (odd) function of $\mathrm{Re}(z)$. For both claims, the integrands are well behaved functions as long as $z \in \mathbb{S}^*_{VIX'^2} \cap \mathbb{S}_w$ where $f^{\text{2-SVCVJ++}}_{VIX'^2}(z;\tau)$ is regular in the strip $\mathbb{S}_{VIX'^2}$ and $\mathbb{S}^*_{VIX'^2}$ is the

conjugate strip, obtained via reflection with respect to the real z axis. The characteristic functions $f^{\text{2-SVCVJ++}}_{VIX'^2}(z;\tau)$ verifies

$$\begin{aligned}\left|f^{\text{2-SVCVJ++}}_{VIX'^2}(-z;\tau)\right| &= \left|E^{\mathbb{Q}}\left[e^{-izVIX'^2_T}\middle|\mathcal{F}_t\right]\right| \\ &\leq E^{\mathbb{Q}}\left[\left|e^{-izVIX'^2_T}\right|\middle|\mathcal{F}_t\right] = f^{\text{2-SVCVJ++}}_{VIX'^2}(-i\,\mathrm{Im}(z);\tau)\end{aligned} \tag{A.17}$$

and therefore, considering the relation in (A.14), determining the strip of regularity $\mathbb{S}^*_{VIX'^2}$ corresponds to analyze the stability of the solutions of the system ODEs in equation (A.67) for $z_k = -i\,\mathrm{Im}(z)a_k(\bar{\tau})/\bar{\tau}$ and $k = 1, 2$. Similar arguments have been considered in Andersen and Piterbarg (2007); Lee et al. (2004); Lord and Kahl (2010) in studying the regularity of the log-price characteristic function $f_x(z;\tau)$ of Heston-like stochastic volatility models. From the second of the (A.3), the solution $B^\sigma_k(-i\,\mathrm{Im}(z)a_k(\bar{\tau})/\bar{\tau};\tau)$ is regular as long as its denominator is not equal to zero, requiring:

$$\mathrm{Im}(z) < \zeta_c^{B^\sigma_k}(\tau) = \frac{\bar{\tau}}{a_k(\bar{\tau})}\frac{1}{\frac{\Lambda_k^2}{2\alpha_k}\left(1-e^{-\alpha_k\tau}\right)} \tag{A.18}$$

which, in addition, guarantees the regularity of $A^\sigma_k(-i\,\mathrm{Im}(z)a_k(\bar{\tau})/\bar{\tau};\tau)$, given in the first of (A.3). Idiosyncratic and correlated co-jumps solutions $C^\sigma_{co}(-i\,\mathrm{Im}(z)a_1(\bar{\tau})/\bar{\tau};\tau)$ and $C^\sigma_{id}(-i\,\mathrm{Im}(z)a_1(\bar{\tau})/\bar{\tau};\tau)$ are regular as long as the argument of the logarithms is not equal to zero, that requires, respectively:

$$\mathrm{Im}(z) < \zeta_c^{C^\sigma_{co}}(\tau) = \frac{\bar{\tau}}{a_1(\bar{\tau})}\min\left(\frac{1}{\mu_{co,\sigma}}, \frac{1}{\frac{\Lambda_1^2}{2\alpha_1}\left(1-e^{-\alpha_1\tau}\right)+\mu_{co,\sigma}e^{-\alpha_1\tau}}\right) \tag{A.19}$$

and

$$\mathrm{Im}(z) < \zeta_c^{C^\sigma_{id}}(\tau) = \frac{\bar{\tau}}{a_1(\bar{\tau})}\min\left(\frac{1}{\mu_{id,\sigma}}, \frac{1}{\frac{\Lambda_1^2}{2\alpha_1}\left(1-e^{-\alpha_1\tau}\right)+\mu_{id,\sigma}e^{-\alpha_1\tau}}\right) \tag{A.20}$$

We notice that, since $\mu_{co,\sigma}, \mu_{id,\sigma} > 0$, we have that $\min\left(\zeta_c^{C^\sigma_{co}}(\tau), \zeta_c^{C^\sigma_{id}}(\tau)\right) < \zeta_c^{B^\sigma_1}(\tau)$, and therefore $\zeta_c(\tau)$ is given by

$$\zeta_c(\tau) = \min\left(\zeta_c^{C^\sigma_{co}}(\tau), \zeta_c^{C^\sigma_{id}}(\tau), \zeta_c^{B^\sigma_2}(\tau)\right) \tag{A.21}$$

A.5 Proof of proposition 9: $E^{\mathbb{Q}}\left[\int_t^T X_s ds\middle|\mathcal{F}_t\right]$

We derive the expression for functions $A_x(\tau)$ and $B_x(\tau)$ in (3.46)

$$E^{\mathbb{Q}}\left[\int_t^T X_s ds\middle|\mathcal{F}_t\right] = A_x(\tau) + B_x(\tau)X_t \tag{A.22}$$

performing the functional derivative of the expression for the expected diffusive quadratic variation in (3.41), whose relevant term we report here for ease of the reader,[1]

$$E^{\mathbb{Q}}\left[\int_t^T \Psi_s^\top X_s ds \middle| \mathcal{F}_t\right] = A_c(t,T;\Psi_{[t,T]}) + B_c^\top(t,T;\Psi_{[t,T]})X_t \tag{A.23}$$

w.r.t. the multiplicative displacement Ψ_t. Without any pretensions to be rigorous, we first introduce the concept of first variation and derivative of a functional. Consider a functional $\mathbf{F}$ of the function $f(x)$

$$\mathbf{F}[f] = \int_{x_0}^{x_1} I_f(x)dx \tag{A.24}$$

where the integrand I_f is assumed to depend on $f(x)$ and possibly on its derivatives and primitives. We will call the functional derivative of $\mathbf{F}$ w.r.t. $f(x)$ the function of x

$$\frac{\delta \mathbf{F}}{\delta f(x)} \tag{A.25}$$

such that the first variation $\delta\mathbf{F} = \mathbf{F}[f+\delta f] - \mathbf{F}[f]$ of $\mathbf{F}$ is (see (Courant and Hilbert, 1953, pp. 186) and (Gelfand et al., 2000, pp. 11))

$$\delta\mathbf{F} = \int_{x_0}^{x_1} \frac{\delta \mathbf{F}}{\delta f(x)}\delta f(x)dx \tag{A.26}$$

where the variation $\delta f(x)$ is an arbitrary sufficiently regular test function.[2] We interpret the expression in (A.23) as a functional $\mathbf{F}_t[\Psi]$ of the multiplicative displacement function $\Psi_t : \mathbb{R}_+ \to \mathbb{R}^n$

$$\mathbf{F}_t[\Psi] = E^{\mathbb{Q}}\left[\int_t^T \Psi_s^\top X_s ds \middle| \mathcal{F}_t\right] + \mathbf{1}^\top \int_t^T \Phi_s ds \tag{A.29}$$

whose variation is

$$\delta\mathbf{F}_t = E^{\mathbb{Q}}\left[\int_t^T \delta\Psi_s^\top X_s ds \middle| \mathcal{F}_t\right] = \int_t^T \delta\Psi_s^\top E^{\mathbb{Q}}\left[X_s \middle| \mathcal{F}_t\right] ds \tag{A.30}$$

---

[1] We disregard the contribution of the Φ-term in the expression (3.41) of $E^{\mathbb{Q}}[\,[\log S]^c_{t,T}\,\big|\,\mathcal{F}_t]$.

[2] In the physics literature, often dealing with functional derivatives of observables (functionals $\mathbf{F}[f]$) of fields (functions $f(x)$) defined on the entire space-time $\mathbb{R}^4$, the definition employed is slightly different, with the variation $\delta f(x)$ inside (A.26) expressed formally in terms of the Dirac delta $\epsilon\delta(y-x)$, and therefore in the scalar case the variation of $\mathbf{F}$ would be

$$\delta\mathbf{F} = \int \frac{\delta\mathbf{F}}{\delta f(x)}\epsilon\delta(x-y)dx = \epsilon\frac{\delta\mathbf{F}}{\delta f(y)} \tag{A.27}$$

with the functional derivative retrieved in the limit of vanishing ϵ as:

$$\frac{\delta\mathbf{F}}{\delta f(x)} = \lim_{\epsilon\to 0}\frac{\mathbf{F}[f+\epsilon\delta(x-y)] - \mathbf{F}[f]}{\epsilon} \tag{A.28}$$

since the delta is symmetric. Good (non technical) introductions can be found in Parisi (1988) and Greiner and Reinhardt (1996).

The last equality is an instance of Fubini theorem and therefore (A.30) holds as long as

$$E^{\mathbb{Q}}\left[\int_t^T |\delta\Psi_s^\top X_s| ds \middle| \mathcal{F}_t\right] < \infty \tag{A.31}$$

but, since the variation $\delta\Psi$ is arbitrary small,

$$|\delta\Psi_s^\top X_s| = \left|\sum_{i=1}^n \delta\psi_{i,s}\sigma_{i,s}^2\right| \leq \sum_{i=1}^n |\delta\psi_{i,s}\sigma_{i,s}^2| \leq \sum_{i=1}^n \sigma_{i,s}^2 \tag{A.32}$$

expression (A.30) holds *a fortiori* if we can interchange the expectation of the volatility factor state vector with its integral

$$E^{\mathbb{Q}}\left[\int_t^T X_s ds \middle| \mathcal{F}_t\right] = \int_t^T E^{\mathbb{Q}}\left[X_s \middle| \mathcal{F}_t\right] ds \tag{A.33}$$

Moreover, the variation $\delta\Psi_s$ has been taken outside of the expectation in (A.30) since it is deterministic. For what was said before, the functional derivative of $\mathbf{F}_t[\Psi]$ w.r.t. Ψ_s, is the conditional expected value of the volatility state vector at time $s \geq t$

$$\frac{\delta \mathbf{F}_t}{\delta \Psi_s} = E^{\mathbb{Q}}\left[X_s \middle| \mathcal{F}_t\right] \tag{A.34}$$

moreover if we assume (A.33), the expected integrated volatility factor state vector is the integral of $\frac{\delta \mathbf{F}_t}{\delta \Psi(s)}$

$$E^{\mathbb{Q}}\left[\int_t^T X_s ds \middle| \mathcal{F}_t\right] = \int_t^T \frac{\delta \mathbf{F}_t}{\delta \Psi_s} ds \tag{A.35}$$

If we now interpret consistently $A_c(t,T;\Psi_t)$ and $B_c(t,T;\Psi_t)$, defined in (3.42), and reported here for ease of the reader,

$$\begin{aligned} A_c(t,T;\Psi_{[t,T]}) &= \int_t^T B_c^\top(s,T;\Psi_{[s,T]}) ds \left(K_0 + \sum_{j=1}^{m_X} \lambda_{0,j}\nabla\theta_j(0)\right) \\ B_c(t,T;\Psi_{[t,T]}) &= \int_t^T e^{\left(K_1^\top + \sum_{j=1}^{m_X} \lambda_{1,j}\nabla\theta_j^\top(0)\right)(s-t)} \Psi(s) ds \end{aligned} \tag{A.36}$$

as functionals of Ψ_t, denoted respectively as $\mathbf{A}_{c,t}[\Psi]$ and $\mathbf{B}_{c,t}[\Psi]$, the linear relation (3.41) allows us to easily compute the functional derivative of $\mathbf{F}_t[\Psi]$ w.r.t. Ψ_s in terms of their own functional derivatives[3]

$$\frac{\delta \mathbf{F}_t}{\delta \Psi(s)} = \frac{\delta \mathbf{A}_{c,t}}{\delta \Psi_s} + \left(\frac{\delta \mathbf{B}_{c,t}}{\delta \Psi_s}\right)^\top X_t \tag{A.37}$$

[3]Observe that

$$\frac{\delta(\mathbf{B}_{c,t}^\top X_t)}{\delta \Psi_s} = \frac{\delta \mathbf{B}_{c,t}^\top}{\delta \Psi_s} X_t = \left(\frac{\delta \mathbf{B}_{c,t}}{\delta \Psi_s}\right)^\top X_t$$

where[4]

$$\begin{aligned}\frac{\delta \mathbf{A}_{c,t}}{\delta \Psi_s} &= \left[\left(\frac{\delta \mathbf{B}_{c,t}}{\delta \Psi_s}\right)^\top - Id_n\right]\left(K_1 + \sum_{j=1}^{m_X} \nabla\theta_j(0)\lambda_{1,j}^\top\right)^{-1}\left(K_0 + \sum_{j=1}^{m_X}\lambda_{0,j}\nabla\theta_j(0)\right) \\ \frac{\delta \mathbf{B}_{c,t}}{\delta \Psi_s} &= e^{\left(K_1^\top + \sum_{j=1}^{m_X}\lambda_{1,j}\nabla\theta_j^\top(0)\right)(s-t)}\end{aligned} \tag{A.40}$$

and we conclude observing that their integrals between time t and T

$$\begin{aligned}\int_t^T \frac{\delta \mathbf{A}_{c,t}}{\delta \Psi_s} ds &= [B_x(\tau) - Id_n\tau]\left(K_1 + \sum_{j=1}^{m_X} \nabla\theta_j(0)\lambda_{1,j}^\top\right)^{-1}\left(K_0 + \sum_{j=1}^{m_X}\lambda_{0,j}\nabla\theta_j(0)\right) \\ \int_t^T \left(\frac{\delta \mathbf{B}_{c,t}}{\delta \Psi_s}\right)^\top ds &= \left[e^{\left(K_1 + \sum_{j=1}^{m_X}\nabla\theta_j(0)\lambda_{1,j}^\top\right)\tau} - Id_n\right]\left(K_1 + \sum_{j=1}^{m_X} \nabla\theta_j(0)\lambda_{1,j}^\top\right)^{-1}\end{aligned} \tag{A.41}$$

are therefore the functions $A_x(\tau)$ and $B_x(\tau)$ of Proposition 9.

A.6 Proof of proposition 11: $F_{VIX}(t,T)$ and $C_{VIX}(K,t,T)$ under the displaced affine framework

By definition of conditional CF (VIX' = VIX/100) and from the results in Proposition 10, we have $z = \mathrm{Re}(z) + i\,\mathrm{Im}(z) \in \mathbb{C}$

$$\begin{aligned}f_{VIX'^2}(z; X_t, t, T) &= E^{\mathbb{Q}}\left[e^{izVIX_T'^2}\middle|\mathcal{F}_t\right] \\ &= e^{iz\left(a + \mathbf{1}^\top I_\Phi(T,T+\bar\tau)\right)/\bar\tau} E^{\mathbb{Q}}\left[e^{izb^\top X_T/\bar\tau}\middle|\mathcal{F}_t\right] \\ &= e^{iz\left(a + \mathbf{1}^\top I_\Phi(T,T+\bar\tau)\right)/\bar\tau} f_\sigma\left(z\frac{b}{\bar\tau}; X_t, t, T\right)\end{aligned} \tag{A.42}$$

[4] In deriving $\frac{\delta \mathbf{A}_{c,t}}{\delta \Psi_s}$ it could be useful the following easy application of the Fubini theorem to perform an interchange of the order of the integrals:

$$\begin{aligned}\int_t^T \left(\int_s^T G(u,s)\Psi(u)du\right)ds &= \int_t^T \left(\int_t^u G(u,s)\Psi(u)ds\right)du \\ &= \int_t^T \left(\int_t^u G(u,s)ds\right)\Psi(u)du\end{aligned} \tag{A.38}$$

which corresponds to two distinct parametrizations of the triangular region $\mathcal{T}_{t,T}$

$$\begin{aligned}\mathcal{T}_{t,T} &= \left\{(u,s) \in \mathbb{R}^2 : s \le u \le T \text{ and } t \le s \le T\right\} \\ &= \left\{(u,s) \in \mathbb{R}^2 : t \le u \le T \text{ and } u \le s \le T\right\}\end{aligned} \tag{A.39}$$

where $f_\sigma(Z; X_t, t, T) = E^{\mathbb{Q}}\left[e^{iZ^\top X_T}\middle|\mathcal{F}_t\right]$ with $Z = \mathrm{Re}(Z) + i\,\mathrm{Im}(Z) \in \mathbb{C}^n$, is the risk-neutral conditional characteristic function of $X_t \in \mathbb{R}^n$. The results in Lewis (2000) and Lewis (2001), based on the regularity theorem for CF of Lukacs (1970), ensure us that $f_{VIX'^2}$ is a regular function in the strip

$$z \in \mathbb{C} \;:\; |\,\mathrm{Im}(z)| < \zeta_c(t,T) \tag{A.43}$$

that will in general depend on the model considered, through f_σ (as discussed in Appendix A.4 for the specific case of the Heston++ model). Recalling the rewritten payoffs

$$\begin{aligned} w_F(VIX'^2_T) &= 100 \times \sqrt{VIX'^2_T} \\ w_C(VIX'^2_T) &= 100 \times \left(\sqrt{VIX'^2_T} - K'\right)^+ \end{aligned} \tag{A.44}$$

and their Fourier transforms

$$\begin{aligned} \hat{w}_F(z) &= 100 \times \frac{\sqrt{\pi}}{2}\frac{1}{(-iz)^{3/2}} \\ \hat{w}_C(z) &= 100 \times \frac{\sqrt{\pi}}{2}\frac{1 - erf(K'\sqrt{-iz})}{(-iz)^{3/2}} \end{aligned} \tag{A.45}$$

that are single-valued regular functions in the upper half of the complex plane $\mathrm{Im}(z) > 0$, we can apply the definition of arbitrage-free pricing. and compute the VIX derivative prices by Fourier inversion of their payoffs. For futures on VIX we have:

$$\begin{aligned} F_{VIX}(t,T) &= E^{\mathbb{Q}}[VIX_T \mid \mathcal{F}_t] \\ &= E^{\mathbb{Q}}[w_F(VIX'^2_T) \mid \mathcal{F}_t] \\ &= E^{\mathbb{Q}}\left[\frac{1}{2\pi}\int_{i\,\mathrm{Im}(z)-\infty}^{i\,\mathrm{Im}(z)+\infty} e^{-izVIX'^2_T}\hat{w}_F(z)dz\middle|\mathcal{F}_t\right] \\ &= \frac{1}{2\pi}\int_{i\,\mathrm{Im}(z)-\infty}^{i\,\mathrm{Im}(z)+\infty} E^{\mathbb{Q}}\left[e^{-izVIX'^2_T} \mid \mathcal{F}_t\right]\hat{w}_F(z)dz \\ &= \frac{1}{2\pi}\int_{i\,\mathrm{Im}(z)-\infty}^{i\,\mathrm{Im}(z)+\infty} f_{VIX'^2}(-z; X_t, t, T)\hat{w}_F(z)dz \end{aligned} \tag{A.46}$$

where we have used Fubini Theorem to move the expectation inside the integral. Considering that the real (imaginary) part of the complex integrand is an even (odd) function of $\mathrm{Re}(z)$, can be rewritten as

$$F_{VIX}(t,T) = \frac{1}{\pi}\int_0^\infty \mathrm{Re}\left[f_{VIX'^2}(-z; X_t, t, T)\hat{w}_F(z)\right]d\,\mathrm{Re}(z) \tag{A.47}$$

with $0 < \mathrm{Im}(z) < \zeta_c$, given in (A.43). Substituting $f_{VIX'^2}$ expression in (A.42) and $\hat{w}_F(z)$ given in (A.45), we get the first of (3.72). Analogously, for call options on VIX,

$$\begin{aligned} C_{VIX}(K,t,T) &= e^{-r\tau} E^{\mathbb{Q}}[(VIX_T - K)^+ \mid \mathcal{F}_t] \\ &= e^{-r\tau} E^{\mathbb{Q}}[w_C(VIX_T'^2) \mid \mathcal{F}_t] \\ &= e^{-r\tau} E^{\mathbb{Q}} \left[\frac{1}{2\pi} \int_{i\,\mathrm{Im}(z)-\infty}^{i\,\mathrm{Im}(z)+\infty} e^{-izVIX_T'^2} \hat{w}_C(z) dz \Big| \mathcal{F}_t \right] \\ &= \frac{e^{-r\tau}}{2\pi} \int_{i\,\mathrm{Im}(z)-\infty}^{i\,\mathrm{Im}(z)+\infty} E^{\mathbb{Q}} \left[e^{-izVIX_T'^2} \mid \mathcal{F}_t \right] \hat{w}_C(z) dz \\ &= \frac{e^{-r\tau}}{2\pi} \int_{i\,\mathrm{Im}(z)-\infty}^{i\,\mathrm{Im}(z)+\infty} f_{VIX'^2}(-z; X_t, t, T) \hat{w}_C(z) dz \\ &= \frac{e^{-r\tau}}{\pi} \int_0^{\infty} \mathrm{Re} \left[f_{VIX'^2}(-z; X_t, t, T) \hat{w}_C(z) \right] d\,\mathrm{Re}(z) \end{aligned} \tag{A.48}$$

with $0 < \mathrm{Im}(z) < \zeta_c$. Substituting $f_{VIX'^2}$ expression in (A.42) and $\hat{w}_C(z)$ given in (A.45), we get the second of (3.72). Similarly, for a put option

$$w_P(VIX_T'^2) = 100 \times max \left(\sqrt{VIX_T'^2} - K' \right) \tag{A.49}$$

with Fourier transform

$$\begin{aligned} \hat{w}_P(z) &= \int_{-\infty}^{\infty} e^{izVIX_T'^2} w_P(VIX_T'^2) dVIX_T'^2 \\ &= 100 \times \left(\frac{iK'}{z} - \frac{\sqrt{\pi}}{2} \frac{erf(K'\sqrt{-iz})}{(-iz)^{3/2}} \right) \end{aligned} \tag{A.50}$$

Therefore, a put option on VIX can be priced either by put-call parity in (2.12), given call and futures prices in (3.72), or directly

$$P_{VIX}(K,t,T) = \frac{e^{-r\tau}}{\pi} \int_0^{\infty} \mathrm{Re} \left[f_{VIX'^2}(-z; X_t, t, T) \hat{w}_P(z) \right] d\,\mathrm{Re}(z) \tag{A.51}$$

with $0 < \mathrm{Im}(z) < \zeta_c$.

A.7 Affinity conservation under displacement transformation of instantaneous volatility

From inspection of VIX derivatives pricing formulas in Propositions 6 or 11, it is clear that VIX futures and options prices depend strongly on the risk-neutral statistical properties of the stochastic volatility process

$$X_t = (\sigma_{1,t}^2, ..., \sigma_{n,t}^2)^\top \in \mathbb{R}^n, \tag{A.52}$$

and only say, *indirectly* (through the VIX affinity coefficients), on the dynamics of the underlying price process S_t. Moreover, by direct inspection of the (a, b) coefficients in Proposition 10, it is clear that they do not depend on the correlation between the diffusive dynamics of S_t and X_t. VIX derivative prices do directly depend on the statistical properties of the volatility factors and the only relevant process to be affine in order for their price to be computable in closed-form is the stochastic volatility process X_t.
This means that to price volatility derivatives, one can either compute the conditional PDF of X_t: $p^{\mathbb{Q}}_{\sigma}(X_T|X_t)$, or more in general can express the pricing formulas, as in Proposition 11, in terms of the conditional CF

$$f_{\sigma}(Z; X_t, t, T) = E^{\mathbb{Q}}\left[e^{iZ^{\top} X_T} \middle| \mathcal{F}_t \right] \tag{A.53}$$

which, as we have seen in Proposition 12, is computable in closed form under our present affine framework for X_t.
The price of equity derivatives instead, depends on the risk-neutral distribution of S_t, to which will in general contribute the dynamics of X_t. In other words, to compute the no-arbitrage price of a contingent claim on S_t, one has to consider either the transition PDF $p^{\mathbb{Q}}_{S}(S_T|S_t)$, or the conditional CF

$$f_{S}(z; S_t, X_t, t, T) = E^{\mathbb{Q}}\left[e^{izS_T} \middle| \mathcal{F}_t \right] \tag{A.54}$$

that will in general be a function of the volatility factors too. The transform analysis of Duffie, Pan and Singleton Duffie et al. (2000) ensures us that the function $f_S(z; S_t, X_t)$ can be computed in closed-form (and in the usual exponential affine form), provided that the complete process

$$(X_t, S_t)^{\top} = (\sigma^2_{1,t}, ..., \sigma^2_{n,t}, S_t)^{\top} \in \mathbb{R}^{n+1} \tag{A.55}$$

is an affine process, according to the affine dependence structure described in (Duffie et al., 2000, Sec 2.2). As will be shown in what follows, if we consider a (Ψ_t, Φ_t)-displaced AJD model, in order for the affinity structure of the complete process $(X_t, S_t)^{\top}$ to hold, binds have to be imposed on the risk-neutral correlation structure between the price process S_t and those stochastic volatility factors $X_{i,t}$ that are displaced. In other terms, if the i-th stochastic volatility factor is displaced, that is

$$V_{c,i}(\sigma^2_{i,t}) = \psi_{i,t}\sigma^2_{i,t} + \phi_{i,t} \tag{A.56}$$

the instantaneous correlation between $dW^S_{i,t}$ and $dW^X_{i,t}$ cannot be chosen arbitrarily in order for the process $(X_t, S_t)^{\top}$ to be affine. We do not make here any general statement and prefer to investigate deeper on this point with a couple of examples of models that fit in the present framework.

Example 1. ***Pacati, Renò and Santilli (2014)*** *In Pacati et al. (2014), the authors consider a jump-diffusion model, labelled* ***2fj++****, in which the price process S_t of a non-dividend paying underlying*

follows the risk-neutral dynamics (refer to main text for details)

$$\begin{aligned} dS_t &= rS_t dt + S_t\sqrt{\sigma_{1,t}^2 + \phi_t} dW_{1,t}^S + \sigma_{2,t} dW_{2,t}^S + k_J S_t dN_t \\ d\sigma_{i,t}^2 &= \alpha_i(\beta_i - \sigma_{i,t}^2)dt + \Lambda_i \sigma_{i,t} dW_{i,t}^\sigma \quad (i = 1, 2) \\ \log(1 + k_J) &\sim \mathcal{N}\left(\log(1 + \bar{k}_J) - \frac{1}{2}\sigma_J^2, \sigma_J^2\right) \end{aligned} \tag{A.57}$$

The contribution to the spot variance $V_c(\sigma_{1,t}^2, \sigma_{2,t}^2)$ of the first stochastic volatility factor is displaced by a non-negative deterministic function $\phi_t \geq 0$

$$\begin{aligned} V_c(\sigma_{1,t}^2, \sigma_{2,t}^2) &= V_{c,1}(\sigma_{1,t}^2) + V_{c,2}(\sigma_{2,t}^2) \\ V_{c,1}(\sigma_{1,t}^2) &= \sigma_{1,t}^2 + \phi_t \\ V_{c,2}(\sigma_{2,t}^2) &= \sigma_{2,t}^2 \end{aligned} \tag{A.58}$$

As they pointed out, the unique functional form of the instantaneous correlation between $dW_{1,t}^S$ and $dW_{1,t}^X$ which guarantees the linearity of the pricing PDE for a contingent claim on S_t is:

$$corr(dW_{1,t}^S, dW_{1,t}^\sigma) = \rho\sqrt{\frac{\sigma_{1,t}^2}{\sigma_{1,t}^2 + \phi_t}} dt \tag{A.59}$$

where $\rho \in [-1, 1]$ is an additional constant.

In the second example that we consider we make explicit the correspondence between a model for $(X_t, S_t)^\top$ with a linear backward Fokker-Planck equation for $f_S(z; S_t, X_t)$, that is the vanilla pricing PDE, and the affinity propriety in the sense of (Duffie et al., 2000, Sec 2.2). This correspondence is an identity and the linearity of the PDE / affinity holds provided a particular form for the correlation structure is imposed.

Example 2. ***Christoffersen, Heston and Jacobs (2009)*** (ψ_t, ϕ_t)***-displaced*** *Consider a filtered probability space $(\Omega, \mathcal{F}, \{\mathcal{F}_t\}_{t\geq 0}, \mathbb{Q})$, satisfying usual assumptions. Under the risk-neutral measure $\mathbb{Q}$, we specify the evolution of the logarithmic price of the underlying S&P500 index $x_t = \log S_t$ as follows*

$$\begin{aligned} dx_t &= \left[r - q - \frac{1}{2}\left(\psi_t\sigma_{1,t}^2 + \phi_t + \sigma_{2,t}^2\right)\right]dt + \sqrt{\psi_t\sigma_{1,t}^2 + \phi_t} dW_{1,t}^S + \sigma_{2,t} dW_{2,t}^S \\ d\sigma_{i,t}^2 &= \alpha_i(\beta_i - \sigma_{i,t}^2)dt + \Lambda_i \sigma_t dW_{i,t}^\sigma \quad (i = 1, 2) \end{aligned} \tag{A.60}$$

where r is the short rate, q is the continuously compounded dividend yield rate, and in which the risk-neutral dynamics of the index is driven by continuous shocks, modeled by the Wiener processes $W_{i,t}^S, i = 1, 2$. The first volatility factor is displaced by two sufficiently regular deterministic functions ψ_t and ϕ_t which verify the conditions (3.27) of our setting

$$\begin{aligned} &\phi_t \geq 0 \ \textit{and} \ \ \phi_0 = 0 \\ &\psi_t \geq 0 \ \textit{and} \ \ \psi_0 = 1 \end{aligned} \tag{A.61}$$

and $\alpha_i, \beta_i, \Lambda_i$ are non-negative constants.[5] *The corresponding dynamics of the index S_t is, by Itō's lemma:*

$$\frac{dS_t}{S_t} = (r-q)dt + \sqrt{\psi_t \sigma_{1,t}^2 + \phi_t} dW_{1,t}^S + \sigma_{2,t} dW_{2,t}^S \tag{A.62}$$

This model is a (ψ_t, ϕ_t)-displaced version of the two-factor model of Christoffersen, Heston and Jacobs Christoffersen et al. (2009), which we will call 2-SV×+. The only non-zero correlations imposed are

$$corr(dW_{1,t}^S, dW_{1,t}^\sigma) = \rho_1(t)dt \tag{A.63}$$

$$corr(dW_{2,t}^S, dW_{2,t}^\sigma) = \rho_2 dt \tag{A.64}$$

with $|\rho_1(t)| \leq 1$ but left otherwise unspecified and $\rho_2 \in [-1,1]$ an additional constant. Consider first the stochastic volatility process $X_t = (\sigma_{1,t}^2, \sigma_{2,t}^2)^\top$ alone. It's easy to check that this process fits in our affine framework, is unaffected by the (ψ_t, ϕ_t)-displacements and its distributional properties can be described by means of the conditional CF

$$f_\sigma^{2\text{-}SV\times+}(z_1, z_2; \sigma_{1,t}^2, \sigma_{2,t}^2, \tau) = E^{\mathbb{Q}}\left[e^{iz_1\sigma_{1,T}^2 + iz_2\sigma_{2,T}^2} \middle| \mathcal{F}_t \right] \tag{A.65}$$

which, from Proposition 12, takes the following exponential affine form

$$\log f_\sigma^{2\text{-}SV\times+}(z_1, z_2; \sigma_{1,t}^2, \sigma_{2,t}^2, \tau) = \sum_{i=1,2} \left(A_i^\sigma(z_i;\tau) + B_i^\sigma(z_i;\tau)\sigma_{i,t}^2 \right) \tag{A.66}$$

where coefficients satisfy the following set of ODEs:

$$\begin{aligned} \frac{\partial A_i^\sigma(z_i;\tau)}{\partial \tau} &= \alpha_i \beta_i B_i^\sigma(z_i;\tau) \\ \frac{\partial B_i^\sigma(z_i;\tau)}{\partial \tau} &= \frac{1}{2}\Lambda_i^2 \left(B_i^\sigma(z_i;\tau)\right)^2 - \alpha_i B_i^\sigma(z_i;\tau) \end{aligned} \tag{A.67}$$

with initial conditions $A_i^\sigma(z_i;0) = 0$ and $B_i^\sigma(z_i;0) = iz_i$. Explicit solutions can be found:

$$\begin{aligned} A_i^\sigma(z_i;\tau) &= -\frac{2\alpha_i\beta_i}{\Lambda_i^2} \log\left(1 - iz_i \frac{\Lambda_i^2}{2\alpha_i}\left(1 - e^{-\alpha_i\tau}\right)\right) \\ B_i^\sigma(z_i;\tau) &= \frac{iz_i e^{-\alpha_i\tau}}{1 - iz_i \frac{\Lambda_i^2}{2\alpha_i}\left(1 - e^{-\alpha_i\tau}\right)} \end{aligned} \tag{A.68}$$

We can conclude that the price of VIX derivatives does not require any specification of the correlations $\rho_1(t), \rho_2$, since it does not depend on them. By direct inspection of Proposition 11, the price of a futures or option written on VIX, depends on the dynamics of S_t only thorough the affinity coefficients of VIX scaled squared

$$\left(\frac{VIX_t^{2\text{-}SV\times+}}{100}\right)^2 = \frac{1}{\bar{\tau}}\left(\sum_{i=1,2} a_i(\bar{\tau}) + b_i(\bar{\tau})\sigma_{i,t}^2 + \int_t^{t+\bar{\tau}} \phi_s ds \right) \tag{A.69}$$

[5] In the present context the Feller condition $2\alpha_i\beta_i \geq \Lambda_i^2, i = 1,2$ is not relevant and we do not consider it further.

which for this 2-SV×+ model take the form ($i = 1, 2$)

$$\begin{aligned} a_i(\bar{\tau}) &= \beta_i\Big(\bar{\tau} - b_i(\bar{\tau})\Big) \\ b_i(\bar{\tau}) &= \frac{1 - e^{-\bar{\tau}\alpha_i}}{\alpha_i} \end{aligned} \tag{A.70}$$

but not on any correlation between $dW^S_{i,t}$ and $dW^\sigma_{j,t}$.
*We now go back to the complete specification of the 2-SV×+ model for $(\sigma^2_{1,t}, \sigma^2_{2,t}, x_t)^\top$ and analyze the role of correlation function $\rho_1(t)$ and begin with the **affine approach** introduced by Duffie, Pan and Singleton in Duffie et al. (2000). Borrowing from their notation, we rewrite the model in 2-SV×+ model in matricial form as*

$$d\begin{pmatrix} \sigma^2_{1,t} \\ \sigma^2_{2,t} \\ x_t \end{pmatrix} = \mu dt + \sigma dW \tag{A.71}$$

where $dW = (dW^{(1)}, dW^{(2)}, dW^{(3)}, dW^{(4)})^\top \in \mathbb{R}^4$ is a 4-dimensional standard Wiener process and the drift is the 3-dimensional vector $\mu = (\mu_{\sigma_1}, \mu_{\sigma_2}, \mu_x)^\top \in \mathbb{R}^3$

$$\begin{aligned} \mu_{\sigma_i} &= \alpha_l(\beta_l - \sigma^2_{l,t}) \quad (i = 1, 2) \\ \mu_x &= r - q - \frac{1}{2}\left(\psi_t\sigma^2_{1,t} + \phi_t + \sigma^2_{2,t}\right) \end{aligned} \tag{A.72}$$

and it's easy to see that μ is an affine function of the complete process $(\sigma_{1,t}, \sigma_{2,t}, x_t)^\top$

$$\mu = K_0 + K_1\begin{pmatrix} \sigma^2_{1,t} \\ \sigma^2_{2,t} \\ x_t \end{pmatrix}$$

$$= \begin{pmatrix} \alpha_1\beta_1 \\ \alpha_2\beta_2 \\ r - q - \frac{1}{2}\phi_t \end{pmatrix} + \begin{pmatrix} -\alpha_1 & 0 & 0 \\ 0 & -\alpha_2 & 0 \\ -\frac{1}{2}\psi_t & -\frac{1}{2} & 0 \end{pmatrix}\begin{pmatrix} \sigma^2_{1,t} \\ \sigma^2_{2,t} \\ x_t \end{pmatrix}$$

The volatility matrix $\sigma \in \mathbb{R}^{3\times 4}$ is given by the following matrix

$$\sigma = \begin{pmatrix} \Lambda_1\sigma_{1,t} & 0 & 0 & 0 \\ 0 & 0 & \Lambda_2\sigma_{2,t} & 0 \\ \rho_1(t)\sqrt{\psi_t\sigma^2_{1,t} + \phi_t} & \sqrt{1 - \rho^2_1(t)}\sqrt{\psi_t\sigma^2_{1,t} + \phi_t} & \rho_2\sigma_{2,t} & \sqrt{1 - \rho^2_2}\sigma_{2,t} \end{pmatrix} \tag{A.73}$$

The complete process is affine in the sense of (Duffie et al., 2000, Sec. 2.2) provided the variance-covariance matrix $\sigma\sigma^\top \in \mathbb{R}^{4\times 4}$ can be written as an affine function of $(\sigma_{1,t}, \sigma_{2,t}, x_t)^\top$

$$\begin{aligned} \sigma\sigma^\top &= H_0 + H_1 \cdot \begin{pmatrix} \sigma^2_{1,t} \\ \sigma^2_{2,t} \\ x_t \end{pmatrix} \\ &= H_0 + H_1^{(1)}\sigma^2_{1,t} + H_1^{(2)}\sigma^2_{1,t} + H_1^{(3)}x_t \end{aligned}$$

for some real symmetric 3×3 matrices H_0 and $H_1^{(i)}, i = 1, 2, 3$. It's easy to realize that, for a general form of $\rho_1(t)$, there are no such matrices. Let us impose the following functional form on the correlation:

$$corr(dW_{1,t}^S, dW_{1,t}^\sigma) = \rho_1(t)dt = \rho_1 \sqrt{\frac{\psi_t \sigma_{1,t}^2}{\psi_t \sigma_{1,t}^2 + \phi_t}} dt \tag{A.74}$$

with $\rho_1 \in [-1, 1]$ an additional constant. With this correlation structure imposed we easily find that ($H_1^{(3)} = \mathbf{0}_{3\times 3}$)

$$\sigma\sigma^\top = \begin{pmatrix} \Lambda_1^2 \sigma_{1,t}^2 & 0 & \rho_1 \Lambda_1 \sqrt{\psi_t} \sigma_{1,t}^2 \\ 0 & \Lambda_2^2 \sigma_{2,t}^2 & \rho_2 \Lambda_2 \sigma_{2,t}^2 \\ \rho_1 \Lambda_1 \sqrt{\psi_t} \sigma_{1,t}^2 & \rho_2 \Lambda_2 \sigma_{2,t}^2 & \psi_t \sigma_{1,t}^2 + \phi_t + \sigma_{2,t}^2 \end{pmatrix}$$

$$= H_0 + H_1^{(1)} \sigma_{1,t}^2 + H_1^{(2)} \sigma_{1,t}^2$$

$$= \begin{pmatrix} 0 & 0 & 0 \\ 0 & 0 & 0 \\ 0 & 0 & \phi_t \end{pmatrix} + \begin{pmatrix} \Lambda_1^2 & 0 & \rho_1 \Lambda_1 \sqrt{\psi_t} \\ 0 & 0 & 0 \\ \rho_1 \Lambda_1 \sqrt{\psi_t} & 0 & \psi_t \end{pmatrix} \sigma_{1,t}^2 + \begin{pmatrix} 0 & 0 & 0 \\ 0 & \Lambda_2^2 & \rho_2 \Lambda_2 \\ 0 & \rho_2 \Lambda_2 & 1 \end{pmatrix} \sigma_{2,t}^2$$

*and therefore the **2-SV**$\times$+ model, equipped with the correlation structure in (A.74), is an affine model in the sense of (Duffie et al., 2000, Sec. 2.2). We conclude this **affine approach** noting that with this ad-hoc form for the correlation, the diffusion matrix σ can be written in the extended canonical form of Collin-Dufresne and Goldstein (2002) and Cheridito et al. (2010)*

$$\sigma_{3\times 4} = \Sigma_{3\times 4} \sqrt{V}_{4\times 4}$$

$$= \begin{pmatrix} \Lambda_1 & 0 & 0 & 0 \\ 0 & 0 & \Lambda_2 & 0 \\ \rho_1 \sqrt{\psi_t} & \sqrt{1 - \rho_{1,t}^2} & \rho_2 & \sqrt{1 - \rho_2^2} \end{pmatrix} \begin{pmatrix} \sqrt{\sigma_{1,t}^2} & 0 & 0 & 0 \\ 0 & \sqrt{\frac{\phi_t}{1-\rho_{1,t}^2} + \psi_t \sigma_{1,t}^2} & 0 & 0 \\ 0 & 0 & \sqrt{\sigma_{2,t}^2} & 0 \\ 0 & 0 & 0 & \sqrt{\sigma_{2,t}^2} \end{pmatrix}$$

and thus satisfies their sufficient condition for affinity.

*Let us now step back to the unspecified correlation $\rho_1(t)$ in (A.63) and follow the standard **PDE approach** for pricing derivatives. Consider the conditional CF of the complete process $(\sigma_{1,t}^2, \sigma_{2,t}^2, x_t)^\top \in \mathbb{R}^3$*

$$f_{x\sigma}^{\text{2-SV}\times+}(z, z_1, z_2; \sigma_{1,t}^2, \sigma_{2,t}^2, x_t, t, T) = E^{\mathbb{Q}} \left[e^{izx_T + iz_1 \sigma_{1,T}^2 + iz_2 \sigma_{2,T}^2} \middle| \mathcal{F}_t \right] \tag{A.75}$$

The Feynmann-Kač theorem states that $f_{x\sigma}$ is a solution of the following boundary value problem[6] (Bjork, 1998, Chap. 5)

$$\begin{aligned} \partial_t f_{x\sigma} + \mu^\top \nabla f_{x\sigma} + \frac{1}{2} Tr\left[\sigma^\top H_{x\sigma} \sigma\right] &= 0 \\ f_{x\sigma}(z, z_1, z_2; \sigma_{1,T}^2, \sigma_{2,T}^2, x_T, T, T) &= e^{izx_T + iz_1 \sigma_{1,T}^2 + iz_2 \sigma_{2,T}^2} \end{aligned} \tag{A.76}$$

[6] $\partial_t f_{x\sigma}$ is for $\frac{\partial f_{x\sigma}}{\partial t}$, $\nabla f_{x\sigma} \in \mathbb{R}^3$ denotes the gradient of $f_{x\sigma}$ w.r.t $(\sigma_{1,t}^2, \sigma_{2,t}^2, x_t)^\top \in \mathbb{R}^3$, $H_{x\sigma} \in \mathbb{R}^{3\times 3}$ is the Hessian matrix of $f_{x\sigma}$ and $Tr[\cdot]$ the trace operator.

where $\mu \in \mathbb{R}^3$ and $\sigma \in \mathbb{R}^{3\times 4}$ have been defined in (A.73) and (A.73), respectively. From the dynamics in (A.60), the PDE for $f_{x\sigma}$ may be written explicitly as follows ($f := f_{x\sigma}, V_i := \sigma^2_{i,t}$)[7]

$$\begin{aligned}0 = \partial_t f &+ \left[r - q - \frac{1}{2}\left(\psi_t V_1 + \phi_t + V_2\right)\right]\partial_x f + \frac{1}{2}(\psi_t V_1 + \phi_t + V_2)\partial^2_{xx} f \\ &+ \sum_{k=1,2}\left[\alpha_k(\beta_k - V_k)\partial_k f + \frac{1}{2}\Lambda_k^2 V_k \partial^2_{kk} f\right] \\ &+ \rho_1(t)\sqrt{\psi_t V_1 + \phi_t}\Lambda_1\sqrt{V_1}\partial^2_{x1} f + \rho_2\Lambda_2 V_2 \partial^2_{x2} f\end{aligned}$$

It's easy to realize that, for a general form of $\rho_1(t)$, the PDE is not analytically tractable, due to the non-linear dependence w.r.t. $V_1 := \sigma^2_{1,t}$ which prevents us from applying a separation argument. Let us impose the correlation in (A.74)

$$corr(dW^S_{1,t}, dW^\sigma_{1,t}) = \rho_1(t)dt = \rho_1\sqrt{\frac{\psi_t V_1}{\psi_t V_1 + \phi_t}}dt \tag{A.77}$$

With this correlation structure, we obtain a linearization of the PDE

$$\begin{aligned}0 = \partial_t f &+ \left[r - q - \frac{1}{2}\left(\psi_t V_1 + \phi_t + V_2\right)\right]\partial_x f + \frac{1}{2}(\psi_t V_1 + \phi_t + V_2)\partial^2_{xx} f \\ &+ \sum_{k=1,2}\left[\alpha_k(\beta_k - V_k)\partial_k f + \frac{1}{2}\Lambda_k^2 V_k \partial^2_{kk} f + \rho_k\Lambda_k V_k \partial^2_{xk} f\right]\end{aligned} \tag{A.78}$$

If we look for a solution of (A.78) with $z = 0$, we are in fact looking for a solution verifying

$$\begin{aligned}f_{x\sigma}(0, z_1, z_2; \sigma^2_{1,t}, \sigma^2_{2,t}, x_t, t, T) &= E^{\mathbb{Q}}\left[e^{iz_1\sigma^2_{1,T} + iz_2\sigma^2_{2,T}}\middle|\mathcal{F}_t\right] \\ &= f_\sigma(z_1, z_2; \sigma^2_{1,t}, \sigma^2_{2,t}, \tau)\end{aligned}$$

that is the conditional CF of the volatility process $X_t = (\sigma^2_{1,t}, \sigma^2_{2,t})^\top$. Since the dynamics of X_t does not depends on x_t, the PDE (A.78) satisfied by f_σ, simplifies to ($f_\sigma := f$)[8]

$$\begin{aligned}\partial_t f + \sum_{k=1,2}\left[\alpha_k(\beta_k - V_k)\partial_k f + \frac{1}{2}\Lambda_k^2 V_k \partial^2_{kk} f\right] &= 0 \\ f_\sigma(z_1, z_2; \sigma^2_{1,T}, \sigma^2_{2,T}, 0) &= e^{iz_1\sigma^2_{1,T} + iz_2\sigma^2_{2,T}}\end{aligned} \tag{A.79}$$

and if we substitute the educated guess of equation A.66

$$f_\sigma(z_1, z_2; \sigma^2_{1,t}, \sigma^2_{2,t}, \tau) = e^{\sum_{k=1,2} A^\sigma_k(z_k;\tau) + B^\sigma_k(z_k;\tau)\sigma^2_{k,t}} \tag{A.80}$$

[7]For ease of notation, in the PDE we will also write $\partial_x f_{x\sigma}$ for $\frac{\partial f_{x\sigma}}{\partial x_t}$, $\partial_k f_{x\sigma}$ for $\frac{\partial f_{x\sigma}}{\partial V_k}$, $\partial^2_{xx} f_{x\sigma}$ for $\frac{\partial^2 f_{x\sigma}}{\partial x_t^2}$, $\partial^2_{ij} f_{x\sigma}$ for $\frac{\partial^2 f_{x\sigma}}{\partial V_i \partial V_j}$, $\partial^2_{xi} f_{x\sigma}$ for $\frac{\partial^2 f_{x\sigma}}{\partial x_t \partial V_i}$.

[8]One can easily realize that the PDE in (A.78), with the terminal condition $f(T) = e^{iz_1\sigma^2_{1,T} + iz_2\sigma^2_{2,T}}$ can be verified by a function independent from x_t, that is verifying $\partial_x f = \partial^2_{xx} f = \partial^2_{xk} f = 0$.

it's a simple check of internal consistency to verify that the coefficients A_k^σ and B_k^σ will satisfy the set of ODEs in (A.67).
We now go back to the full linear PDE in (A.78) and look for a solution with $z_1 = z_2 = 0$, that is we look for the conditional CF of the log-price, needed in pricing equity derivatives Lewis (2000, 2001)

$$\begin{aligned} f_{x\sigma}(z,0,0;\sigma_{1,t}^2,\sigma_{2,t}^2,x_t,t,T) &= E^{\mathbb{Q}}\left[e^{izx_T}\middle|\mathcal{F}_t\right] \\ &= f_x(z,\sigma_{1,t}^2,\sigma_{2,t}^2,t,T) \end{aligned}$$

Since the dynamics of $x_t = \log S_t$ depends on the dynamics of the volatility factors X_t, the choice $z_1 = z_2 = 0$ will only modifies the terminal condition, otherwise leaving the PDE in (A.78) unchanged ($f_x := f$)

$$\begin{aligned} \partial_t f + \left[r - q - \frac{1}{2}\left(\psi_t V_1 + \phi_t + V_2\right)\right]\partial_x f + \frac{1}{2}(\psi_t V_1 + \phi_t + V_2)\partial_{xx}^2 f + \\ \sum_{k=1,2}\left[\alpha_k(\beta_k - V_k)\partial_k f + \frac{1}{2}\Lambda_k^2 V_k \partial_{kk}^2 f + \rho_k \Lambda_k V_k \partial_{xk}^2 f\right] = 0 \\ f_x(z;\sigma_{1,T}^2,\sigma_{2,T}^2,x_T,T,T) = e^{izx_T} \end{aligned} \tag{A.81}$$

Now we substitute in (A.77) the educated guess

$$\log f_x(z;V_1,V_2,x_t,t,T) = i(x_t + (r-q)\tau)z + \sum_{k=1,2}\left(A_k^x(z,t,T) + B_k^x(z,t,T)\sigma_{k,t}^2\right) - \frac{1}{2}z(i+z)I_\phi(t,T) \tag{A.82}$$

where $I_\phi(t,T) = \int_t^T \phi_s ds$, it's easy to show that the coefficients $A_k^x(z;t,T)$ and $B_k^x(z;t,T)$ solve the following set of ODEs

$$\begin{aligned} \partial_t A_k^x &= -\alpha_k \beta_k B_k^x \\ \partial_t B_1^x &= -\frac{1}{2}\Lambda_1^2 \left(B_1^x\right)^2 + \left(\alpha_1 - iz\rho_1\Lambda_1\right)B_1^x + \frac{1}{2}z(i+z)\psi_t \\ \partial_t B_2^x &= -\frac{1}{2}\Lambda_2^2 \left(B_2^x\right)^2 + \left(\alpha_2 - iz\rho_2\Lambda_2\right)B_2^x + \frac{1}{2}z(i+z) \end{aligned} \tag{A.83}$$

with null initial conditions at $t = T$. For generic ψ_t the Riccati equation for B_1^x (and thus A_1^x) does not have a closed-form solution, but can be easily integrate numerically, whereas the others can be given explicitly:

$$\begin{aligned} A_1^x(z;\tau) &= \frac{\alpha_1\beta_1}{\Lambda_1^2}\left[(c_1 - d_1)\tau - 2\log\left(\frac{1 - g_1 e^{-d_1\tau}}{1 - g_1}\right)\right] \\ B_1^x(z,\tau) &= \frac{c_1 - d_1}{\Lambda_1^2}\frac{1 - e^{-d_1\tau}}{1 - g_1 e^{-d_1\tau}} \end{aligned} \tag{A.84}$$

where we have defined the auxiliary parameters:

$$\begin{aligned} c_k &= \alpha_k - iz\rho_k\Lambda_k \\ d_k &= \sqrt{c_k^2 + z(i+z)\Lambda_k^2} \\ g_k &= \frac{c_k - d_k}{c_k + d_k} \end{aligned} \tag{A.85}$$

This examples suggest that (Ψ_t, Φ_t)-displaced affine models of the volatility factor process X_t are in general subjected to restrictions in their correlation structure (such as those in equations A.59 and A.74) in order for the affinity to be extended to the complete $(X_t, S_t)^\top$ process. Moreover, this last example shows the problems arising from the presence of the displacement functions in two different perspectives. On one side the restriction on the correlation structure allows the variance-covariance matrix of the complete process to be an affine function of $(X_t, \log S_t)^\top$, as required by the *affinity* definition in Duffie et al. (2000). On the other side, the *ad-hoc* correlation structure leads to a separable equity pricing PDE (for the log-price CF f_x), therefore easily numerically or even analytically integrable, but it does not affect the separable VIX derivatives pricing PDE (for the factor process CF f_σ), consistently with the fact that X_t is affine despite the non-affinity of the complete process $(X_t, S_t)^\top$.

References

Abramowitz, M. and I. Stegun (1965). *Handbook of mathematical functions*. Courier Dover Publications. 62

Aït-Sahalia, Y. and A. W. Lo (1998). Nonparametric estimation of state-price densities implicit in financial asset prices. *The Journal of Finance 53*(2), 499–547. 25, 80

Allen, P., S. Einchcomb, and N. Granger (2006). Conditional variance swaps. *Product note, JP Morgan Securities, London*. 17

Amengual, D. and D. Xiu (2012). Delving into risk premia: reconciling evidence from the S&P 500 and VIX derivatives. *Work in progress*. 31

Andersen, L. B. and V. V. Piterbarg (2007). Moment explosions in stochastic volatility models. *Finance and Stochastics 11*(1), 29–50. 79, 113, 125

Andersen, T., L. Benzoni, and J. Lund (2002). An empirical investigation of continuous-time equity return models. *Journal of Finance 57*, 1239–1284. 1, 40, 47, 49, 55, 79, 111

Bakshi, G., C. Cao, and Z. Chen (1997). Empirical performance of alternative option pricing models. *Journal of Finance 52*, 2003–2049. 3, 25, 39, 42, 57, 59, 79, 80

Baldeaux, J. and A. Badran (2014). Consistent modelling of VIX and equity derivatives using a 3/2 plus jumps model. *Applied Mathematical Finance 21*(4), 299–312. 43, 53

Bandi, F. and R. Renò (2015). Price and volatility co-jumps. *Journal of Financial Economics*. Forthcoming. 56, 100, 111

Bardgett, C., E. Gourier, and M. Leippold (2013). Inferring volatility dynamics and risk premia from the S&P 500 and VIX markets. *Swiss Finance Institute Research Paper* (13-40). 1, 38, 40, 49, 50, 55, 61, 80, 111, 119

Bates, D. (1996). Jumps and stochastic volatility: Exchange rate processes implicit in deutsche mark options. *Review of financial studies 9*(1), 69–107. 3, 39, 42, 59, 79

Bates, D. (2000). Post-'87 crash fears in the S&P 500 futures option market. *Journal of Econometrics 94*, 181–238. 59, 95, 119

Bates, D. S. (2012). Us stock market crash risk, 1926–2010. *Journal of Financial Economics 105*(2), 229–259. 30, 49, 55, 79

Bayer, C., J. Gatheral, and M. Karlsmark (2013). Fast ninomiya–victoir calibration of the double-mean-reverting model. *Quantitative Finance 13*(11), 1813–1829. 51

Bjork, T. (1998). *Arbitrage theory in continuous time*. Wiley. 8, 135

Black, F. (1976). The pricing of commodity contracts. *Journal of Financial Economics 3*, 167–179. 25, 27, 28, 29, 49, 83

Black, F. and M. Scholes (1973). The pricing of options and corporate liabilities. *Journal of Political Economy 81*, 637–659. 18, 25, 26, 49, 82

Bossu, S., E. Strasser, and R. Guichard (2005). Just what you need to know about variance swaps. *JPMorgan Equity Derivatives report 4*. 72

Branger, N., A. Kraftschik, and C. Völkert (2014). The fine structure of variance: Consistent pricing of VIX derivatives. In *Paris December 2012 Finance Meeting EUROFIDAI-AFFI Paper*. x, 1, 26, 40, 48, 54, 55, 61, 65, 67, 71, 74, 77, 111

Brigo, D. and F. Mercurio (2001). A deterministic-shift extension of analytically-tractable and time-homogenous short-rate models. *Finance & Stochastics 5*, 369–388. x, 2, 55, 56

Britten-Jones, M. and A. Neuberger (2000). Option Prices, Implied Price Processes, and Stochastic Volatility. *The Journal of Finance 55*(2), 839–866. 17, 18

Broadie, M., M. Chernov, and M. Johannes (2007). Model Specification and Risk Premia: Evidence from Futures Options. *The Journal of Finance 62*(3), 1453–1490. 59, 119

Broadie, M. and A. Jain (2008). The effect of jumps and discrete sampling on volatility and variance swaps. *International Journal of Theoretical and Applied Finance 11*(08), 761–797. 72

Bru, M.-F. (1991). Wishart processes. *Journal of Theoretical Probability 4*(4), 725–751. 110

Carr, P. and R. Lee (2009). Volatility derivatives. *Annu. Rev. Financ. Econ. 1*(1), 319–339. 1, 17

Carr, P. and K. Lewis (2004). Corridor variance swaps. *RISK-LONDON-RISK MAGAZINE LIMITED- 17*(2), 67–72. 17

Carr, P. and D. Madan (1999). Option valuation using the fast Fourier transform. *Journal of computational finance 2*(4), 61–73. 32, 38

Carr, P. and D. Madan (2001). Towards a theory of volatility trading. *Option Pricing, Interest Rates and Risk Management, Handbooks in Mathematical Finance*, 458–476. 18, 73

Carr, P. and L. Wu (2006). A tale of two indices. *The Journal of Derivatives 13*(3), 13–29. 73

Carr, P. and L. Wu (2009). Variance risk premiums. *Review of Financial Studies 22*(3), 1311–1341. 72, 73

Chen, H. and S. Joslin (2012). Generalized transform analysis of affine processes and applications in finance. *Review of Financial Studies 25*(7), 2225–2256. 39, 61

Chen, K. and S.-H. Poon (2013). Consistent pricing and hedging volatility derivatives with two volatility surfaces. *Available at SSRN 2205582*. 40, 45, 47, 55, 59, 111, 122

Cheridito, P., D. Filipović, and R. L. Kimmel (2010). A note on the dai–singleton canonical representation of affine term structure models*. *Mathematical Finance 20*(3), 509–519. 5, 6, 57, 135

Christoffersen, P., S. Heston, and K. Jacobs (2009). The shape and term structure of the index option smirk: Why multifactor stochastic volatility models work so well. *Management Science 55*(12), 1914–1932. 4, 40, 45, 51, 59, 67, 95, 100, 122, 133

Chung, S.-L., W.-C. Tsai, Y.-H. Wang, and P.-S. Weng (2011). The information content of the S&P 500 index and VIX options on the dynamics of the S&P 500 index. *Journal of Futures Markets 31*(12), 1170–1201. 1, 26

Collin-Dufresne, P. and R. Goldstein (2002). Do bonds span the fixed income markets? Theory and evidence for unspanned stochastic volatility. *Journal of Finance 57*(4), 1685–1730. 135

Collin-Dufresne, P., R. S. Goldstein, and C. S. Jones (2008). Identification of maximal affine term structure models. *The Journal of Finance 63*(2), 743–795. 5, 6, 57

Cont, R. and T. Kokholm (2013). A consistent pricing model for index options and volatility derivatives. *Mathematical Finance 23*(2), 248–274. 52, 72, 73

Courant, R. and D. Hilbert (1953). Methods of mathematical physics. 126

Cox, J., J. Ingersoll, and S. Ross (1985). A theory of the term structure of interest rates. *Econometrica 53*, 385–406. 3, 6, 28, 35, 42, 79

Da Fonseca, J. and M. Grasselli (2011). Riding on the smiles. *Quantitative Finance 11*(11), 1609–1632. 100, 110

Da Fonseca, J., M. Grasselli, and C. Tebaldi (2007). Option pricing when correlations are stochastic: an analytical framework. *Review of Derivatives Research 10*(2), 151–180. 110

Da Fonseca, J., M. Grasselli, and C. Tebaldi (2008). A multifactor volatility Heston model. *Quantitative Finance 8*(6), 591–604. 100

Dai, Q. and K. Singleton (2000). Specification analysis of affine term-structure models. *Journal of Finance 55*(5), 1943–1978. 5

Dai, Q. and K. Singleton (2002). Expectation puzzles, time-varying risk premia, and affine models of the term structure. *Journal of Financial Economics 63*, 415–441. 57

Demeterfi, K., E. Derman, M. Kamal, and J. Zou (1999). More than you ever wanted to know about volatility swaps. *Goldman Sachs quantitative strategies research notes 41*. 17, 18, 72, 73

Detemple, J. and C. Osakwe (2000). The valuation of volatility options. *European Finance Review 4*(1), 21–50. 28, 29

Dotsis, G., D. Psychoyios, and G. Skiadopoulos (2007). An empirical comparison of continuous-time models of implied volatility indices. *Journal of Banking & Finance 31*(12), 3584–3603. 30

Duan, J.-C. and C.-Y. Yeh (2010). Jump and volatility risk premiums implied by VIX. *Journal of Economic Dynamics and Control 34*(11), 2232–2244. 33, 60, 123

Duffie, D., D. Filipović, and W. Schachermayer (2003). Affine processes and applications in finance. *Annals of applied probability*, 984–1053. 5

Duffie, D. and N. Garleanu (2001). Risk and valuation of collateralized debt obligations. *Financial Analysts Journal 57*(1), 41–59. 69

Duffie, D. and R. Kan (1996). A yield-factor model of interest rates. *Mathematical Finance 6*(4), 379–406. 3, 67, 69, 79, 113

Duffie, D., J. Pan, and K. Singleton (2000). Transform analysis and asset pricing for affine jump-diffusions. *Econometrica 68*(6), 1343–1376. ix, x, 2, 4, 6, 7, 8, 12, 32, 34, 39, 40, 45, 46, 59, 65, 67, 68, 69, 70, 77, 78, 95, 120, 122, 131, 132, 134, 135, 138

Duffie, D. and K. Singleton (1999). Modeling term structures of defaultable bonds. *Review of Financial Studies 12*(4), 687–720. 67

Duffie, D. and K. J. Singleton (2012). *Credit Risk: Pricing, Measurement, and Management: Pricing, Measurement, and Management*. Princeton University Press. 69

Egloff, D., M. Leippold, and L. Wu (2010). The term structure of variance swap rates and optimal variance swap investments. *JOURNAL OF FINANCIAL AND QUANTITATIVE ANALYSIS 45*(5), 1279–1310. x, 33, 49, 55, 65, 66, 67, 68, 69, 79

Eraker, B. (2004). Do Stock Prices and Volatility Jump? Reconciling Evidence from Spot and Option Prices. *The Journal of Finance 59*(3), 1367–1404. 4, 59, 79

Eraker, B., M. Johannes, and N. Polson (2003). The impact of jumps in volatility and returns. *Journal of Finance 58*, 1269–1300. 59

Exchange, C. B. O. (2009). The cboe volatility index–VIX. *White Paper*. 18, 19

Fang, F. and C. W. Oosterlee (2008). A novel pricing method for european options based on fourier-cosine series expansions. *SIAM Journal on Scientific Computing 31*(2), 826–848. 38, 49

Gatheral, J. (2008). Consistent modeling of SPX and VIX options. In *Bachelier Congress*. 37, 39, 51, 55

Gelfand, I. M., S. V. Fomin, and R. A. Silverman (2000). *Calculus of variations*. Courier Corporation. 126

Geman, H., N. El Kauroui, and J. C. Rochet (1994). Changes of numeraire, changes of probability measures and option pricing. *Journal of Applied Probability 32*, 443–458. 4, 8, 12, 14

Goard, J. and M. Mazur (2013). Stochastic volatility models and the pricing of VIX options. *Mathematical Finance 23*(3), 439–458. 53

Gourieroux, C. and R. Sufana (2004). Derivative pricing with multivariate stochastic volatility: Application to credit risk. *Les Cahiers du CREF of HEC Montreal Working Paper No. CREF*, 04–09. 110

Gourieroux, C. and R. Sufana (2010). Derivative pricing with wishart multivariate stochastic volatility. *Journal of Business & Economic Statistics 28*(3), 438–451. 110

Greiner, W. and J. Reinhardt (1996). *Field quantization*. Springer Science & Business Media. 126

Gruber, P. H., C. Tebaldi, and F. Trojani (2010). Three make a smile–dynamic volatility, skewness and term structure components in option valutation. *CAREFIN Research Paper* (02). 110

Gruber, P. H., C. Tebaldi, and F. Trojani (2015). The price of the smile and variance risk premia. *Swiss Finance Institute Research Paper* (15-36). 119

Grünbichler, A. and F. A. Longstaff (1996). Valuing futures and options on volatility. *Journal of Banking & Finance 20*(6), 985–1001. 21, 28

Heston, S. (1993). A closed-form solution for options with stochastic volatility with applications to bond and currency options. *Review of Financial Studies 6*, 327–343. ix, 1, 3, 33, 34, 37, 38, 39, 49, 52, 100

Jiang, G. J. and Y. S. Tian (2007). Extracting model-free volatility from option prices: An examination of the VIX index. *The Journal of Derivatives 14*(3), 35–60. 73

Kaeck, A. and C. Alexander (2012). Volatility dynamics for the S&P 500: Further evidence from non-affine, multi-factor jump diffusions. *Journal of Banking & Finance 36*(11), 3110–3121. 1, 40, 47, 49, 55, 79

Kallsen, J., J. Muhle-Karbe, and M. Voß (2011). Pricing options on variance in affine stochastic volatility models. *Mathematical Finance 21*(4), 627–641. 53

Kokholm, T., M. Stisen, B. Buchanan, and B. Buchanan (2015). Joint pricing of VIX and SPX options with stochastic volatility and jump models. *The Journal of Risk Finance 16*(1). 40, 42, 43, 59, 122

Lee, R. W. et al. (2004). Option pricing by transform methods: extensions, unification and error control. *Journal of Computational Finance 7*(3), 51–86. 125

Leippold, M. and F. Trojani (2008). Asset pricing with matrix jump diffusions. *Available at SSRN 1274482*. 110

Leippold, M., L. Wu, and D. Egloff (2007). Variance risk dynamics, variance risk premia, and optimal variance swap investments. In *EFA 2006 Zurich Meetings Paper*. x, 33, 65, 66, 68, 70

Lewis, A. L. (2000). Option valuation under stochastic volatility. *Option Valuation under Stochastic Volatility*. 38, 60, 61, 76, 110, 123, 124, 129, 137

Lewis, A. L. (2001). A simple option formula for general jump-diffusion and other exponential lévy processes. *Available at SSRN 282110*. 38, 60, 61, 76, 123, 124, 129, 137

Lian, G.-H. and S.-P. Zhu (2013). Pricing VIX options with stochastic volatility and random jumps. *Decisions in Economics and Finance 36*(1), 71–88. 25, 39, 40, 41, 42, 59, 61, 77, 122

Lin, Y.-N. (2007). Pricing VIX futures: Evidence from integrated physical and risk-neutral probability measures. *Journal of Futures Markets 27*(12), 1175–1217. 33, 34, 35, 36, 39, 41, 59, 60, 123

Lin, Y.-N. and C.-H. Chang (2009). VIX option pricing. *Journal of Futures Markets 29*(6), 523–543. 25

Lo, C.-L., P.-T. Shih, Y.-H. Wang, and M.-T. Yu (2013). Volatility model specification: Evidence from the pricing of VIX derivatives. 40, 45, 46, 47, 55, 59

Lord, R. and C. Kahl (2010). Complex logarithms in heston-like models. *Mathematical Finance 20*(4), 671–694. 125

Lukacs, E. (1970). Characteristics functions. *Griffin, London*. 129

Mencía, J. and E. Sentana (2013). Valuation of VIX derivatives. *Journal of Financial Economics 108*(2), 367–391. 1, 23, 25, 27, 29, 30, 31, 32, 40, 47, 49, 54, 55, 79

Mortensen, A. (2005). Semi-analytical valuation of basket credit derivatives in intensity-based models. *Available at SSRN 663425*. 69

Pacati, C., G. Pompa, and R. Renò (2015a). It' time to relax (the Feller condition). Working paper. 111

Pacati, C., G. Pompa, and R. Renò (2015b). Smiling twice: The Heston++ model. Working paper.

Pacati, C., R. Renò, and M. Santilli (2014). Heston model: shifting on the volatility surface. *RISK* (November), 54–59. x, 2, 55, 57, 131

Pan, J. (2002). The jump-risk premia implicit in options: Evidence from an integrated time series study. *Journal of Financial Economics 63*, 3–50. 79, 119

Papanicolaou, A. and R. Sircar (2014). A regime-switching Heston model for VIX and S&P 500 implied volatilities. *Quantitative Finance 14*(10), 1811–1827. 25, 52, 53, 65

Parisi, G. (1988). *Statistical field theory*. Addison-Wesley. 126

Pitt, M. K. and N. Shephard (1999). Filtering via simulation: Auxiliary particle filters. *Journal of the American statistical association 94*(446), 590–599. 50, 119

Psychoyios, D. and G. Skiadopoulos (2006). Volatility options: Hedging effectiveness, pricing, and model error. *Journal of Futures Markets 26*(1), 1–31. 30

Rhoads, R. (2011). *Trading VIX Derivatives: Trading and Hedging Strategies Using VIX Futures, Options, and Exchange Traded Notes*, Volume 503. John Wiley & Sons. 19, 26

Sepp, A. (2008a). Pricing options on realized variance in the Heston model with jumps in returns and volatility. *Journal of Computational Finance 11*(4), 33–70. 40, 61, 77

Sepp, A. (2008b). VIX option pricing in a jump-diffusion model. *Risk Magazine*, 84–89. x, 39, 40, 43, 44, 45, 49, 55, 59, 61, 65, 67, 77

Song, Z. and D. Xiu (2014). A tale of two option markets: Pricing kernels and volatility risk. *Fama-Miller Working Paper, Forthcoming*, 12–10. 1

Todorov, V. and G. Tauchen (2011). Volatility jumps. *Journal of Business & Economic Statistics 29*(3), 356–371. 56, 72

Vasicek, O. (1977). An equilibrium characterization of the term structure. *Journal of Financial Economics 5*, 177–188. 3

Wang, Z. and R. T. Daigler (2011). The performance of VIX option pricing models: empirical evidence beyond simulation. *Journal of Futures Markets 31*(3), 251–281. 30

Whaley, R. E. (1993). Derivatives on market volatility: Hedging tools long overdue. *The journal of Derivatives 1*(1), 71–84. 28, 49

Zhang, J. E., J. Shu, and M. Brenner (2010). The new market for volatility trading. *Journal of Futures Markets 30*(9), 809–833. 21, 24, 33, 34, 35, 36, 60, 61

Zhang, J. E. and Y. Zhu (2006). VIX futures. *Journal of Futures Markets 26*(6), 521–531. 30, 34, 35, 39, 42

Zhao, B. (2013). Unifying variance swap term structures, SPX and VIX derivatives. *SPX and VIX Derivatives (January 21, 2013)*. 65, 67, 74

Zhu, S.-P. and G.-H. Lian (2012). An analytical formula for VIX futures and its applications. *Journal of Futures Markets 32*(2), 166–190. 36, 37, 39, 41, 59

Zhu, Y. and J. E. Zhang (2007). Variance term structure and VIX futures pricing. *International Journal of Theoretical and Applied Finance 10*(01), 111–127. 34, 35, 36